INTERFACIAL TENSION AND VISCOSITY OF RESERVOIR FLUIDS

by

ABHIJIT YESHWANT DANDEKAR

Submitted for the Degree of Doctor of Philosophy

Department of Petroleum Engineering

Heriot-Watt University

Edinburgh, UK

February 1994

Dedicated to my Beloved Grandfather.

ABSTRACT

Interfacial tension (IFT) and viscosity are the two important fluid properties which have a particular significance in various reservoir engineering calculations and mathematical simulations. Therefore, there exists a need to develop practical methods to accurately determine them for reservoir fluids particularly for application to gas injection schemes and development of gas condensate reservoirs.

Part A of this thesis on interfacial tension presents a novel technique for measuring this property, which has the advantage of carrying out the simultaneous measurements of interfacial tension along with other phase properties, without any extra efforts. The developed expression relating the interfacial tension to other measurable properties is simple and rigorous and hence, does not involve any empiricism. Results on various binary and multicomponent synthetic hydrocarbon mixtures, and real gas condensate fluids using the above technique have been presented along with literature data in order to demonstrate the accuracy and reliability of the method. Similarly, interfacial tension data determined by the conventional pendant drop technique on real volatile and black oil fluids has also been furnished.

A critical evaluation of the predictive techniques for interfacial tension, namely; the scaling law and the parachor method has also been presented using a large number of data on interfacial tension of binary hydrocarbon mixtures from literature. Based on this evaluation and employing the same literature data on interfacial tension of binary hydrocarbon mixtures modifications of the existing predictive techniques are proposed by relating the exponents in the equations to the molar density difference between the vapour and liquid phases. Results obtained for various multicomponent synthetic hydrocarbon mixtures and real reservoir fluids, by implementing the above

mentioned modifications have shown significant improvement compared to the original methods.

Part B of this thesis on viscosity presents a comparative study for pure hydrocarbon components and their mixtures by using various viscosity prediction methods. Also presented is a tuning study on various real reservoir fluids by employing the popularly used residual viscosity and corresponding states methods respectively. The drawbacks of these techniques have also been highlighted.

The residual viscosity method is critically evaluated and it has been proved that the variation of residual viscosity with respect to reduced density is not uniform for all fluids, particularly in the dense fluid phase. Based on a large number of data on pure hydrocarbon compounds in the dense fluid phase from literature, the residual method is modified by relating the residual viscosity of a fluid to its molecular weight along with its reduced density in dense fluid phase conditions. The modified method has been applied to various pure hydrocarbon compounds and their mixtures, and real reservoir fluids. The superiority of the new method has been demonstrated by comparing the results with those of the original methods and those based on the principle of corresponding states.

TABLE OF CONTENTS

LIST OF SYMBOLS

Nomenclature

A_c = Scaling Law Constant

a = Capillary Constant

a_0-a_6 = Constants in Fanchi's Parachor Correlation

B = Scaling Law Constant ($B = CZ_c^n$)

C = Constant in Sugden's Equation

d_e = Equatorial Diameter of a Pendant Drop

d_s = Diameter of the Pendant Drop Measured at a Distance d_e Above the Tip of the Drop

d_t = Inside Diameter of the Tip

E = Exponent in Scaling Law and Parachor Method

g = Acceleration due to Gravity

H = Drop Shape Factor/Herzog's Parameter

h = Height of a Film/Capillary Rise

K = Permeability

M = Molecular Weight

n = Total Number of Components in the System

N_b = Bond Number

P = Pressure/Parachor

P_c = Capillary Pressure

r = Radius of the Capillary

R_1, R_2 = Principal Radii of Curvature

S = Function of d_s and d_e ($S = \frac{d_s}{d_e}$)

S_{or} = Residual Oil Saturation

T = Temperature

U = Darcy Velocity

V	=	Volume
X	=	Liquid Phase Mole Fraction
Y	=	Vapour Phase Mole Fraction
Z	=	Compressibility Factor

Greek Letters

α_c	=	Riedel Parameter
β	=	Scaling Law Exponential Constant
δ	=	Partial Differential
Δ	=	Difference Operator
μ	=	Viscosity
ρ	=	Density
σ	=	Interfacial Tension
θ	=	Scaling Law Exponential Constant

Subscripts

a	=	Capillary Constant/Atmospheric
b	=	Boiling Point
c	=	Critical Value
i	=	Component Index
l	=	Liquid Phase
m	=	Molar/Mixture
n	=	Number of Components
r	=	Reduced Value
v	=	Vapour Phase

Abbreviations

AAD	=	Average Absolute Deviation
CCE	=	Constant Composition Expansion
CVD	=	Constant Volume Depletion
EOR	=	Enhanced Oil Recovery
EOS	=	Equations of State
GOR	=	Gas Oil Ratio
HWU	=	Heriot-Watt University
IFT	=	Interfacial Tension
MBC	=	Multiple Backward Contact
MFC	=	Multiple Forward Contact
PR	=	Peng-Robinson
STDEV	=	Standard Deviation
V-L-E	=	Vapour-Liquid-Equilibrium

LIST OF TABLES

LIST OF FIGURES

ACKNOWLEDGEMENTS

First of all, I am extremely grateful to Professors Ali Danesh, Dabir Tehrani and Adrian Todd for providing me this excellent opportunity to study under their guidance.

To Professor Ali Danesh I am highly indebted for his continual interest and invaluable guidance in my work. His expertise and profound knowledge of the subject have all been important factors in the consummation of this work.

I would like to express my special appreciation to Professor Dabir Tehrani for his constructive criticism and suggestions in the course of the research reported here.

I would also like to thank Professor Adrian Todd for his interest in my work and providing continual encouragement during the course of this study.

On the experimental side, I am particularly indebted to Ian Baille, Keith Bell and Ken Malcolm for performing all of the high-pressure and high-temperature PVT tests on various synthetic and real reservoir fluids, from which all of the interfacial tension data reported in this work were generated. I would also like to thank Jim Pantling for his novel design and construction contributions to many associated items of equipment used in this study.

Sincere thanks are extended to Andrew Kidd, David Parker and Radheshyam Sarkar for their invaluable assistance in computer related problems, and to Donghai Xu for providing me the FPE (Fluid Phase Equilibria) program for phase behaviour calculations.

I sincerely thank to all of my family members and friends who gave me moral support and encouragement during the course of this study.

Finally, I am very grateful to the oil companies who supported the various projects, without which the production of this manuscript would have been doubtful to say the least.

INTRODUCTION

As a contribution to a major reservoir fluids study project in the Department of Petroleum Engineering at Heriot-Watt University the author was assigned to conduct research in interfacial tension (IFT) between hydrocarbon vapours and liquids and the viscosity of hydrocarbon fluids both at a wide range of temperature, pressure and compositions. The basic objective of this work was to develop and evaluate reliable techniques for measuring and predicting these two properties of reservoir fluids.

This thesis, therefore, is composed of two main parts:

Part A - Interfacial Tension (IFT)

Part B - Viscosity

The following main points summarise the work reported in this thesis in the above two areas:

A - INTERFACIAL TENSION

Chapter 1 Deals with various definitions of interfacial tension, and its significance in reservoir engineering. Work carried out by various researchers on studying the effect of interfacial tension on increased oil recovery, for example, by reduction in the capillary pressure and increase in gravity drainage is discussed in detail here. Also discussed here is the effect of temperature and pressure on interfacial tension, and various examples from the literature and the results reported in this

work are furnished to study the effect of these variables on interfacial tension.

Chapter 2 Various techniques for measuring interfacial tension are reviewed in this chapter. Interfacial tension between the oil and gas phases is normally measured by the conventional pendant drop technique in the petroleum industry. An assessment of the pendant drop device installed in the gas condensate cell and the vapour-liquid equilibrium (V-L-E) apparatus of Heriot-Watt University is presented in detail. The other experimental techniques which are reviewed in this chapter are the, newly developed Laser Light Scattering technique (LLS), which is considered to be highly accurate and reliable for determining very low interfacial tension values. Also discussed are the conventional methods of measuring the interfacial tension by the capillary rise technique and the ring method. The meniscus method is saved for a more detailed treatment in the next chapter.

Chapter 3 A novel technique developed during the course of this study, based on the rise of a liquid film over a flat vertical wall, called the gas-liquid curvature technique or the meniscus method is discussed and presented in detail. This chapter also provides a large number of accurate and reliable data measured on interfacial tension of synthetic, binary and multicomponent hydrocarbon mixtures, gas condensates, volatile and black oil systems using the meniscus method and the conventional pendant drop technique. All the data reported were generated at a wide range of temperature and pressure conditions from the experiments performed on the above mentioned fluids in the gas condensate and the vapour liquid equilibrium (V-L-E) facilities. An

error analysis for the meniscus technique and the pendant drop method is furnished at the end of the chapter.

Chapter 4 This chapter covers the techniques for prediction of interfacial tension (IFT) using other available fluid data such as density and parachor. Interfacial tension of reservoir fluids is commonly predicted by the scaling law and the parachor method in the petroleum industry. These two popularly used methods are reviewed in details in this chapter. Some of the non-conventional methods such as the gradient theory of inhomogeneous fluids is also discussed. Although the method has not been thoroughly studied for engineering purposes, it is presented in this chapter for the purpose of completeness of the review of the predictive techniques.

Chapter 5 A critical evaluation of the scaling law and the parachor method, based on a large number of data from the literature on binary hydrocarbon mixtures at a wide range of temperature and pressure conditions is presented in this chapter. It is shown that both methods underpredict the interfacial tension at high pressure conditions (low IFT) and overpredict at low pressure conditions (high IFT). The two methods are modified by making the exponents in the scaling law and the parachor method a function of the molar density difference between the vapour and the liquid phases. The accuracy of the modified methods is demonstrated by applying them to both synthetic multicomponent hydrocarbon mixtures and real reservoir fluids at wide range of temperature and pressure conditions.

Chapter 6 The conclusions drawn from the study are presented along with recommendations for future work.

B - VISCOSITY

The study carried out on viscosity can be summarised as follows:

Chapter 1 General aspects of viscosity such as definition, the effect of temperature, pressure and composition are discussed in this chapter. Also presented is the significance of viscosity in reservoir engineering and fluid mechanics.

Chapter 2 A detailed review of the various viscosity correlations is presented in this chapter. Broadly the viscosity of reservoir fluids can be predicted by either the residual viscosity method or the principle of corresponding states method. However, the most commonly used method in the compositional reservoir simulators is the residual viscosity method, which has gained popularity due to its simplicity and is fairly easily tuned to the experimental data. The one reference, two reference and the extended principle of corresponding states methods have not achieved the same degree of success, yet due to their complex mathematical formulations.

Chapter 3 Many viscosity correlations relate the viscosity of the fluid to its density, especially the residual viscosity method. Most of these correlations show a high degree of sensitivity to the values of density used in the pertinent correlations. Hence, this chapter is aptly dedicated to the review of two equations of state (EOS) for estimating the density of hydrocarbon liquids and vapours for use in the viscosity correlations. Also presented is a small section showing the importance of accurate and reliable density values used in the viscosity correlations.

Chapter 4 A comparative study carried out on various predictive techniques using a large number of data on pure hydrocarbons and their mixtures is presented here. Also furnished is a useful tuning study carried out on the residual viscosity method and the principle of corresponding states method using a number of data sets on viscosity of real reservoir fluids.

Chapter 5 Conclusions drawn from chapter 4 once again confirmed that the residual viscosity method was the simplest and most efficient technique for estimating the viscosity of gas and liquid phases alike. However, the study also revealed certain drawbacks (large underprediction of viscosity of dense phase fluids) of this approach, which are demonstrated in this chapter. Based on these conclusions a modification of the residual viscosity method is presented, which has significantly improved the performance of this method. The accuracy of the modified method is demonstrated by applying it to pure hydrocarbons, their mixtures and real reservoir fluids and the results are also compared with the two most popularly used methods from the group of principle of corresponding states.

Chapter 6 The conclusions drawn from this study and the recommendations for future work are provided in this chapter.

PART A - INTERFACIAL TENSION

CHAPTER 1 : INTRODUCTION - INTERFACIAL TENSION

1.1 : INTRODUCTION

Surface forces play a major role in multiphase flow of gas - liquid systems in hydrocarbon reservoirs and pipelines. A quantitative index of the molecular behaviour at the interface is defined as the interfacial tension (IFT), defined as the force exerted at the interface per unit length usually expressed in the units of dyne/cm (mN/m). Various definitions have been reported for this surface property such as -

1) Measure of the specific surface free energy between two phases having different compositions[1] (erg/cm^2).

2) Boundary tension at an interface between a liquid and a gas or vapour[2] (mN/m).

3) Measure of free energy of a fluid interface[2] (erg/cm^2).

Nearly all of the common specific properties of fluids, such as density, boiling and freezing points, viscosity and thermal conductivity, are properties of the main body of fluids, whereas interfacial tension is the best known property of fluid interfaces. In this chapter the significance of interfacial tension in reservoir engineering and the effect of temperature and pressure on interfacial tension is described. In earlier periods the IFT was simply referred to as 'surface tension' when the tension between liquid and air or liquid and its vapour at atmospheric conditions was considered.

1.2 : SIGNIFICANCE OF INTERFACIAL TENSION IN RESERVOIR ENGINEERING

Interfacial tension (IFT) is a very important property as the relative magnitudes of surface, gravitational and viscous forces affect the recovery of reservoir fluids. It has been well

established that the relative permeability relationships which determine the flow behaviour of reservoir fluids strongly depend on the IFT at high pressure conditions.

Lowering of IFT between fluid phases play a particularly important role in the success of most tertiary recovery processes in hydrocarbon reservoirs. In miscible systems, for example, enhanced hydrocarbon recovery relies on the interaction between the displacing and the in - place fluids producing near zero IFT. Here, mixing and mass transfer take place across the phase boundary producing changes in fluid properties which lead to thermodynamic miscibility and reduced capillary pressures. This results in low liquid saturation, and is the ultimate objective in such processes as, miscible and surfactant flooding.

For a particular class of reservoirs, gas condensates, hydrocarbons exist as a single phase above the dew point. During depletion when the pressure falls below the dew - point the fluid in pores separates into its constituent liquid and vapour phases. Here, the composition and hence the IFT between the phases varies with pressure. The volume of liquid condensing in the formation is often very small, which may lead to permanently trapped liquid hydrocarbon, and reduced gas flow to the producing well. Such situations often result in a loss of revenue, and can present technical difficulties, since in extreme cases liquid build up near the wells can stop gas production altogether. Improved recovery methods for these reservoirs include gas recycling, full and partial pressure maintenance, and possibly water flooding. Laboratory experiments[3,4,5,14,15] using condensate fluids show that flow rates are considerably improved and residual saturation's of liquids much reduced when IFT is low (< 0.04 mN/m). These works demonstrate the importance of low IFT in correlating improved flow rates and lower residual saturation's with fluid composition, and hence reservoir pressures.

Wagner and Leach[6] studied the effects of IFT on displacement efficiency by performing immiscible displacement tests in a consolidated sandstone core over the IFT range from less than 0.01 to 5 mN/m to better define how IFT reduction can lead to increased oil recovery. Their study revealed that displacement efficiency under both oil - wet and water - wet conditions can be markedly improved by a sufficient reduction in IFT. In the particular medium used by them and the low pressure gradients employed, the reduction of IFT below

about 0.07 mN/m, resulted in large increases in displacement efficiencies. They obtained increased recoveries at pressure gradients which were well below those which can exist in the interwell area of a reservoir under water flood. Also, experiments have shown that the residual oil, S_{or}, is related to the capillary number, $\frac{\mu v}{\sigma}$, where μ is the viscosity, v is the velocity and σ is the interfacial tension. In case of an immiscible displacement, the effect of oil/water interfacial tension on residual oil saturation can be illustrated by Figure 1.2.1[12]. Where the oil saturation is plotted vs. capillary number, which is an approximate measure of the ratio of viscous to capillary forces. Over ranges of velocity, oil viscosity, and oil/water IFT found in conventional waterflooding, residual oil saturation is insensitive to capillary number. Figure 1.2.1 shows that a drastic reduction in IFT between oil and water, by several orders of magnitude or more, would be required to achieve a significant reduction in S_{or}. However, in case of a miscible displacement the interfacial tension effect is even more pronounced, since the objective is to achieve miscibility and hence by eliminating the IFT completely between the displacing fluid and the oil (capillary number infinite), residual oil saturation can be reduced to its minimal value.

Alonso and Nectoux[7] investigated the primary depletion of a near critical fluid in a very rich gas condensate reservoir. It was reported from their study that gravity segregation of liquids was important when the IFT was low. As the IFT increases the gravitational forces are overtaken by the capillary forces which result in a classical gas - drive type experiment. It has also been observed that the mode of drainage mainly relies on the density differences and IFT between gas and oil phases.

A dimensionless number which defines the ratios of gravitational to surface forces, is called 'the Bond number' and is defined by :

$$N_b = \frac{\Delta\rho g k}{\sigma} \qquad (1.2.1)$$

Where,

N_b = the Bond number

$\Delta\rho$ = the density difference between the vapour and liquid.

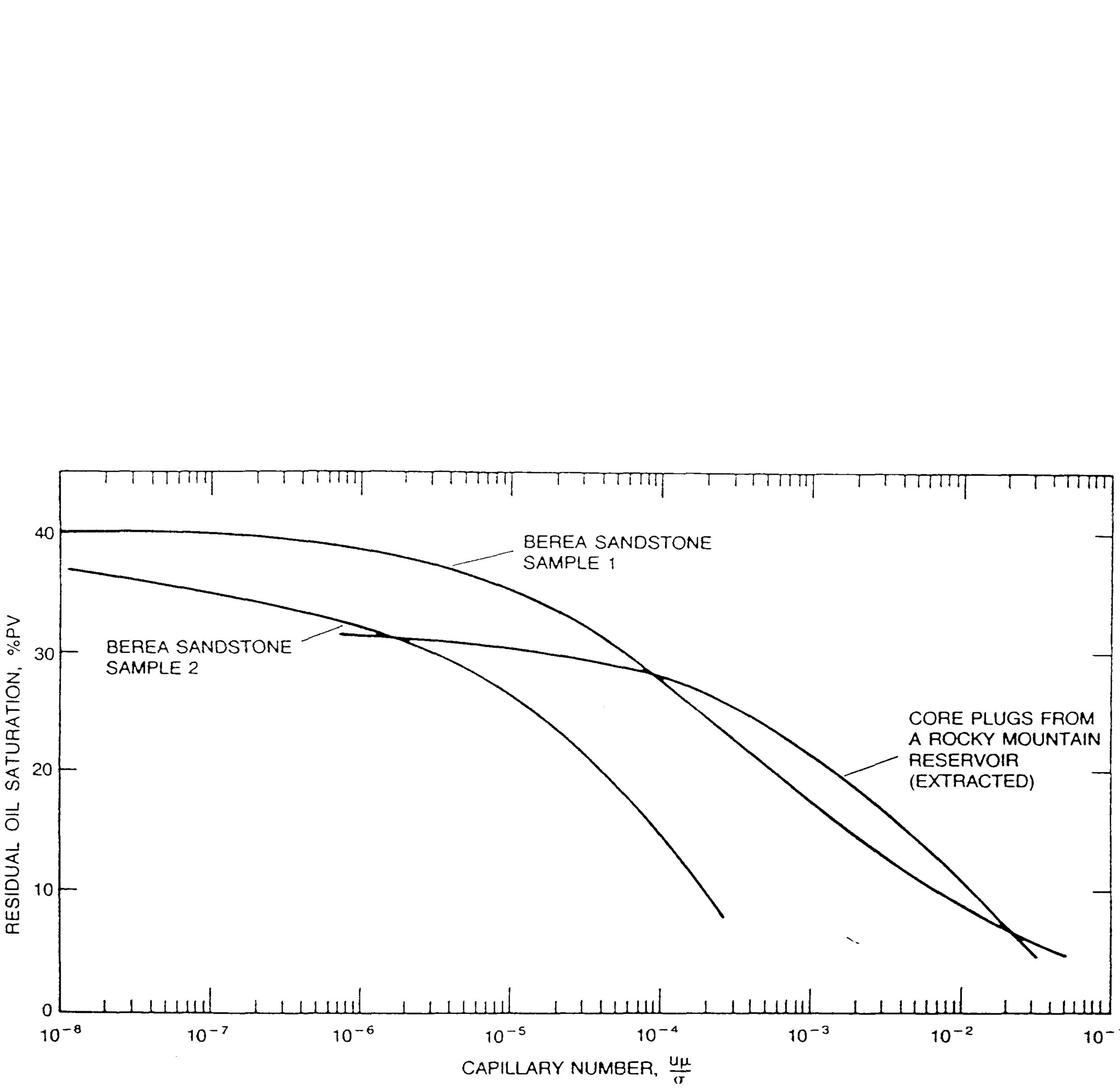

Figure 1.2.1 - Dependence of Residual Oil Saturation on Capillary Number (from Reference 12).

g = the acceleration due to gravity

k = permeability and

σ = the interfacial tension

one can see from Eq. 1.2.1 that the lower the IFT the greater is the gravitational influence.

In gas - condensate systems the initial IFT is very low and approaches zero in the critical region, but it increases rapidly as the pressure falls below the dew - point. Therefore when the initial IFT is very low this should allow a more efficient drainage of condensate as shown by the Bond number.

Another quantity which defines the IFT effects on the recovery, is the capillary pressure. The residual oil remaining in the rock after oil is displaced with water or gas is greatly dependent on the capillary forces. The capillary pressure itself is a function of interfacial tension and the principal radii of curvature through Young-Laplace Eq. as follows :

$$P_c = \sigma\left(\frac{1}{R_1} + \frac{1}{R_2}\right) \qquad (1.2.2)$$

Where,

P_c = the capillary pressure

σ = the interfacial tension and

R_1 & R_2 = the principal radii of curvature

Reduction of interfacial tension will decrease the capillary pressure which will reduce the residual oil saturation. In any two phase system, as the wetting phase saturation increases the capillary pressure decreases. In a gas condensate system, however, the IFT initially is very small and increases as the pressure decreases, which tends to increase the capillary pressure. As can be seen from Eq. 1.2.2, when the IFT is low, the capillary pressure will be suppressed and the pores may be unable to retain the condensate wetting phase. As the IFT increases the ability of capillary forces to retain condensate will increase, until the radius of mean curvature of the condensate reaches a maximum and the pore is full.

Hence, when a gas - condensate reservoir is depleted gravitational forces can be initially dominant, but become balanced by capillary forces as the IFT increases. A gas - condensate recovery project conducted in the Department of Petroleum Engineering of this University[8,9], performed experiments, in two dimensional glass micromodels and different types of sandstone cores concluded that the, gravity drainage of condensate was most effective at very low IFTs, but occurs throughout the region of retrograde condensation. The increase of IFT resulted in retention of the condensate by capillary forces and the flow of condensate become capillary controlled[8,9].

1.3 : EFFECT OF TEMPERATURE ON IFT

The kinetic agitation of the molecules and the tendency of the molecules to fly outwards increases as the temperature rises[10]. Hence, as a matter of fact, the interfacial tension almost invariably decreases with rising temperature, the only exceptions known being with a few substances over a restricted range of temperature. As the temperature rises towards the critical value, the restraining force on the surface molecules diminishes and the vapour pressure increases, when the critical temperature is reached, of course, the IFT vanishes altogether. Figures 1.3.1-1.3.3[13] illustrate the effect of temperature on interfacial tension.

1.4 : EFFECT OF PRESSURE ON IFT

In most cases a high pressure vapour over the surface of a liquid would result in a low IFT by bringing a fairly large number of gaseous molecules within reach of the surface. The attractions of these molecules on the surface molecules of the liquid would neutralise, to some extent, the inward attraction on the surface molecules, and so diminish IFT. High compression of the gas above the liquid is equivalent to putting a second liquid, of rather small attraction for the first, in place of gas.

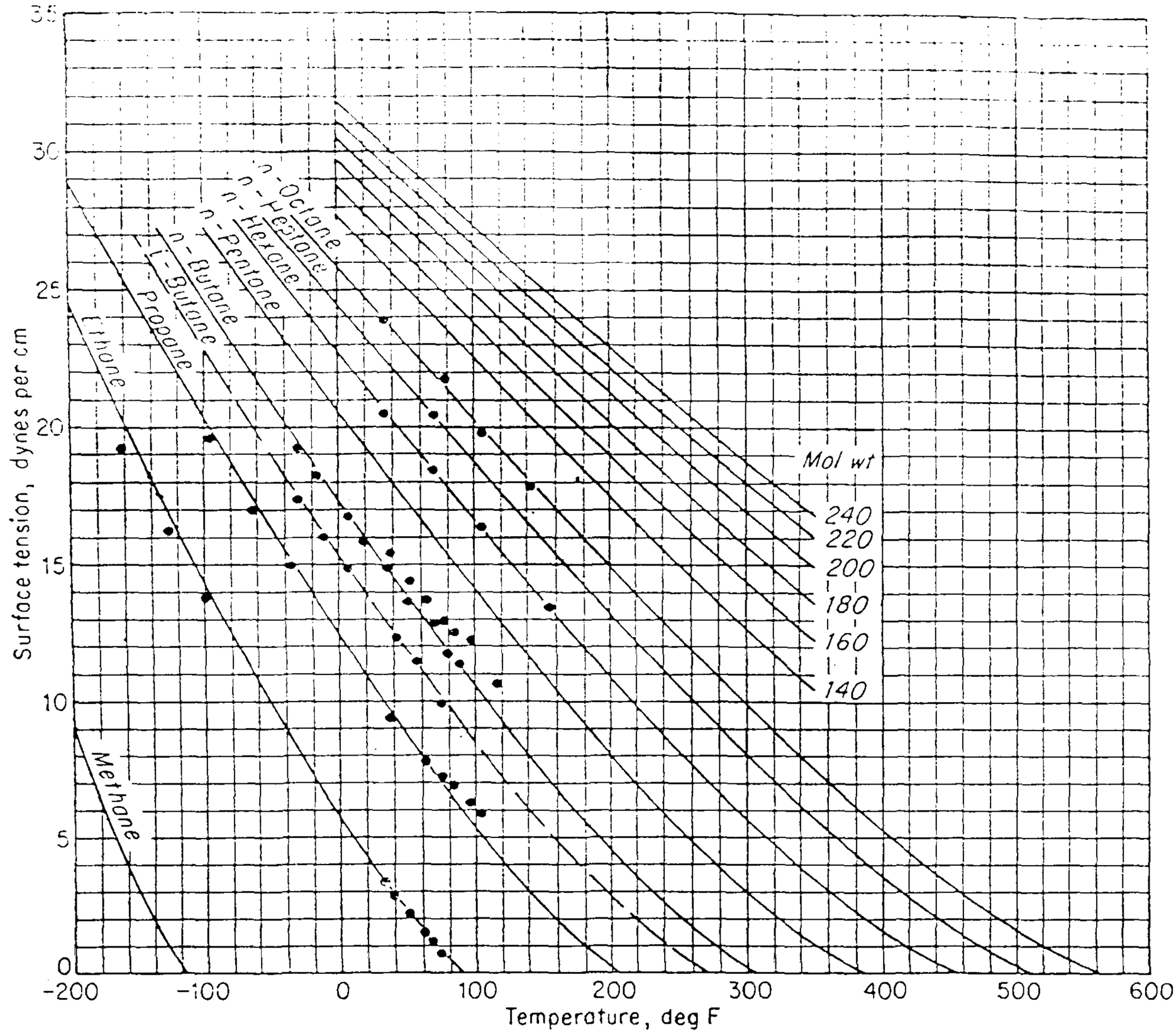

Figure 1.3.1 - Effect of Temperature on Interfacial Tension of Pure Hydrocarbons (from Reference 13).

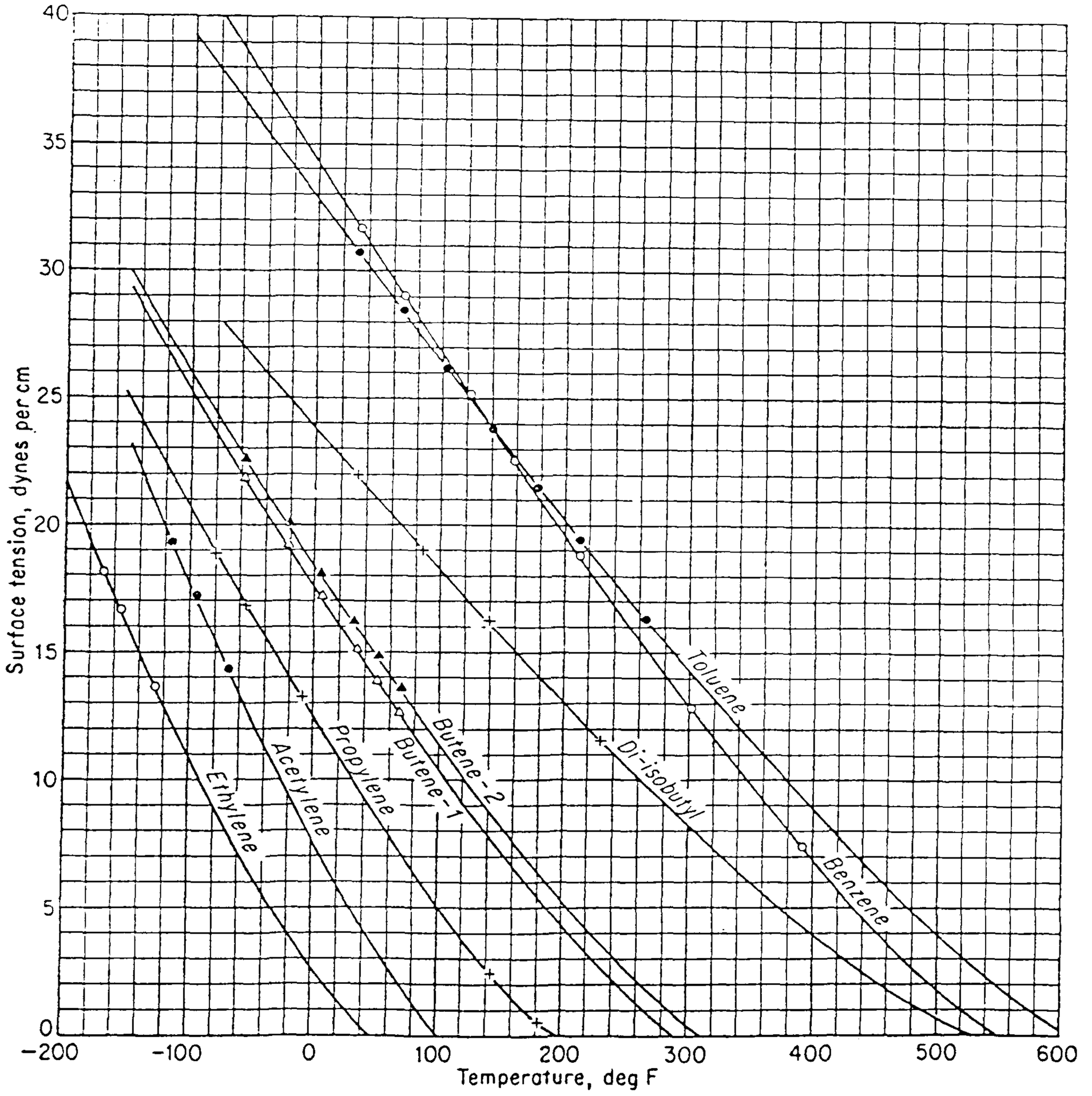

Figure 1.3.2 - Effect of Temperature on Interfacial Tension of Pure Hydrocarbons (from Reference 13).

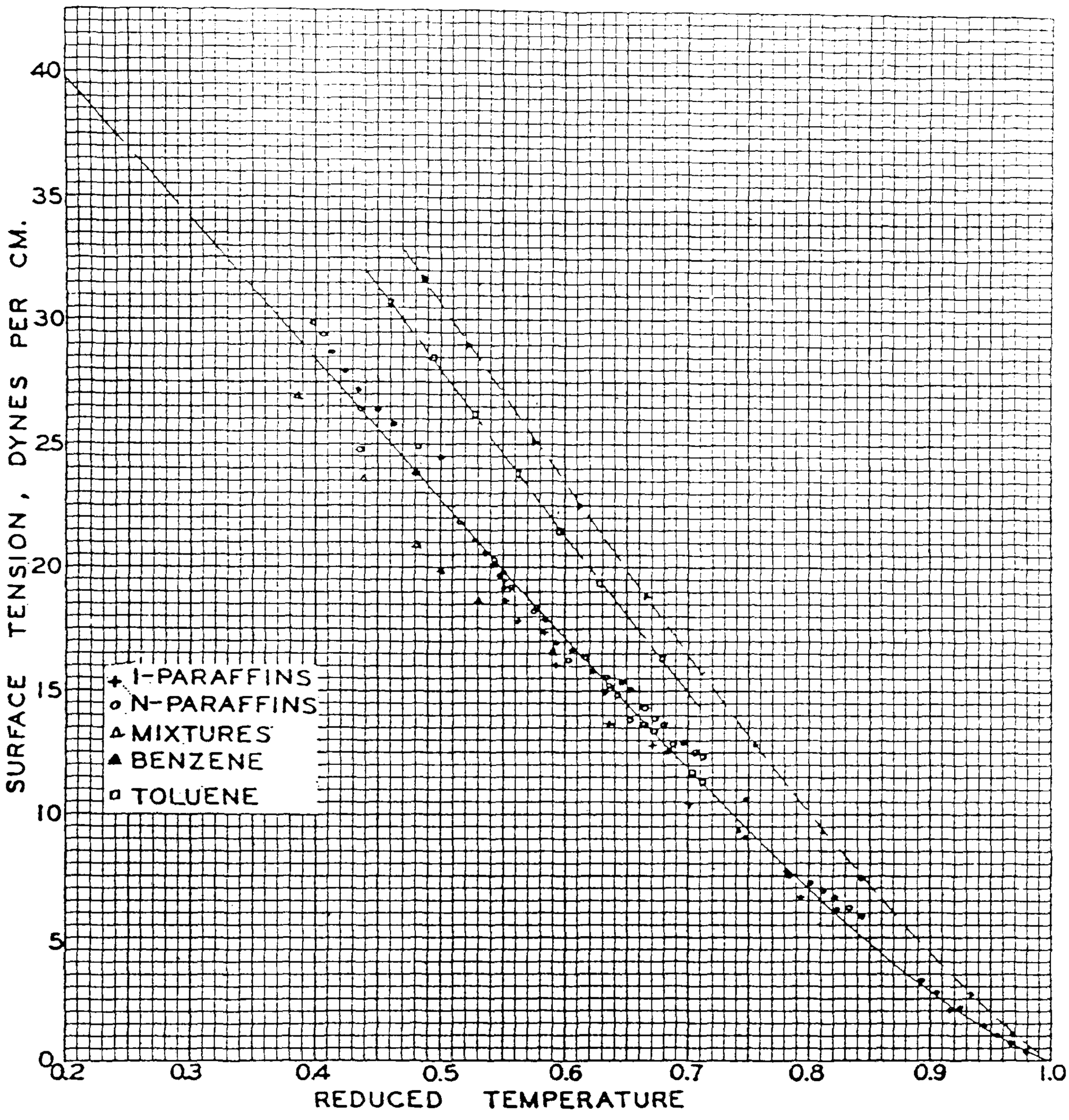

Figure 1.3.3 - Interfacial Tension as a Function of Reduced Temperature for Pure Hydrocarbons and Mixtures (from Reference 13).

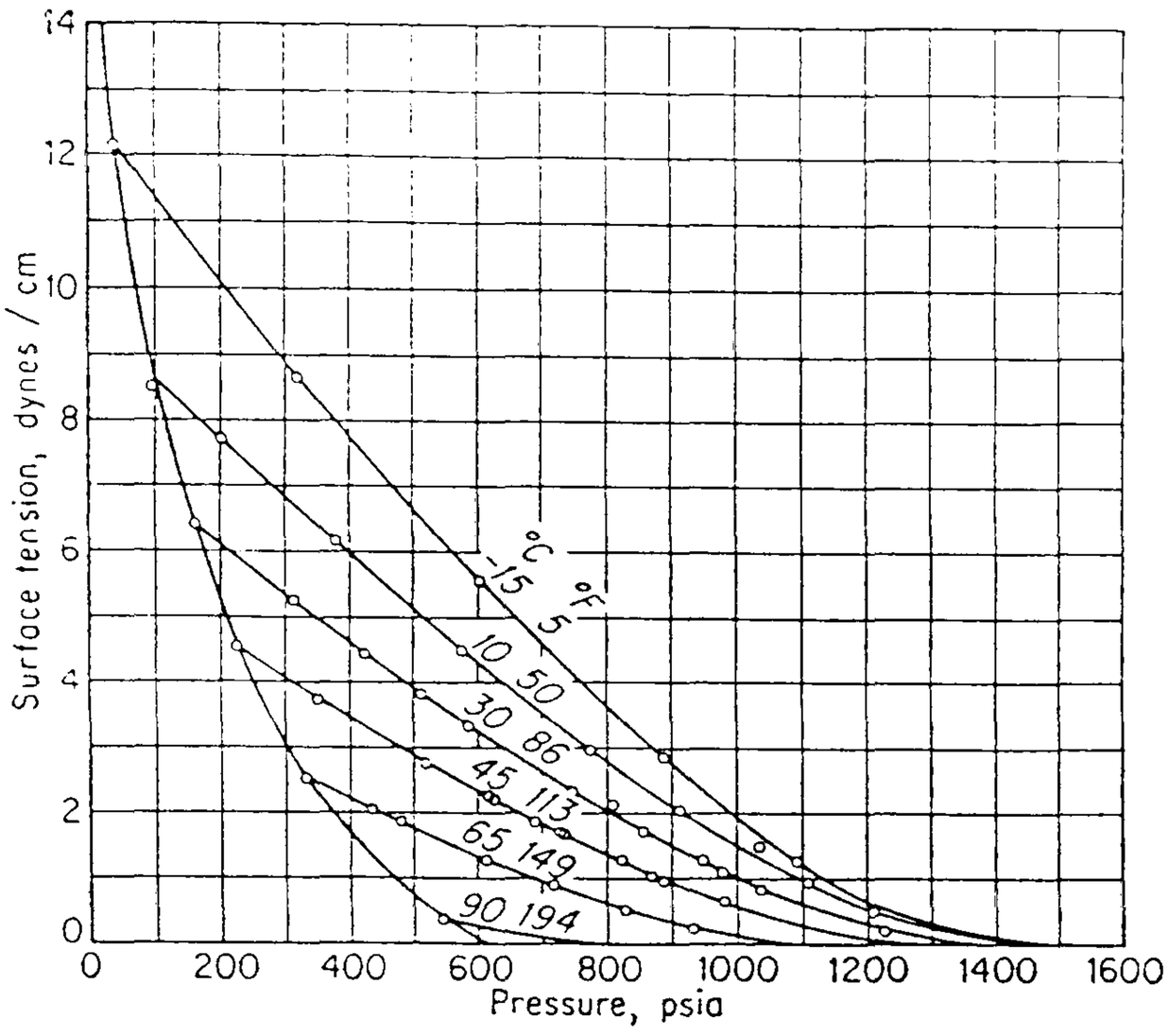

Figure 1.4.1 - Interfacial Tension of a Methane-Propane System (from Reference 13).

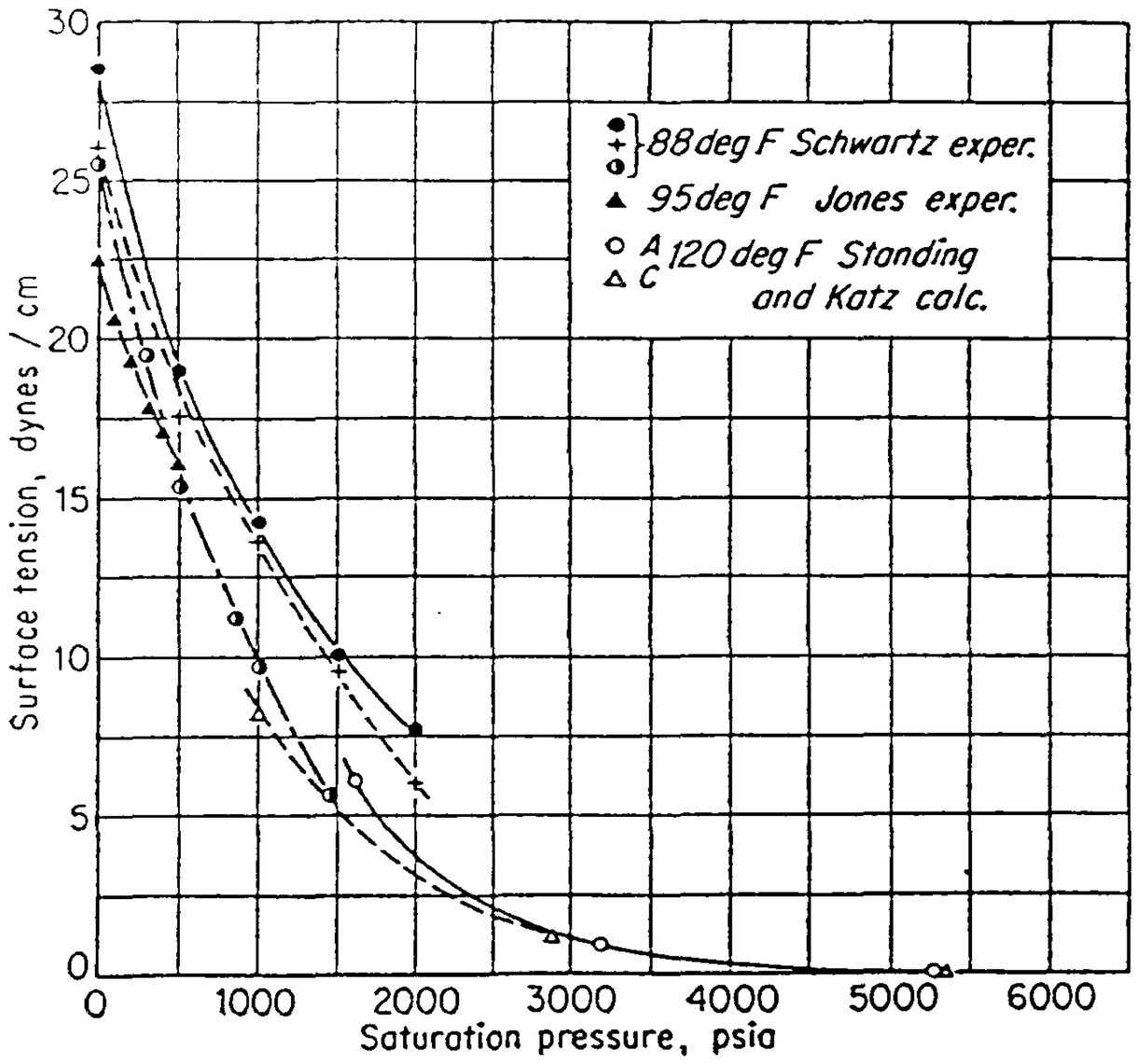

Figure 1.4.2 - Interfacial Tension of Crude Oils (from Reference 13).

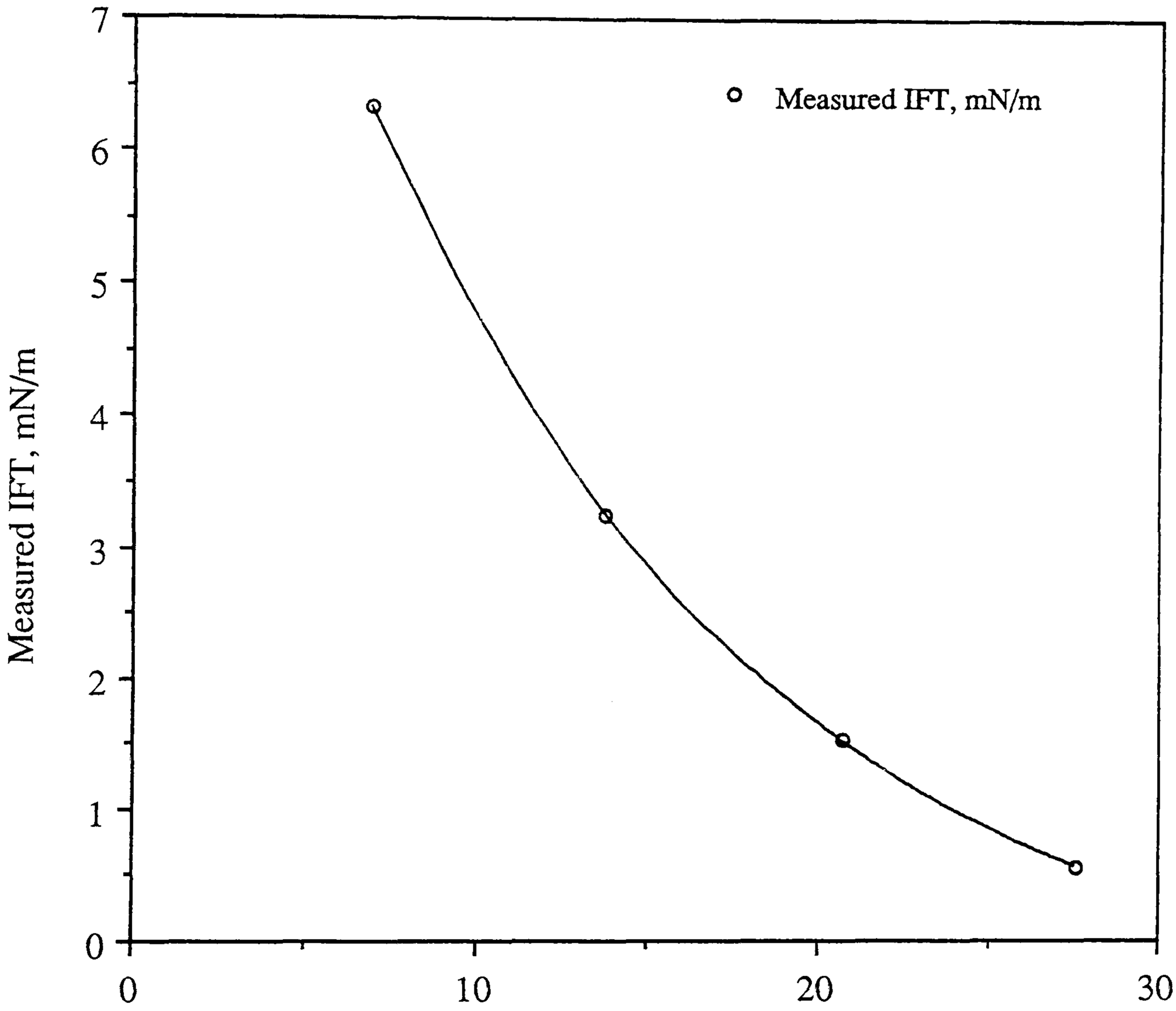

Figure 1.4.3 - Effect of Pressure on a Real Gas Condensate Fluid C3 at 140 deg C (Chapter 3, Section 3.6.1).

Kundt's measurements[11] confirm this expectation and show decrease in the IFT of several common liquids, with increase of pressure of the gas above them; the decrease amounted to some 50 % in some cases at about 150 atm. The amount of decrease in IFT as the result of a given amount of increase in pressure depends on the type of gas in contact with liquid. For example, when IFT between hydrogen and diethyl ether (DEE) is compared with IFT between air and DEE and carbon dioxide and DEE, for a given increase in pressure, the decrease in IFT of hydrogen-DEE will be less than this decrease in IFT of air-DEE, which in turn will be less than the decrease in IFT of carbon dioxide-DEE[11]. Figure 1.4.1 and 1.4.2 show the effect of pressure on interfacial tension for a methane-propane system and crude oils respectively[13] and Figure 1.4.3 illustrates the effect of pressure on a real gas condensate fluid (results for this fluid C_3 are discussed in Chapter 3, Section 3.6.1).

References

1) Hough, E.W., Wood, B.B. and Rzasa, M.J.: "Adsorption at H_2O,- He, -CH_4, -N_2 Interfaces at Pressures to 15,000 PSIA", *J. Phys. Chem.*, Vol. 56, pp. 996, (1952).

2) Andreas, J.M., Hauser, E.A. and Tucker, W.B.: "Boundary Tension by Pendant Drops", Presented at the Fiftieth Colloid Symposium, held at Cambridge, Massachusetts, (Jun., 1938).

3) Bardon, C. and Longeron, .: "Influence of Very Low Interfacial Tensions on Relative Permeability", *Society of Petroleum Engineers Journal (SPEJ)*, pp. 391-401, (Oct., 1980).

4) Asar, H.K.: "Influence of Interfacial Tension on Gas Oil Relative Permeability in Gas- Condensate Systems", PhD Thesis, University of Southern California, (May, 1980).

5) Amafuele, J.O., and Handy, L.L.: "The Effect of Interfacial Tension on Relative Oil Water Permeabilities on Consolidated Porous Media", *Society of Petroleum Engineers Journal (SPEJ)*, pp 371-381 (June, 1982).

6) Wagner, O.R., and Leach, R.O.: "Effects of Interfacial Tension on Displacement Efficiency", *Society of Petroleum Engineers Journal (SPEJ)*, pp 335-344, (Dec., 1966).

7) Alonso, M.E., and Nectoux, A.C.: "Experimental and Numerical Investigations of the Primary Depletion of a Critical Fluid", Presented at the 59th Annual Technical Conference and Exhibition held in Houston, Texas, September 16-19, SPE 13266, (1984).

8) Danesh, A., Henderson, G.D., Krinis, D. and Peden, J.M.: "Experimental Investigation of Retrograde Condensation in Porous media at Reservoir Conditions", SPE 18316, (1988).

9) Danesh, A., Krinis, D., Henderson, G.D., Peden, J.M: "Visual Investigation of Retrograde Phenomenon and Gas Condensate Flow in Porous Media", *Revue De L Institut Francais Du Petrole*, Vol. 45, No. 1, pp. 79-87, (1990).

10) Adam, N.K.: "The Physics and Chemistry of Surfaces", Oxford University Press, London, 3rd Edition, (1941).

11) Kundt, Ann. Physik, 12, 538 ; *International Critical Tables*, 4, 475, (1881).

12) Stalkup, Jr, F. I.: "Miscible Displacement", Monograph Volume 8, Henry L. Doherty Series, *Society of Petroleum Engineers of AIME*, (1984)

13) Katz, D. L.: "Handbook of Natural Gas Engineering", McGraw-Hill Book Company, New York, (1959).

14) Haniff, M.S. and Ali, J.K.: "Relative Permeability and Low Tension Fluid Flow in Gas Condensate Systems", SPE 20917, Presented at Europec 90, The Hague, Netherlands, 22-24 October (1990).

15) Ali, J.K., Butler, S., Allen, L. and Wardle, P.: "The Influence of Interfacial Tension on Liquid Mobility in Gas Condensate Systems", SPE 26783, Presented at the Offshore European Conference held in Aberdeen, 7-10 September (1993).

CHAPTER 2 : EXPERIMENTAL TECHNIQUES FOR MEASURING INTERFACIAL TENSION

2.1 : INTRODUCTION

Interfacial tension (IFT) of reservoir fluids is commonly measured by the conventional pendant drop technique in the petroleum industry. It is perhaps, the most widely used method for measuring the IFT of wide ranging type of fluids with established accuracy and reliability. In this chapter the pendant drop technique is discussed in detail along with the experimental evaluation of this device employed in HWU's gas condensate cell. A brief discussion of the pendant drop spout installed in a vapour liquid equilibrium (V-L-E) cell is also presented. Also, discussed is the very recent method of measuring the IFT by the Laser Light Scattering technique (LLS), which has gained considerable importance in recent years because of its reliable and accurate measurements at very low values of interfacial tension. The capillary rise method and the ring method still employed by some investigators are also reviewed. The novel technique based on the rise of a liquid film over a flat vertical wall, the gas-liquid interface or the meniscus method developed during the course of this study will be discussed in detail in the next chapter.

2.2 : PENDANT DROP TECHNIQUE

A literature survey carried out on IFT showed that the majority of experimental data on IFT has been generated using the pendant drop technique for pure as well as multicomponent systems. Table (2.2.1), lists the data on pendant drop technique employed for various hydrocarbon systems, highlighting its popularity.

In this technique, a liquid droplet is allowed to hang from a narrow tube or a spout or a syringe from its tip in a high pressure cell surrounding the drop with the vapour in equilibrium. The schematic of a pendant drop is shown in Figure (2.2.1). In Figure (2.2.1),

Table 2.2.1 - List of IFT Data Measured by Pendant Drop Technique.

No	Reference No.	Temp Range °F	Pressure Range psia	IFT Range
1	4	100 - 190°F	1300 - 1900 psia	0 - 2.2 mN/m
2	9	100 - 200°F	500 - 2400 psia	0 - 7.6 mN/m
3	10	100 - 175°F	650 - 1200 psia	0 - 3 mN/m
4	11	100 - 190°F	1500 - 5300 psia	0 - 10 mN/m
5	12	74 - 280°F	15 - 15,000 psia	25 - 75 mN/m
6	13	77°F	-	0.001 mN/m
7	14	77°F	-	10 - 370 mN/m
8	15	160°F	1000 - 1580 psia	0.0096 - 6 mN/m
9	16	160, 220°F	900 - 2380 psia	0.008 - 7.8 mN/m
10	17	115 - 220°F	300 - 1155 psia	0.026 - 5.7 mN/m
11	18	160°F	1600 - 2376 psia	0.000 - 4 mN/m

Table 2.2.2 - Tabulated Values of the Drop Shape Factors, $(\frac{1}{H})$, (from Reference 2).

S	0	1	2	3	4	5	6	7	8	9
0.67	.90174	.89822	.89471	.89122	.88775	.88430	.88087	.87746	.87407	.87069
0.68	.86733	.86399	.86067	.85736	.85407	.85080	.84755	.84431	.84110	.83790
0.69	.83471	.83154	.82839	.82525	.82213	.81903	.81594	.81287	.80981	.80677
0.70	.80375	.80074	.79774	.79477	.79180	.78886	.78593	.78301	.78011	.77722
0.71	.77434	.77148	.76864	.76581	.76299	.76019	.75740	.75463	.75187	.74912
0.72	.74639	.74367	.74097	.73828	.73560	.73293	.73028	.72764	.72502	.72241
0.73	.71981	.71722	.71465	.71208	.70954	.70700	.70448	.70196	.69946	.69698
0.74	.69450	.69204	.68959	.68715	.68472	.68230	.67990	.67751	.67513	.67276
0.75	.67040	.66805	.66571	.66338	.66107	.65876	.65647	.65419	.65192	.64966
0.76	.64741	.64518	.64295	.64073	.63852	.63632	.63414	.63196	.62980	.62764
0.77	.62550	.62336	.62123	.61912	.61701	.61491	.61282	.61075	.60868	.60662
0.78	.60458	.60254	.60051	.59849	.59648	.59447	.59248	.59050	.58852	.58656
0.79	.58460	.58265	.58071	.57878	.57686	.57494	.57304	.57114	.56926	.56738
0.80	.56551	.56364	.56179	.55994	.55811	.55628	.55446	.55264	.55084	.54904
0.81	.54725	.54547	.54370	.54193	.54017	.53842	.53668	.53494	.53322	.53150
0.82	.52978	.52808	.52638	.52469	.52300	.52133	.51966	.51800	.51634	.51470
0.83	.51306	.51142	.50980	.50818	.50656	.50496	.50336	.50176	.50018	.49860
0.84	.49702	.49546	.49390	.49234	.49080	.48926	.48772	.48620	.48468	.48316
0.85	.48165	.48015	.47865	.47716	.47568	.47420	.47272	.47126	.46980	.46834
0.86	.46690	.46545	.46401	.46258	.46116	.45974	.45832	.45691	.45551	.45411
0.87	.45272	.45134	.44996	.44858	.44721	.44585	.44449	.44313	.44178	.44044
0.88	.43910	.43777	.43644	.43512	.43380	.43249	.43118	.42988	.42858	.42729
0.89	.42600	.42472	.42344	.42216	.42089	.41963	.41837	.41711	.41586	.41462
0.90	.41338	.41214	.41091	.40968	.40846	.40724	.40602	.40481	.40361	.40241
0.91	.40121	.40001	.39882	.39764	.39646	.39528	.39411	.39294	.39178	.39062
0.92	.38946	.38831	.38716	.38602	.38488	.38374	.38260	.38147	.38035	.37922
0.93	.37810	.37699	.37588	.37477	.37367	.37256	.37147	.37037	.36928	.36819
0.94	.36711	.36603	.36495	.36387	.36280	.36173	.36067	.35960	.35854	.35749
0.95	.35643	.35338	.35433	.35328	.35224	.35120	.35016	.34913	.34809	.34706
0.96	.34604	.34501	.34398	.34296	.34195	.34093	.33991	.33890	.33789	.33688
0.97	.33587	.33487	.33386	.33286	.33186	.33086	.32986	.32887	.32787	.32688
0.98	.32588	.32849	.32930	.32290	.32191	.32092	.31992	.31893	.31793	.31694
0.99	.31594	.31494	.31394	.31294	.31194	.31093	.30992	.30891	.30790	.30688
1.00	.30586	.30483	.30379							

d_e is called the equatorial diameter or the maximum horizontal diameter of the drop, d_s is the diameter of the drop measured at a distance d_e above the tip of the drop and d_t is the tip inside diameter as observed on a photographic image. The quantity d_{tw} is already known which represents the original tip inside diameter which is taken as a reference value for calculating the magnification. The drop dimensions are correlated by balancing the gravitational and surface forces to give the IFT in the form given below :

$$\sigma = \frac{g d_e^2}{H} (\rho_l - \rho_v) \qquad (2.2.1)$$

Where,

g = acceleration due to gravity

σ = interfacial tension

ρ_l & ρ_v = liquid and vapour phase densities (mass) respectively

in Eq. 2.2.1, H, which is a function of $S = \frac{d_s}{d_e}$, is called the drop shape factor, the values of which have been derived using the Laplace/Young equation as applied to the drops and reported by several workers[1,2] against S.

Hence the values of H can be known after measuring the drop dimensions and subsequently calculating the value of S. Table (2.2.2), gives the tabulated values of $\frac{1}{H}$ vs. S from Reference[2].

2.2.1 : Discussion of Results on Pendant Drop Device in the Gas Condensate Equilibrium Cell

As an initial approach towards the measurement of interfacial tension between gas and condensate phases in equilibrium, a pendant drop device was installed in the gas condensate cell as shown in Figure (2.2.1.1). The device installed consisted of a spout attached to the orifice of a regulating valve which is located in the wall of the cell adjacent to the window. The valve forms the part of the direct sampling system (see Section 3.2 for details of the

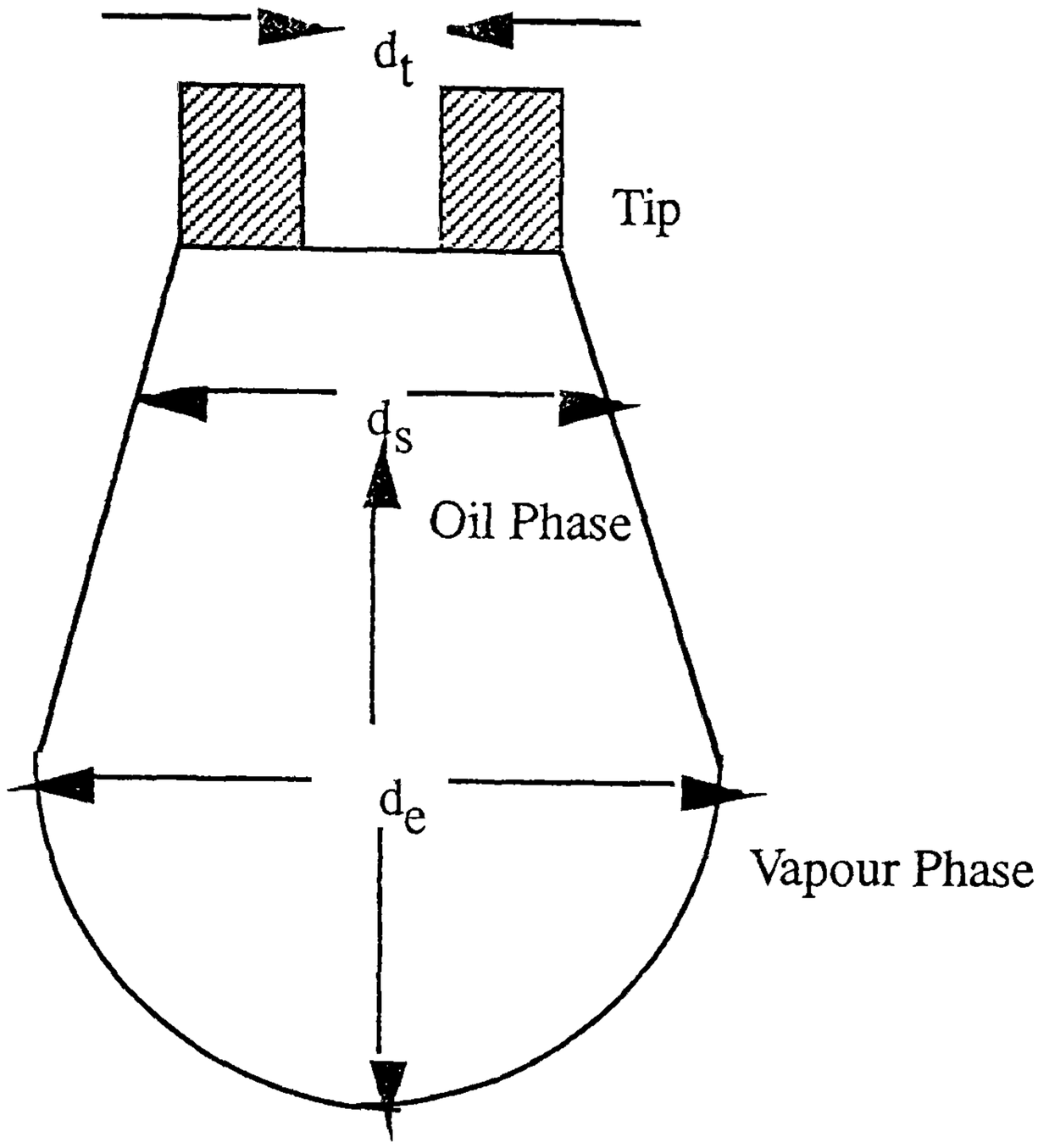

Figure 2.2.1 - Pendant Drop Hanging from a Tube, in Vapour.

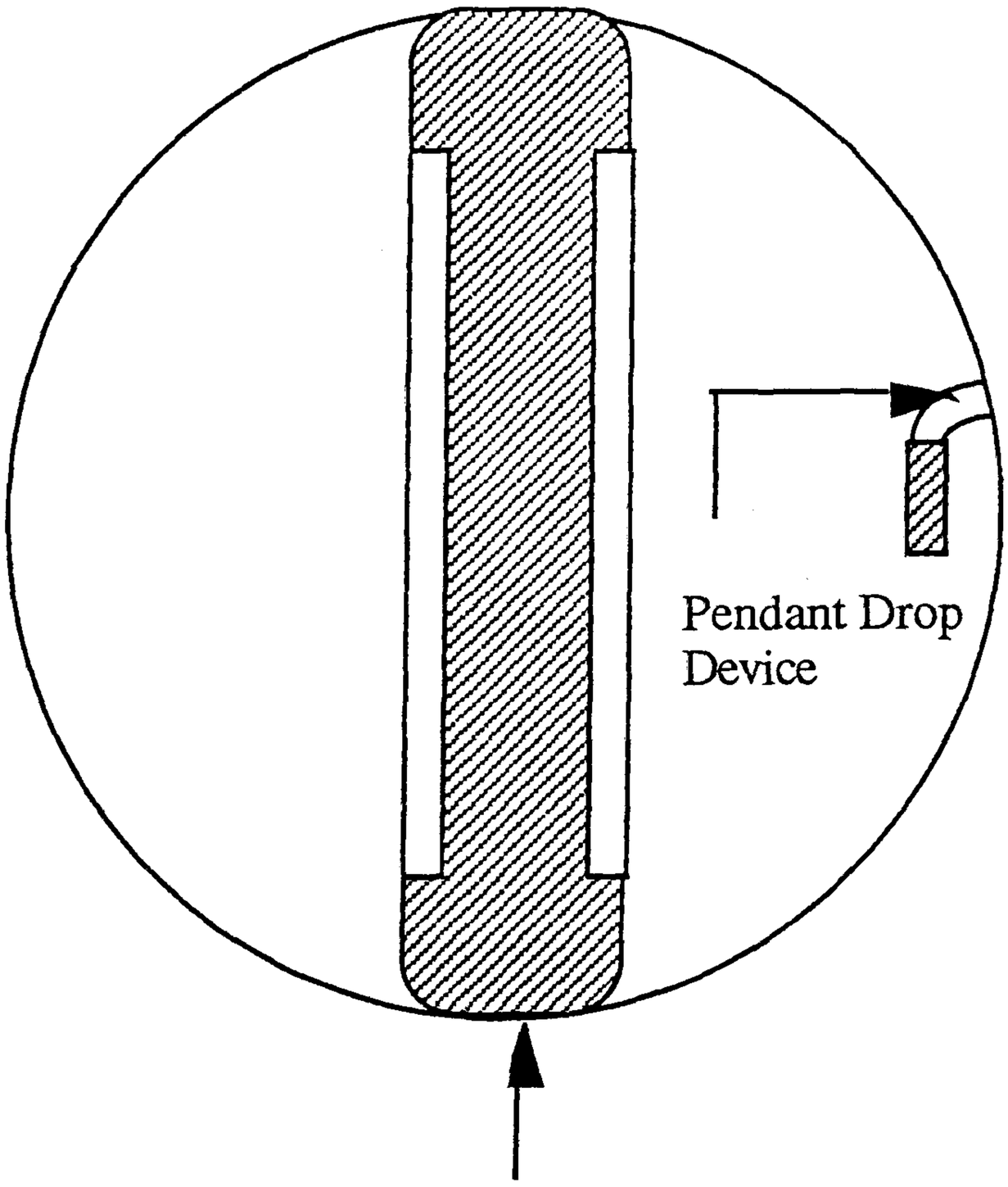

Figure 2.2.1.1 - Schematic of the Pendant Drop Device in the Gas Condensate Cell of Heriot-W att University.

Table 2.2.1.1 - Interfacial Tension Data of Methane - n - Butane System at 80°C.

No	Pressure, MPa	Pendant-Drop, (Measured) mN/m	Sugdens Equation[5], mN/m	Parachor Method[8], mN/m	Literature[4] (Measured) mN/m
1	9.06	0.48	0.17	0.37	0.74
2	7.68	1.49	1.20	0.92	1.70
3	6.30	2.00	1.95	1.70	2.15
4	4.92	2.06	2.82	2.65	-

Table 2.2.1.2 - Interfacial Tension Data of Methane - n - Decane System at 71.1°C.

Method	Interfacial Tension, mN/m
Pendant - Drop (Measured)	0.73
Sugden Equation[5]	0.64
Parachor Method[8]	0.38
Stegemeier (Measured)[11]	0.57

experimental facility) and by manipulation of fluids contained within the circulation loop it is possible to suspend a drop of liquid at the tip of the spout. Interfacial tension can then be calculated after measuring the drop dimensions as mentioned in the previous section. In order to test the pendant drop facility incorporated into the cell two binary systems namely methane-n-butane and methane-n-decane, at 80°C and 71.1°C respectively, were studied.

The methane-n-butane system exhibited retrograde condensation and had a two phase region between 4.92 MPa and 11.09 MPa. IFTs in the range of 0.5 to 2 mN/m were measured by the pendant drop technique. Table (2.2.1.1), lists the IFT measurements by the pendant drop device and those reported in the literature[4], along with those calculated by the predictive techniques[5,8]. The measured methane and n - decane interfacial tension at 71.1°C and 31.11 MPa and the value given by Stegemeier et.al.[11] along with predicted values are tabulated in Table (2.2.1.2). Reasonable agreement between the values obtained from our measurements, predicted values and reported by Stegemeier et. al.[11] can be seen. As it can be seen from Table (2.2.1.1), the values matched reasonably well at high IFTs but it was found that the lowest limit of IFT measurable by our pendant drop method was 1 dyne/cm. The measurement of IFT at fairly low values requires very small diameter drops to be formed which was very difficult with the present spout size which was 0.65 mm. The insertion of a spout of smaller size would involve large changes in the cell structure which was thought to be unfeasible. So the pendant drop method merely served the purpose of quantitative assessment. And the values measured by our pendant drop spout at low values could not be quoted with certainty. These were the initial results which proved to be conducive for the development of a novel technique based on the rise of a film of liquid over a flat vertical wall. A complete account of this method with the obtained results are furnished in the next chapter.

2.2.2 : Pendant Drop Device in the Vapour-Liquid Equilibrium (V-L-E) Cell

A pendant drop spout was installed in the V-L-E cell in order to carry out the measurement of interfacial tension during the processes of gas injection involving real volatile and black oils. The details of the arrangement are shown in Figure 2.2.2.1 which shows the pendant drop

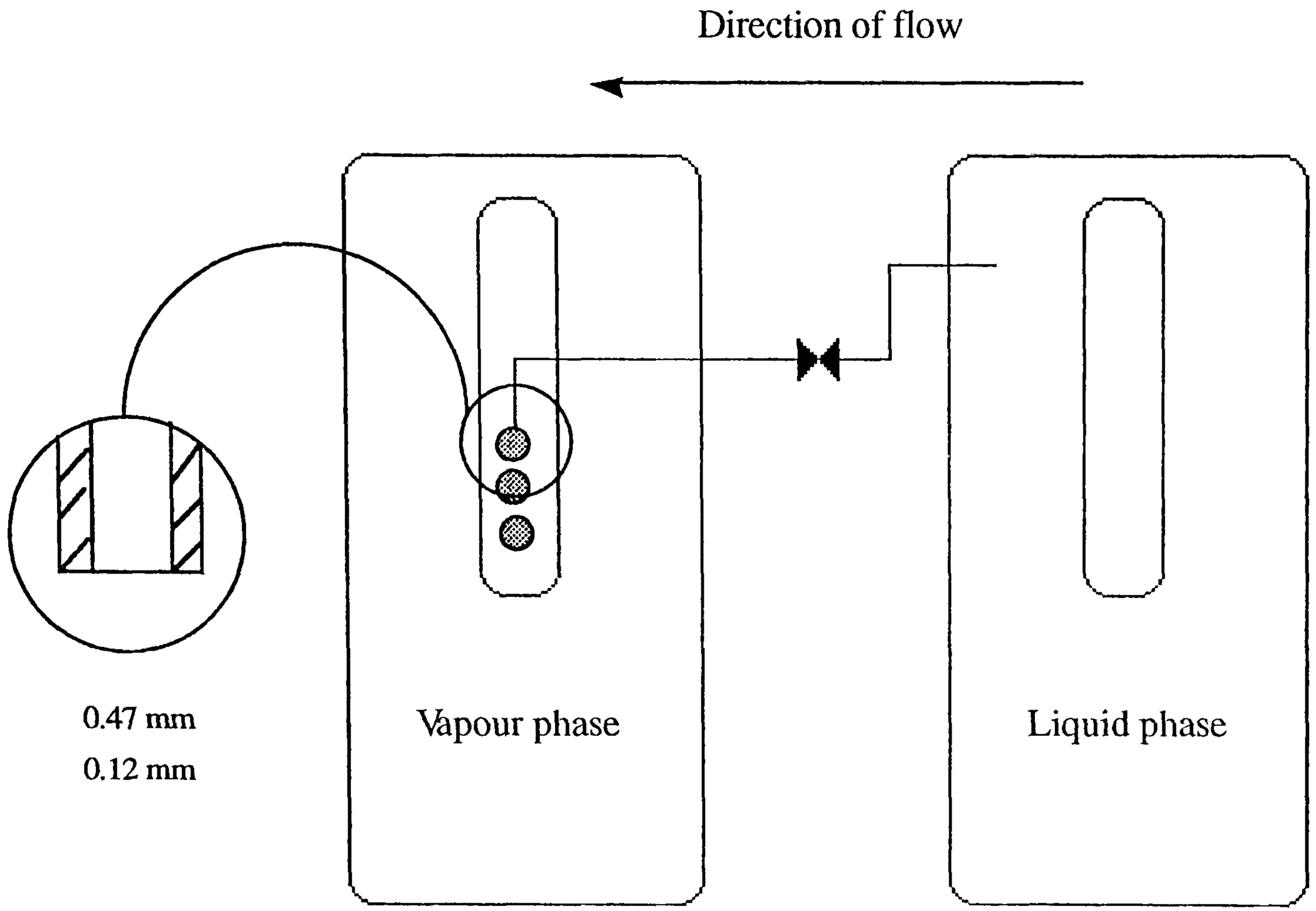

Figure 2.2.2.1 - Schematic of Pendant Drop in the V-L-E Facility.

tubing, pipework and isolation valve, that are introduced between two, 200 cc Ruska windowed VLE cells, in such a way that liquid phase could be introduced and dropped through its equilibrium vapour, via a small bore (0.47 mm external diameter, 0.12 mm internal diameter) stainless steel capillary tube. By extending the horizontal length of this pipe, a droplet of the liquid could be dropped from its distal tip. This event and the vapour-liquid interface boundary could then be video recorded and subsequently dimensioned using the VMS scalar unit for IFT calculations.

It was first decided to test the validity of the developed gas-liquid curvature (meniscus) method and the installed pendant drop method by measuring interfacial tension data for a known system for which values in the literature would be available. So that these measurement techniques could be applied with confidence to the injection processes for determining the interfacial tension. A binary mixture of methane-n-decane at 71.1°C was selected for this purpose. Stegemier[11] has measured IFT of this binary mixture at different isotherms by the pendant drop technique. The range of IFTs reported is from 0.002-10 dyne/cm. A detailed discussion of the experiment carried out is provided in Chapter 3. Interfacial tension measurements were carried out at various pressures below the dew point of 35.3 MPa. Both the pendant drop and gas-liquid meniscus methods were found to be in reasonable agreement with the data presented in the literature. Plots for comparison are presented in Chapter 3. This exercise proved that the meniscus method could also be applied in the V-L-E cell for condensate type fluids with near zero contact angles and at the same time validated the newly installed pendant drop device.

It was then decided to test both the methods for a real volatile oil system. This oil was flashed at several pressures below its bubble point of 34.92 MPa at 100°C. The IFTs were measured similar to the previous experiment at three different pressures and were compared with those predicted by the modified parachor method (no previous measurements were reported for this system). This comparison indicated that the values measured by the pendant drop were in reasonable agreement with those predicted whereas the meniscus values were significantly low. This is apparently due to the partial wetting ($90° > \text{contact angle} > 0°$) of the cell windows by the oil phase (also contact angle increases as IFT increases) as against the

condensate phase which exhibits a full wetting behaviour. Perfect wetting has been one of the assumption in developing the expression for the gas-liquid curvature technique. Another explanation for these differences is because of the presence of surface active agents such as asphaltenes in the oil systems. Hence it was decided to use the pendant drop method for these wetting type of fluids in future studies. A detailed description of this experiment involving the real volatile oil is furnished in Chapter 3.

2.3 : LASER LIGHT SCATTERING TECHNIQUE

Laser Light Scattering (LLS) technique is a fairly new technique especially suited for measuring IFTs near the critical point or at very high pressures. Recently Pearce and Haniff[6], measured the IFT of a methane-propane binary mixture by LLS technique in the range of 0.001 to 1 mN/m. Similarly the same authors[7], have measured IFT of a carbon dioxide system near the critical region in the range of 0.01 to 2 mN/m.

Measurement of surface properties such as the interfacial tension, and viscosity by the LLS technique is based on the thermally excited waves which exist at the interface separating the vapour and liquid phases. These waves are studied by measuring the statistical properties of the light scattered at the interface using the LLS technique. A laser beam is focused on to the surface of the liquid, such that both the reflected and scattered light are collected at a photo multiplier. A recently developed technique called the photon correlation spectroscopy is used to detect the signals. Here, the scattered and reflected lights are mixed to produce a beat frequency which can be measured using either a spectrum analyser to produce a power spectrum in the frequency domain or an auto-correlator to give a correlation function in the time domain. The correlation functions or power spectra thus provides the characteristics of the surface waves. In order to interpret the correlation functions one uses a dispersion equation which relates the properties of the fluid to a description of the wave propagations. Finally the correlation function is solved by a numerical procedure, since it does not have any analytical solutions, to give the values of interfacial tension and viscosity directly.

As far as the advantages of the LLS technique are concerned, it is a non - perturbative technique, needs only a small volume of liquid for measurements, and it is also capable of measuring interfacial tensions close to the critical point[6,7]. The LLS technique requires density data of equilibrated phases. Compositional data on the fluids tested are also needed if predictive methods are to be evaluated against experimental IFT data. The measurements of IFT by the LLS technique are required to be carried out in the specific apparatus where it is difficult to match the same compositions that exist in the equipment for conventional phase behaviour measurements. However, compared to the LLS technique, the set-up described in this thesis which directly provides all the density, compositional and volumetric data required for measurement and prediction of the interfacial tension is much more convenient and practical.

2.4 : CAPILLARY RISE TECHNIQUE

The capillary rise method is another technique employed for measuring interfacial tension which relies on the fundamentals of capillarity and uses some basic equations to measure the IFT from it. Weinaug and Katz[8], have measured the IFTs of the methane-propane binary mixture at various temperature and pressure conditions using the capillary rise method. This method basically involves the use of a fine capillary tube through which a liquid is allowed to rise, this particular rise is predominantly dependant upon the interfacial tension, or the adhesive and cohesive forces. The surface force of IFT is then balanced against the liquid head which enables to define the following relationship :

$$2\pi r\sigma = \pi r^2 h\,(\rho_l - \rho_v)g \qquad (2.4.1)$$

the quantity on the left hand side of the Eq. 2.4.1, is the force due to IFT and that on the right hand side is the force due to the liquid head which allows the calculation of IFT:

$$\sigma = \frac{g\Delta\rho hr}{2} \qquad (2.4.2)$$

Where,

σ = interfacial tension

r = radius of the capillary

h = the height of liquid column in the capillary

g = acceleration due to gravity and

ρ_l & ρ_v = liquid and vapour phase densities (mass)

In Eq. 2.4.1 & 2.4.2 the contact angle between the liquid and the tube wall is assumed to be zero.

Weinaug and Katz[8], used a double glass equilibrium cell to permit visual observation of the capillary rise of the liquid mixture. They used a glass capillary tube of less than 0.5 mm inside diameter which was mounted in the aforementioned cell with the help of two small springs. This capillary tube was calibrated in place with chemically pure grade benzene in order to include the correction for the rise of the liquid outside the tube in the computed radius of the capillary. The radius determined by this method is not the true radius but the pseudo radius containing a correction factor. The usual formula, corrected for the liquid in the meniscus and the density of the vapour, enables the computation of the IFT from the rise of the liquid in the capillary above that in the gauge :

$$\sigma = \frac{1}{2} rg(h + \frac{r}{3}) (\rho_l - \rho_v) \qquad (2.4.3)$$

here, r, is the pseudo radius of the tube, g, is the acceleration due to gravity and h, is the height of rise of the liquid column through the capillary.

Swartz[19], measured the interfacial tension of gas saturated crude oil by applying the technique of capillary rise. Measurements were performed at a temperature of 31°C ranging from 4 to 28 mN/m. Swartz[19], has justified the use of this method for its simplicity and sufficient accuracy.

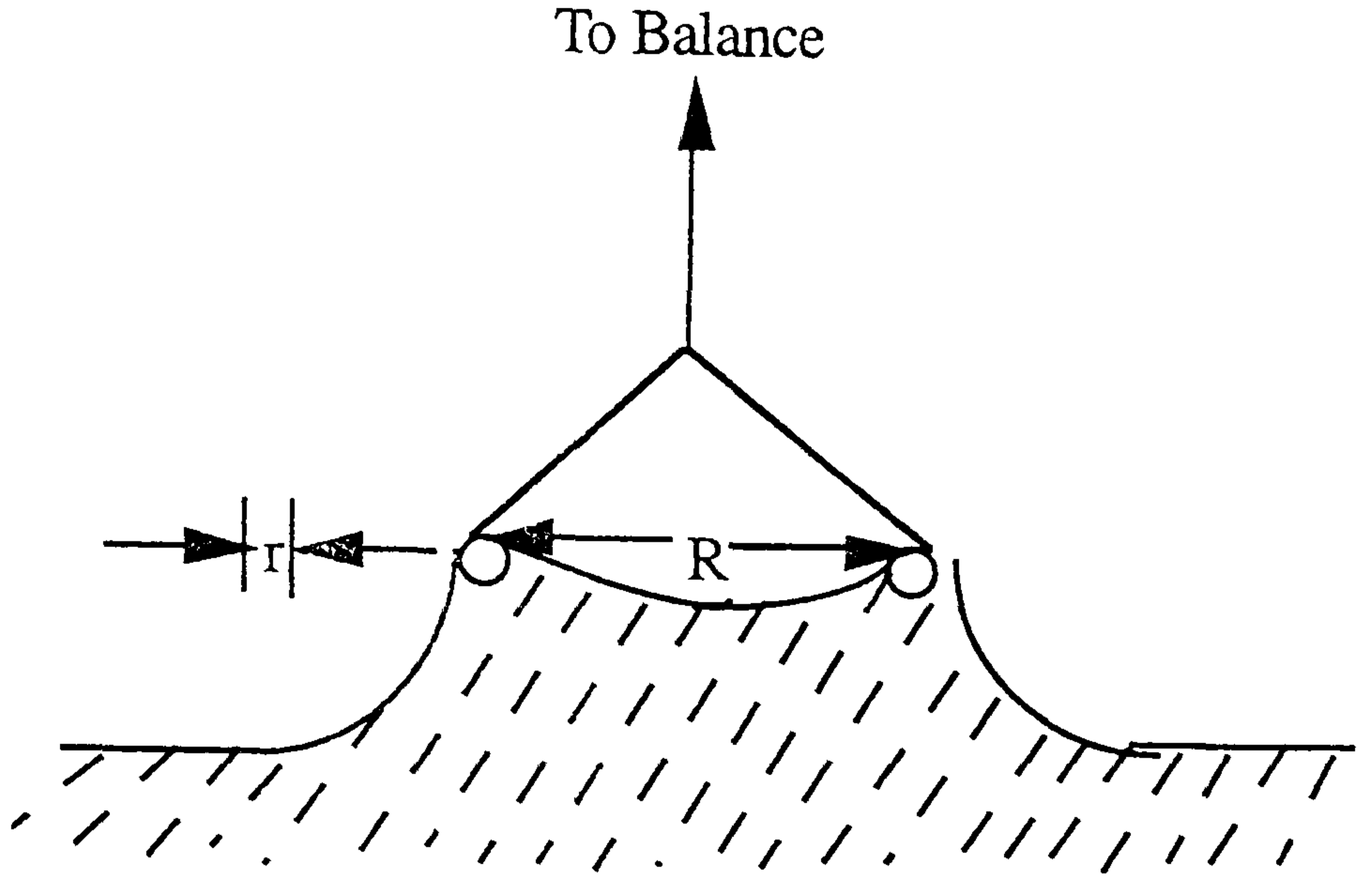

Figure 2.5.1 - The Ring Method (from Reference 20).

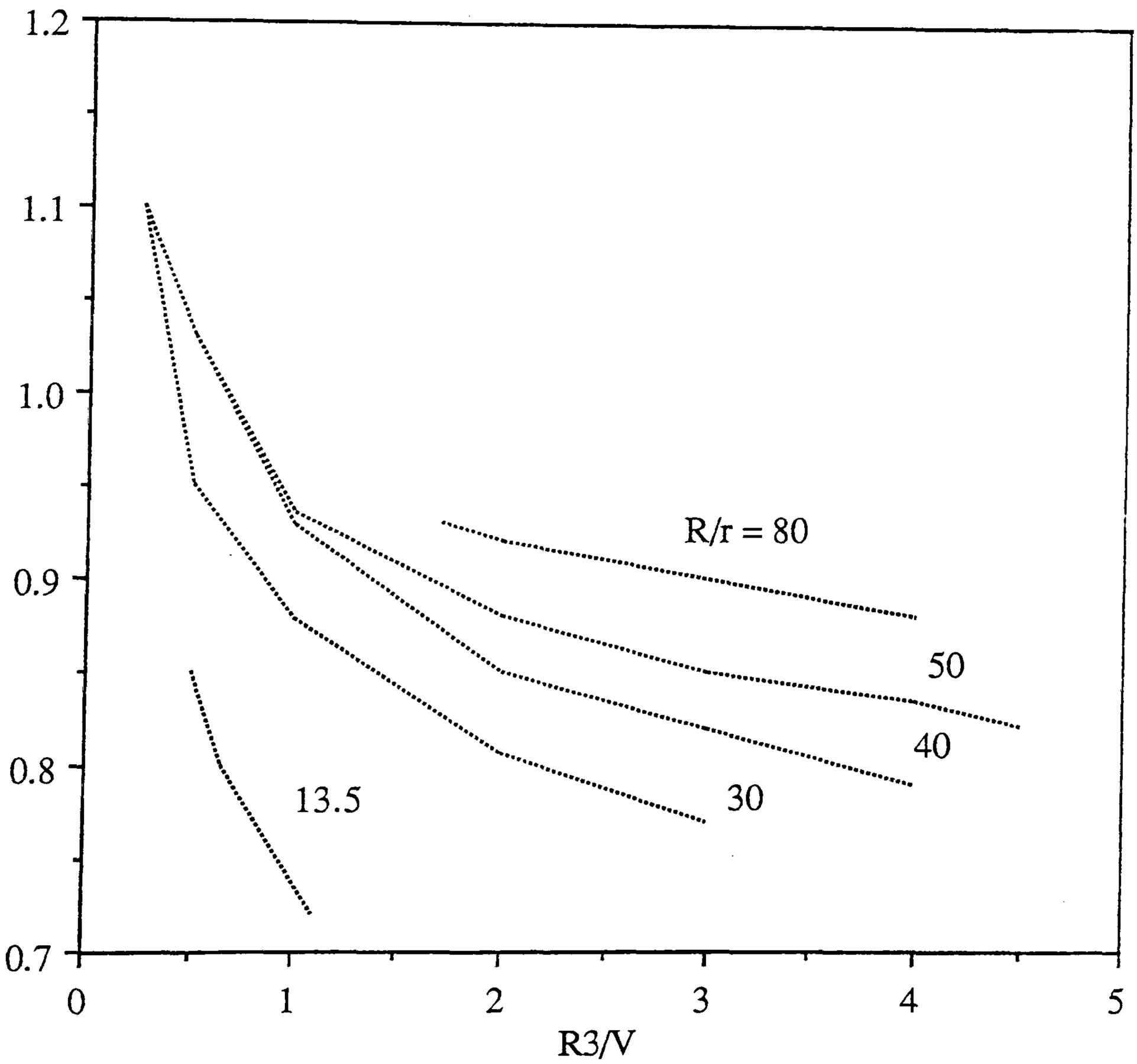

Figure 2.5.2 - Correction Factor Plots for the Ring Method (from Reference 21).

Although this method appears to be simple for application, its use at very high pressure conditions, where the IFT is small, is not practical as the rise of liquid in the capillary tube is very small.

2.5 : THE RING METHOD

The ring method is generally attributed to du Nouy[20]. The method belongs to the family of detachment methods, where a first approximation to the detachment force is given by the surface tension multiplied by the periphery of the surface detached. Thus, for a ring, as illustrated in Figure (2.5.1),

$$W_{tot} = W_{ring} + 4\pi R\sigma \qquad (2.5.1)$$

Harkins and Jordan[21] found, however, that Eq. 2.5.1 was generally in serious error and worked out an empirical correction factor, which is given by the following expression:

$$f = \left(\frac{\sigma}{p}\right) = f\left(\frac{R^3}{V}, \frac{R}{r}\right) \qquad (2.5.2)$$

where p denoted the "ideal" surface tension calculated from Eq. 2.5.1 and V is the meniscus volume. Figure (2.5.2) shows the correction factor plots for the ring method. Eq. 2.5.1 & 2.5.2 used in conjunction with Figure (2.5.2) can be used to determine the interfacial tension.

References

1) Andreas, J.M., Hauser, E.A., and Tucker, W.B.: "Boundary Tension by Pendant Drops", Presented at the Fiftieth Colloid Symposium, held at Cambridge, Massachusetts, (Jun., 1938).

2) Niederhauser, D.O. and Bartell, F.E.: "A Corrected Table for Calculation of Boundary Tensions by Pendant Drop Method", Research on Occurrence and

Recovery of Petroleum, A Contribution from API Research Project 27, pp. 114-146, (Mar., 1947).

3) Bashforth, F. and Adams, J.C.: "An Attempt to test the Theories of Capillary Action", University Press, Cambridge, England, (1883).

4) Pennington, B.F. and. Hough, E.W.: "Interfacial Tension of the Methane Normal Butane System", *Producers Monthly*, pp. 4, (Jul., 1965).

5) Hough, E.W. and Warren, H.G.: "Correlation of Interfacial Tension of Hydrocarbons", *Society of Petroleum Engineers Journal (SPEJ)*, pp. 345-349, (Dec., 1966).

6) Haniff, M.S. and Pearce, A.J.: "Measuring Interfacial Tension in a Methane - Propane Gas - Condensate System Using a Laser Light Scattering Technique", SPE 19025, (1988).

7) Pearce, A.J. and Haniff, M.S.: "Light Scattering Experiments from a Carbon Dioxide Surface Near the Critical Point : A Data Reduction Procedure", *J. Col. & Int. Sci.*, Vol. 119, No. 2, pp. 315-325, (Oct., 1987).

8) Weinaug, C.F. and Katz, D.L.: "Surface Tension of Methane - Propane Mixtures", *Industrial & Engineering Chemistry (I & EC)*, Vol. 35, No. 2, pp. 239-247, (Feb., 1943).

9) Stegemeier, G.L. and Hough, E.W.: "Interfacial Tension of the Methane Normal Pentane System", *Producers Monthly*, pp. 6-9, (Nov., 1961).

10) Brauer, E.B. and Hough, E.W.: "Interfacial Tension of the Normal Butane Carbon Dioxide System", *Producers Monthly*, pp. 13, (Aug., 1965).

11) Stegemeier, G.L., Pennington, B.F., Brauer, E.B. and Hough, E.W.: "Interfacial Tension of the Methane - Normal Decane System", *Society of Petroleum Engineers Journal (SPEJ)*, pp. 257-260, (Sep., 1980).

12) Hough, E.W., Rzasa, M.J. and Wood, B.B.: "Interfacial Tensions At Reservoir Pressures and Temperatures; Apparatus and the Water - Methane System", *Petroleum Transactions of AIME*, Vol. 192, pp. 58-60, (1951).

13) Jennings, H.Y. Jr.: "Apparatus for Measuring Very Low Interfacial Tensions", *The Review of Scientific Instruments*, Vol. 28, No. 10, pp. 774-777, (Oct., 1957).

14) Andreas, J.M., Hauser, E.A. and Tucker, W.B.: "Boundary Tension by Pendant Drops", Presented at the Fiftieth Colloid Symposium, held at Cambridge, Massachusetts, pp. 9-11, (Jun., 1938).

15) Nagarajan, N. and Robinson, R.L.Jr.: "Equilibrium Phase Compositions, Phase Densities, and Interfacial Tensions for CO_2 + Hydrocarbon Systems. 3. CO_2 + Cyclohexane. 4. CO_2 + Benzene", *Journal of Chemical and Engineering Data*, Vol. 32, No.3, pp. 369-371, (1987).

16) Nagarajan, N. and Robinson, R.L.Jr.: "Equilibrium Phase Compositions, Phase Densities, and Interfacial Tensions for CO_2 + Hydrocarbon Systems. 2. CO_2 + n - Decane", *Journal of Chemical and Engineering Data*, Vol. 31, No.2, pp. 168-171, (1986).

17) Hsu, Jack, J.C, Nagarajan, N. and Robinson, R.L.Jr.: "Equilibrium Phase Compositions, Phase Densities, and Interfacial Tensions for CO_2 + Hydrocarbon Systems. 1. CO_2 + n - Butane", *Journal of Chemical and Engineering Data*, Vol. 30, No.4, pp. 485-491, (1985).

18) Gasem, K.A.M., Dickson, K.B., Dulcamara, P.B., Nagarajan, N. and Robinson, R.L.Jr.: "Equilibrium Phase Compositions, Phase Densities, and Interfacial Tensions for CO_2 + Hydrocarbon Systems. 5. CO_2 + n - Tetradecane", *Journal of Chemical and Engineering Data*, Vol. 34, No.2, pp. 191-195, (1989).

19) Swartz, C.A.: "The Variation in the Surface Tension of Gas Saturated Petroleum With Pressure of Saturation", *Physics*, Vol. 1, pp.245-253, (Oct., 1931).

20) du Nouy, P. Lecomte, *J. Gen. Physiol.*, 1, 521 (1919).

21) Harkins, W.D. and Jordan, H.F.: "A Method for the Determination of Surface Tension and Interfacial Tension from the Maximum Pull on a Ring", *J. Am. Chem. Soc.*, 52, 1751, (1930).

CHAPTER 3 : DEVELOPMENT OF A NOVEL TECHNIQUE FOR MEASURING INTERFACIAL TENSION OF GAS CONDENSATE SYSTEMS

3.1 : INTRODUCTION

As discussed earlier in Section 2.2.1, a narrow spout was inserted in the gas condensate port at the neck to form liquid droplets by pumping condensate through the analysis loop. The droplets were observed through the window, magnified and recorded on video. A number of fluids for which literature IFT data were available, were tested. The measured results agreed with the literature data for fluids with interfacial tension higher than about 1mN/m. The spout diameter was however, too large to yield properly shaped droplets at low IFT. Although the unit could be improved by inserting a thin wire in the spout, to form smaller droplets, the method was abandoned in favour of the gas-liquid meniscus technique at low IFT conditions, which is discussed in detail in this chapter.

The gas - liquid interface, as seen on a monitor, during a pressure depletion study of a gas condensate is presented in Figures (3.1.1) to (3.1.4). The thick black band running vertically through the window is the stirrer shaft which is used to enhance the achievement of equilibrium between the two phases. The clear area in the upper half of the window is the gas phase and the hazy area in the lower part is the liquid phase. The horizontal black band in the centre of the window is the gas - liquid meniscus as seen on the monitor. Note the changes in the gas - liquid interface thickness as the pressure is reduced below the dew - point. As pressure declines during the process of depletion for a retrograde condensation, compositional changes in the gas and liquid phases give rise to increase in interfacial tension between the two phases. At pressures close to the dew - point, Figure (3.1.1), the interface is thin and flat. As pressure falls further below the dew - point, Figure (3.1.2), and Figure (3.1.3), the interface curvature steadily increases as shown by thickening of the band, until at pressures much below the dew - point, Figure (3.1.4), where the interface exhibits a considerable amount of curvature.

Figure 3.1.1 - Gas Liquid Interface Below the Dew Point.

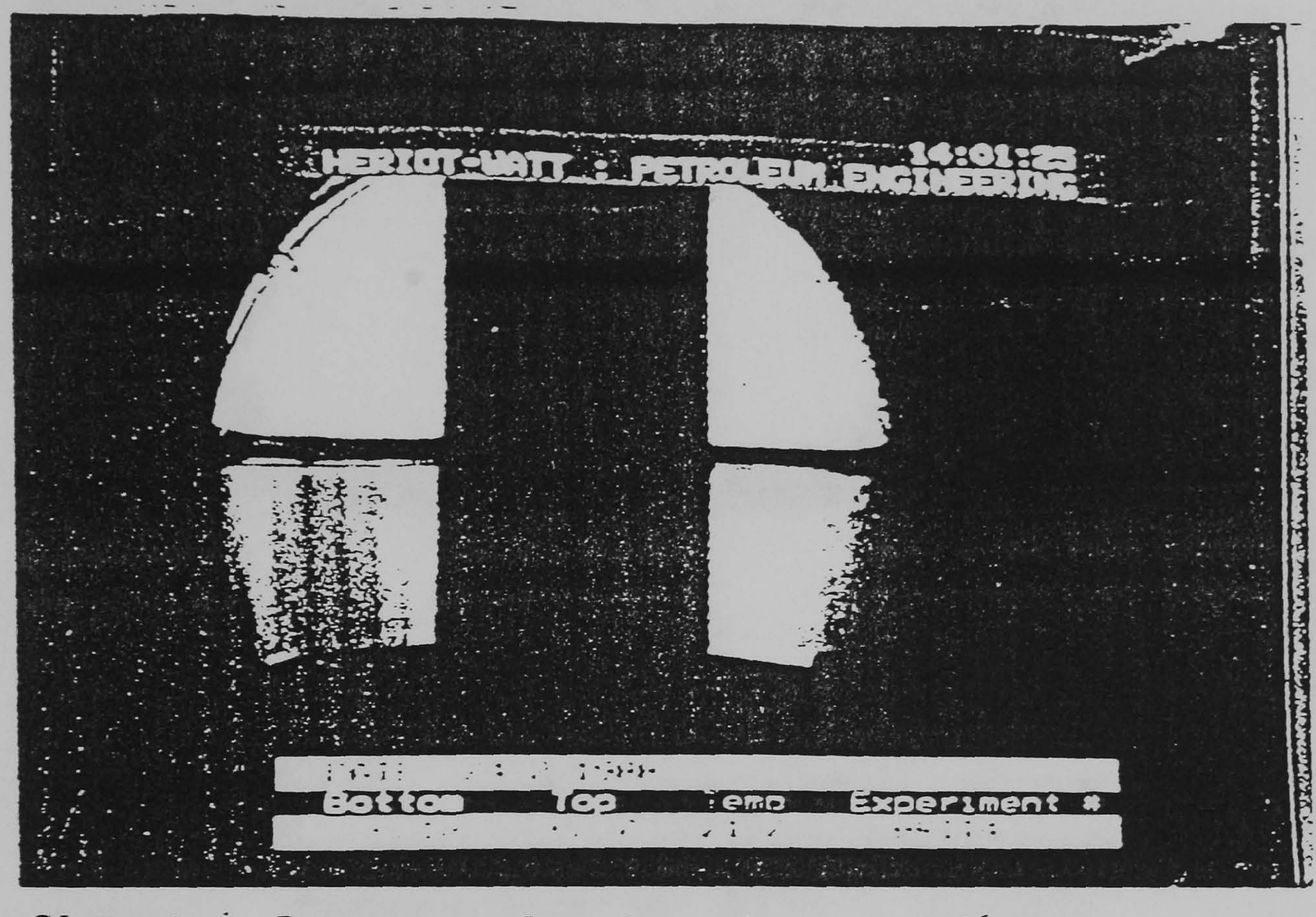

Plate 1 Pressure below dew-point = 0.56MPa
Interface thickness = 0.08cm

Figure 3.1.2 - Gas Liquid Interface Below the Dew Point.

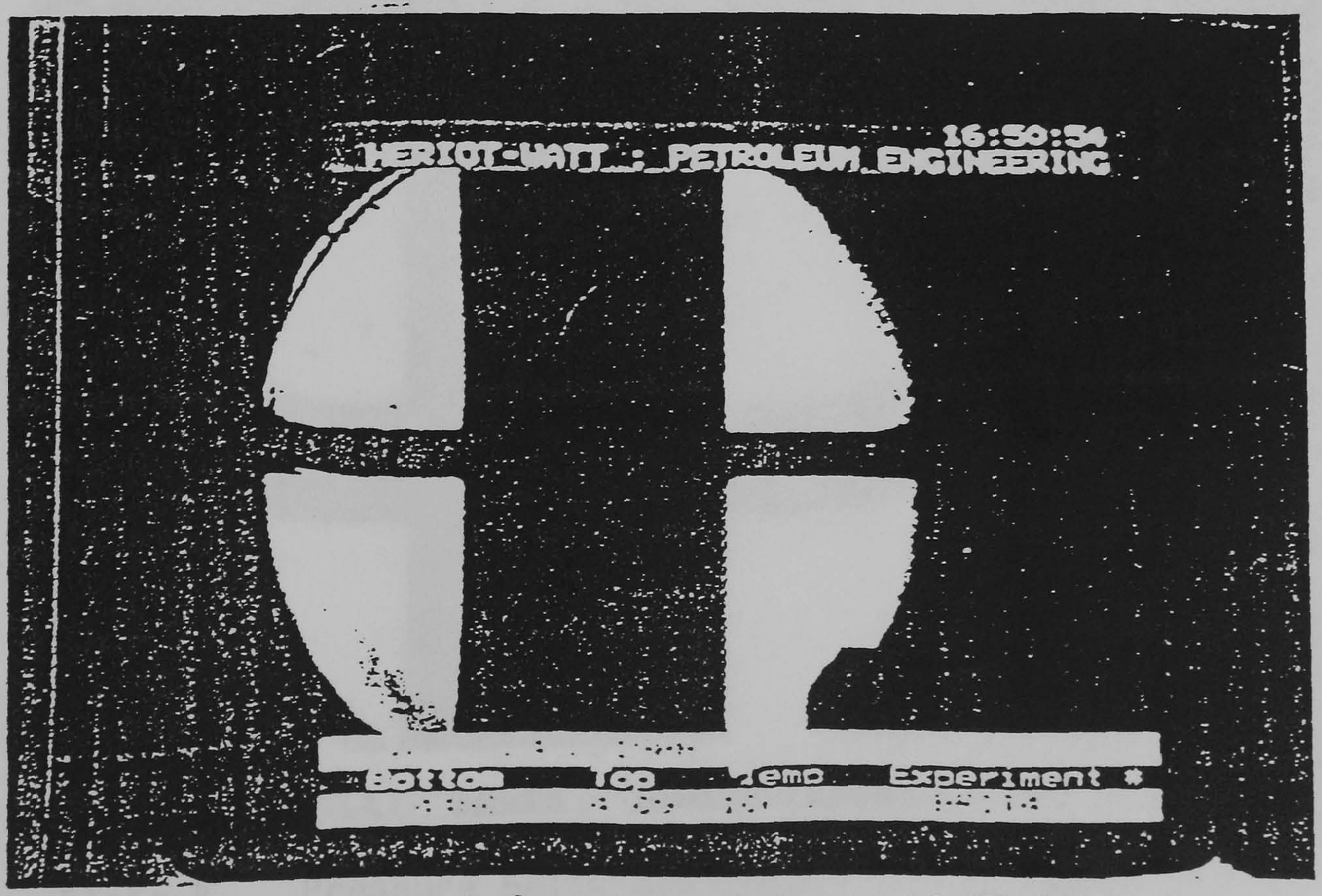

Plate 2 Pressure below dew-point = 12.55MPa
Interface thickness = 0.21cm

Figure 3.1.3 - Gas Liquid Interface Below the Dew Point.

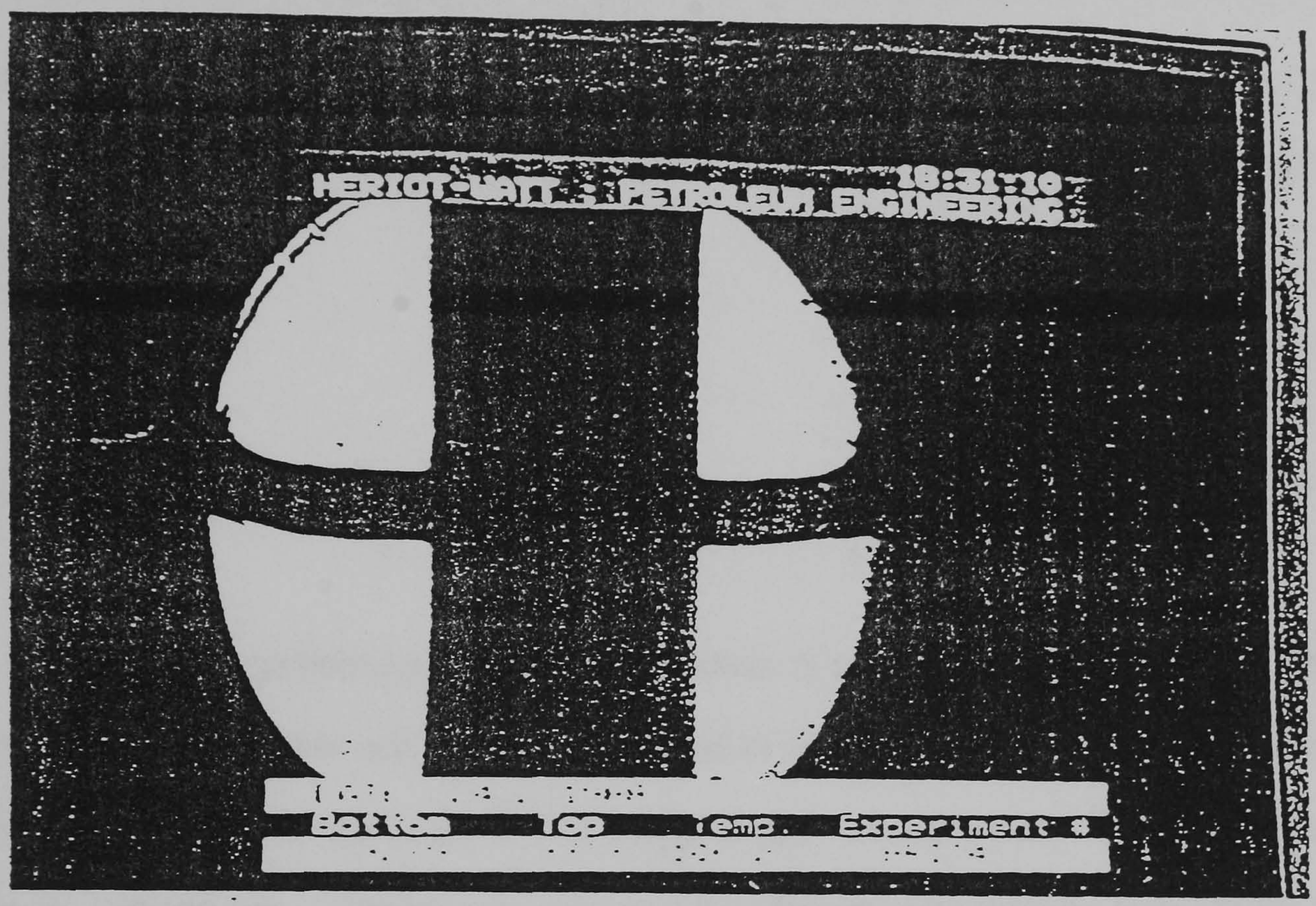

Plate 3 Pressure below dew-point = 20.83MPa
Interface thickness = 0.31cm

Figure 3.1.4 - Gas Liquid Interface Below the Dew Point.

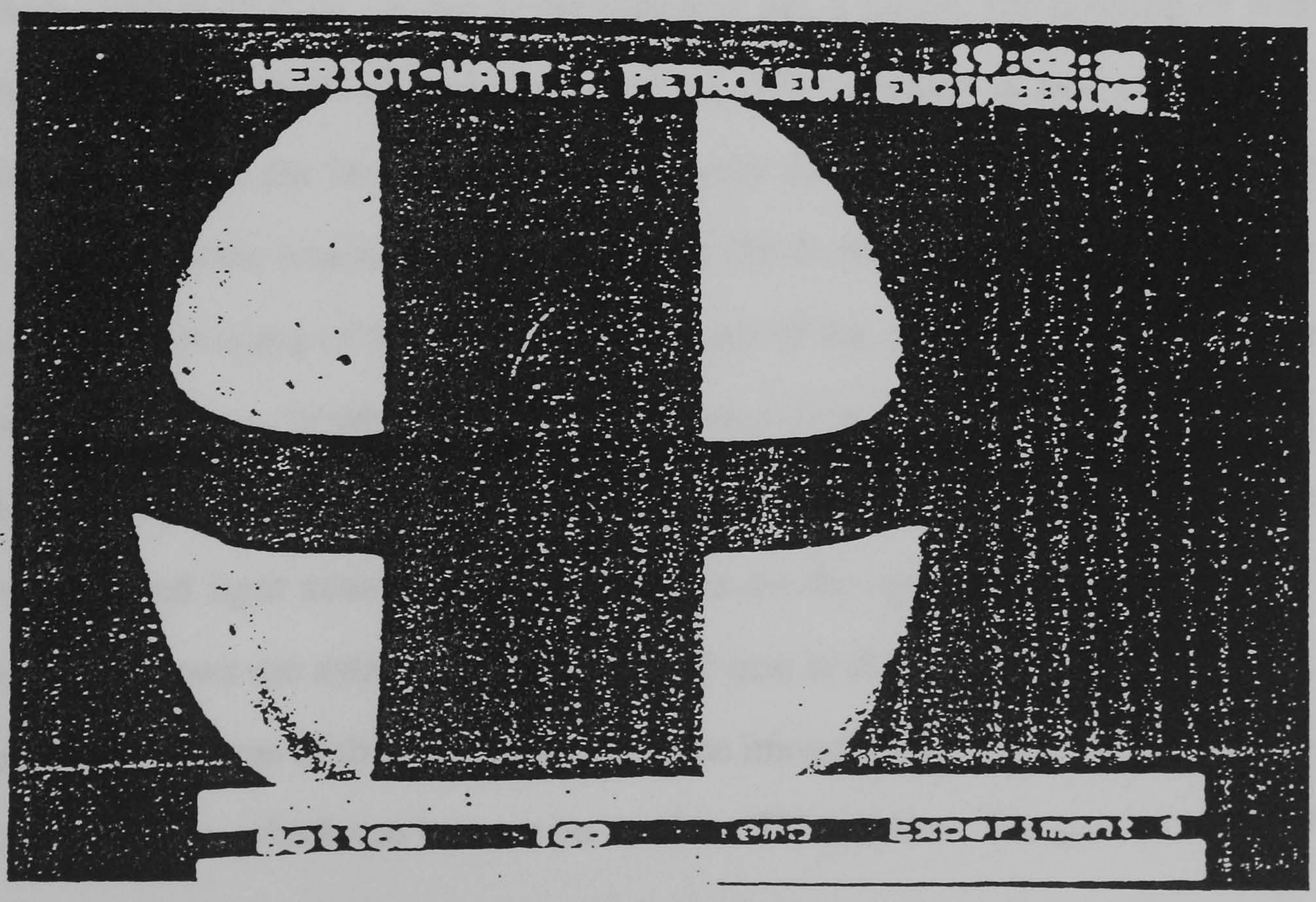

Plate 4 Pressure below dew-point = 21.72MPa
Interface thickness = 0.40cm

The above observations led to the development of a novel technique for determining the interfacial tension of gas condensate fluids tested in the gas condensate facility. It was also attempted to employ this technique in the vapour-liquid equilibrium (V-L-E) facility for volatile and black oils, but, it was unsuccessful due to the contact angle considerations (Section 2.2.2). However, the method was successfully applied in the V-L-E facility for gas condensate type fluids (Section 3.5.2). Interfacial tension data measured on various binary and multicomponent synthetic hydrocarbon mixtures and real reservoir fluids is presented in this chapter.

3.2 : EXPERIMENTAL SET - UP FOR GAS CONDENSATE CELL

The gas - condensate equilibrium cell used in the study is manufactured by A.C.B. of France under license from Elf. This cell has been modified in certain areas from its original set - up and made more flexible to use in the P-V-T study of gas - condensates. The equipment is a typical large volume gas - condensate cell, and equipment with similar features by other manufacturers is also available for which the proposed methods can be applied.

The cell consists of a large upper chamber and a small lower chamber connected together by a narrow neck, Figure (3.2.1). In the upper chamber lies a piston, the position of which is controlled by pumping mercury into the top of the cell. Mercury is also pumped into the lower chamber through the bottom of the cell, thereby forming a 'liquid piston' in the lower chamber. The volume available to hydrocarbon fluids within the cell can therefore be controlled by the pumping of the mercury into or out of the cell. The cell is housed into a thermo-static enclosure, in which the air can be cooled or heated. Visual information is achieved by means of two sapphire windows mounted opposite each other in the neck of the vessel with a fitted light source and a TV camera on the opposite sides, Figure (3.2.1). Although the windows are small, approximately 10 mm in diameter, visual information can still be achieved by virtue of the magnification of the image which is approximately 32 times the actual dimensions, which can be seen on a colour TV monitor. The gas - condensate (or

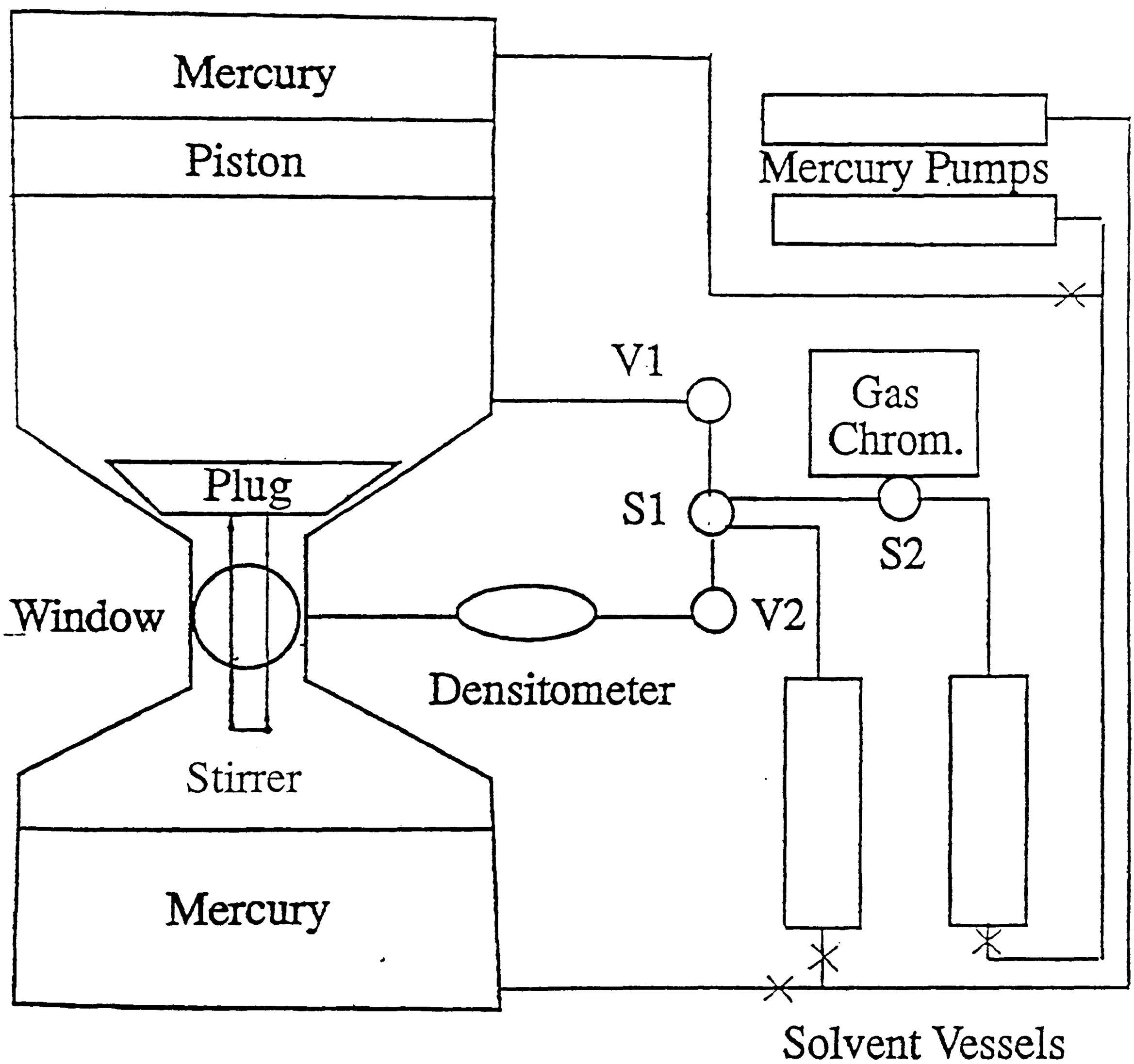

Figure 3.2.1 - Gas-Condensate Equilibrium Cell Set-Up.

condensate - mercury) interface can be located in the window by adding and withdrawing equal volumes of mercury to the top and bottom of the cell (or vice versa) and moving the cell hydrocarbon contents up and down at constant pressure and volume. The total and phase volumes are determined by monitoring the volume of mercury pumped. The actual side views and the front views of the gas - liquid interface are shown in Figure (3.2.3) and Figure (3.2.4) and Figure (3.2.2), show the cross section of the view of the sapphire window. Located within the neck is a stirring mechanism which terminates in the upper chamber with a paddle to speed up the achievement of equilibrium between the phases. The unique feature of this cell is the stirrer shaft which is about 2.5 mm in diameter and can be lowered or raised as required in order to isolate the upper and lower chambers by plugging the neck top with a Teflon plug which is mounted on the stirrer below the paddle in the upper chamber. The cell has two inlet/outlet ports located in the upper chamber and in the neck as the same levels as the window. An analysis loop connects the two ports and hence the cell contents can flow through it when the neck is plugged and mercury is pumped into or out of the cell. After achieving equilibrium between gas and condensate phases, with the interface and the window, the neck is plugged and the system pressure is slightly raised to ensure that both the retrograde gas and condensate remains as a single phase while flowing through the analysis loop.

The analysis loop consists of three multiport valves and a densitometer (Figure (3.2.1)) and is connected to the cell via two isolating valves located in the cell wall. The total volume of the sampling loop is about 4 cc and is considered to be the part of the cell volume when the isolating valves are opened. The loop is entirely within the oven and is kept at the test temperature with a maximum working pressure of 41.45 MPa limited by the high pressure Paar oscillating densitometer. Valves V_1 and V_2 (Figure (3.2.1)) are used to provide cleaning, evacuation and, feeding of the cell as well as conventional sampling. Sample capturing for direct compositional analysis is achieved through a two position six - port valve S_1 for both gases and liquids by the solvent pinch technique. The details of the sampling technique are voluminous and can be found elsewhere[1,2]. Figure (3.2.5) through (3.2.9) show the external view of the cell showing overall details of the gas - condensate equilibrium cell facility.

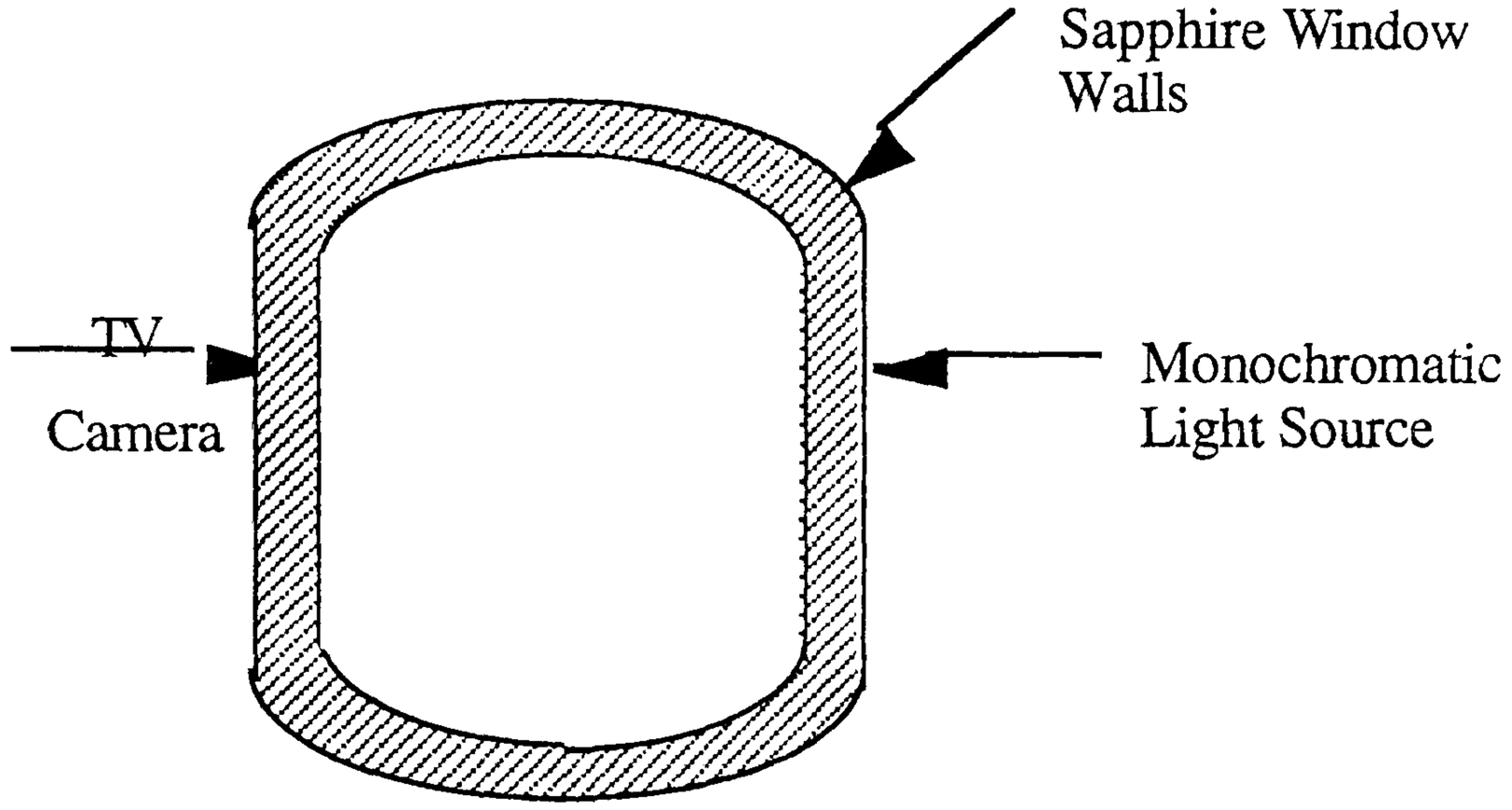

Figure 3.2.2 - Cross Sectional Top View of the Sapphir e Window.

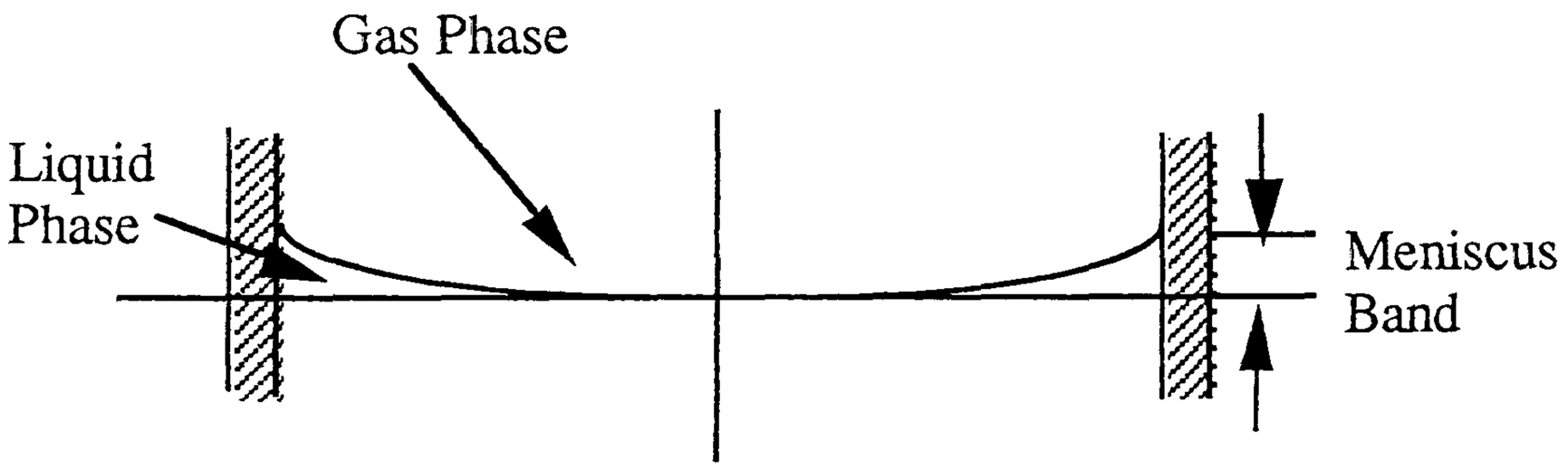

Figure 3.2.3 - Side View of the Gas-Liquid Interface.

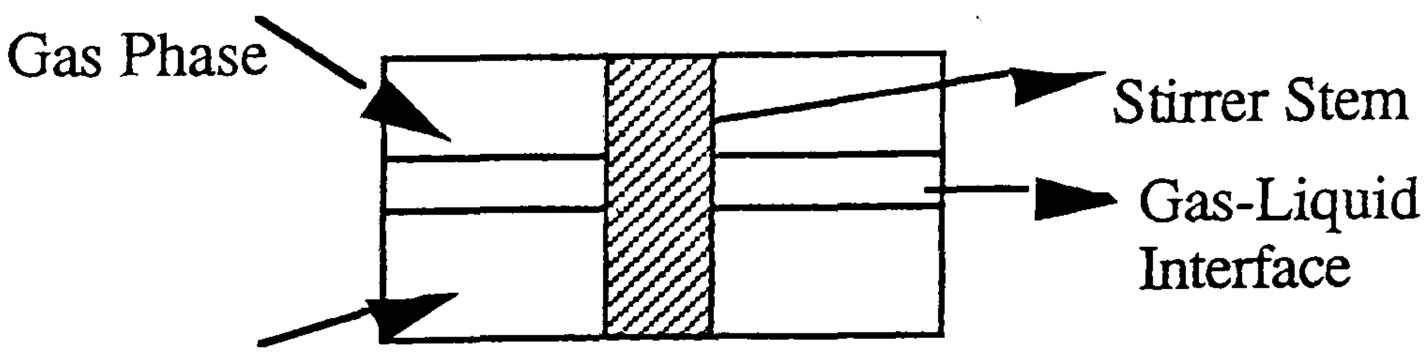

Figure 3.2.4 - Front View of the Gas-Liquid Interface (as seen on the TV monitor).

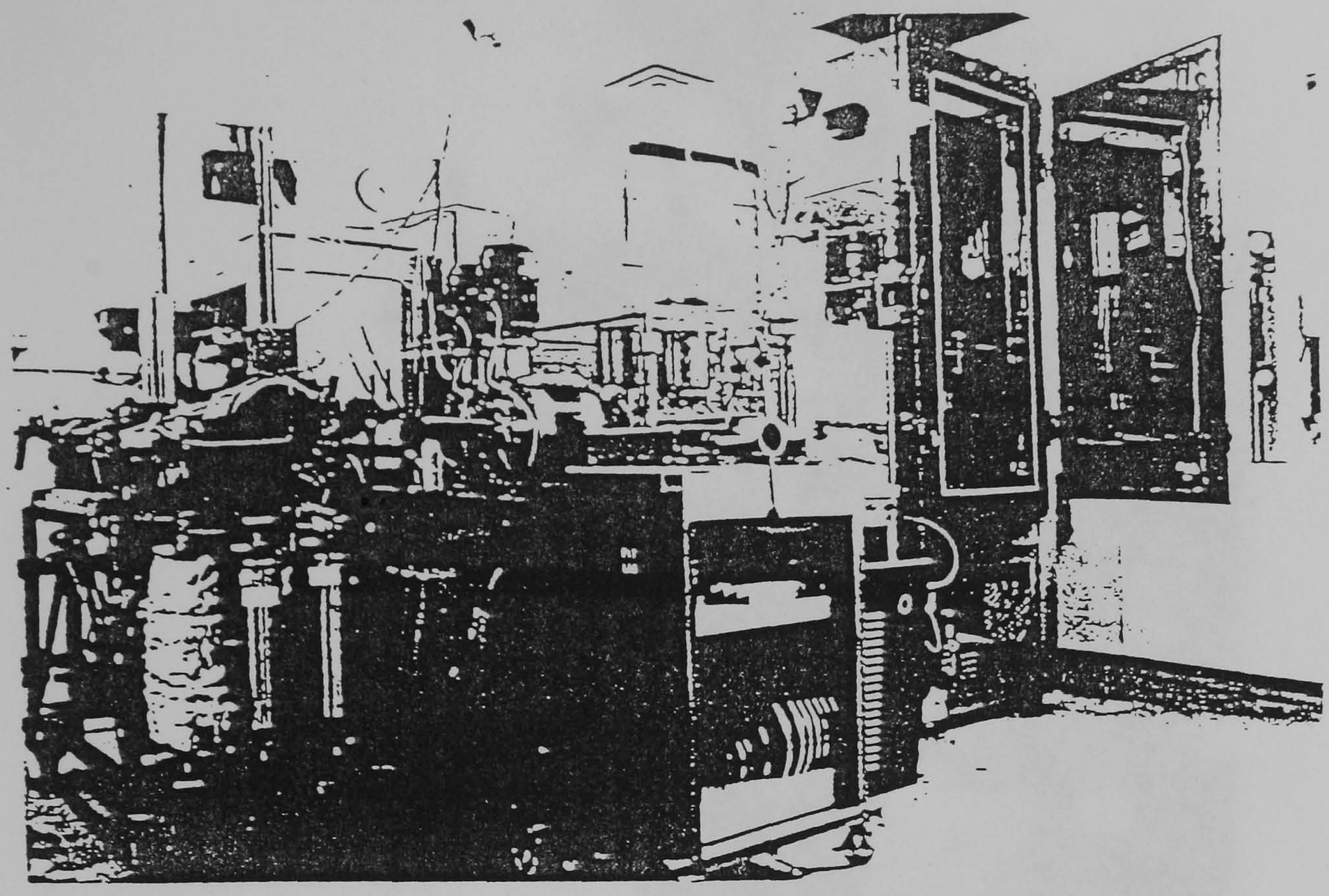

Figure 3.2.5 - General View of the Condensate Facility.

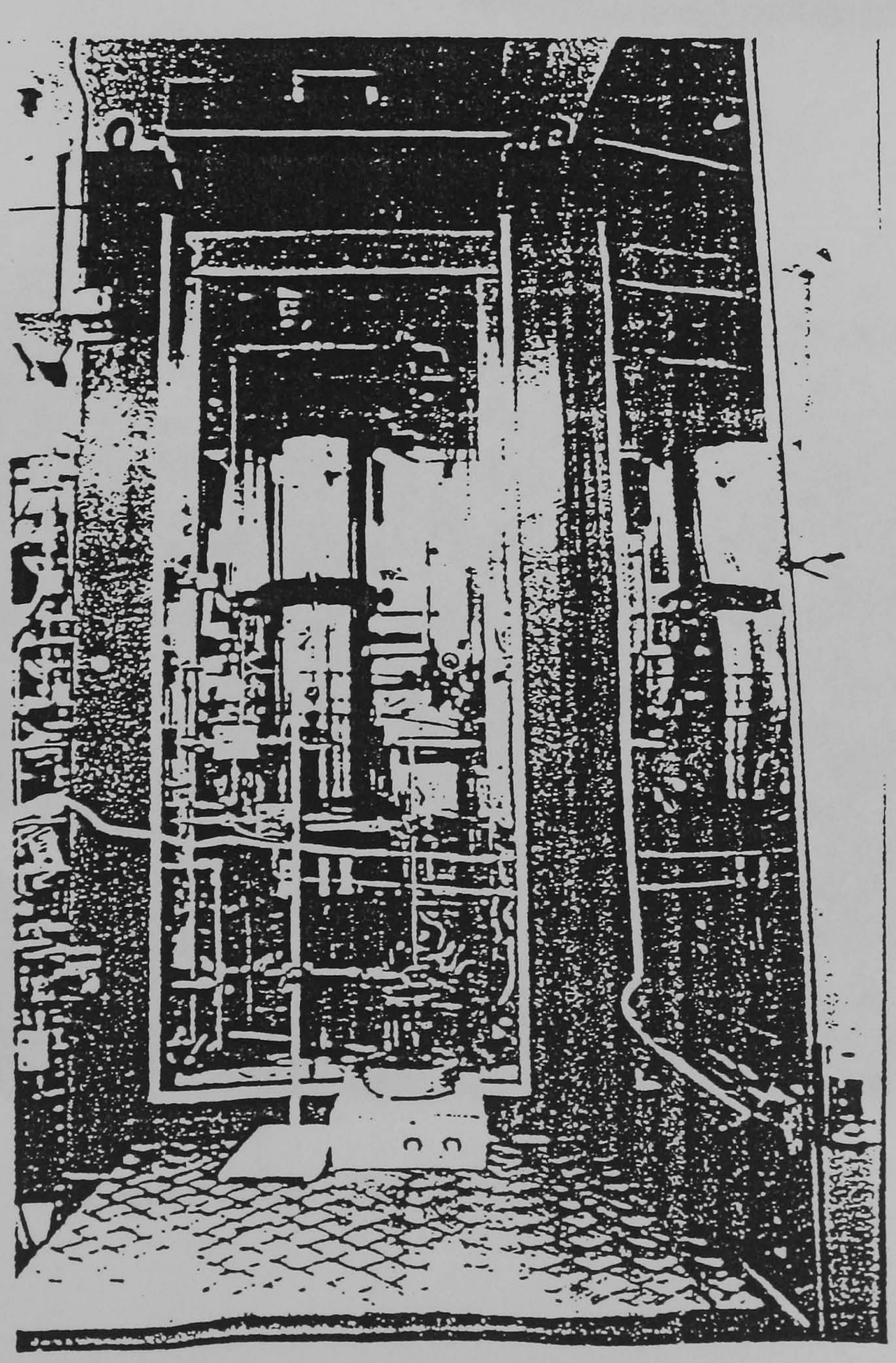

ate Cell in its Enclosure.

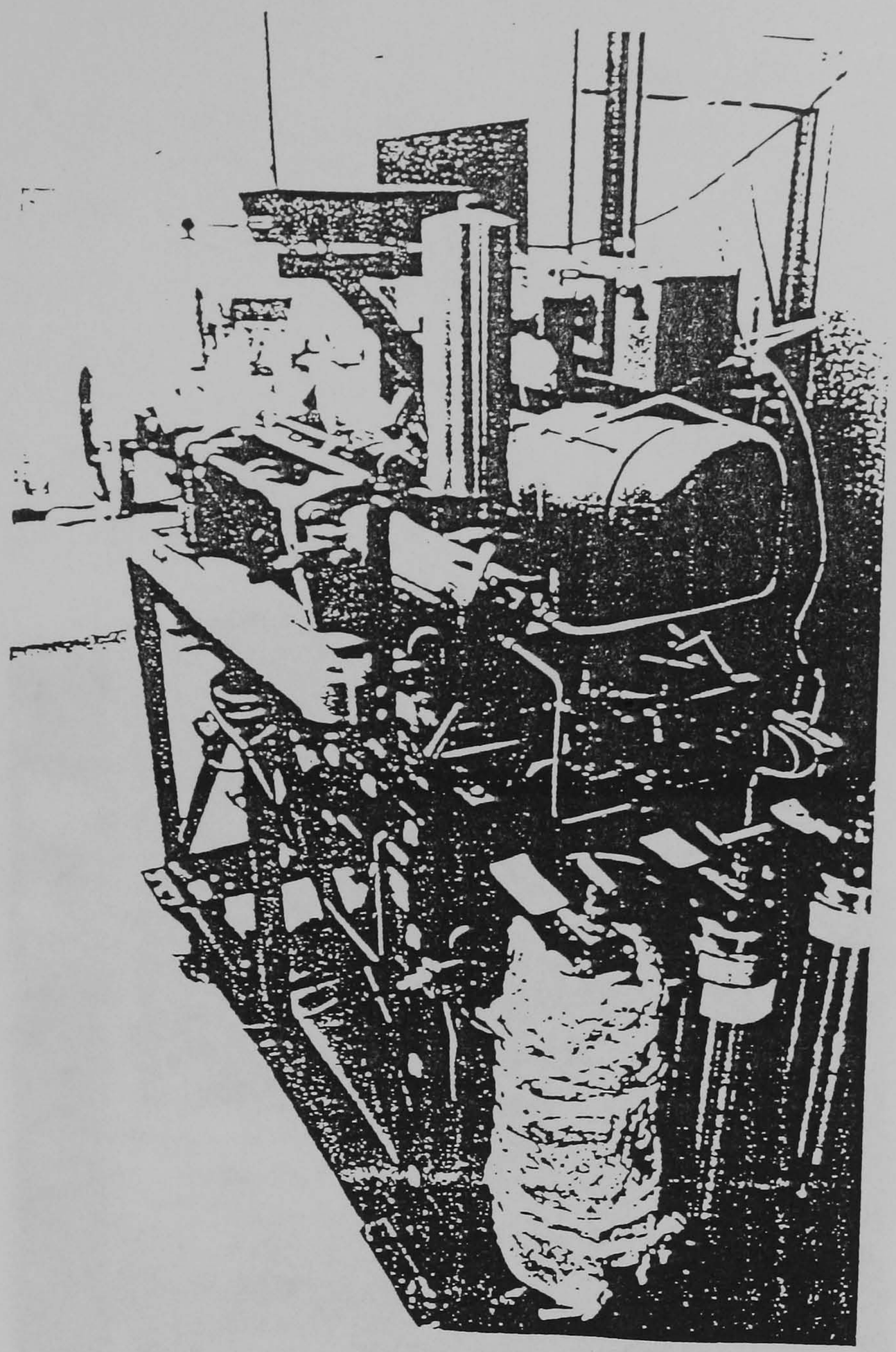

Figure 3.2.7 - The Pumping Rig.

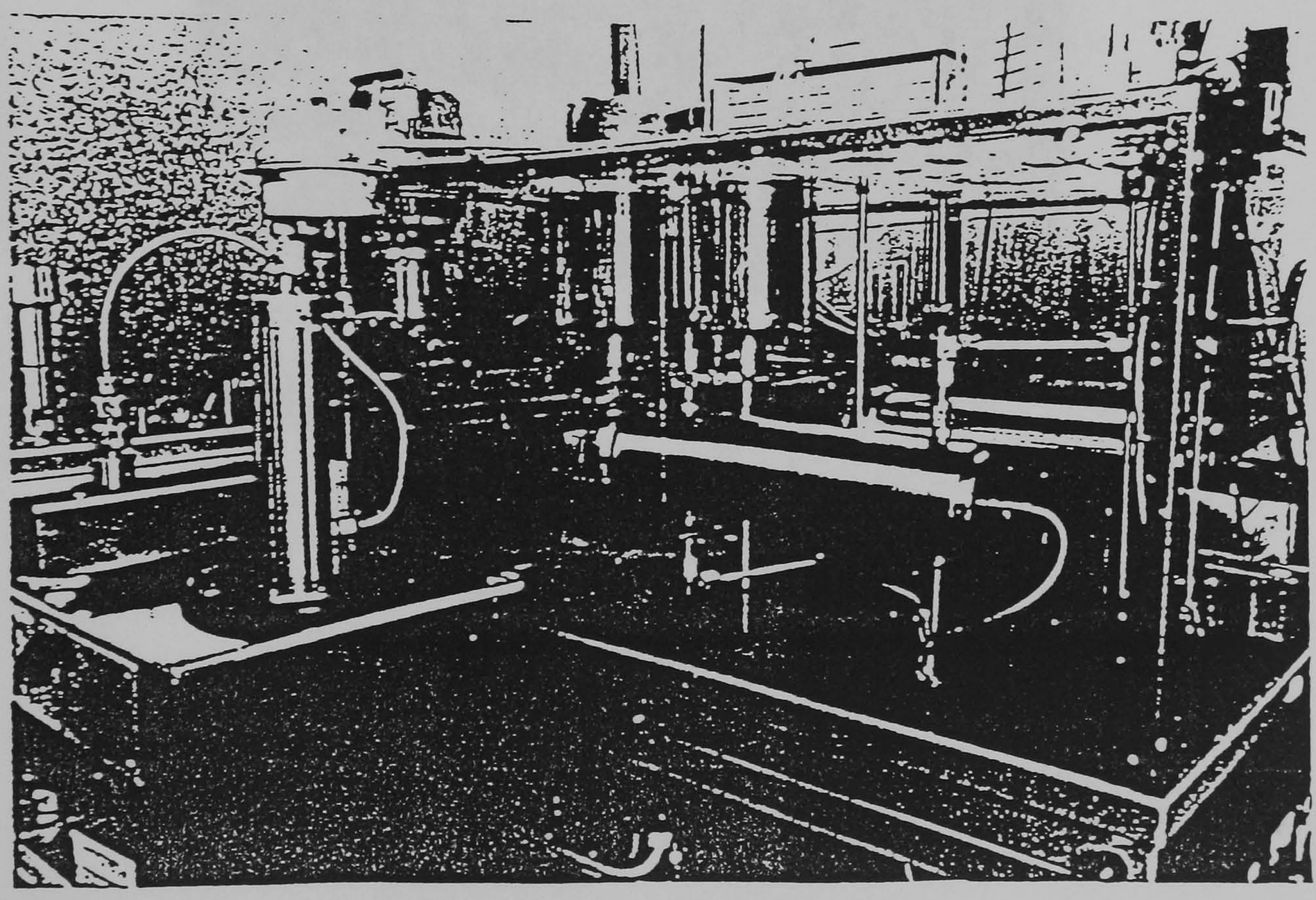

Figure 3.2.8 - The ROP Mercury Pumps.

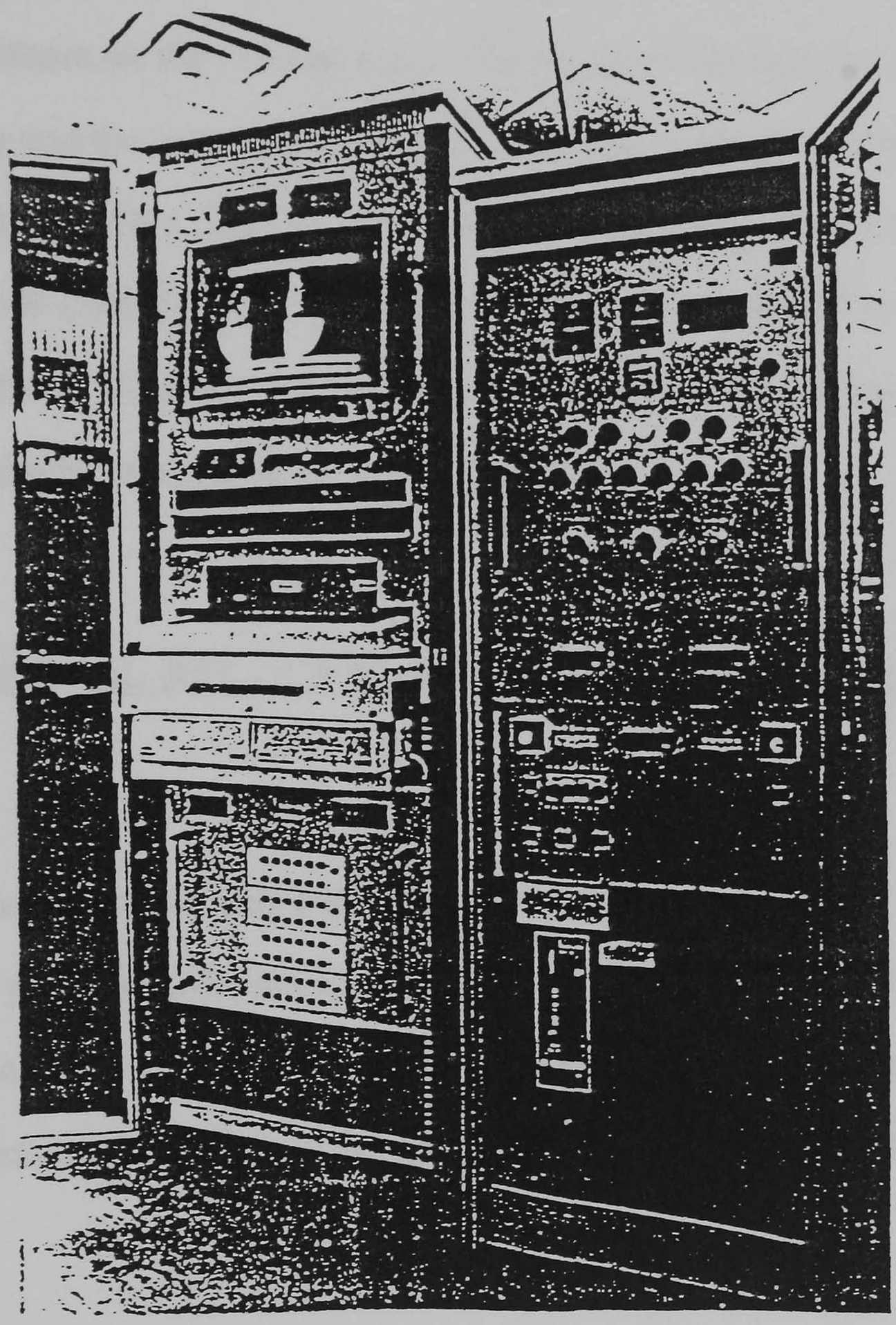

Figure 3.2.9 - Instrumentation Cabinets.

An Olympus High Precision Video Scaling Unit (VMS300) is used to assist with the measurement of meniscus width (film height) for use in the calculation of IFT. This allows two horizontal and two vertical lines to be superimposed onto either a TV monitor or directly recorded onto video cassette. The unit has proved to be a quick and accurate method for measurement of the meniscus width. The unit can measure to ± 0.011mm on the horizontal scale and to ± 0.008mm on the vertical scale. The image of the meniscus is magnified by 32 times its actual size and the actual diameter of the stirrer (2.5mm) is used to calibrate the scalar unit. A Time Base Corrector (TBC) is also used to stabilise and synchronise the signal from the Video Cassette Recorder (VCR) through the VMS300 scaling unit to improve the quality of the image obtained. Readings are taken for each pressure point below the dew - point where the IFT measurements are desired.

3.3 : EXPERIMENTAL SET - UP FOR VAPOUR-LIQUID-EQUILIBRIUM (V-L-E) APPARATUS

The V-L-E apparatus is a two-cell PVT rig which is used to study the phase behaviour of black and volatile oils, experimentally, in simulated gas injection processes. Forward and backward contact experiments can be performed to investigate the leading and trailing edge, respectively, of a gas displacement. At present the V-L-E experimental facility is configured to perform :

1) Phase volume measurement
2) Phase density measurement
3) Phase compositional analysis and
4) Interfacial tension (IFT) measurements using the pendant drop and meniscus techniques.

More conventional PVT tests may of course be performed; saturation pressure determination, gas oil ratio (GOR) measurement and oil formation volume factor estimation, for instance. Experimental operating limits for temperature and pressure are, at present, 100°C and 34.6 MPa respectively.

The schematic of the V-L-E experimental facility is shown in Figure 3.3.1. Two, 200cc Ruska VLE windowed cells mounted within a thermostatically controlled airbath, controllable to within ± 0.1°C, are employed to contain the experimental fluids. Each VLE cell is fitted, front and rear with high pressure glass windows, to assist in phase volume, liquid droplet and meniscus (for IFT) measurements. Viewing the vapour/liquid interface is further aided by lighting from the rear of the cells, while viewing from the front with a magnifying boroscope. The event of falling of a liquid droplet through its equilibrium vapour is recorded on a video cassette along with the gas-liquid meniscus for IFT calculations. The droplet and the meniscus are later dimensioned by the previously mentioned VMS300 scalar unit. The image of a droplet is magnified by 53 times of its actual size. The external diameter of the pendant drop spout (0.47mm) is used to calibrate the scalar unit.

Once the interface has been identified the distance from the interface to the cell top can be measured by a linear transducer, mounted on the boroscope traversing stage. The measured distance is then translated to volume, each cell having a slightly different calibration conversion factor. To accelerate equilibrium after, say injecting a gas into an oil, or, dropping the system pressure, to determine the saturation pressure of a fluid contained within one of the VLE cells, they are mounted on a plate which can be rotated. This also allows for the total inversion of the cells for phase volume measurement, where large vapour volumes are involved. Communication between the V-L-E cells is by pipework, which has been kept as short as possible, to minimise phase disruption when filling the route. Incorporated within the pipework is a calibrated oscillating density cell (Anton Paar) and an high pressure liquid chromatography (HPLC) sampling valve (Valco). The density cell, as well as giving measurements of phase densities also indicates when the phase is homogeneous, by displaying a steady reading over time. When the sample is homogeneous it may be analysed compositionally. Each analysis only removes approximately 0.2cc of fluid. By operating the HPLC valve the sample fluid is introduced, as a slug, into a mobile solvent transport column. After a pre-set time the centre of the fluid slug will be present inside a second HPLC valve fitted with a 0.6microlitre internal valve capacity. When operated this valve injects that fraction of the fluid directly into the column of an Hewlett Packard 5880A gas chromatograph

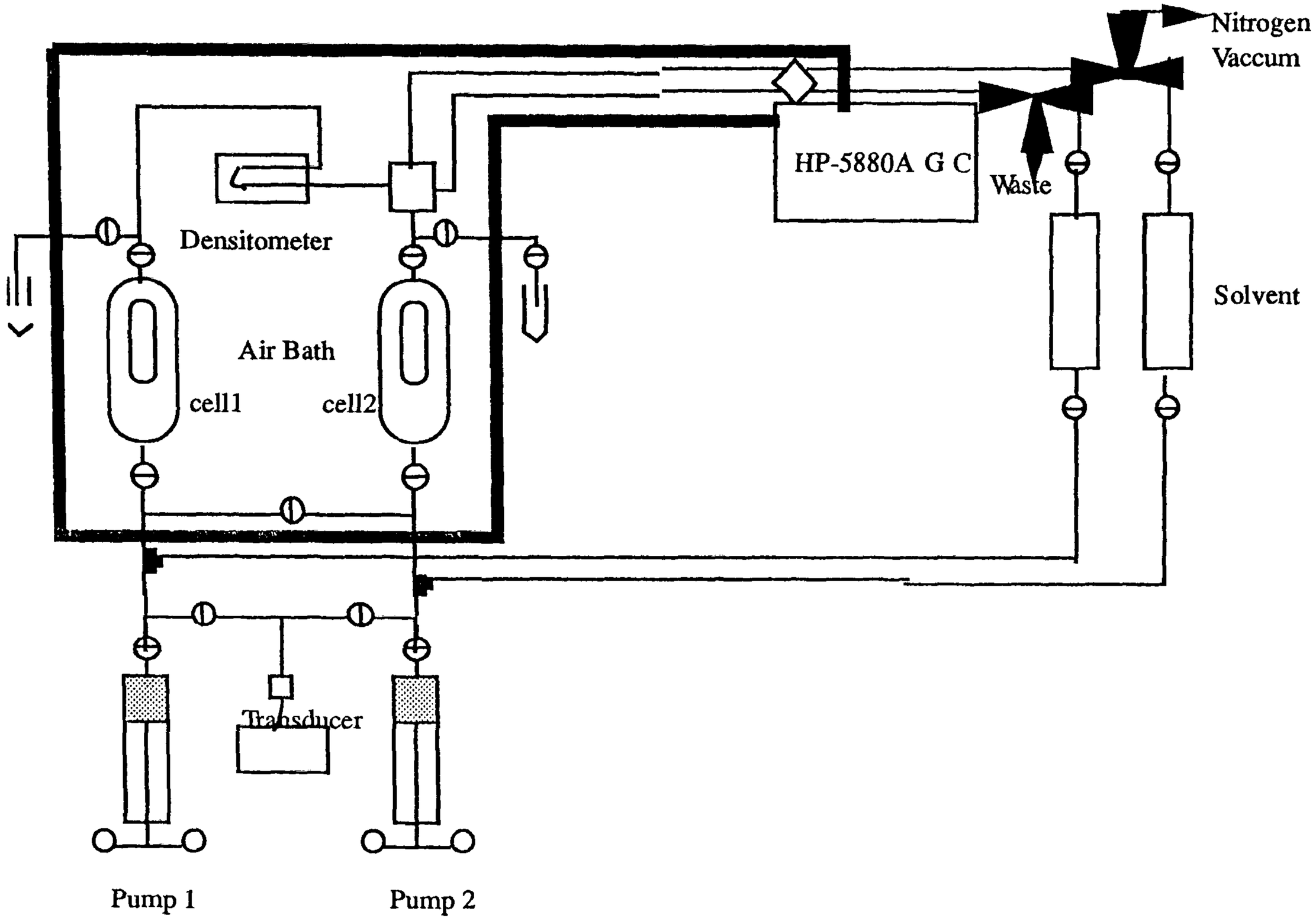

Figure 3.3.1 - Vapour-Liquid Equilibrium (V -L-E) Facility

fitted with a flame ionisation detector (FID). The description of this V-L-E facility is also available elsewhere in more details[2].

3.4 : LITERATURE SURVEY

Groenveld[3], studied the withdrawal of flat plates from the liquid bath which had a significant importance in the processes of dip coating, lubrication, freezing and, drying rolls, and in the coating of photographic film and paper. He proposed a new theory for withdrawal from viscous Newtonian liquids by vertical plates. In his work the thickness of the liquid layer on the withdrawn plate was determined experimentally by a light adsorption method. But his work was more relevant as far as the textile and certain chemical engineering applications were concerned.

Wilson and Jones[4], studied a similar phenomenon concerning the case of liquid film running down a vertical wall and entering a large pool creating horizontal ripples, he also studied a case similar to that of Groenveld[3], in which a case of flat vertical wall running downwards through a liquid column was analysed, but both the cases studied were relevant to other applications whereas our case was, in which the wall was stationary and the liquid film was moving.

Similarly other researchers have done an extensive work in the area of withdrawal of flat plates from liquid columns[5,6,7]. Extensive research has also been carried out concerning the withdrawal of cylinders from liquid baths, mostly considering the Newtonian fluids[8,9,10].

White and Tallmadge[11], considered the case of static meniscus on the outside of cylinders and a special case of meniscus outside the flat plate. They also derived an equation relating the meniscus profile and the film height. Kennedy and Burley[12], applied the geometry of fluid interfaces in the shape of figures of revolution to external fluid dynamics. The work of the above two researchers are closely related to the observations made in our work, hence, applied to derive a rigorous relationship for measuring interfacial tension.

3.4.1 : Theoretical Background of the Developed Technique

In this section a detailed derivation of the relationship developed is given, beginning with the fundamental equation of capillarity by Young and Laplace[23].

If a liquid surface is curved, the pressure is greater on the concave side than on the convex, by an amount which depends on the interfacial tension and the curvature. This is because the displacement of a curved surface , parallel to itself, results in an increase in area as the surface moves towards the convex side, and work has to be done to increase the area. This work is supplied by the pressure difference moving the surface[23].

The calculation may be made by considering the energy involved in a displacement of the surface, as shown in Figure (3.4.1.1), ABCD is a small part of the surface with sides at right angles; now this area is displaced parallel to itself, away from the concave side, by a distance δN, with the normals to the boundaries in the displaced position A'B'C'D' the same as the normals in the original position. The normals at A and B meet at O_1, those at B and C at O_2. Let the radius of curvature of the arc AB be R_1 and that of BC be R_2. Now the Sin of angle θ_1 or AO_1B is :

$$\text{Sin}(\theta_1) = \text{Sin}(AO_1B) = \frac{\text{Opposite Side}}{\text{Hypotenuse}} \qquad (3.4.1.1)$$

$$= \frac{AB}{R_1} \qquad (3.4.1.2)$$

similarly Sin of angle θ_2 or BO_2C will be :

$$\text{Sin}(\theta_2) = \text{Sin}(BO_2C) = \frac{BC}{R_2} \qquad (3.4.1.3)$$

and the area of the element of surface after the displacement is :

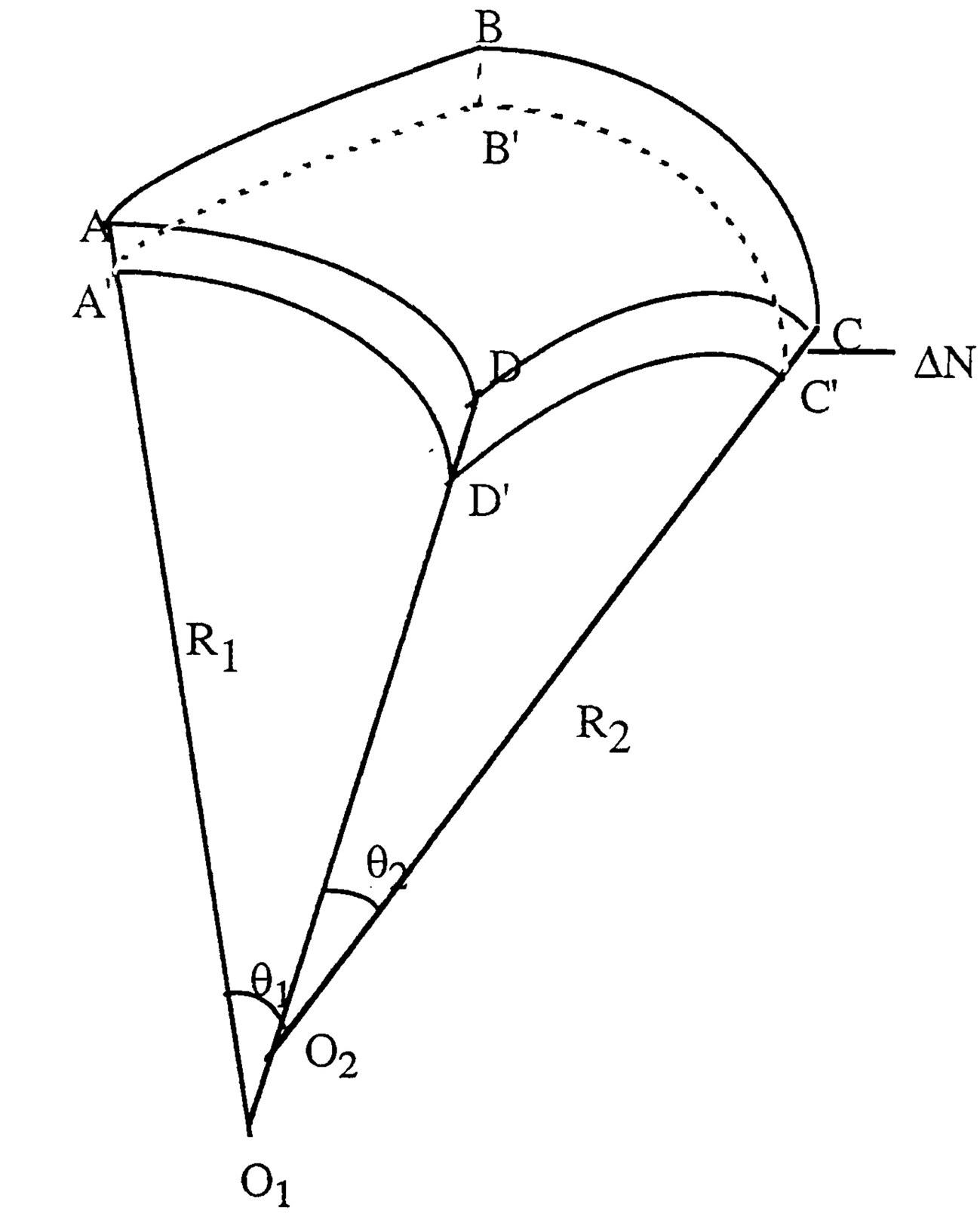

Figure 3.4.1.1 - Schematic of a Liquid Surface.

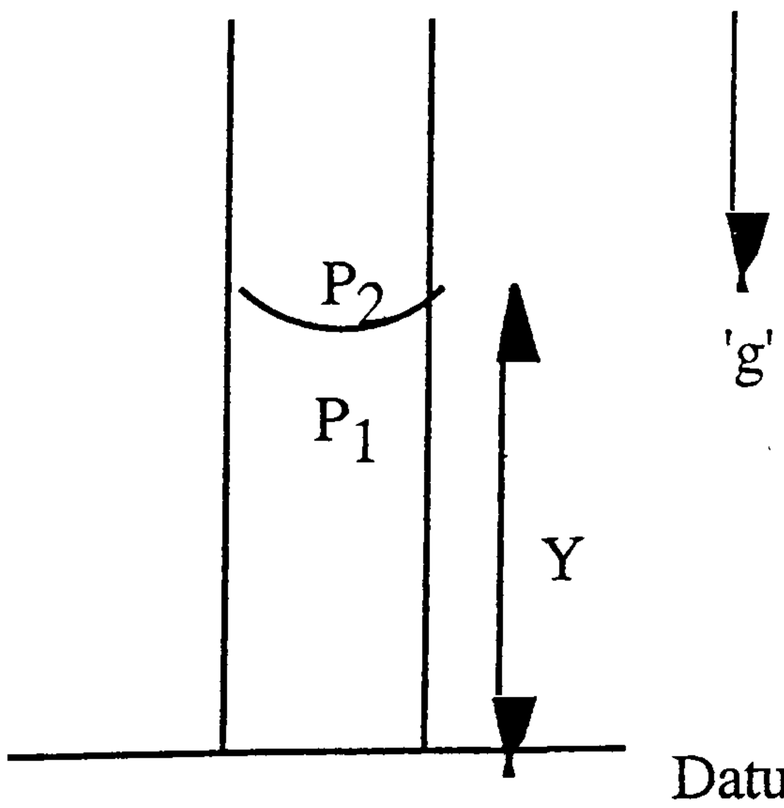

Figure 3.4.1.2 - Pressure Differential Across a Capillary.

$$\text{Area} = \left(AB + \frac{AB}{R_1}\Delta N \right) \left(BC + \frac{BC}{R_2}\Delta N \right) \qquad (3.4.1.4)$$

$$\text{Area} = AB{\times}BC + \frac{AB{\times}BC}{R_2}\Delta N + \frac{AB{\times}BC}{R_1}\Delta N + \frac{AB{\times}BC}{R_1R_2}\Delta N^2 \qquad (3.4.1.5)$$

neglecting the second order quantities and taking AB×BC common :

$$\text{Area} = AB{\times}BC \left[1 + \frac{\Delta N}{R_1} + \frac{\Delta N}{R_2} \right] \qquad (3.4.1.6)$$

and, $AB{\times}BC = ABCD$ (3.4.1.7)

finally,

$$\text{Area} = ABCD \left[1 + \frac{\Delta N}{R_1} + \frac{\Delta N}{R_2} \right] \qquad (3.3.1.8)$$

where,

$$\Delta\text{Area} = ABCD \left[1 + \frac{\Delta N}{R_1} + \frac{\Delta N}{R_2} \right] - ABCD \qquad (3.3.1.8\ a)$$

$$= ABCD{\times}\Delta N \left[\frac{1}{R_1} + \frac{1}{R_2} \right] \qquad (3.3.1.8\ b)$$

The work done against the free energy or interfacial tension is therefore :

$$\text{Work} = \sigma{\times}\Delta\text{Area} \qquad (3.4.1.9)$$

$$= ABCD{\times}\Delta N \left(\frac{1}{R_1} + \frac{1}{R_2} \right)\sigma \qquad (3.4.1.9\ a)$$

now if the pressure on the concave side is P_1 and on the convex side is P_2 then, the work done by this pressure differential is given by :

$$\text{Work} = (P_1 - P_2)\ ABCD{\times}\Delta N \qquad (3.4.1.10)$$

when these two work done are equated from Eq. 3.4.1.9 a and Eq. 3.4.1.10:

$$ABCD\times\Delta N\left(\frac{1}{R_1}+\frac{1}{R_2}\right)\sigma=(P_1-P_2)\,ABCD\times\Delta N \qquad (3.4.1.11)$$

finally,

$$\Delta P=(P_1-P_2)=\sigma\left(\frac{1}{R_1}+\frac{1}{R_2}\right) \qquad (3.4.1.12)$$

Eq. 3.4.1.12, which is called the Young-Laplace equation is the fundamental equation of capillarity. This has been extensively used in several applications, it also forms the basis of the derivation of the relationship developed in this work for the measurement of interfacial tension. The application of Eq. 3.4.1.12, is given in the following lines.

Now, for any figure of revolution explicit expressions for the two principal radii of curvature R_1 and R_2 can be written by choosing the plane of the first radius of curvature in such a way to pass through the axis of revolution[1].

$$R_1=\frac{\left[1+\left(\frac{dx}{dy}\right)^2\right]^{3/2}}{\left(\frac{d^2x}{dy^2}\right)} \qquad (3.4.1.13)$$

$$R_2=x\frac{Sqrt\left[1+\left(\frac{dx}{dy}\right)^2\right]}{\left(\frac{dx}{dy}\right)} \qquad (3.4.1.13a)$$

The curvature of interface for the tested conditions (IFT < 5 dyne/cm) as observed and measured on the cell flat windows indicated that, $\frac{1}{R_1}>>\frac{1}{R_2}$, hence :

$$\Delta P = \frac{\sigma \left(\frac{d^2x}{dy^2} \right)}{\left[1 + \left(\frac{dx}{dy} \right)^2 \right]^{3/2}} \qquad (3.4.1.14)$$

the pressure differential across the interface is balanced by the gravity at each point see Figure (3.4.1.2), hence we can write :

$$\Delta P = (\rho_l - \rho_v) \, gy \qquad (3.4.1.15)$$

Eq. 3.4.1.14 and 3.4.1.15 can thus be equated which gives:

$$(\rho_l - \rho_v) \, gy = \frac{\sigma \left(\frac{d^2x}{dy^2} \right)}{\left[1 + \left(\frac{dx}{dy} \right)^2 \right]^{3/2}} \qquad (3.4.1.16)$$

after introducing capillary constant, a, and making the left hand side of Eq. 3.4.1.16 dimensionless we get :

$$a = \left[\frac{2\sigma}{(\rho_l - \rho_v) \, g} \right]^{1/2} \qquad (3.4.1.17)$$

$$\frac{\left(\frac{d^2X}{dY^2} \right)}{\left[1 + \left(\frac{dX}{dY} \right)^2 \right]^{3/2}} = 2Y \qquad (3.4.1.18)$$

where, $Y = \frac{y}{a}$ and $X = \frac{x}{a}$, the contact angle, θ, on the window from Figure (3.4.1.3) for gas - condensate is defined by :

$$\tan(\theta) = - \frac{dX}{dY} \text{, at } X = 0 \qquad (3.4.1.19)$$

Now substituting Eq. 3.4.1.19 in Eq. 3.4.1.18 and solving for Y gives :

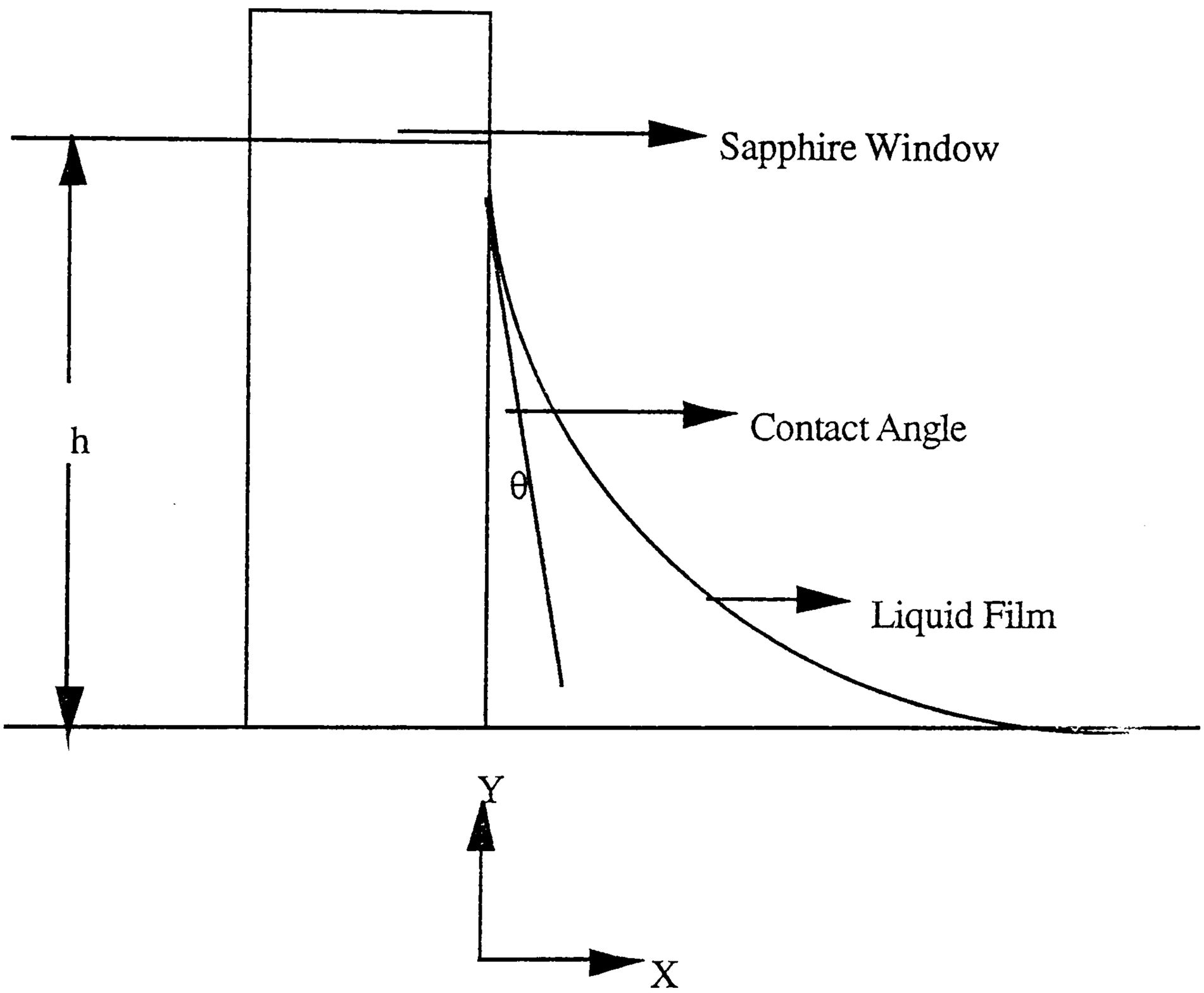

Figure 3.4.1.3 - Rise of a Condensate Over the Cell Window .

$$Y = (1 - \sin\theta)^{1/2}, \text{ at } X = 0 \qquad (3.4.1.20)$$

hence the rise of condensate on the window (meniscus band), h, is given by Figure (3.2.3) :

$$h = \left[\frac{2\sigma}{(\rho_l - \rho_v)\, g} \right]^{1/2} (1 - \sin\theta)^{1/2} \qquad (3.4.1.21)$$

For gas - condensate systems, where the interfacial tension is low, the condensate may be assumed to completely wet the window[13,14], i.e. contact angle, $\theta = 0$.

Hence,

$$\sigma = \frac{(\rho_l - \rho_v)\, g h^2}{2} \qquad (3.4.1.22)$$

Eq. 3.4.1.22, is the relationship derived which has been used throughout this work for measuring the interfacial tensions of various fluids tested. The results obtained are presented in the following sections.

3.5 : INTERFACIAL TENSION MEASUREMENTS OF SYNTHETIC MIXTURES

After developing the new technique based on the gas-liquid interface observed during experimentation with gas-condensates, it was decided to test the method against literature data on simple binary hydrocarbon systems. This section is dedicated for describing the measurements carried out on various synthetic mixtures. A comparison with the literature data is also presented wherever the relevant measurements have been previously reported.

3.5.1 : Methane-n-Butane System

At a temperature of 80°C the mixture has a two phase region in the range of 4.23 MPa to 10.78 MPa and exhibits retrograde condensation[15]. Table (3.5.1.1 a) and (3.5.1.1 b) give

Table 3.5.1.1 (a) - Liquid Phase Composition and Densities at 80°C for the Methane - n - Butane System.

1.- > Methane 2.-> n - Butane

No	Pressure, MPa	X_1, Mole Fraction	X_2, Mole Fraction	Liquid Density, gm/cc
1	10.78	0.4547	0.5453	0.3483
2	10.34	0.4293	0.5707	0.3620
3	9.75	0.3971	0.6029	0.3783
4	9.06	0.3621	0.6379	0.3947
5	7.68	0.2974	0.7026	0.4212
6	6.30	0.2365	0.7635	0.4424
7	4.92	0.1762	0.8238	0.4614
8	4.23	0.1457	0.8543	0.4702

Table 3.5.1.1 (b) - Vapour Phase Composition and Densities at 80°C for the Methane - n - Butane System.

1.- > Methane 2.-> n - Butane

No	Pressure, MPa	Y_1, Mole Fraction	Y_2, Mole Fraction	Vapour Density, gm/cc
1	10.78	0.6857	0.3143	0.1683
2	10.34	0.6971	0.3029	0.1557
3	9.75	0.7074	0.2926	0.1404
4	9.06	0.7141	0.2859	0.1252
5	7.68	0.7171	0.2829	0.1015
6	6.30	0.7098	0.2902	0.0823
7	4.92	0.6855	0.3145	0.0649
8	4.23	0.6615	0.3385	0.0569

Table 3.5.1.2 - Film Heights Measured at Each Pressure Stage for the Methane - n - Butane System at 80°C.

No	Pressure, MPa	Film Heights, mm
1	10.78	0.3319
2	10.34	0.4400
3	9.75	0.5837
4	9.06	0.7400
5	7.68	0.9660
6	6.30	1.0477
7	4.92	1.2145
8	4.23	1.3293

Table 3.5.1.3 - Data on Interfacial Tension for the Methane - n - Butane System at 80°C.

No	Pressure, MPa	Parachor Method, mN/m	Scaling Law, mN/m	Measured, mN/m	Literature[16], mN/m
1	10.78	0.146	0.131	0.097	-
2	10.34	0.252	0.222	0.196	-
3	9.75	0.445	0.387	0.397	-
4	9.06	0.734	0.631	0.724	0.740
5	7.68	1.449	1.224	1.463	1.700
6	6.30	2.322	1.935	2.135	2.150
7	4.92	3.409	2.807	2.868	-
8	4.23	4.019	3.290	3.582	-

the densities and phase compositions for the mixture from 10.78 MPa to 4.23 MPa, both phase compositions and densities were taken from Reference[15]. These values were employed in calculating IFT by the newly developed meniscus technique and the predictive methods. Table (3.5.1.2) gives the film heights measured directly from the TV monitor. The figures reported here are actual film heights after taking into account the magnification used. Table (3.5.1.3), reports values of IFT measured by the equation proposed in this work (Eq. 3.4.1.22) and those predicted by the parachor and scaling law. From this data it can be very well seen that except the IFTs close to the dew - point all other values were in reasonable agreement with the scaling (column 4) and parachor (column 3) methods, and those reported in the literature (column6)[16]. Although there is a disagreement between some values this could be possibly because of the poor optical system which was available in the beginning, and was improved greatly for the study of later systems. The use of literature density data could have also contributed to the error.

3.5.2 : Methane - n - Decane System

This binary system was also studied for making the assessment of pendant drop device employed in the cell in the beginning, which proved unsatisfactory for measurements below 1 dyne/cm. The study was performed only at one pressure and video recordings were available for it. A mixture comprising of 93 mole % methane and 7 mole % n-decane was used at 71.1°C. The dew - point pressure of the mixture at 71.1°C was determined at 34.79 MPa. The IFT measurement was carried out only at one pressure below the dew - point, 31.03 MPa. The compositions and densities of the gas and condensate phases were measured by the facilities present in the experimental set - up. Table (3.5.2.1 a) gives the condensate phase compositions and densities and Table (3.5.2.1 b) gives gas phase compositions and densities. In Table (3.5.2.2) the data on film height and the IFT measured by Eq. 3.4.1.22, the scaling law, and the parachor method are given. The value measured by Stegemeier[17], at these conditions is 0.57 mN/m, which agrees with our value within 7 %.

Table 3.5.2.1 (a) - Liquid Phase Compositions and Densities at 71.1°C for the Methane - n - Decane System.

1.- > Methane 2.- > n - Decane

Preussure, MPa	X_1, Mole Fraction	X_2, Mole Fraction	Liquid Density, gm/cc
31.03	0.7724	0.2276	0.5110

Table 3.5.2.1 (b) - Vapour Phase Compositions and Densities at 71.1°C for the Methane - n - Decane System.

1.- > Methane 2.- > n - Decane

Preussure, MPa	Y_1, Mole Fraction	Y_2, Mole Fraction	Vapor Density, gm/cc
31.03	0.9635	0.0365	0.2360

Table 3.5.2.2 - Data on Interfacial Tension for the Methane -n- Decane System at 71.1°C.

Pressure, MPa	Film Height, mm	Parachor Method, mN/m	Scaling Law, mN/m	Measured, mN/m	Reference[17], mN/m
31.03	0.625	0.480	0.590	0.530	0.570

The above mixture was previously studied in the gas condensate PVT cell. The following lines describe the experiment carried out on the same system in the V-L-E cell for validating the gas-liquid interface technique and the pendant drop technique by comparing both measurements with the literature data.

As mentioned previously Stegemeier[17] has measured IFT of the methane-n-decane system at different isotherms by the pendant drop method. The measurements at 71.1°C were selected for comparison since the data had a wide range of IFTs from 0.002-10 dyne/cm, and the temperature most suited the operating conditions of the V-L-E cell. A mixture of methane (89 mole %) and n-decane (11 mole %) was prepared gravimetrically and introduced into the cell. The mixture did not pass through an exact critical pressure but reached a near critical dew-point of 35.30 MPa. A constant composition expansion test was performed at pressures ranging from 34.47 to 10.34 MPa. The entire experiment was video recorded and the measurements of gas-liquid interface and the droplets for the pendant drop were carried out by the VMS300 video scalar unit. Density was measured of both the liquid and vapour phases except for a few high pressure data points where the liquid density could not be measured due to operational problems of the densitometer. These data were however obtained by interpolation or extrapolation of the available measurements. A comparison between the density differences measured in this work and by Sage and Lacey[18] is shown in Figure 3.5.2.1, which shows a reasonably good agreement. The average differences between both liquid and vapour phase densities were less than 1.5 % compared to Sage and Lacey[18]. Interfacial tension data were calculated using both sets of density differences and are shown in Figures 3.5.2.2 and 3.5.2.3. The average differences between IFT values measured by the pendant drop method and those reported in Reference 17 were less than 10 %. These plots prove the reliability of the IFT measurements carried out in the VLE apparatus using both methods, which also proves the fact that the gas-liquid interface technique can also be applied to the V-L-E rig for model fluids.

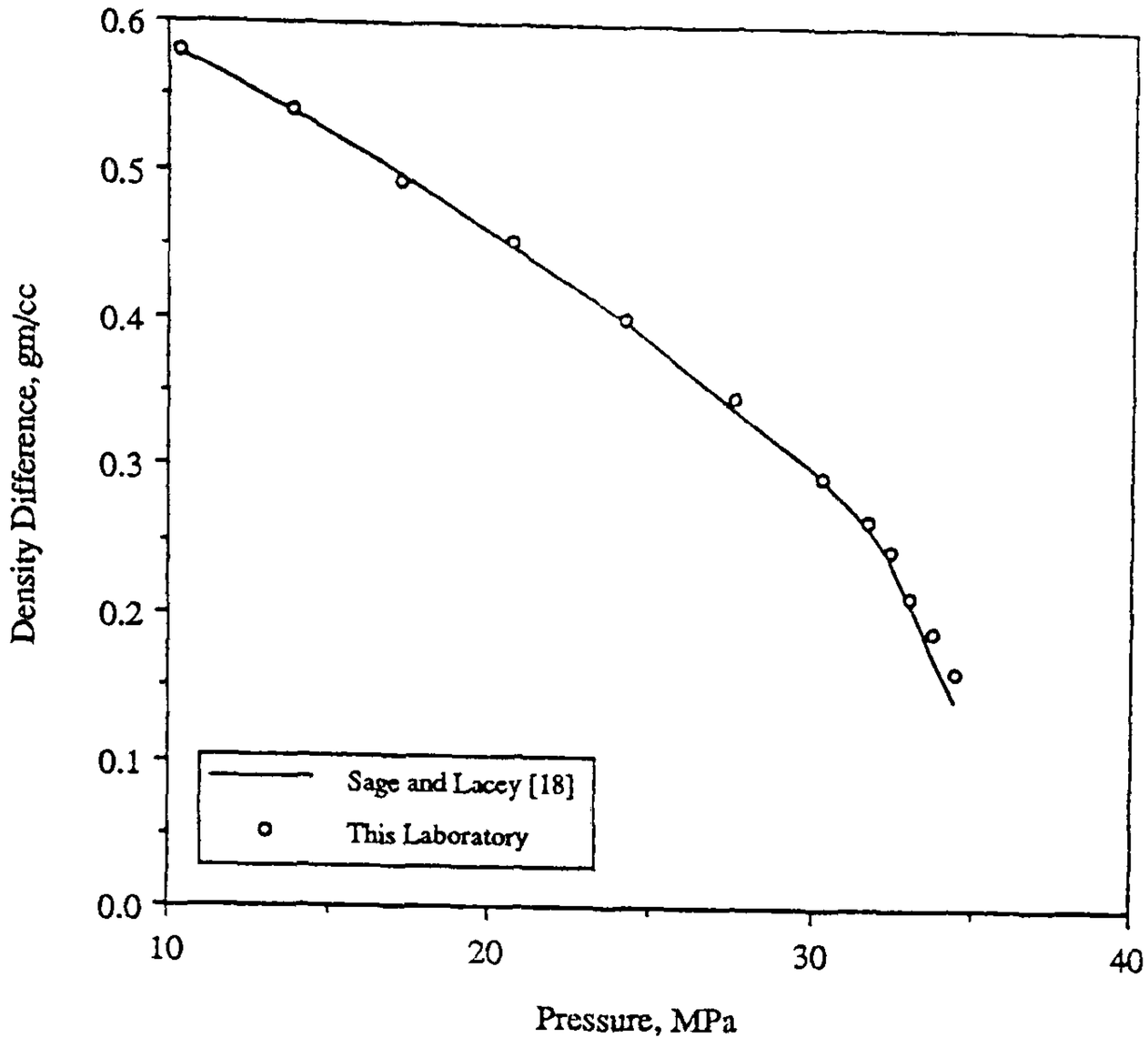

Figure 3.5.2.1 - Comparison of the Liquid-Gas Density Difference for the C1-nC10 Mixture at 71.1 deg C.

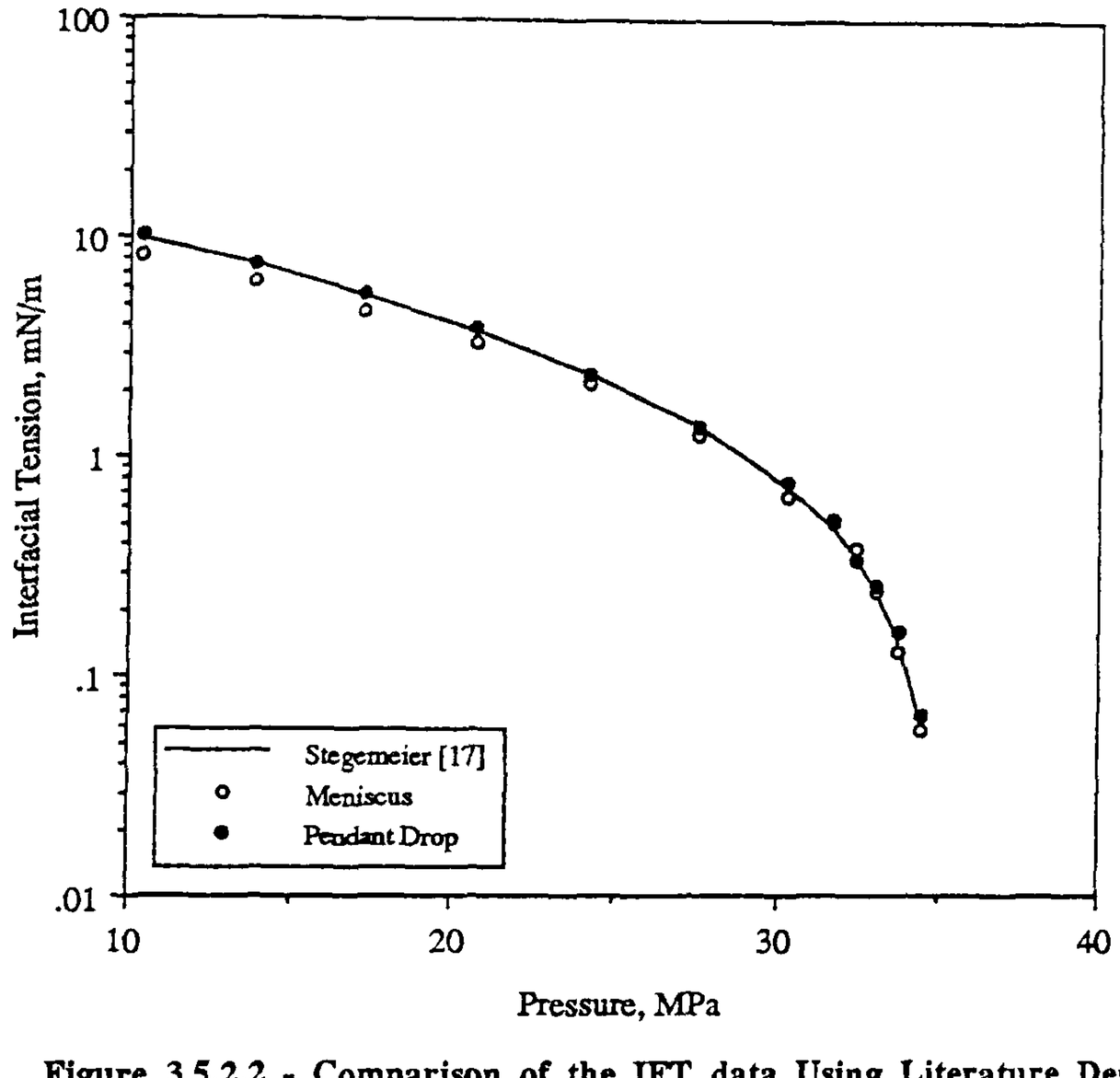

Figure 3.5.2.2 - Comparison of the IFT data Using Literature Density Differences for the C1-nC10 Mixture at 71.1 deg C.

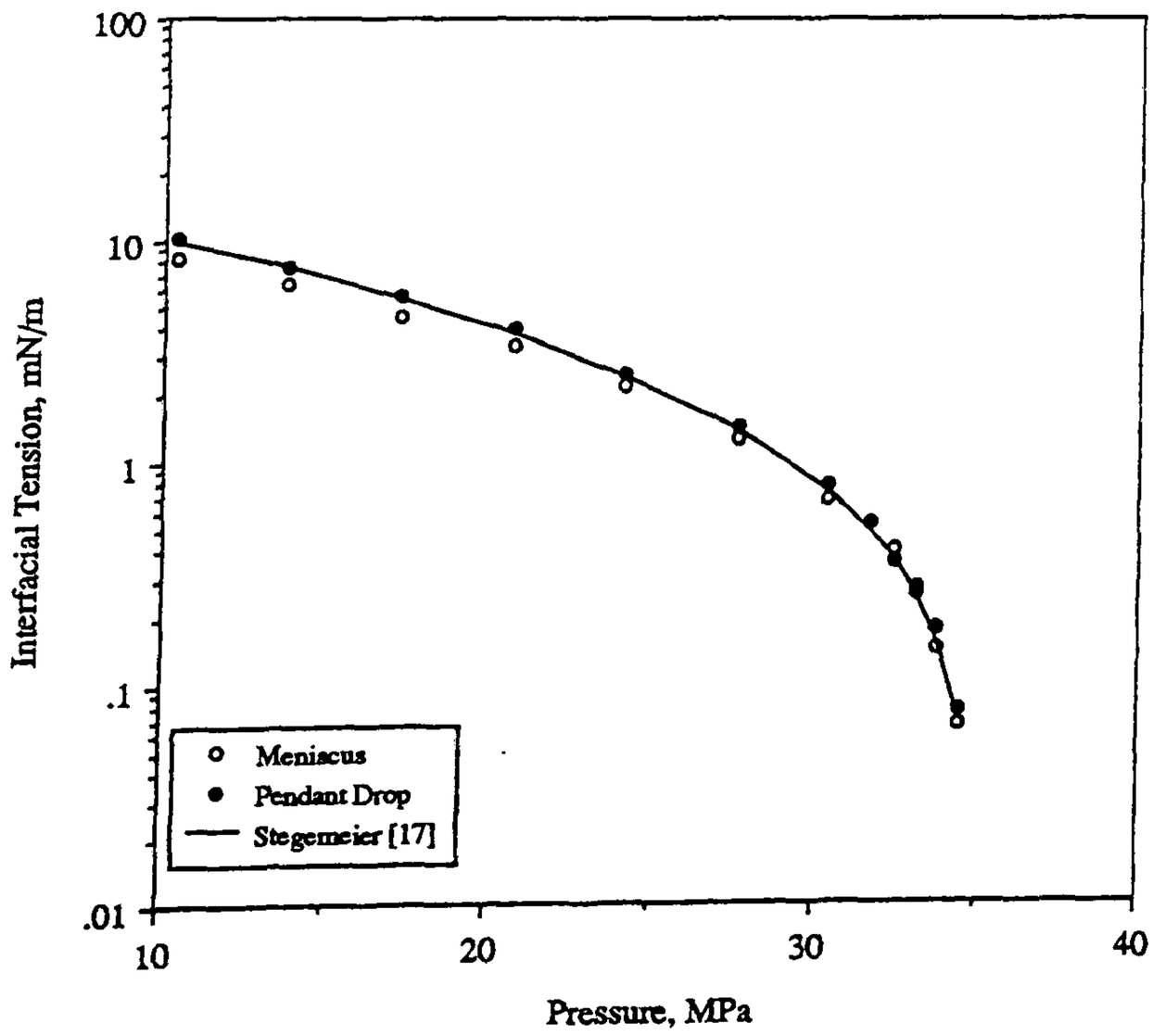

Figure 3.5.2.3 - Comparison of the IFT data Using Density Data Measured in this Laboratory for the C1-nC10 Mixture at 71.1 deg C.

5.5.3 : Methane - Propane System

After getting some encouraging results from the previously studied mixtures, it was decided to do a complete study of IFT against a recently published literature data on IFT of gas - condensate systems. Reliable literature data on IFT at high pressure conditions vis - a - vis low IFT data is scarce.

Haniff and Pearce[19], measured interfacial tension of a methane - propane binary at five isotherms by a laser light scattering technique. They used the compositional and density data of Sage and Lacey[20,21], for evaluating IFTs. They reported a dew - point of 9.39 MPa at 33.6°C for a mixture of (methane = 0.62 mol fraction).

A complete compositional and density analysis supported by the IFT measurements was done at 33.6°C to check the reliability of our measurement technique for IFT and to check the accuracy of our sampling facility. The dew - point measured in our laboratory was reported as 8.98 MPa. A mixture of the same compositions were prepared independently and tested by a research laboratory[1] determined the dew point as 8.99 MPa.

A full compositional, density and IFT study was carried out at pressures, of; 8.89, 8.74, 8.68, 8.47, and 7.16 MPa at 33.6°C. Since the dew - point measurement of our Laboratory did not match the measurements reported by Haniff and Pearce[19], density differences were taken as the datum instead of pressure to compare our IFT measurements. Table (3.5.3.1 a & 3.5.3.1 b) provide the condensate and vapour phase compositions and densities at various stages below the dew point pressure.

The IFTs tabulated by Haniff and Pearce[19], for density differences measured by them at 33.6°C were plotted on a semi - logarithmic scale in order to interpolate the values of IFTs for density differences measured by us at prevailing pressures. Figure (3.5.3.1) shows the plotted data of IFT vs. density differences reported by Haniff and Pearce[19], and in Table (3.5.3.2) are the values of IFTs read from Figure (3.5.3.1) for the density differences measured by us at the conditions studied.

Table 3.5.3.1 (a) - Liquid Phase Compositions and Densities at 33.6°C for the Methane Propane System.

1.- > Methane 2.- > Propane

No	Pressure, MPa	X_1, Mole Fraction	X_2, Mole Fraction	Liquid Density, gm/cc
1	8.89	0.5095	0.4905	0.2627
2	8.74	0.4833	0.5167	0.2991
3	8.68	0.4749	0.5251	0.3041
4	8.47	0.4617	0.5383	0.3143
5	7.16	0.3496	0.6504	0.3640

Table 3.5.3.1 (b) - Vapour Phase Compositions and Densities at 33.6°C for the Methane Propane System.

1.- > Methane 2.- > Propane

No	Pressure, MPa	Y_1, Mole Fraction	Y_2, Mole Fraction	Vapour Density, gm/cc
1	8.89	0.6159	0.3841	0.1831
2	8.74	0.6141	0.3859	0.1698
3	8.68	0.6125	0.3875	0.1603
4	8.47	0.6334	0.3666	0.1466
5	7.16	0.6294	0.3706	0.1050

Table 3.5.3.2 - Data of Haniff and Pearce[19], on Interfacial Tension Interpolated, for the Density Differences Measured in our Laboratory, from Figure (3.3.3.1).

No	Density Difference, gm/cc	Interfacial Tension, mN/m
1	0.0796	0.018
2	0.1293	0.058
3	0.1438	0.077
4	0.1677	0.122
5	0.2590	0.662

Table 3.5.3.3 - Data on Interfacial Tension for the Methane - Propane System at 33.6°C.

No	Pressure, MPa	Film Heights, mm	Scaling Law, mN/m	Parachor Method, mN/m	Measured mN/m	Haniff and* Pearce[19], mN/m
1	8.89	0.2221	0.006	0.006	0.019	0.018
2	8.74	0.2902	0.045	0.045	0.054	0.058
3	8.68	0.3169	0.070	0.069	0.071	0.077
4	8.47	0.4695	0.126	0.127	0.181	0.122
5	7.16	0.8165	0.656	0.685	0.847	0.662

* From Table 3.5.3.2 above

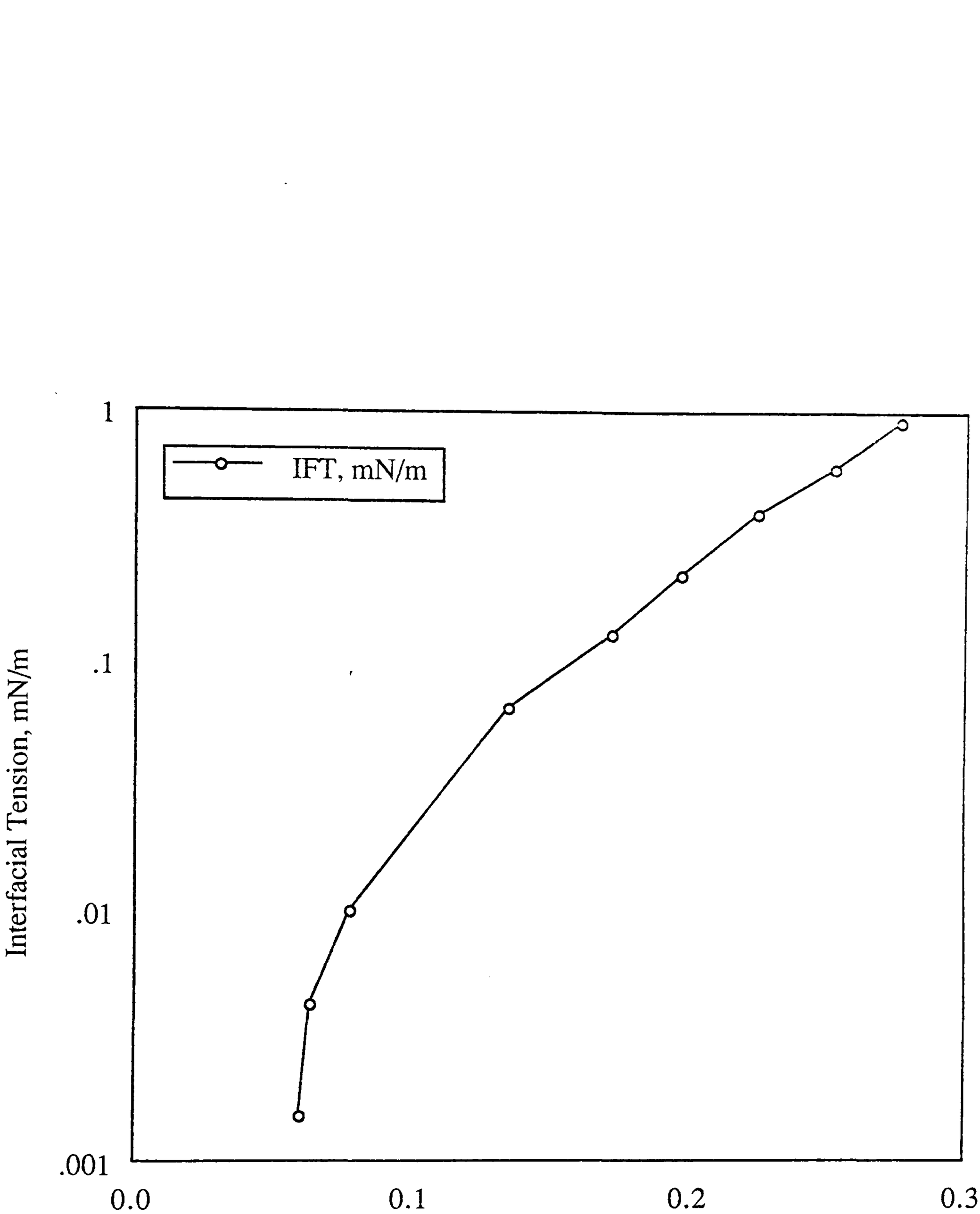

Figure 3.5.3.1 - Data of Haniff and Pearce [19], on IFT of Methane-Propane Mixture at 33.6 deg C.

IFT data obtained by predictive techniques, reported by Haniff and Pearce[19], and measured by Eq. 3.4.1.22 is furnished in Table (3.5.3.3), the tabulated values clearly indicate an acceptable agreement of IFTs measured by us with that obtained by the predictive techniques and those reported by Haniff and Pearce[19]. The IFT data measured by us at the last two pressure conditions is significantly different from Haniff and Pearce, which could be due to the error in accurately measuring the meniscus bandwidth.

3.5.4 : Carbon Dioxide - n - Tetradecane System

Gasem et al[22], have carried out a complete study on CO_2 + n - tetradecane mixture at 71.1°C reporting full compositional and density data along with data on IFTs, measured by the conventional pendant drop technique. A mixture of 92.4 mole % carbon dioxide and 7.6 mole % n - tetradecane was prepared for this purpose. The dew - point measured by us for this mixture matched very closely the one reported in Reference[22], the value reported by us was 16.36 MPa compared to 16.34 MPa reported in Reference[22]. The gas densities measured by us were 2 % higher than those reported in Reference[22], and the condensate phase densities measured by us were 0.5 % higher than those reported in Reference[22]. Compositional and density data measured by us for the gas and condensate phases is shown in Table (3.5.4.1), and a comparison of the density differences is shown in Figure (3.5.4.1).

The variation of IFT with the density difference between the liquid and gas phases are shown in Figure (3.5.4.2). The IFT is proportional to the liquid - gas density differences which is small at low IFT conditions or at high pressure conditions. Because of the disparities in our density measurements with those in Reference[22], the IFTs were calculated using both the density difference data sets measured by us and reported in Reference[22], the IFTs were recalculated for the pendant drop measurements reported in Reference[22] for our density differences and vice - versa for our IFT measurements. The IFT data generated for both density differences and both methods is tabulated in Table (3.5.4.2). The uncertainty figures reported in Table (3.5.4.2) are higher at low IFT conditions because of the errors involved in

Table 3.5.4.1 - Constant Composition Expansion Phase Data of Carbon Dioxide - n - Tetradecane System at 71.1°C.

No	Pressure, MPa	Density, gm/cc		CO_2, Mole Fraction	
		Condensate	Gas	Gas	Condensate
1	20.79 (Initial)	0.7622		0.9239	
2	16.24	0.7446	0.6785	0.9557	0.8875
3	16.21	0.7470	0.6701	0.9581	0.8838
4	16.13	0.7485	0.6640	0.9614	0.8815
5	15.93	0.7528	0.6451	0.9686	0.8636
6	14.48	0.7600	0.5339	0.9881	0.8055
7	12.41	0.7607	0.3897	0.9970	0.7402
8	11.03	0.7579	0.3064	0.9982	0.6489
9	20.79 (Final)	0.7622		0.9238	

Table 3.5.4.2 - Data on Interfacial Tension for the Carbon Dioxide - n - Tetradecane System at 71.1°C.

No	Pressure, MPa	Reference[22] Density Data		This Work Density Data		Deviation* %	Uncertainty** %
		Ref[22]	This Work	Ref[22]	This Work		
		mN/m		mN/m			
1	16.24	0.022	0.020	0.019	0.017	11	11
2	16.21	0.027	0.026	0.025	0.025	0	10
3	16.13	0.044	0.048	0.039	0.043	10	9
4	15.93	0.094	0.102	0.089	0.096	8	7
5	14.48	0.728	0.689	0.733	0.695	5	3
6	12.41	2.490	2.520	2.459	2.489	1	2
7	11.03	4.030	4.168	4.002	4.139	3	1

* percentage deviation between interfacial tension values measured in this work and those reported in Reference 22 for density data measured in this laboratory.

** uncertainty calculated for interfacial tension data measured in this work using the densities measured in this laboratory, considering the errors in measuring densities and meniscus bandwidths

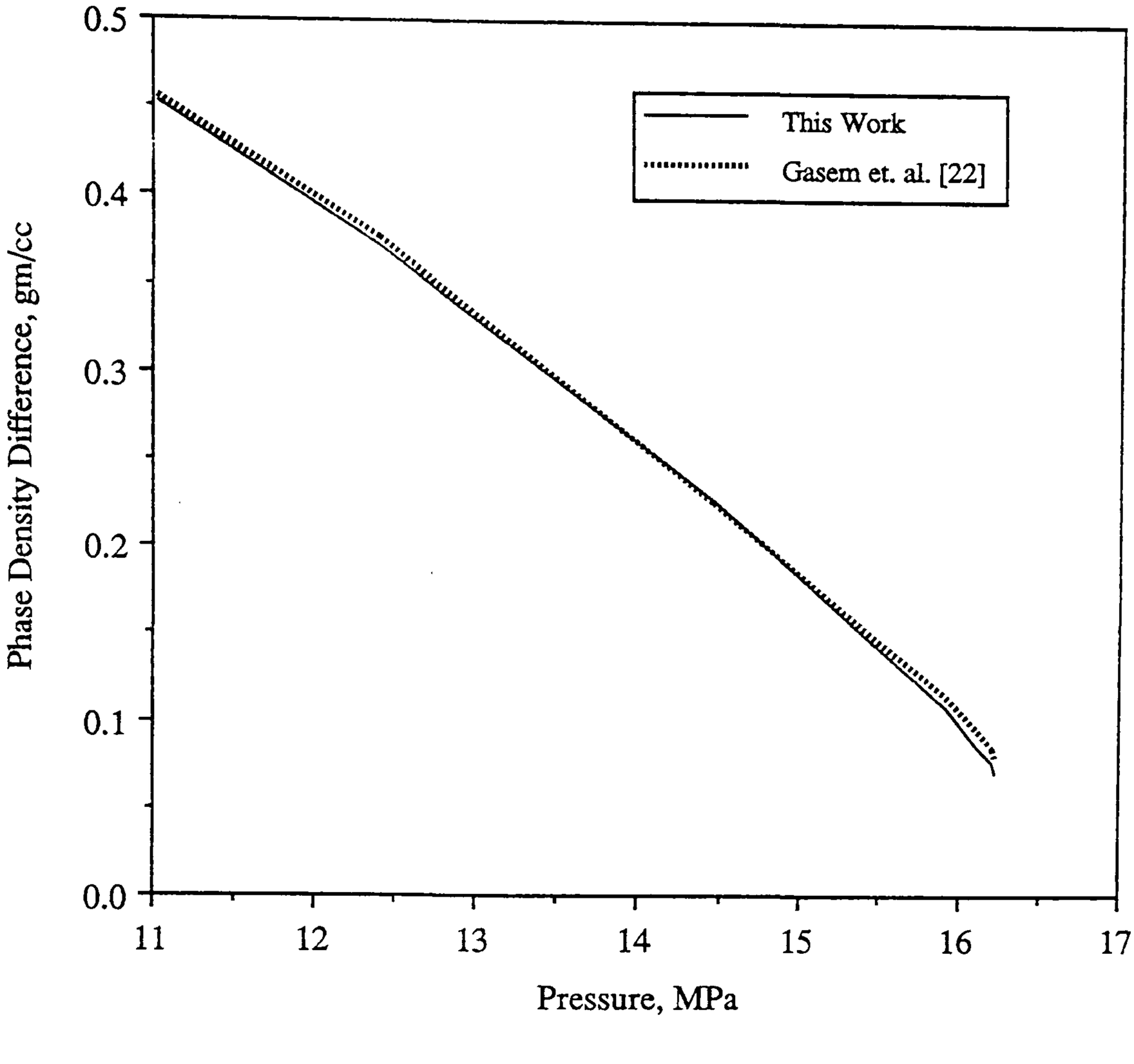

Figure 3.5.4.1 - Comparison of Density Difference Data, for the Carbon Dioxide - n - Tetradecane System at 71.1 deg C.

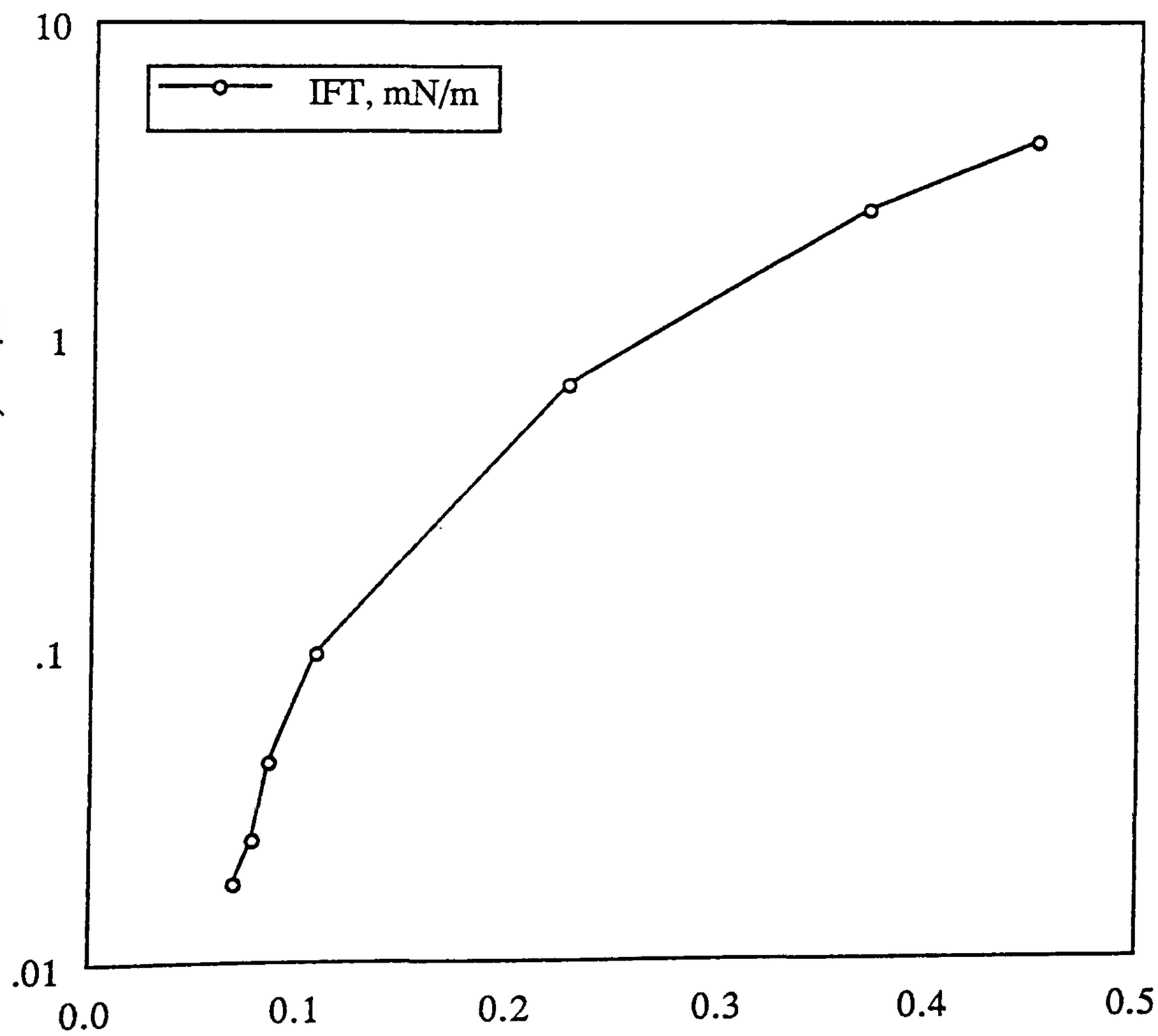

Figure 3.5.4.2 - Variation of IFT With Density Difference, for the CO2-n C14 Mixture at 71.1 deg C.

measuring the film heights at these conditions, which are quite small, subsequently these uncertainties reduce at high IFT conditions since the errors in measuring the film heights get minimised at low pressure or high IFT conditions.

The results in Table (3.5.4.2), clearly indicate the reliability and accuracy of our proposed measurement technique also highlighting its simplicity in carrying out the measurements and the ease with which reliable IFT data can be generated.

3.5.5 : Methane-Propane-n-Decane System

A four stage forward contact study was conducted in the vapour-Liquid-equilibrium (V-L-E) apparatus, between pure methane and a ternary mixture comprising of methane, propane and normal decane. This study was performed to generate data on phase densities, phase volumes and interfacial tensions to support the work on dynamic validation of phase behaviour models.

A ternary mixture comprising of methane (46 mole %), propane (39 mole %) and normal decane (15 mole %) was contacted with pure methane at 20.68 MPa and 37.78°C. The event of suspending the liquid droplets into its surrounding equilibrium vapour and the meniscus at the interface were video recorded for IFT measurements. The liquid and vapour phase densities at equilibrium were also measured. The experiment progressed to the second stage in which the equilibrium vapour was retained to contact with a fresh liquid. However the second contact resulted in complete miscibility. The experiment was stopped at this stage and a pressure of 13.79 MPa was selected to carry out the necessary number of contacts required for the dynamic validation study. The experiment was continued for four stages. The phase densities, pendant drops and meniscus widths were recorded at each contact point. The video recordings were later dimensioned to measure the interfacial tension for both the pendant drop and the meniscus technique. The measured IFT values and phase densities are furnished in Table 3.5.5.1. The predicted liquid and vapour phase compositions are provided in Table 3.5.5.2 a and 3.5.5.2 b respectively.

3.5.6 : Methane-Carbon Dioxide-Propane-n-Pentane-n-Decane-n-Hexadecane System

A series of constant composition expansion (CCE) and gas cycling tests were performed on a six component synthetic mixture comprising of CO_2, CH_4, C_3H_8, nC_5, nC_{10} and nC_{16}. The tests were carried out at a temperature of 100°C and 22.75 MPa. Interfacial tension data was measured using the gas-liquid interface technique during the cycling test with a gas composed of 59.35% CH_4 and 40.65% CO_2 at 22.75 MPa. The measured IFT data and phase densities are provided in Table 3.5.6.1. The predicted liquid phase compositions are given in Table 3.5.6.2 a and measured vapour phase compositions are provided in Table 3.5.6.2 b.

3.5.7 Interfacial Tension Measurements on a Synthetic Near Critical Fluid

A complete set of tests were planned for a **near critical real reservoir fluid** to be tested in the VLE and gas condensate experimental facilities. As a forerunner to that a six component synthetic mixture comprised of methane, ethane, propane and normal pentane, octane and decane, was gravimetrically prepared. A constant composition expansion (CCE) test was performed on this fluid at 38.0°C in the gas-condensate PVT cell. The mixture exhibited a near critical dew point of about 33 MPa. The phase volumes, densities and meniscus widths were recorded from 31.72 to 24.13 MPa. The meniscus widths were later dimensioned using a video scalar unit from which the IFT values were measured. The values of interfacial tension for this near critical fluid ranged from 0.0017 to 0.235 dyne/cm and are furnished for various points of CCE in Table 3.5.7.1 and Figure 3.5.7.1. The single phase composition for this fluid is given in Table 3.5.7.2, however, no measurements or predictions for the two phase compositions for this fluid were carried out.

Table 3.5.5.1 - Interfacial Tension Measurements on a Ternary Mixture of CH_4-C_3H_8-n-$C_{10}H_{22}$ for a Forward Multiple Contact Study With CH_4 at 37.8°C.

Stage Number	Liquid Density gm/cc	Vapour Density gm/cc	Measured IFT mN/m
		20.68 MPa	
1	0.4918	0.2442	0.457
		13.79 MPa	
1	0.5495	0.1493	2.375
2	0.4964	0.1794	1.166
3	0.4894	0.1914	0.907
4	0.4874	0.2003	0.697

Table 3.5.6.1 - Interfacial Tension Measurements on a Six Component Synthetic Gas Condensate for a Gas Cycling Study at 22.75 MPa and 100°C.

Stage Number	Liquid Density gm/cc	Vapour Density gm/cc	Measured IFT mN/m
0	0.5700	0.2410	0.853
1	0.6050	0.2390	1.359
2	0.6260	0.2390	1.742
3	0.6400	0.2360	2.123
4	0.6490	0.2380	2.347

Table 3.5.7.1 - Interfacial Tension Measurements on a Near Critical Synthetic Gas Condensate at 38°C.

Pressure (MPa)	Liquid Density gm/cc	Vapour Density gm/cc	Measured IFT mN/m
31.72	0.5013	0.3733	0.002
30.34	0.5245	0.3431	0.010
28.96	0.5456	0.3219	0.037
27.58	0.5567	0.3095	0.078
24.13	0.5749	0.2880	0.235

Table 3.5.5.2 (a) - Liquid Phase Compositions* at 37.8°C for a Forward Multiple Contact Study with Methane and a Ternary Mixture of Methane-Propane-n-Decane.

1.- > Methane **2.- > Propane** **3.- > n-Decane**

Stage Number	X_1, Mole Fraction	X_2, Mole Fraction	X_3, Mole Fraction
<u>20.68 MPa</u>			
1	0.6090	0.2053	0.1857
<u>13.79 MPa</u>			
1	0.4604	0.2919	0.2477
2	0.4834	0.3606	0.1560
3	0.4904	0.3707	0.1389
4	0.4921	0.3727	0.1352

Table 3.5.5.2 (b) - Vapour Phase Compositions* at 37.8°C for a Forward Multiple Contact Study with Methane and a Ternary Mixture of Methane-Propane-n-Decane.

1.- > Methane **2.- > Propane** **3.- > n-Decane**

Stage Number	Y_1, Mole Fraction	Y_2, Mole Fraction	Y_3, Mole Fraction
<u>20.68 MPa</u>			
1	0.8553	0.1287	0.0160
<u>13.79 MPa</u>			
1	0.8556	0.1404	0.0040
2	0.7955	0.1988	0.0057
3	0.7822	0.2116	0.0062
4	0.7792	0.2145	0.0063

* Predicted by the three parameter Peng-Robinson EOS

Table 3.5.6.2 (a) - Predicted Liquid Phase Compositions (PR 3 Par EOS) for a Gas Cycling Study on a Six Component Synthetic Gas Condensate at 22.75 MPa and 100°C.

1.- > Methane 2.- > Carbon Dioxide 3.- > Propane 4.- > n - Pentane 5.- > n - Decane 6.- > n - Hexadecane

Stage Number	X_1, Mole Fraction	X_2, Mole Fraction	X_3, Mole Fraction	X_4, Mole Fraction	X_5, Mole Fraction	X_6, Mole Fraction
0	0.2295	0.2740	0.1376	0.1761	0.0942	0.0885
1	0.2274	0.2784	0.1406	0.1982	0.0944	0.0608
2	0.2273	0.2785	0.1413	0.2057	0.0954	0.0517
3	0.2273	0.2785	0.1414	0.2077	0.0958	0.0492
4	0.2273	0.2785	0.1415	0.2081	0.0960	0.0489

Table 3.5.6.2 (b) - Measured Vapour Phase Compositions for a Gas Cycling Study on a Six Component Synthetic Gas Condensate at 22.75 MPa and 100°C.

1.- > Methane 2.- > Carbon Dioxide 3.- > Propane 4.- > n - Pentane 5.- > n - Decane 6.- > n - Hexadecane

Stage Number	Y_1, Mole Fraction	Y_2, Mole Fraction	Y_3, Mole Fraction	Y_4, Mole Fraction	Y_5, Mole Fraction	Y_6, Mole Fraction
0	0.6678	0.2087	0.0692	0.0371	0.0115	0.0057
1	0.6400	0.2774	0.0432	0.0247	0.0092	0.0055
2	0.6232	0.3193	0.0280	0.0168	0.0075	0.0052
3	0.6139	0.3443	0.0187	0.0117	0.0062	0.0052
4	0.6087	0.3599	0.0125	0.0081	0.0051	0.0057

Table 3.5.7.2 - Single Phase Composition of the Synthetic Near Critical Fluid.

Component	Mole %
Methane	76.58
Ethane	7.79
Propane	5.17
n-Pentane	3.95
n-Octane	2.80
n-Hexadecane	3.71
Total	100

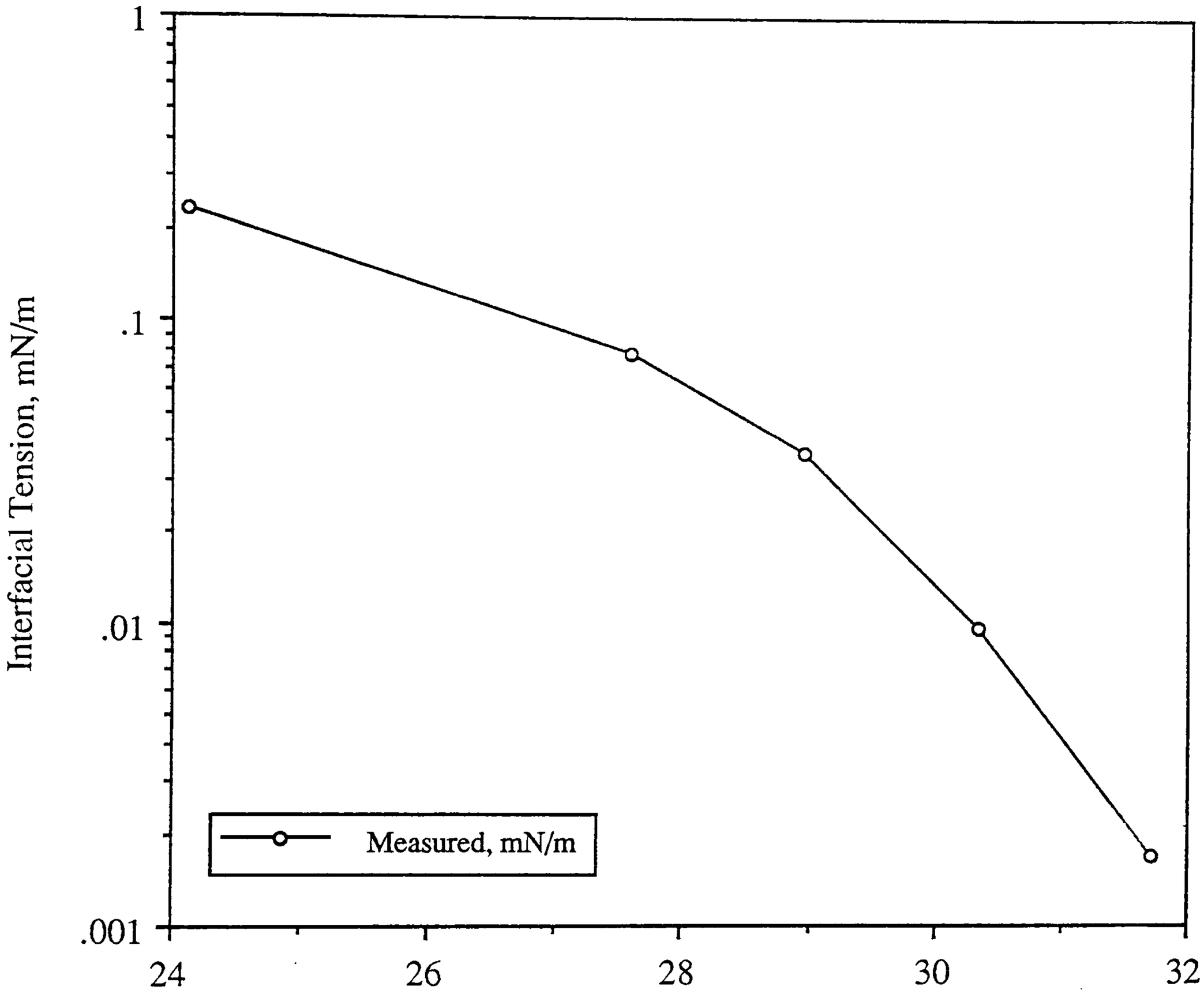

Figure 3.5.7.1 - Interfacial Tension data on a Near Critical Synthetic Gas Condensate at 38 deg C.

3.6 : INTERFACIAL TENSION MEASUREMENTS OF REAL RESERVOIR FLUIDS

This section presents IFT measurements on one gas condensate, volatile oil, black oil and one near critical fluid at various values of temperature, using the gas-liquid meniscus method and the pendant drop method in the gas-condensate PVT cell and the V-L-E cell respectively. A constant composition expansion (CCE), constant volume depletion (CVD) and gas cycling test were carried out on the gas condensate, and IFTs were measured during these processes. Interfacial tension measurements are presented for the volatile oil for a flash test and a backward multiple contact study involving an injection gas mixture of methane and carbon dioxide. A backward multiple contact study was also carried out for the black oil involving methane as an injection gas and IFTs were measured during this process. Similarly interfacial tension measurements which were carried out on the black oil during a forward multiple contact study with methane and a binary mixture of methane and carbon dioxide respectively are also presented. Interfacial tension values determined for the near critical fluid at temperatures ranging from 25 to 140°C in the V-L-E set up and the gas condensate facility by applying the gas-liquid interface technique are also furnished.

3.6.1 : Gas Condensate Fluid C_3

A real gas condensate fluid (bottom hole sample) identified as fluid C_3 for which the single phase composition is given in Table 3.6.1.1 was used for the CCE, CVD and gas cycling test with methane. All the tests were carried out at a temperature of 140°C in the gas condensate PVT cell described in section 3.2. Interfacial tension values were measured during these tests using the gas-liquid interface technique developed during the course of this study.

The purpose of carrying out these experiments was to simulate the production of gas and condensate by depletion down to about 27.58 MPa and to simulate gas cycling there after. This fluid exhibited a dew-point pressure of 42.20 MPa. The fluid was first subjected to Constant Composition Expansion (CCE) test. The two phase compositions, densities,

Table 3.6.1.1 - Single Phase Composition of Fluid C_3.

Component	Feed Composition Mole %
N_2	0.57
C_1	71.74
CO_2	2.33
C_2	7.86
C_3	4.14
iC_4	0.62
nC_4	1.67
iC_5	0.52
nC_5	0.75
C_6	1.04
C_7	1.62
C_8	1.40
C_9	1.07
C_{10}	0.55
C_{11}	0.49
C_{12}	0.48
C_{13}	0.44
C_{14}	0.52
C_{15}	0.46
C_{16}	0.26
C_{17}	0.21
C_{18}	0.20
C_{19}	0.15
C_{20+}	0.91
Total	100.00

volumes and meniscus widths were measured at pressures from 27.58 to 6.89 MP in the intervals of 6.89 MPa. The liquid and vapour compositions were measured with the direct sampling facility, except at 13.79 and 6.89 MPa the vapour phase compositions were calculated using the material balance. Liquid and vapour phase densities were measured using the Paar densitometer. The meniscus widths were measured using the VMS300 video scalar unit. The compositional data has been furnished in Table 3.6.1.2 and the data on phase densities and IFTs measured is presented in Table 3.6.1.3.

After completion of the CCE the sample was recompressed to single phase and a partial Constant Volume Depletion Study (CVD) performed from dew point pressure to 27.58 MPa. During CVD the phase densities and phase compositions were measured at 31.03 and 27.58 MPa together with all the other relevant data. The meniscus widths were also recorded as usual for IFT measurements. The measured compositions are provided in Table 3.6.1.4 and the data on phase densities and IFTs measured is presented in Table 3.6.1.3.

At a pressure of 27.58 MPa the CVD was stopped in order to carry out the methane cycling test into the depleted sample to simulate a gas injection process in the reservoir. This pressure was selected because it was close to the point of maximum liquid drop out for this fluid. The test was performed using 99.99% pure methane at 140°C and 27.58 MPa into the cell and allowing the resultant vapour to contact with the liquid until equilibrium was attained. The data obtained from this test comprised of phase volumes, densities, vapour phase compositions and meniscus widths for IFT calculations. The liquid composition could not be measured due to the fact that the liquid cannot be removed in a gas cycling test. Information on vapour phase compositions is provided in Table 3.6.1.5. The sample was returned to the initial volume by removing vapour from the cell. The test was progressed through four cycles of methane addition. The phase densities and interfacial tension values measured during the four stages of gas addition test are provided in Table 3.6.1.3.

Table 3.6.1.2 - Phase Compositions of Fluid C_3 for a CCE Test at 140°C.

	27.58 MPa		**20.68 MPa**		**13.79 MPa**		**6.89 MPa**	
	Vapour	**Liquid**	**Vapour**	**Liquid**	**Vapour**	**Liquid**	**Vapour**	**Liquid**
Component	Mole %	Mole %	Mole %	Mole %	Mole %	Mole %	Mole %	Mole %
N_2	0.61	0.3	0.61	0.22		0.15		0.07
C_1	75.22	48.77	75.84	39.59		28.97		16.22
CO_2	2.41	1.8	2.44	1.59		1.20		0.73
C_2	7.92	7.4	8.10	6.95		5.94		4.03
C_3	4.05	4.75	4.11	4.89		4.74		3.59
iC_4	0.59	0.81	0.59	0.88		0.92		0.78
nC_4	1.57	2.32	1.57	2.58		2.78		2.50
iC_5	0.47	0.83	0.46	0.98	*Calculated*	1.12	*Calculated*	1.12
nC_5	0.67	1.23	0.66	1.46	*by*	1.72	*by*	1.76
C_6	0.86	1.95	0.85	2.28	*Material*	2.83	*Material*	3.21
C_7	1.35	3.38	1.34	4.36	*Balance*	5.58	*Balance*	6.77
C_8	1.12	3.2	1.10	4.24		5.55		7.21
C_9	0.80	2.71	0.80	3.67		4.99		6.74
C_{10}	0.39	1.6	0.36	2.18		3.05		4.20
C_{11}	0.30	1.6	0.27	2.24		2.90		4.08
C_{12}	0.28	1.65	0.30	2.25		2.99		4.16
C_{13}	0.24	1.78	0.15	2.45		3.25		4.45
C_{14}	0.29	2.22	0.17	2.97		4.00		5.50
C_{15}	0.24	1.97	0.16	2.53		3.05		4.07
C_{16}	0.11	1.38	0.06	1.76		2.14		2.98
C_{17}	0.08	1.08	0.04	1.09		1.36		1.75
C_{18}	0.07	1.08	0.02	1.51		1.85		2.44
C_{19}	0.05	0.89	0.01	1.07		1.28		1.66
C_{20+}	0.32	5.3	0.00	6.25		7.64		9.98
Total	100.00	100.00	100.00	100.00		100.00		100.00

Table 3.6.1.3 - Interfacial Tension Measurements on Fluid C_3 for CCE, CVD and Gas Cycling (27.58 MPa) Tests at 140°C.

Pressure (MPa)/ Stage Number	Liquid Density gm/cc	Vapour Density gm/cc	Measured IFT mN/m
			<u>CCE</u>*
27.58	0.5760	0.2260	0.564
20.68	0.6040	0.1650	1.523
13.79	0.6390	0.1050	3.251
6.89	0.6740	0.0520	6.335
			<u>CVD</u>**
31.03	0.5630	0.2630	0.253
27.58	0.5770	0.2280	0.622
			<u>Gas Cycling</u>***
1	0.5890	0.2023	0.994
2	0.6024	0.1990	1.173
3	0.6231	0.1882	1.519
4	0.6345	0.1731	1.785

* See Table 3.6.1.2 for compositions
** See Table 3.6.1.4 for compositions
*** See Table 3.6.1.5 for compositions

Table 3.6.1.4 - Phase Compositions of Fluid C_3 for a CVD Test at 140°C.

	31.03 MPa		27.58 MPa	
	Vapour	Liquid	Vapour	Liquid
Component	Mole %	Mole %	Mole %	Mole %
N_2	0.60	0.34	0.62	0.29
C_1	74.02	52.73	74.83	46.70
CO_2	2.35	1.90	2.39	1.77
C_2	7.86	7.58	7.85	7.65
C_3	4.05	4.69	4.02	4.83
iC_4	0.60	0.78	0.59	0.84
nC_4	1.59	2.22	1.56	2.40
iC_5	0.49	0.78	0.47	0.86
nC_5	0.70	1.15	0.68	1.27
C_6	0.93	1.70	0.89	1.87
C_7	1.46	3.09	1.40	3.46
C_8	1.20	2.86	1.14	3.23
C_9	0.92	2.43	0.84	2.83
C_{10}	0.47	1.44	0.43	1.66
C_{11}	0.40	1.37	0.38	1.73
C_{12}	0.36	1.49	0.33	1.76
C_{13}	0.32	1.56	0.26	2.24
C_{14}	0.36	1.91	0.31	2.20
C_{15}	0.35	1.70	0.31	1.82
C_{16}	0.16	1.20	0.15	1.09
C_{17}	0.12	0.74	0.07	1.46
C_{18}	0.11	1.06	0.08	1.13
C_{19}	0.08	0.79	0.05	0.96
C_{20+}	0.51	4.52	0.35	5.98
Total	100.00	100.00	100.00	100.00

Table 3.6.1.5 - Vapour Phase Compositions of Fluid C_3 for a Gas Cycling Test with Methane at 27.58 MPa and 140°C.

	Stage 1	Stage 2	Stage 3	Stage 4
Component	Mole%	Mole%	Mole%	Mole%
N_2	0.66	0.67	0.70	0.72
C_1	81.54	83.27	85.98	89.26
CO_2	1.76	1.56	1.24	0.82
C_2	5.89	5.26	4.25	3.11
C_3	2.94	2.63	2.12	1.53
iC_4	0.44	0.39	0.32	0.23
nC_4	1.16	1.05	0.85	0.63
iC_5	0.36	0.32	0.26	0.20
nC_5	0.51	0.46	0.38	0.28
C_6	0.65	0.59	0.50	0.40
C_7	0.99	0.91	0.78	0.64
C_8	0.79	0.74	0.65	0.55
C_9	0.60	0.55	0.49	0.42
C_{10}	0.29	0.28	0.25	0.21
C_{11}	0.25	0.23	0.21	0.18
C_{12}	0.22	0.21	0.19	0.16
C_{13}	0.23	0.21	0.20	0.17
C_{14}	0.17	0.16	0.14	0.12
C_{15}	0.17	0.16	0.15	0.13
C_{16}	0.08	0.07	0.07	0.06
C_{17}	0.05	0.05	0.05	0.03
C_{18}	0.04	0.04	0.04	0.02
C_{19}	0.03	0.02	0.02	0.02
C_{20+}	0.19	0.17	0.16	0.11
Total	100.00	100.00	100.00	100.00

3.6.2 : Real Volatile Oil Volatile Oil (A)

A real volatile oil sample was used for carrying out the flash (CCE) and a backward multiple contact study using a mixture of methane and carbon dioxide. The single phase feed composition of the oil is available in Table 3.6.2.1. Both CCE and the contact study were carried out at a temperature of 100°C. These tests were performed in the vapour-liquid-equilibrium facility (V-L-E) cell described in Section 3.3. The interfacial tension data was measured using the pendant drop method because the gas-liquid interface technique was found unsuitable due to the contact angle considerations as mentioned in Section 2.2.2 of the previous chapter.

A flash test was performed on this oil at 100°C below the saturation pressure of 34.92 MPa. The test was conducted from 6.89 to 35.26 MPa. The phase volumes, densities and compositions were measured at 6.89, 10.34 and 13.79 MPa. The two phase compositions are presented in Table 3.6.2.2. The event of falling of a droplet into its surrounding equilibrium vapour was recorded at the three pressures mentioned above. These tapes were later used for dimensioning the drops, using the VMS300 video scalar unit to calculate the pendant drop IFT. The measured liquid and vapour phase densities and IFT values are furnished in Table 3.6.2.3.

Application of gas injection in the field, to both maintain reservoir pressure and as an aid to enhanced oil recovery (EOR) has been popular for many years now. A series of multiple contact experiments are conducted to study the effect of mass transfer between the original injection gas and the reservoir oil as the fluids migrate towards the production well. A four stage backward contact study was carried out on the real volatile oil employing an injection gas mixture of methane (60 mole %) and carbon dioxide (40 mole %) at 35.26MPa and 100°C.

A previously calculated amount of oil was loaded into the cell and was allowed to contact the fresh injection gas in the first stage. The phase densities were measured and the equilibrium liquid was allowed to flow through the spout into its equilibrium vapour for interfacial tension

Table 3.6.2.1 - Single Phase Composition of Real Volatile Oil (A).

Component	Feed Composition Mole%
C_1	57.53
C_2	10.16
C_3	5.83
iC_4	1.22
nC_4	2.06
iC_5	1.01
nC_5	1.70
C_6	1.40
C_7	2.16
C_8	2.55
C_9	2.00
C_{10}	1.55
C_{11}	1.10
C_{12}	1.00
C_{13}	0.99
C_{14}	0.78
C_{15}	0.85
C_{16}	0.72
C_{17}	0.49
C_{18}	0.60
C_{19}	0.51
C_{20+}	3.81
Total	100.00

Table 3.6.2.2 - Phase Compositions of Real Volatile Oil (A) for a CCE Test at 100°C.

	13.79 MPa		10.34 MPa		6.89 MPa	
	Vapour	Liquid	Vapour	Liquid	Vapour	Liquid
Component	Mole %	Mole %	Mole %	Mole %	Mole %	Mole %
C_1	76.120	29.875	75.315	23.961	72.933	16.920
C_2	11.250	9.878	11.677	8.961	12.350	7.617
C_3	5.120	7.330	5.507	7.485	6.131	7.177
iC_4	0.848	1.730	0.905	1.856	1.008	1.891
nC_4	1.350	3.172	1.453	3.437	1.692	3.596
iC_5	0.512	1.725	0.536	1.965	0.611	2.099
nC_5	0.869	3.012	0.927	3.433	1.145	3.739
C_6	0.619	2.635	0.597	2.951	0.827	3.395
C_7	0.789	4.306	1.180	4.914	1.390	5.689
C_8	0.870	5.266	1.271	6.071	1.909	7.224
C_9	0.643	4.375	0.632	2.915	0.005	3.209
C_{10}	0.374	2.869	0.000	5.257	0.000	6.140
C_{11}	0.255	2.382	0.000	2.650	0.000	3.183
C_{12}	0.215	2.185	0.000	2.492	0.000	2.877
C_{13}	0.157	2.010	0.000	2.390	0.000	2.760
C_{14}	0.000	1.827	0.000	2.046	0.000	2.352
C_{15}	0.000	1.759	0.000	2.123	0.000	2.484
C_{16}	0.000	1.585	0.000	1.648	0.000	1.931
C_{17}	0.000	1.177	0.000	1.394	0.000	1.613
C_{18}	0.000	1.260	0.000	1.457	0.000	1.686
C_{19}	0.000	1.219	0.000	1.247	0.000	1.481
C_{20+}	0.000	8.423	0.000	9.346	0.000	10.936
Total	100.000	100.000	100.000	100.000	100.000	100.000

Table 3.6.2.3 - Interfacial Tension Measurements on Real Volatile Oil (A) for a CCE* test at 100°C.

No	Pressure MPa	Liquid Density gm/cc	Vapour Density gm/cc	Measured IFT mN/m
1	13.79	0.6900	0.1170	7.046
2	10.34	0.7060	0.0860	10.313
3	6.849	0.7260	0.0580	13.519

* See Table 3.6.2.2 for compositions

Table 3.6.2.4 - Interfacial Tension Measurements on Real Volatile Oil (A) for a Backward Multiple Contact Study * * **with CH_4+CO_2 at 35.26 MPa and 100°C.**

Stage No	Liquid Density gm/cc	Vapour Density gm/cc	Measured IFT mN/m
1	0.6378	0.3581	0.663
2	0.6898	0.3660	1.420
3	0.7248	0.3636	2.170
4	0.7565	0.3505	3.239

* * See Table 3.6.2.5 for compositions

Table 3.6.2.5 - Predicted Phase Compositions of Real Volatile Oil (A) for a MBC Study with CH4+CO2 at 35.26 MPa and 100°C.

	Stage 1		Stage 2		Stage 3		Stage 4	
	Vapour	Liquid	Vapour	Liquid	Vapour	Liquid	Vapour	Liquid
Component	Mole %	Mole %	Mole %	Mole %	Mole %	Mole %	Mole %	Mole %
C_1	64.910	42.035	60.047	36.717	58.275	33.791	58.823	31.815
CO_2	16.130	14.113	29.156	24.029	36.156	28.499	39.213	29.662
C_2	6.396	5.720	2.941	2.643	1.029	0.928	0.146	0.131
C_3	3.470	3.789	1.776	2.030	0.728	0.867	0.132	0.162
iC_4	0.702	0.853	0.377	0.493	0.167	0.233	0.035	0.051
nC_4	1.149	1.541	0.647	0.947	0.307	0.486	0.070	0.120
iC_5	0.543	0.810	0.322	0.527	0.163	0.290	0.041	0.080
nC_5	0.893	1.415	0.545	0.949	0.284	0.544	0.076	0.159
C_6	0.690	1.279	0.445	0.934	0.254	0.599	0.079	0.213
C_7	0.999	2.131	0.673	1.667	0.411	1.173	0.146	0.488
C_8	1.052	2.855	0.752	2.477	0.505	2.003	0.221	1.075
C_9	0.780	2.363	0.569	2.136	0.396	1.824	0.188	1.088
C_{10}	0.553	1.948	0.415	1.849	0.300	1.682	0.157	1.137
C_{11}	0.359	1.471	0.274	1.459	0.205	1.406	0.117	1.071
C_{12}	0.306	1.398	0.237	1.425	0.181	1.423	0.109	1.165
C_{13}	0.268	1.459	0.209	1.548	0.163	1.626	0.106	1.486
C_{14}	0.179	1.229	0.142	1.361	0.113	1.504	0.078	1.536
C_{15}	0.182	1.380	0.144	1.552	0.114	1.752	0.081	1.872
C_{16}	0.133	1.216	0.105	1.404	0.083	1.634	0.061	1.871
C_{17}	0.079	0.857	0.063	1.006	0.050	1.195	0.037	1.429
C_{18}	0.085	1.089	0.066	1.302	0.052	1.578	0.039	1.971
C_{19}	0.062	0.953	0.047	1.156	0.037	1.424	0.028	1.843
C_{20+}	0.080	8.091	0.047	10.387	0.028	13.537	0.016	19.573
Total	100.000	100.000	100.000	100.000	100.000	100.000	100.000	100.000

measurement. The equilibrium liquid phase was kept intact and was allowed to come in contact with the fresh injection gas in the second stage and this process continued till the vapour phase remained similar to the original gas that is being injected. The measured liquid and vapour phase densities and interfacial tension data is furnished in Table 3.6.2.4 for all four stages. The predicted liquid and vapour phase compositions are provided in Table 3.6.2.5.

3.6.3 : Real Black Oil RFS-1

Three multiple contact tests were performed on the real black oil RFS-1 at 34.58 MPa and 100°C. Similar to the previously mentioned backward contact study on the real volatile oil, a four stage backward contact study was performed with pure methane as an injection gas, and two multiple forward contacts were performed with pure methane and a mixture of methane (79. 86 mole %) and carbon dioxide (20.14 mole %) respectively. These experiments were conducted in the vapour-liquid-equilibrium (V-L-E) facility.

The original single phase liquid composition of the real black oil is given in Table 3.6.3.1. About 100cc of this oil were loaded into one of the windowed PVT cells. Into this oil about 70cc of pure methane was injected. The mixture was then taken to equilibrium, at 34.58 MPa and the phase volumes, densities and compositions were recorded. The contact study was performed for altogether four stages till the resultant equilibrium vapour phase composition was virtually equal to 100 % methane. The two phase compositions are presented in Table 3.6.3.2. The event of equilibrium liquid droplets suspended on the pendant drop spout surrounded by its equilibrium vapour phase was recorded for each stage. The video recordings were subsequently employed to dimension the droplets and calculate the interfacial tension from it. The liquid and vapour phase densities and interfacial tension values for this test are provided in Table 3.6.3.3.

In the first forward contact test, about 50cc of the original RFS-1 oil were loaded into one of the windowed PVT cells. Into this oil about 120cc of pure methane was injected. The

Table 3.6.3.1 - Single Phase Composition of Real Black Oil RFS-1.

Component	Feed Composition Mole %
C_1	23.979
C_2	3.978
C_3	5.647
iC_4	1.998
nC_4	4.118
iC_5	2.090
nC_5	2.890
C_6	4.104
C_7	6.248
C_8	6.552
C_9	5.197
C_{10}	4.059
C_{11}	3.308
C_{12}	2.638
C_{13}	2.357
C_{14}	2.179
C_{15}	1.947
C_{16}	1.615
C_{17}	1.283
C_{18}	1.265
C_{19}	1.046
C_{20+}	11.503
Total	100

Table 3.6.3.2 - Phase Compositions for a Real Black Oil RFS-1 for a Four Stage Backward Contact Study with CH_4 at 34.58 MPa and 100°C.

	Stage 1		Stage 2		Stage 3		Stage 4	
	Vapour	Liquid	Vapour	Liquid	Vapour	Liquid	Vapour	Liquid
Component	Mole %	Mole %	Mole %	Mole %	Mole %	Mole %	Mole %	Mole %
C_1	83.413	59.623	88.856	58.553	92.375	59.343	95.039	59.094
C_2	1.809	1.782	0.798	0.804	0.285	0.292	0.086	0.089
C_3	2.207	2.632	1.095	1.402	0.457	0.627	0.171	0.254
iC_4	0.734	0.962	0.379	0.556	0.174	0.280	0.074	0.140
nC_4	1.278	1.945	0.735	1.244	0.356	0.656	0.161	0.339
iC_5	0.651	1.022	0.378	0.704	0.202	0.433	0.103	0.244
nC_5	0.763	1.354	0.491	1.001	0.271	0.614	0.143	0.377
C_6	1.108	2.067	0.797	1.734	0.580	1.303	0.370	0.996
C_7	1.486	3.271	1.079	2.984	0.787	2.453	0.514	1.963
C_8	1.362	3.559	1.030	3.482	0.748	3.086	0.515	2.628
C_9	1.002	2.734	0.756	2.850	0.600	2.690	0.425	2.457
C_{10}	0.730	2.279	0.584	2.495	0.470	2.509	0.343	2.405
C_{11}	0.515	1.756	0.410	1.984	0.336	2.013	0.249	1.936
C_{12}	0.407	1.441	0.337	1.761	0.285	1.977	0.215	2.109
C_{13}	0.330	1.319	0.279	1.628	0.240	1.820	0.178	1.937
C_{14}	0.310	1.247	0.266	1.628	0.236	1.831	0.186	1.976
C_{15}	0.239	1.092	0.220	1.394	0.188	1.664	0.146	1.909
C_{16}	0.197	1.014	0.184	1.343	0.172	1.580	0.129	1.695
C_{17}	0.116	0.673	0.109	0.938	0.103	1.126	0.083	1.358
C_{18}	0.125	0.728	0.112	0.993	0.103	1.194	0.078	1.376
C_{19}	0.098	0.617	0.089	0.856	0.082	1.032	0.063	1.201
C_{20+}	1.121	6.889	1.023	9.672	0.952	11.482	0.735	13.525
Total	100.000	100.000	100.000	100.000	100.000	100.000	100.000	100.000

Table 3.6.3.3 - Interfacial Tension Measurements on a Real Black Oil RFS-1 for a Backward Multiple Contact Study with CH_4 at 34.58 MPa and 100°C (Compositions in Table 3.6.3.2).

Stage No	Liquid Density gm/cc	Vapour Density gm/cc	Measured IFT* mN/m
2	0.6870	0.2390	2.189
3	0.7200	0.2170	3.319
4	0.7460	0.2060	4.515

* insufficient vapour in equilibrium did not allow IFT measurements for stage 1

Table 3.6.3.5 - Interfacial Tension Measurements on a Real Black Oil RFS-1 for a Forward Multiple Contact Study with CH_4 at 34.58 MPa and 100°C (Compositions in Table 3.6.3.4).

Stage No	Liquid Density gm/cc	Vapour Density gm/cc	Measured IFT mN/m
1	0.6920	0.2370	2.091
2	0.6420	0.2780	0.987
3	0.6110	0.3100	0.437

Table 3.6.3.7 - Interfacial Tension Measurements on a Real Black Oil RFS-1 for a Forward Multiple Contact Study with CH_4 (79.86 mole %) and Carbon Dioxide (20.14 mole %) at 34.58 MPa and 100°C (Compositions in Table 3.6.3.6).

Stage No	Liquid Density gm/cc	Vapour Density gm/cc	Measured IFT** mN/m
1	0.7070	0.3110	1.168
2	0.6430	0.3570	0.325

** insufficient vapour in equilibrium did not allow IFT measurements for stage 3

Table 3.6.3.4 - Phase Compositions for a Real Black Oil RFS-1 for a Three Stage Forward Contact Study with CH_4 at 34.58 MPa and 100°C.

	Stage 1		Stage 2		Stage 3	
	Vapour	Liquid	Vapour	Liquid	Vapour	Liquid
Component	Mole %	Mole %	Mole %	Mole %	Mole %	Mole %
C_1	91.795	59.191	86.883	60.110	83.323	60.485
C_2	0.740	0.684	1.507	1.365	2.157	1.911
C_3	1.024	1.273	1.817	2.222	2.142	2.896
iC_4	0.342	0.502	0.615	0.818	0.809	1.027
nC_4	0.687	1.161	1.212	1.799	1.589	2.198
iC_5	0.329	0.666	0.562	0.958	0.720	1.106
nC_5	0.438	0.953	0.741	1.354	0.954	1.531
C_6	0.585	1.462	0.888	1.855	1.116	1.972
C_7	0.844	2.780	1.264	3.212	1.558	3.275
C_8	0.874	3.450	1.280	3.771	1.558	3.748
C_9	0.566	2.627	0.799	2.694	0.970	2.566
C_{10}	0.439	2.547	0.606	2.358	0.747	2.190
C_{11}	0.309	2.103	0.421	1.965	0.521	1.738
C_{12}	0.227	2.005	0.305	1.681	0.378	1.494
C_{13}	0.170	1.737	0.233	1.398	0.293	1.244
C_{14}	0.148	1.451	0.194	1.187	0.244	1.045
C_{15}	0.132	1.423	0.172	1.165	0.223	1.004
C_{16}	0.092	1.173	0.120	0.914	0.162	0.813
C_{17}	0.066	0.956	0.090	0.769	0.116	0.652
C_{18}	0.059	1.049	0.079	0.731	0.108	0.639
C_{19}	0.044	0.938	0.061	0.638	0.084	0.526
C_{20+}	0.091	9.869	0.151	7.034	0.230	5.939
Total	100.000	100.000	100.000	100.000	100.000	100.000

Table 3.6.3.6 - Phase Compositions for a Real Black Oil RFS-1 for a Three Stage Forward Contact Study with CH_4 (79.86 mole %) and Carbon Dioxide (20.14 mole %) at 34.58 MPa and 100°C.

	Stage 1		Stage 2		Stage 3	
	Vapour	Liquid	Vapour	Liquid	Vapour	Liquid
Component	Mole %	Mole %	Mole %	Mole %	Mole %	Mole %
C_1	73.763	48.830	70.706	51.221	67.920	53.904
CO_2	16.897	14.329	14.039	12.176	11.322	10.553
C_2	0.766	0.727	1.513	1.412	2.184	2.039
C_3	1.087	1.288	2.031	2.249	2.809	2.952
iC_4	0.368	0.490	0.674	0.810	0.920	1.021
nC_4	0.745	1.125	1.347	1.763	1.820	2.137
iC_5	0.358	0.625	0.629	0.915	0.842	1.058
nC_5	0.473	0.887	0.828	1.268	1.115	1.444
C_6	0.632	1.336	1.034	1.730	1.345	1.849
C_7	0.922	2.479	1.448	2.896	1.895	2.935
C_8	0.994	3.152	1.534	3.455	2.012	3.349
C_9	0.656	2.377	0.975	2.430	1.287	2.272
C_{10}	0.525	2.174	0.763	2.150	1.016	1.940
C_{11}	0.378	1.862	0.537	1.655	0.730	1.463
C_{12}	0.288	1.667	0.397	1.384	0.540	1.198
C_{13}	0.231	1.509	0.318	1.259	0.432	1.070
C_{14}	0.195	1.334	0.261	1.074	0.358	0.891
C_{15}	0.180	1.346	0.229	1.018	0.348	0.833
C_{16}	0.127	1.092	0.169	0.814	0.226	0.659
C_{17}	0.100	0.959	0.127	0.678	0.193	0.534
C_{18}	0.086	0.915	0.114	0.668	0.176	0.525
C_{19}	0.068	0.785	0.090	0.579	0.140	0.442
C_{20+}	0.161	8.713	0.236	6.397	0.370	4.934
Total	100.000	100.000	100.000	100.000	100.000	100.000

mixture was then taken to equilibrium, at 34.58 MPa and the phase volumes, densities and compositions were recorded. The contact study was performed for altogether three stages till there was no mass transfer between the rich vapour and the fresh oil added as a feed at the start of each stage. The two phase compositions are presented in Table 3.6.3.4. The event of equilibrium liquid droplets suspended on the pendant drop spout surrounded by its equilibrium vapour phase was recorded for each stage. The video recordings were subsequently employed to dimension the droplets and calculate the interfacial tension from it. The liquid and vapour phase densities and interfacial tension values for this test are provided in Table 3.6.3.5. In the second forward contact test with the injection gas mixture consisting of methane and carbon dioxide, again 50cc of the original RFS-1 oil were loaded into one of the windowed PVT cells. Into this oil about 110cc of the methane (79.86 mole %) and carbon dioxide (20.14 mole %) gas mixture was injected. The mixture was then taken to equilibrium at 34.58 MPa and the phase volumes, densities and compositions were recorded. This study was performed for altogether three stages till the test was on the verge of approaching miscible conditions. The two phase compositions for this test are presented in Table 3.6.3.6 and the two phase densities and interfacial tension values are provided in Table 3.6.3.7.

3.6.4 : Near Critical Fluid

A series of constant composition expansion (CCE) tests were performed on a near critical real fluid at 50, 80, 100, 120, 140°C. The CCE test at 140°C was carried out in the gas condensate facility whereas the tests were performed in the VLE facility at other temperatures. The gas-liquid interface thickness was recorded at various different temperatures below the dew point pressure for various isotherms. These recordings were later dimensioned for calculating the interfacial tension values. The measured IFT values are furnished in Table 3.6.4.1 and Figure 3.6.4.1. The single phase composition of this fluid is given in Table 3.6.4.2, no compositional measurements or predictions were carried out for this fluid.

Table 3.6.4.1 - Interfacial Tension Measurements on a Real Near Critical Fluid at Various Temperatures.

Pressure (MPa)	Liquid Density gm/cc	Vapour Density gm/cc	Measured IFT mN/m
<u>50°C</u>			
30.34	0.5004	0.3832	0.0210
28.96	0.5241	0.3514	0.0659
27.58	0.5455	0.3261	0.1333
<u>80°C</u>			
31.72	0.4653	0.3892	0.0045
31.03	0.4803	0.3606	0.0139
30.34	0.4947	0.3443	0.0383
28.96	0.5171	0.3151	0.1179
27.58	0.5348	0.2915	0.2237
<u>100°C</u>			
31.72	0.4622	0.3614	0.0062
31.03	0.4811	0.3387	0.0236
30.34	0.4922	0.3221	0.0404
28.96	0.5110	0.2943	0.1109
27.58	0.5257	0.2732	0.2092
<u>120°C</u>			
31.72	0.4566	0.3470	0.0029
31.03	0.4728	0.3251	0.0172
30.34	0.4834	0.3098	0.0443
28.96	0.5025	0.2837	0.1120
27.58	0.5164	0.2617	0.2193
<u>140°C</u>			
30.34	0.4613	0.3102	0.0036
28.96	0.4866	0.2800	0.0339
27.58	0.5010	0.2634	0.0850
13.79	0.6130	0.1077	2.3610

Table 3.6.4.2 - Single Phase Composition of Real Near Critical Fluid.

Component	Feed Composition Mole %
N_2	0.36
C_1	69.95
CO_2	0.29
C_2	10.04
C_3	4.27
iC_4	0.50
nC_4	1.50
iC_5	0.31
nC_5	0.85
C_6	0.91
C_7	1.77
C_8	1.99
C_9	1.59
C_{10}	1.15
C_{11}	0.75
C_{12}	0.56
C_{13}	0.59
C_{14}	0.43
C_{15}	0.36
C_{16}	0.26
C_{17}	0.23
C_{18}	0.13
C_{19}	0.17
C_{20+}	1.05
Total	100.00

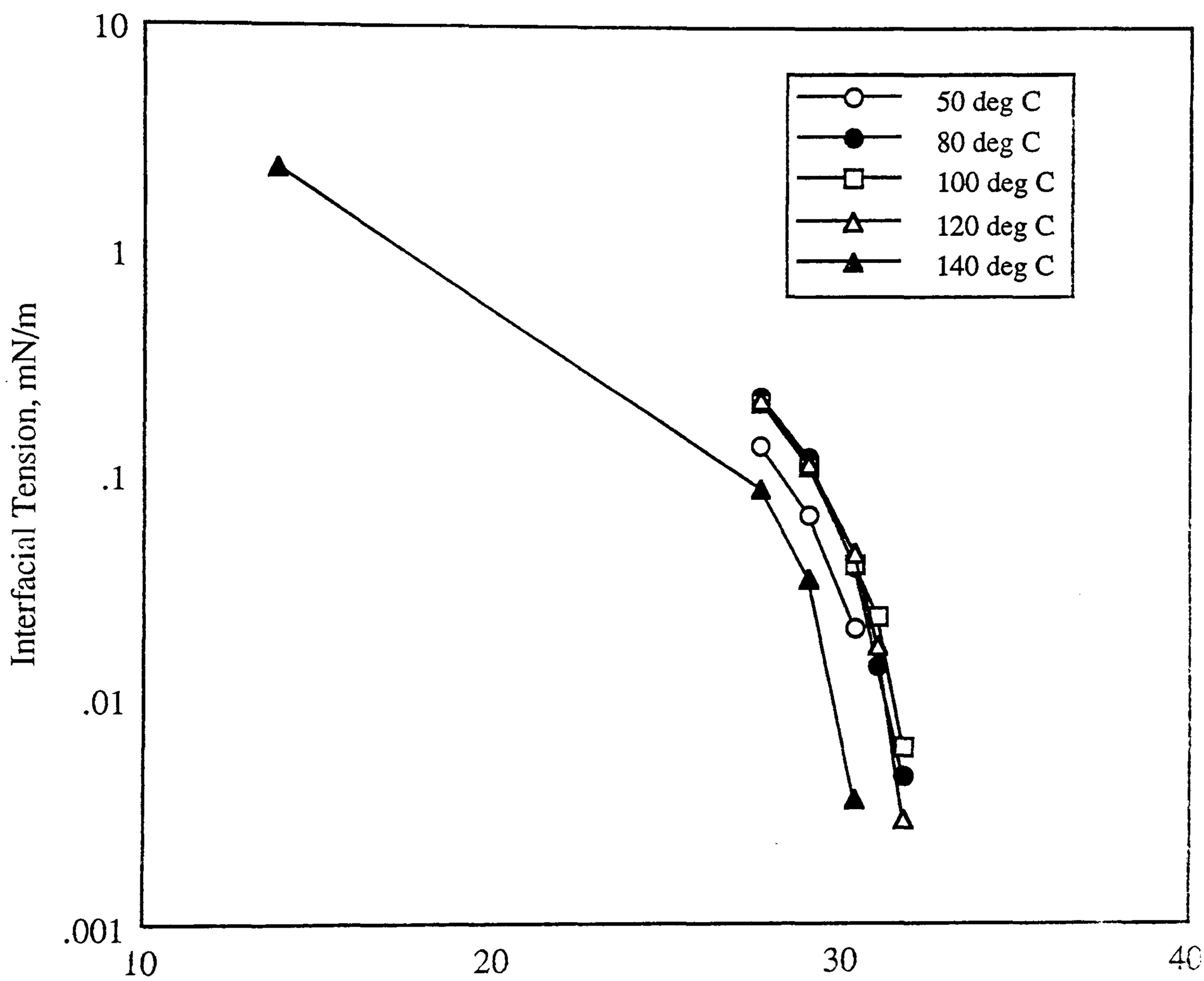

Figure 3.6.4.1 - Interfacial Tension data on a Real Near Critical Fluid at Various Temperatures.

3.7 : ERROR ANALYSIS

This section presents the error analysis carried out on the newly developed gas-liquid curvature technique and the pendant drop method in the gas condensate PVT cell and the vapour-liquid-equilibrium (V-L-E) apparatus respectively. The data of synthetic mixtures for which the interfacial tensions were measured using these methods are used to estimate the inaccuracies in measurement. The inaccuracies are calculated for different ranges of IFT measured.

The correlation used for the gas-liquid interface technique (Eq. 3.4.1.22) is :

$$\sigma = \frac{1}{2} h^2 g(\rho_l - \rho_v) \qquad (3.7.1)$$

Where,

σ = interfacial tension

h = the meniscus bandwidth or the interface thickness

$\rho_l - \rho_v$ = the difference between the liquid and vapour phase densities and

g = acceleration due to gravity

Taking partial derivatives of Eq. 3.7.1 with respect to the film height h, liquid density ρ_l and gas density ρ_v :

$$\frac{d\sigma}{dh} = gh\Delta\rho$$

$$\frac{d\sigma}{d\rho_l} = \frac{gh^2}{2}$$

$$\frac{d\sigma}{d\rho_v} = -\frac{gh^2}{2} \qquad (3.7.2\ a, b, c)$$

Using the above set of equations a single differential equation can be formed to represent the error in measuring interfacial tension :

$$d\sigma = \frac{d\sigma}{dh}\Delta h + \frac{d\sigma}{d\rho_l}\Delta\rho_l + \frac{d\sigma}{d\rho_v}\Delta\rho_v \qquad (3.7.3)$$

Whereas Δh, $\Delta\rho_l$ and $\Delta\rho_v$ are the errors in measuring the gas-liquid interface height, liquid density and the vapour density. Hence, the percentage inaccuracy in measuring the interfacial tension can be calculated from :

$$\text{Inaccuracy} = \frac{d\sigma}{\sigma} * 100\ \% \qquad (3.7.4)$$

The estimated error in measuring the gas-liquid interface height h, using the VMS300 video scalar unit is $\pm$ 0.011mm, for the liquid density is 0.0003gm/cc and for the vapour density is 0.0001gm/cc. Employing these errors estimated and the interfacial tension data measured for various synthetic mixtures, the estimated errors for the gas-liquid interface technique are furnished in Table 3.7.1.

Similar analysis has been performed for the pendant drop method. The basic correlation for using the pendant drop method is (Eq. 2.2.1):

$$\sigma = \frac{(\rho_l - \rho_v)g d_e^2}{H} \qquad (3.7.5)$$

Where,

σ = interfacial tension

$\rho_l - \rho_v$ = the density difference between the liquid and vapour phases

d_e = the maximum horizontal (equatorial) diameter of the drop

H = the drop shape factor and

g = acceleration due to gravity

Taking partial derivatives of Eq. 3.7.5 with respect to the equatorial diameter d_e, liquid density ρ_l and vapour density ρ_v :

Table 3.7.1 - Error Analysis for the Gas-Liquid Interface Technique.

IFT, mN/m	Error (%)
0.01-0.1	7.5
0.1-1	3.7
1-10	1.8

Table 3.7.2 - Error Analysis for the Pendant Drop Technique.

IFT, mN/m	Error (%)
0.07-0.1	5.0
0.1-1	3.3
1-10	1.9

$$\frac{d\sigma}{dd_e} = \frac{2\Delta\rho g d_e}{H}$$

$$\frac{d\sigma}{d\rho_l} = \frac{g d_e^2}{H}$$

$$\frac{d\sigma}{d\rho_v} = -\frac{g d_e^2}{H} \qquad (3.7.6\ a, b, c)$$

Similar to Eq. 3.7.3 we have :

$$d\sigma = \frac{d\sigma}{dd_e}\Delta d_e + \frac{d\sigma}{d\rho_l}\Delta\rho_l + \frac{d\sigma}{d\rho_v}\Delta\rho_v \qquad (3.7.7)$$

Whereas Δd_e, $\Delta\rho_l$ and $\Delta\rho_v$ are the errors in measuring the equatorial diameter, liquid and vapour density. The estimated error in measuring d_e is $\pm$ 0.008mm, for the liquid density is 0.0003 gm/cc and for the vapour density is 0.0001 gm/cc. Hence from Eq. 3.7.4 the errors for the pendant drop method can also be estimated and are presented in Table 3.7.2.

References

1) Danesh, A., Todd, A.C., Somerville, J. and Dandekar, A.: "Direct Measurement of Interfacial Tension, Density, Volume, and Compositions of Gas - Condensate System", *Trans IChem E*, Vol. 68, *Part A*, pp. 325-330, (Jul., 1990).

2) Danesh, A. and Todd, A.C.: "A Novel Sampling Method for Compositional Analysis of High Pressure Fluids", *Fluid Phase Equilibria*, Vol. 57, pp. 161-171, (1990).

3) Groenveld, P.: "High Capillary Number Withdrawal from Viscous Newtonian Liquids by Flat Plates", *Chemical Engineering Science*, Vol. 25, pp. 33-40, (1970).

4) Wilson, S.D.R. and Jones, A.F.: "The Entry of a Falling Film into a Pool and Air Entrainment Problem", *J. Fluid Mech.*, Vol. 128, pp. 219-230, (1983).

5) Lee, Chien. Y. and Tallmadge, J.A.: "Meniscus Shapes in Withdrawal of Flat Sheets from Liquid Baths. 2. A Quasi - one - Dimensional Flow Model for Low Capillary Numbers", *Industrial & Engineering Chemistry (I & EC) Fundamentals*, Vol. 14, No. 2, pp. 120-126, (1975).

6) Inverarity, G.: "Dynamic Wetting of Glass Fibre and Polymer Fibre", *British Polymer Journal*, Vol. 1, pp. 245-251, (Nov., 1969).

7) Burley, R. and Kennedy, B.S.: "A Study of the Dynamic Wetting Behaviour of Polyester Tapes", *The British Polymer Journal*, pp. 140-143, (Dec., 1976).

8) White, D.A. and Tallmadge, J.A.: "A Theory of Withdrawal of Cylinders from Liquid Baths", *AIChEJ*, Vol. 12, No. 2, (Mar., 1966).

9) Tallmadge, J.A. and White, D.A.: "Film Properties and Design Procedures in Cylinder Withdrawal", *Industrial & Engineering Chemistry (I & EC) Process Design & Development*, Vol. 7, No. 4, pp. 503-508, (Oct., 1968).

10) White, D.A. and Tallmadge, J.A.: "A Gravity Corrected Theory for Cylinder Withdrawal", *AIChEJ*, Vol. 13, No. 4, pp. 745-750, (Jul., 1967).

11) White, D.A. and Tallmadge, J.A.: "Static Menisci on the Outside of Cylinders", *J. Fluid Mech.* Vol. 23, Part 2, pp. 325-335, (1965).

12) Kennedy, B.S. and Burley, R.: "Dynamic Fluid Interface Displacement and Prediction of Air Entrainment", *J. Col. & Int. Sci.*, Vol. 62, No.1, pp. 48-62, (Oct., 1977).

13) Danesh, A., Henderson, G.D., Krinis, D. and Peden J.M.: Paper Presented at the SPE 63 rd Annual Tech. Conf., Houston, Texas, SPE 18316, (1988).

14) Cahn, J.W.: "Critical Point Wetting", *The J. Chem. Physics*, Vol. 66, No. 8, pp. 3667-3672, (April, 1977).

15) Sage, B.H., Hicks, B.L. and Lacey, W.N.: "Phase Equilibria in Hydrocarbon Systems, The Methane - n - Butane System in the Two Phase Region", *Industrial & Engineering Chemistry (I & EC)*, Vol. 32, No. 8, pp. 1088-1091.

16) Pennington, B.F. and Hough, E.W.: "Interfacial Tension of the Methane - Normal Butane System", *Producers Monthly*, pp. 4, (Jul., 1965).

17) Stegemeier, G.L., Pennington, B.F., Brauer, E.B. and Hough, E.W.: "Interfacial Tension of the Methane - Normal Decane System", *Society of Petroleum Engineers Journal (SPEJ)*, pp. 257-260, (Sep., 1962).

18) Sage, B.H. and Lacey, W.N.:"Thermodynamic Properties of the Lighter Paraffin Hydrocarbons and Nitrogen", API, New York, (1950).

19) Haniff, M.S. and Pearce, A.J.: "Measuring Interfacial Tension in a Methane - Propane Gas - Condensate System Using a Laser Light Scattering Technique", SPE 19025, (1988).

20) Sage, B.H, Lacey, W.N. and Schaefsma, J.G.: "Phase Equilibria in Hydrocarbon Systems", *Industrial & Engineering Chemistry (I & EC)*, Vol. 26, pp. 214-217, (1934).

21) Reamer, H.H, Sage, B.H. and Lacey, W.N.: "Phase Equilibria in Hydrocarbon Systems", *Industrial & Engineering Chemistry (I & EC)*, Vol. 42, pp. 534-539, (1950).

22) Gasem, K.A.M., Dickson, K.B., Dulcamara, P.B., Nagarajan, N. and Robinson, R.L.Jr.: "Equilibrium Phase Compositions, Phase Densities, and Interfacial Tensions for CO_2 + Hydrocarbon Systems. 5. CO_2 + n - Tetradecane", *J. Chem & Engg. Data*, Vol. 34, No.2, pp. 191-195, (1989).

23) Adam, N.K.: "The Physics and Chemistry of Surfaces", Oxford University Press, London, 3rd Edition, (1941).

CHAPTER 4 : PREDICTIVE TECHNIQUES FOR INTERFACIAL TENSION

4.1 : INTRODUCTION

In this chapter some of the predictive techniques for estimating the interfacial tension (IFT) are reviewed in details. The IFT of hydrocarbon mixtures at high pressures can be estimated by several methods. Although all the methods have theoretical foundations, they rely to certain extent on experimentally determined parameters.

The lack of reliable experimental data and the need for good IFT values have sustained a continuous interest for past sixty years in the development of correlations to predict this property. Several methods have been devised which make use of the various properties of the fluids, such as density[2,3,4,5], liquid compressibility[6,7], and the enthalpy of vaporisation[8]. More recently, Sivaraman et. al.[9], used the latent heat of vaporisation to predict IFT of pure alkanes, napthenic and aromatic compounds over a wide range of temperature from freezing to the critical point of the fluids. Here the most widely used correlations in the petroleum industry are discussed in details.

4.2 : PARACHOR METHOD

This is the most commonly used method, which correlates the density difference of the liquid and vapour phases with the IFT. It was first developed by Macleod[3], for pure component systems, and later modified by Sugden[4], who introduced the parachor concept. Weinaug and Katz[5], introduced simple mixing rules to allow the prediction of the IFT of mixtures.

It was first observed by Macleod[3], that the interfacial tension (σ) of pure components was related to the density difference between the liquid and saturated vapour by the expression :

$$\sigma = C (\Delta\rho)^E \qquad (4.2.1)$$

Eq. 4.2.1, was later modified by Sugden[4], to obtain the following:

$$\sigma^{1/E} = [P] \frac{\Delta\rho}{M} \qquad (4.2.2)$$

The quantity [P], is the property called parachor, which is the property of each compound and is discussed further in Section 4.2.1. E, is the exponent equal to 4 as proposed by Macleod[3], in the original Eq. 4.2.2, and M, is the molecular weight of the pure compound. Weinaug and Katz[5], improved Eq. 4.2.2 to make it applicable to mixtures and proposed the following:

$$\sigma^{1/E} = \sum_{i=1}^{n} \rho_{lm}(P_i X_i) - \rho_{vm}(P_i Y_i) \qquad (4.2.3)$$

Where,

σ = interfacial tension

E = the exponent ; = 4

ρ_{lm} = the molar liquid density

P_i = the parachor of the ith component

X_i = liquid mole fraction of the ith component

ρ_{vm} = the molar vapour density and

Y_i = vapour mole fraction of the ith component

It is evident that a simple molar mixing rule is used to obtain the parachors of the liquid ($\Sigma P_i X_i$) and the vapour ($\Sigma P_i Y_i$) respectively. For prediction of IFT of hydrocarbons, the compositional and density data obtained either from experimentation or from EOS models can be used. The parachor values for various pure components have been reported by several authors[4,5,8]. Hough and Stegemeier[8], have given a plot of parachor against the carbon numbers for normal paraffins ranging from C_1 to C_{20} (Figure 4.2.1), it follows a well

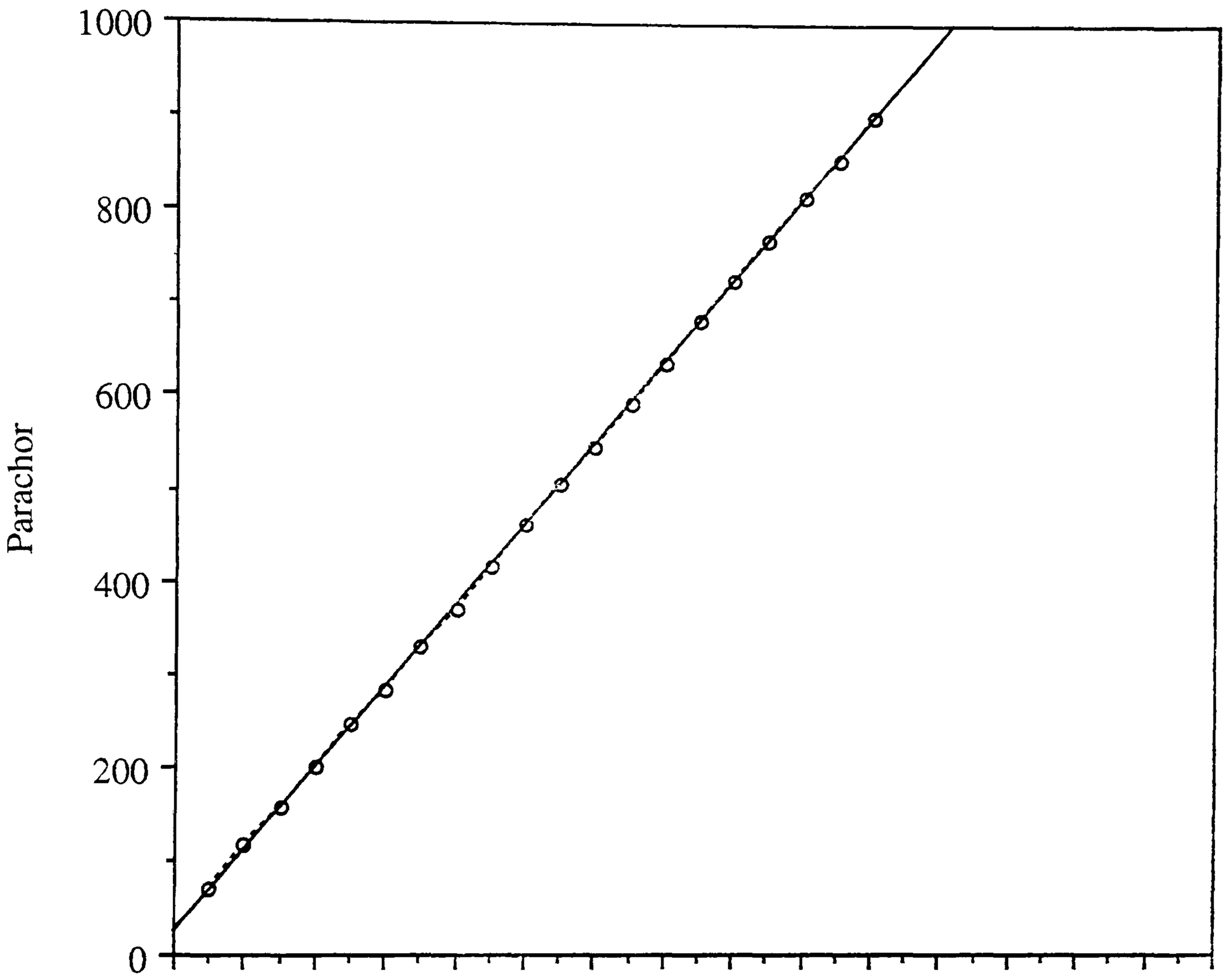

Figure 4.2.1 - Plot of Carbon Number vs. Parachor for normal Alkanes (from Reference 8).

defined linear relationship which can be used for evaluating parachor values for normal paraffins hydrocarbons for predicting IFTs using Eq. 4.2.2 or 4.2.3. From Figure 4.2.1:

$$P_\sigma = 23.85 + 43.73C_N \qquad (4.2.4)$$

where,

P_σ = parachor of a normal paraffin and

C_N = carbon number

This method is suitable only for synthetic mixtures with well defined compositions. However, for the real reservoir fluids the exact composition is usually not known. All isomers are combined in groups such as C_6's, C_7's etc. To obtain the parachors for such groups, correlations of parachors with molecular weight of the hydrocarbon compounds were introduced by Katz and Monroe[22], Figure 4.2.2. They measured the surface tension of C_{7+} residues of various crudes to prepare Figure 4.2.2. However, it has been indicated by Firoozabadi et. al.[11] that this approach underestimates the interfacial tension in a certain range. This could be attributed to the limited range of data employed in the approach of Katz et. al.[22]. In order to circumvent this problem, Firoozabadi et al[11], determined parachors of a wide range of crude oil fractions with a broad band of molecular weights and proposed the following correlation (Figure 4.2.3):

$$P_\sigma = -11.4 + 3.23\ M - 0.0022\ M^2 \qquad (4.2.5)$$

Where,

$P\sigma$ = the parachor of the plus fraction of a real reservoir fluid and

M = the molecular weight of the plus fraction of a real reservoir fluid

Eq. 4.2.5, should not be used to evaluate parachor of the oil heavy end, which generally contains a high concentration of asphaltic materials.

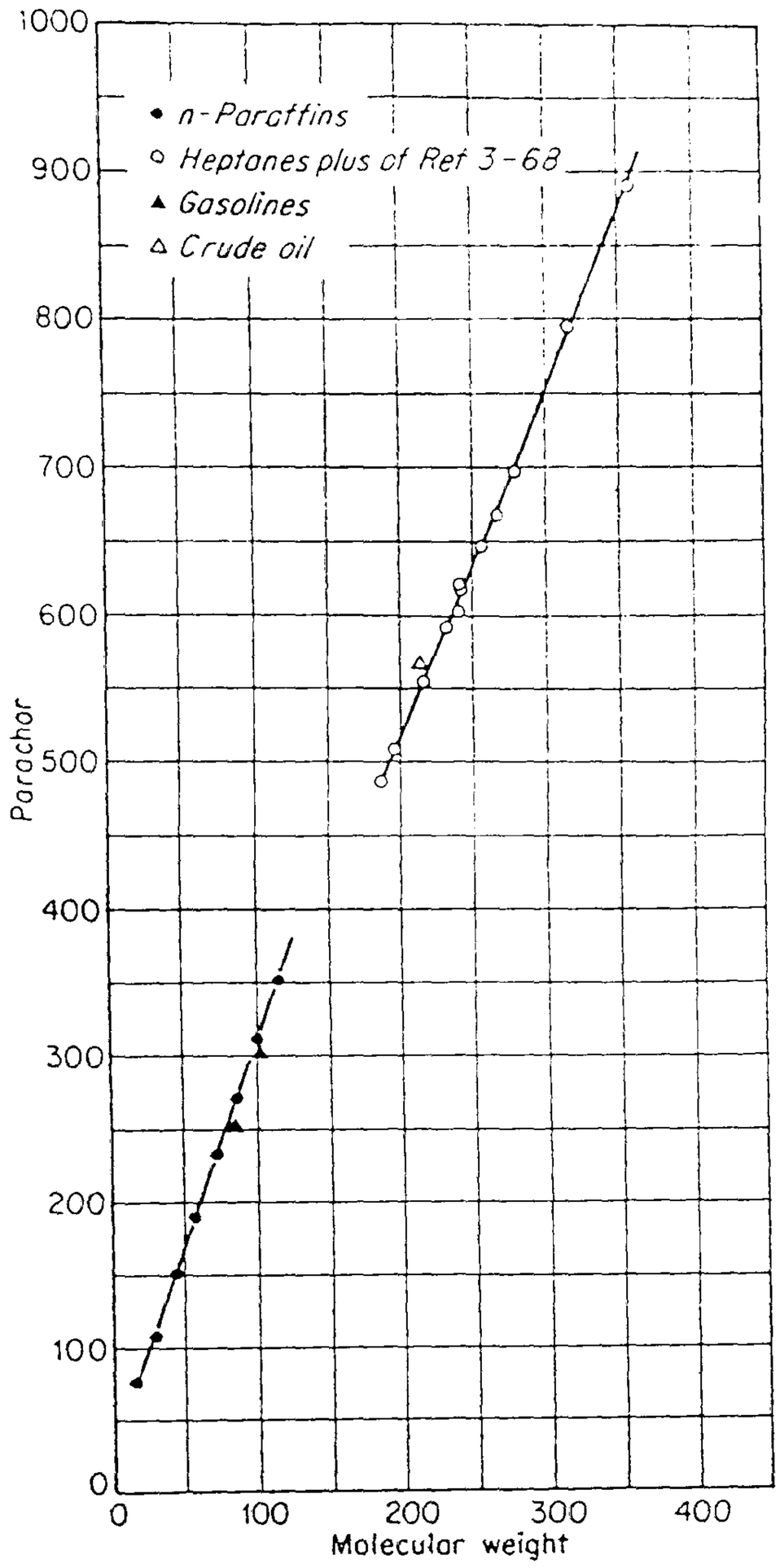

Figure 4.2.2 - Parachors for Hydrocarbons (from Reference 22).

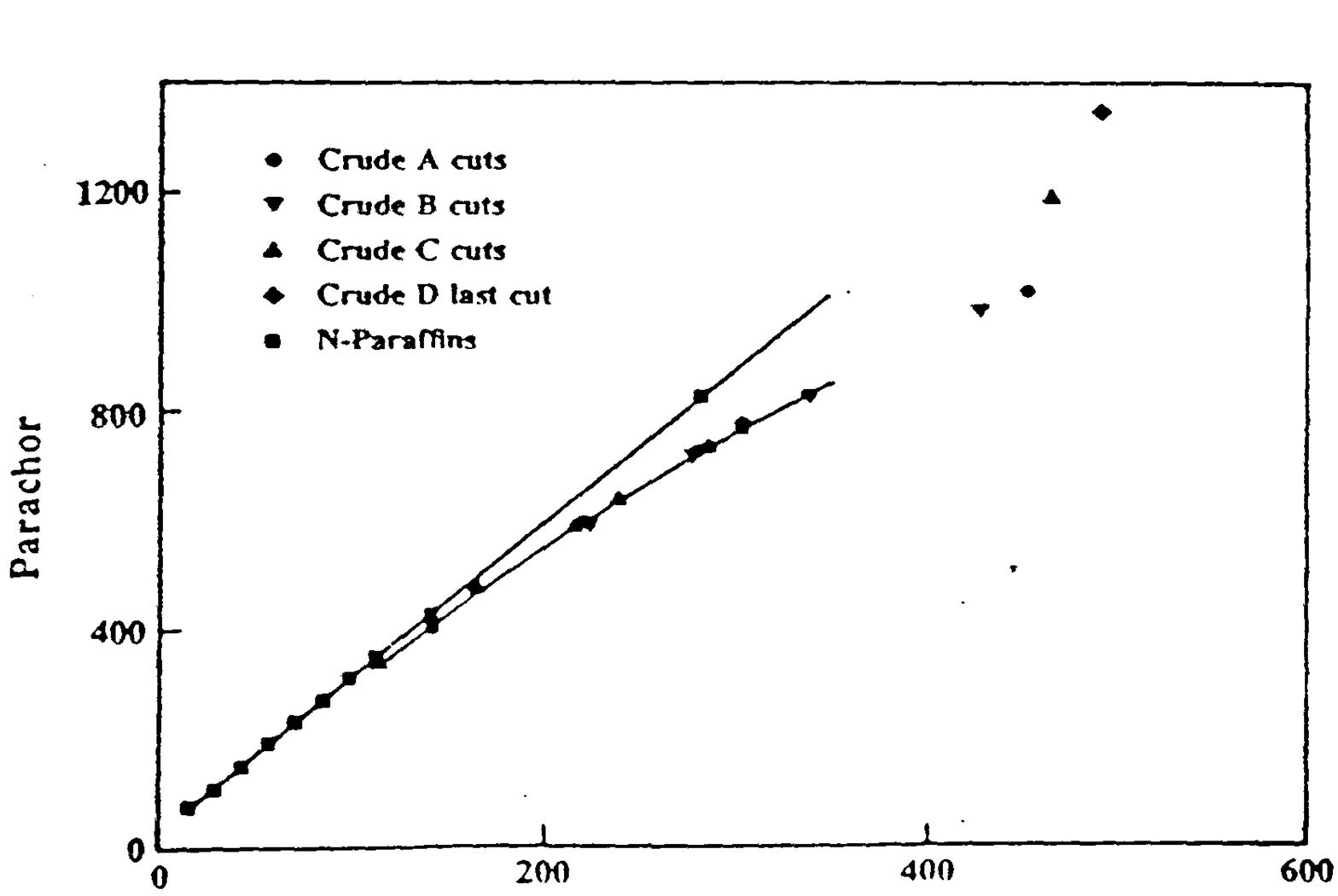

Figure 4.2.3 - Parachors vs. Molecular Weight for Crude Cuts and n-Paraffins. (from Reference 11).

4.2.1 : Hough and Stegemeier's Method

The correlation proposed by the above authors[8] is based on the approximate relationships between the physical and critical properties of pure normal paraffins. It has been observed[8] that the following relationships are good approximations for relating the surface tension, difference between density of the liquid and vapour, absolute temperature and critical temperature for propane and n-butane.

For Propane,

$$\Delta\rho = 0.80\ (1-T/T_c)^{0.326} \qquad (4.2.1.1)$$

$$\sigma = 49.5\ (1-T/T_c)^{1.20} \qquad (4.2.1.2)$$

$$\sigma/\Delta\rho = 61.9\ (1-T/T_c)^{0.874} \text{ and} \qquad (4.2.1.3)$$

$$\sigma = 112.5\ \Delta\rho^{3.68} \qquad (4.2.1.4)$$

For n-butane

$$\Delta\rho = 0.86\ (1-T/T_c)^{0.333} \qquad (4.2.1.5)$$

$$\sigma = 52.5\ (1-T/T_c)^{1.22} \qquad (4.2.1.6)$$

$$\sigma/\Delta\rho = 61.0\ (1-T/T_c)^{0.887} \text{ and} \qquad (4.2.1.7)$$

$$\sigma = 91.2\ \Delta\rho^{3.66} \qquad (4.2.1.8)$$

Guggenheim's[23] values for these constants, not specifically for hydrocarbons, are :

$$\Delta\rho = C'\ (1-T/T_c)^{1/3} \qquad (4.2.1.9)$$

$$\sigma = C'' (1-T/T_c)^{11/9} \qquad (4.2.1.10)$$

$$\sigma/\Delta\rho = C''' (1-T/T_c)^{8/9} \text{ and} \qquad (4.2.1.11)$$

$$\sigma = C \Delta\rho^{11/3} \qquad (4.2.1.12)$$

where,

$\Delta\rho$ = difference in density of the liquid and vapour phases

σ = surface tension

T = absolute temperature

T_c = critical temperature and

C', C'', C''' = constants

Eq. 4.2.1.12 may be recognised as the surface tension-density difference relationship leading to Sugden's[4] parachor, (Eq. 4.2.1) with the exponent "3/11" rather than "1/4". That is:

$$P = M C^{3/11} = \frac{M \sigma^{3/11}}{\Delta\rho} \qquad (4.2.1.13)$$

where,

P = parachor and

M = molecular weight

Hence, Eq. 4.2.3 can be applied to multicomponent mixtures with the exponent value of E = 3.67 instead of 4 as Hough-Stegemeier's approach[8].

4.2.2 : Sugden's Parachor

In this section a brief description on the physical significance of parachors is given. It has long been recognised that the molecular volume of an organic compound depends on its

chemical constituents, and may be used in the case of liquids of uncertain constitution as a guide to estimate their composition. The principle underlying this view is that different atomic groupings have characteristic shapes and sizes and will therefore probably occupy characteristic volumes in liquids, the total volume of the liquid being the sum of the characteristic volumes of the separate groups of the molecules. The difficulty in practical application has always been that the volumes of liquids change with temperature, as the thermal motions of the molecules gradually overcome the cohesional forces between them, and no really satisfactory basis for choosing the correct temperature at which to compare the molecular volumes was found for a long time. Sugden[14], however pointed out that MacLeod's[3], relationship of density difference against IFT can form a good basis for the comparison of molecular volumes under conditions where the effect of temperature is neutralised by taking into account the IFT.

Now from Eq. 4.2.2 the constant [P] equals :

$$[P] = \frac{M}{\Delta\rho}\sigma^{1/E} \qquad (4.2.2.1)$$

the right hand side of the Eq. 4.2.2.1, is the product of IFT raised to a quarter (when a value of, E=4, is taken) and the molecular volume which is molecular weight divided by the density difference between liquid and vapour phase.

This particular term [P] on the left hand side of Eq. 4.2.2.1 has been termed by Sugden[14], as 'parachor'. Parachor is a property independent from pressure and temperature. Hence, by experimentation the parachor can be evaluated for each pure compound if the measured interfacial tension, density difference between liquid and vapour phases, and the molecular weights are substituted in Eq. 4.2.2.1.

4.2.3 : Fanchi's Method for Estimating Parachor

Fanchi[12], performed a linear regression analysis relating the critical properties (V_c and T_c) and parachor of normal paraffins ranging from C_1 to C_7 to develop an expression for the

prediction of parachors. The following equation resulted after the analysis for the parachor, P_σ:

$$P_\sigma = a_0 + a_1 V_c + a_2 T_c + a_3 H + a_4 H^2 + a_5 H^3 + \frac{a_6}{H} \qquad (4.2.3.1)$$

Where H denotes the Herzog's[13] parameter and is defined by :

$$H = V_c^{5/6} T_c^{1/4} \qquad (4.2.3.2)$$

Where,

V_c = critical volume of the compound and

T_c = critical temperature of the compound

The coefficients of the regression equation ; a_0-a_6 have the following values :

$a_0 = -72.765582$

$a_1 = -9166.37732$

$a_2 = -1.07786869$

$a_3 = 2197.28955$

$a_4 = -111.984168$

$a_5 = 20.4550431$

$a_6 = 55.9694357$

The above correlation gives a very good match of parachor values with those reported by Amyx et al[10], for pure normal paraffin hydrocarbons from C_1 to C_7, but values of parachors estimated by the above method for components having carbon number greater than seven gives substantially high values which subsequently results in very high IFTs. This could be attributed to the use of limited data, only upto C_7, in regression analysis, hence the extrapolation beyond C_7 would obviously result in unreliable values for the parachor.

In a recent publication Fanchi[17] provided an updated regression analysis for calculation of parachors, by adding data of hydrocarbons for C_8 up to C_{20} for pure components to the

original data set of C_1 to C_7 in order to improve the estimation of parachors for high-molecular weight components. The regression equation was maintained in its original form[12], since the trial of a number of functional relationships based on the data of Amyx et al[10], had revealed that the original expression best describes a relationship between parachor, critical volume and critical temperature. The new regression coefficients have the following values:

$$a_0 = 176.05005$$

$$a_1 = -7472.9807$$

$$a_2 = -0.87458088$$

$$a_3 = 1560.4793$$

$$a_4 = 19.309439$$

$$a_5 = 0.05013801$$

$$a_6 = -25.691718$$

4.3 : SCALING LAW

As the interfacial tension (IFT) vanishes at the critical point its variation can be scaled according to the proximity of the test condition to the critical point. The reduction of IFT with increasing temperature can be expressed via a relationship :

$$\sigma \sim (1 - T_r)^{\theta} \qquad (4.3.1)$$

Brock and Bird[2], incorporated a proportionality constant A_c, a parameter based on the law of the corresponding states, so that Eq. 4.3.1, becomes :

$$\sigma = A_c (1 - T_r)^{\theta} \qquad (4.3.2)$$

A_c can be evaluated from :

$$A_c = P_c^{2/3} T_c^{1/3} (0.133\alpha_c - 0.281) \quad (4.3.3)$$

and $\theta = \frac{11}{9}$

the Riedel parameter, α_c, is directly obtained from Reid and Sherwood[16], or it can be evaluated from the following expression suggested by Miller[15]:

$$\alpha_c = 0.9076 \left[1.0 + \frac{\frac{T_b}{T_c} \ln \frac{P_c}{P_a}}{1-\frac{T_b}{T_c}} \right] \quad (4.3.4)$$

Where,

σ = interfacial tension

T_r = reduced temperature

θ = the scaling law constant exponent

A_c = proportionality constant, defined by Eq. 4.3.3

P_c = critical pressure

T_c = critical temperature

α_c = the Riedel parameter, defined by Eq. 4.3.4

T_b = boiling temperature and

P_a = atmospheric pressure

Lee and Chien[15] replaced the quantity of scale temperature by proposing density difference as :

$$(\rho_l - \rho_v) \sim (T_c - T)^{\beta} \quad (4.3.5)$$

substituting ($\beta = \frac{5}{16}$) into Eq. 4.3.5 and introducing a proportionality constant B':

$$(\rho_l - \rho_v) = B'(T_c - T)^{\beta} \quad (4.3.6)$$

after performing the dimensional analysis to define the relationship between the density difference and critical temperature differences :

$$\frac{\rho_l - \rho_v}{\rho_c} = B(1- T_r)\beta \qquad (4.3.7)$$

where B is defined as :

$$B = C\, Z_c^n \qquad (4.3.8)$$

where,

C = dimensionless constant in Eq. 4.3.8

Z_c = critical compressibility factor and

n = exponent to be fitted in Eq. 4.3.8

substituting Eq. 4.3.7 and Eq. 4.3.8 into Eq. 4.3.2 yields :

$$\sigma^{\beta/\theta} = [P] (\rho_{lm} - \rho_{vm}) \qquad (4.3.9)$$

Where:

$$[P] = \frac{A_c^{\beta/\theta} V_c}{B} \qquad \text{and} \qquad \rho_c = \frac{M}{V_c}$$

and substituting the values of, θ and β, in Eq. 4.3.9:

$$\sigma^{0.25568} = [P] (\rho_{lm} - \rho_{vm}) \qquad (4.3.10)$$

Eq. 4.3.10 is very similar to the one fourth power rule (E = 0.25) suggested by Macleod and Sugden[3,4], here ($\rho_{lm} - \rho_{vm}$) stand for the molar density difference and [P] is the mixture parachor. Expression for parachor can be derived from previous set of Equations as :

$$[P] = \frac{A_c^{\beta/\theta} V_c}{B} \qquad (4.3.11)$$

constant B can be obtained from Reference[15] where B values calculated from measured surface tension data for normal paraffins are tabulated for methane to n - hexadecane, Table 4.3.1. For hydrocarbons ranging from C_2 to C_8, B can be accurately estimated from the following expression suggested by Lee and Chien[15]:

$$B = 1.854426\, Z_c^{-0.52402} \qquad (4.3.12)$$

The set of equations proposed by Lee and Chien[15] predicts the parachor values of pure components within 1 % of those reported by other methods.

Eq. 4.3.10, 4.3.11 and 4.3.12 can easily be employed for estimating the IFT of a single component and mixtures. Considering the approach of Weinaug and Katz[5], from Eq. 4.3.10 :

$$\sigma^{0.25568} = \rho_{lm}\,[P_l] - \rho_{vm}\,[P_v] \qquad (4.3.13)$$

where $[P_l]$ and $[P_v]$ are the parachors for the liquid phase and vapour phase of the mixtures respectively. One can observe that Eq. 4.2.3 is the same as Eq. 4.3.13 but in which simple compositional mixing rule is used.

Following are the mixing rules proposed by Lee and Chien[15] to calculate the parameters for calculating the liquid and vapour phase parachors for use in Eq. 4.3.13:

Table 4.3.1 - Calculated Values of B from Measured Surface Tension Data for normal Paraffins (from Reference 15).

Compound	B
CH_4	3.409
C_2H_6	3.630
C_3H_8	3.681
nC_4	3.687
nC_5	3.695
nC_6	3.726
nC_8	3.852
nC_9	3.865
nC_{10}	3.855
nC_{11}	3.641
nC_{12}	3.815
nC_{13}	3.872
nC_{14}	3.820
nC_{15}	3.795
nC_{16}	3.822

$$V_{cl} = \sum_{i=1}^{n} X_i V_{ci}$$

$$B_l = \sum_{i=1}^{n} X_i B_i$$

$$P_{cl} = \sum_{i=1}^{n} X_i P_{ci}$$

$$T_{cl} = \sum_{i=1}^{n} X_i T_{ci}$$

$$\alpha_{cl} = \sum_{i=1}^{n} X_i \alpha_{ci}$$

(4.3.14 - 4.3.18)

$$V_{cv} = \sum_{i=1}^{n} Y_i V_{ci}$$

$$B_v = \sum_{i=1}^{n} Y_i B_i$$

$$P_{cv} = \sum_{i=1}^{n} Y_i P_{ci}$$

$$T_{cv} = \sum_{i=1}^{n} Y_i T_{ci}$$

$$\alpha_{cv} = \sum_{i=1}^{n} Y_i \alpha_{ci}$$

(4.3.19 - 4.3.23)

Eq. 4.3.14 to 4.3.18 can be employed to get the liquid phase parameters, to be used in the Eq. 4.3.11, for the liquid phase mixture :

$$[P_l] = \frac{A_{cl}\beta/\theta V_{cl}}{B_l} \qquad (4.3.24)$$

and Eq. 4.3.19 to 4.3.23 can be employed to get the vapour phase parameters:

$$[P_v] = \frac{A_{cv}\beta/\theta V_{cv}}{B_v} \qquad (4.3.25)$$

and for A_{cl}, and A_{cv}

$$A_{cl} = P_{cl}^{2/3} T_{cl}^{1/3} (0.133\alpha_{cl} - 0.281) \qquad (4.3.26)$$

$$A_{cv} = P_{cv}^{2/3} T_{cv}^{1/3} (0.133\alpha_{cv} - 0.281) \qquad (4.3.27)$$

Lee and Chien[15], have proposed another approach similar to Weinaug and Katz[5] for calculating the IFT which is to calculate the pure component parachors from Eq. 4.3.3, 4.3.4 and 4.3.11, and using Eq. 4.2.3, with an exponent value of E=3.911111...., instead of E=4. However Eq. 4.3.13 has been used in this work as the scaling law approach. Lee and Chien[15] have quoted an average absolute deviation (AAD), of 3.7% for 45 data sets of binary mixtures and 7.3 % for the carbon dioxide reservoir oil data studied by them. These deviations were reported by them to be 50 % less than those reported by the Weinaug and Katz[5], approach.

4.4 : GRADIENT THEORY

In this section the most non - conventional approach for predicting the interfacial tension between gas and liquid phases is presented. The method has not been thoroughly studied for engineering applications and is presented here merely for the purpose of completeness of the review of the predictive methods.

The interface of the two phases at equilibrium has been considered as a third phase with properties varying between those at the bulk of liquid and gas. This approach known as the gradient theory of inhomogeneous fluid, uses an equation of state to evaluate the required properties by thermodynamic relations. Any EOS can be used for the above purpose, though for each compound an experimentally determined parameter should be known for that EOS[1]

Carey and Scriven[18], reported the predictions of IFT of several normal paraffin binary mixtures using the gradient theory of inhomogeneous fluids and reported the predicted IFTs lying within 2 % of the observed experimental data. The actual theory behind the application is given below.

Given an in homogeneous system at temperature T, volume V with N_i particles of species i = 1,2 then the differential equation which governs the density variations through a planar surface is given by[19] :

$$\sum_{j=1}^{2}\nabla_{r\_}(C_{ij}\nabla_{r}n_j)-\frac{1}{2}\sum_{j,k=1}^{2}\left(\frac{\partial C_{ij}}{\partial n_{\alpha i}}\right).\nabla_{r\_n_k}.\nabla_{r\_n_j}=\mu^{o}{}_{i}(\underline{n})-\mu_i \qquad \text{for i = 1 to 2} \qquad (4.4.1)$$

where,

$$C_{ij}=\frac{KT}{6}\int_{v}S^2C_0{}^{ij}(S,n\_)d^3s \qquad (4.4.2)$$

A more convenient approach is given by Vargas[20], :

$$C_{ij}=\frac{1}{2}\omega_2{}^{ij}+\frac{1}{8}\sum_{k=1}^{2}n_k\left[\left(\frac{\partial\omega_2{}^{ik}}{\partial n_j}\right)-\left(\frac{\partial\omega_2{}^{jk}}{\partial n_i}\right)\right] \qquad (4.4.3)$$

$$\omega_2{}^{ij}=-\frac{1}{3}\int S^2U_{ij}(S)g_{ij}(S;n\_)d^3S \qquad (4.4.4)$$

Where,

$C_0{}^{ij}$ = direct correlation function between a pair of particles of type i and j

$\mu_o{}^{i}$(n) = local chemical potential of species *i* in a homogeneous state at composition n

μ_i = chemical potential of species *i*

g_{ij}(s,n) = pair correlation function between particles *i* and *j*

u_{ij} = pair potential function between the corresponding molecules

ω = grand thermodynamic potential and

n = number density

considering the work of McCoy and Davis[21], it can be assumed that the surface and density profiles of simple one - component fluids are not greatly influenced by the density dependence of the influence factor (β). With this assumption Eq. 4.4.1 for a planar interface reduces to :

$$\sum_{j=1}^{2} C_{ij} \frac{d^2 n_j}{dx^2} = \mu^0{}_i(n\_) - \mu_i, i = 1,2 \qquad (4.4.5)$$

C_{ij} for species 1 & 2 can be given as :

$$C_{12} = \beta\sqrt{C_{11}C_{22}} \qquad (4.4.6)$$

where, β, is an adjustable parameter, C_{11} and C_{22} are to be determined from the pure component interfacial tension data. Hence IFT equation corresponding to Eq. 4.4.1, is given by [19,20], :

$$\sigma = \int_{-\infty}^{\infty} \sum_{i,j=1}^{2} C_{ij} \left(\frac{dn_i}{dx}\right)\left(\frac{dn_j}{dx}\right) dx \qquad (4.4.7)$$

$$\sigma = \int_{n_i 1}^{n_i 2} \sqrt{2\left[\omega(n\_) - \omega(n\_^{bulk})\right]} \sqrt{\sum_{j,k=1} C_{kj} \left(\frac{dn_k}{dn_i}\right)\left(\frac{dn_j}{dn_i}\right)} dn_i \qquad (4.4.8)$$

Eq. 4.4.8 is a profile independent equation. Where n_{i1} & n_{i2} are the bulk densities for species i which are computed via equalities of bulk pressures and chemical potentials for each species. $\omega(n)$, represents the grand thermodynamic potential defined by :

$$\omega(n\_) = f^0(n\_) - \sum_i n_i \mu_i \qquad (4.4.9)$$

Where $f^0(n\_)$ the local Helmholtz free energy density of homogeneous fluid at composition ($^{n}\_$) can be determined from an EOS.

A more detailed application of Eq. 4.4.7 or 4.4.8 for prediction of interfacial tension of mixtures is given in Reference[18]. As the method relies significantly on the empiricism, defined by Eq. 4.4.6, and major thermodynamic calculations, it has not been widely applied.

References

1) Nitsche, J.M., Teletzke, G.E., Scriven, L.E., and Davis, H.T.: "Behaviour of Water, Carbon dioxide and Decane", *Fluid Phase Equilibria*, Vol. 14, pp. 203-208, (1980).

2) Brock, J.R. and Bird, R.B.: "Surface Tension and the Principle of Corresponding states", *AIChEJ*, Vol. 1, No. 2, pp. 174-177, (Jun., 1955).

3) MaCleod, D.B.: "On a Relation Between Surface Tension, Density", *Transactions of Faraday Soc.*, Vol. 19, pp. 38-43, (1923).

4) Sugden S.: "A Relation between Surface Tension, Density and, Chemical Composition", *J. Chem. Soc.*, Vol. 168, pp. 1177-1189, (1924).

5) Weinaug, C.F. and Katz, D.L.: "Surface Tension of Methane - Propane Mixtures", *Industrial & Engineering Chemistry (I & EC)*, pp. 239-246, (1943).

6) Mayer, S.W.: "A Molecular Parameter Relationship between Surface Tension and Liquid Compressibility", *J. Phys. Chem.*, Vol. 67, pp. 2160-2164, (1963).

7) Sanchez, I.C.: "Liquids : Surface Tension, Compressibility and Invariants", *J. Chem Phys.*, Vol. 79, pp. 405-415, (1983).

8) Hough, E.W. and Stegemeier, G.l.: "Correlation of Surface and Interfacial Tension of Light Hydrocarbons in the Critical Region", *Society of Petroleum Engineers Journal (SPEJ)*, pp. 259-263, (Dec., 1961).

9) Sivaraman, A., Ziga, J. and Kobayashi, R.: "Correlation for Prediction of Interfacial Tensions of Pure Alkane, Napthenic and Aromatic Compounds between their Freezing and Critical Points", *Fluid Phase Equilibria*, Vol. 18, pp. 225-235, (1984).

10) Amyx, J.W., Bass, D.M. and Whiting, R.L.: "Petroleum Reservoir Engineering", McGraw Hill, pp. 306-308, (1960).

11) Firoozabadi, A. Katz, D.L. Soroosh, H. and Sajjadian, V.A.: "Surface Tension of Reservoir Crude Oil/Gas Systems Recognising Asphalt in the Heavy Fraction", *Society of Petroleum Engineers Journal (Reservoir Engineering)*, pp. 265-272, (Feb., 1988).

12) Fanchi, J.R.: "Calculation of Parachors for Compositional Simulation", *Journal of Petroleum Technology*, pp. 2049-2050, (Nov., 1985).

13) Reid, R.C. and Sherwood, T.K.: "The Properties of Gases and Liquids", McGraw Hill Book Co., Inc., New York City, pp. 205-211, (1973).

14) Sugden, S.: "The Parachors and Valency (Routledge, 1930); A List of Parachors", Brit. Assoc. Report, (1932).

15) Lee, S.T. and Chien, M.C.H.: "A New Multicomponent Surface Tension Correlation Based on Scaling Theory", Presented at the SPE/DOE Fourth Symposium on Enhanced Oil Recovery held in Tulsa, Oklahoma, SPE/DOE, 12643, April 15-18, (1984).

16) Reid, R.C. and Sherwood, T.K.: "The Properties of Gases and Liquids", McGraw Hill Book Co., Inc., New York City, Second Edition, pp. 571-584, (1966).

17) Fanchi, J.R.: "Calculation of Parachors for Compositional Simulation" : An Update, *Society of Petroleum Engineers Journal (Reservoir Engineering)*, pp. 433-436, (Aug., 1990).

18) Carey, B.S., Scriven, L.E. and Davis, H.T.: "Semiempirical Theory of Surface Tension of Binary Systems", *AIChEJ*, Vol. 26, No. 5, pp. 705-711, (Sep., 1980).

19) Bongiorno, V., Scriven, L.E. and Davis, H.T.: "Molecular Theory of Fluid Interfaces", *J. Col. Int. Sci.*, Vol. 57, p. 462, (1976).

20) Vargas, A.: "On the Molecular Theory of Dense Fluids and Fluid Interfaces", PhD Thesis, Univ., Minn., Minneapolis, (1976).

21) McCoy, B.F. and Davis, H.T.: "On the Free Energy Theory of Inhomogeneous Fluids", *Phys. Rev. A 20*, p. 1201, (1978).

22) Katz, D. L.: "Handbook of Natural Gas Engineering", McGraw-Hill Book Company, New York, (1959).

23) Guggenheim, E. A.: "Thermodynamics", Third Ed., North Holland Publishing Co., Amsterdam, (1957).

CHAPTER 5 : IMPROVEMENT OF PREDICTIVE TECHNIQUES FOR INTERFACIAL TENSION - SCALING LAW AND PARACHOR METHOD

5.1 : INTRODUCTION

In order to study the predictive capabilities and carry out possible improvements in the predictive techniques namely, the scaling law[1], and the parachor method[2], a study was carried out on a five component mixture comprising of methane, propane, n-pentane, n-decane, and n-hexadecane at temperatures of 30 (Fluid B), 35 (Fluid B), 40 (Fluid A) and 80°C (Fluid A), and a twenty component mixture (Fluid C) comprising of normal paraffins from methane to n-eicosane, at 65.5, 93.3 and 121.1°C. Interfacial tensions for these mixtures were measured using the gas-liquid interface technique proposed in this work, and were also calculated using the predictive techniques[1,2]. Measured compositional and density data were used wherever available whereas predicted phase compositions were employed where the measured data was unavailable.

The above study is discussed in Section 5.2 below and the proposed modifications of the scaling law and the parachor method are furnished in detail in Section 5.3. The modified methods have been tested against interfacial tension data measured on multicomponent synthetic mixtures (Section 5.4) and real reservoir fluids (Section 5.5) from this work and those reported in the literature.

5.2 : COMPARISON OF PREDICTED AND MEASURED INTERFACIAL TENSION DATA

The data on two phase compositions and densities are presented in Table (5.2.1) to Table (5.2.7), for the five (Fluid A & B) and twenty (Fluid C) component mixtures for the studied conditions (the single phase compositions of these fluids is provided in Table 5.4.1 of Section

Table 5.2.1 (a) - Liquid Phase Compositions and Densities at 30°C for a Five Component Mixture (Fluid B).

1.- > Methane 2.- > Propane 3.- > n - Pentane 4.- > n - Decane 5.- > n - Hexadecane

No	Pressure, MPa	X_1, Mole Fraction	X_2, Mole Fraction	X_3, Mole Fraction	X_4, Mole Fraction	X_5, Mole Fraction	Liquid Density, gm/cc
1	30.42	0.7085	0.1043	0.0760	0.0455	0.0657	0.5240
2	29.04	0.6831	0.1085	0.0824	0.0524	0.0736	0.5480
3	27.66	0.6613	0.1122	0.0901	0.0577	0.0787	0.5640
4	26.29	0.6432	0.1157	0.0945	0.0623	0.0843	0.5720
5	23.53	0.6038	0.1245	0.1076	0.0733	0.0908	0.5980
6	19.39	0.5449	0.1394	0.1314	0.0869	0.0974	0.6180

Table 5.2.1 (b) - Vapour Phase Compositions and Densities at 30°C for a Five Component Mixture (Fluid B).

1.- > Methane 2.- > Propane 3.- > n - Pentane 4.- > n - Decane 5.- > n - Hexadecane

No	Pressure, MPa	Y_1, Mole Fraction	Y_2, Mole Fraction	Y_3, Mole Fraction	Y_4, Mole Fraction	Y_5, Mole Fraction	Vapour Density, gm/cc
1	30.42	0.8552	0.0851	0.0480	0.0172	0.0145	0.4000
2	29.04	0.8477	0.0830	0.0445	0.0145	0.0103	0.3690
3	27.66	0.8557	0.0812	0.0428	0.0128	0.0075	0.3490
4	26.29	0.8621	0.0799	0.0416	0.0109	0.0055	0.3280
5	23.53	0.8741	0.0771	0.0381	0.0079	0.0028	0.2950
6	19.39	0.8908	0.0736	0.0313	0.0043	0.0000	0.2430

Table 5.2.2 (a) - Liquid Phase Compositions and Densities at 35°C for a Five Component Mixture (Fluid B), (Predicted Compositional Data and Interpolated Density Data).

1.- > Methane 2.- > Propane 3.- > n - Pentane 4.- > n - Decane 5.- > n - Hexadecane

No	Pressure, MPa	X_1, Mole Fraction	X_2, Mole Fraction	X_3, Mole Fraction	X_4, Mole Fraction	X_5, Mole Fraction	Liquid Density, gm/cc
1	30.42	0.7638	0.1007	0.0634	0.0322	0.0399	0.5000
2	29.04	0.7408	0.1056	0.0691	0.0374	0.0470	0.5230
3	27.66	0.7187	0.1103	0.0748	0.0425	0.0536	0.5370
4	26.29	0.6975	0.1148	0.0807	0.0475	0.0595	0.5470
5	24.91	0.6765	0.1194	0.0867	0.0525	0.0648	0.5590

Table 5.2.2 (b) - Vapour Phase Compositions and Densities at 35°C for a Five Component Mixture (Fluid B), (Predicted Compositional Data and Interpolated Density Data).

1.- > Methane 2.- > Propane 3.- > n - Pentane 4.- > n - Decane 5.- > n - Hexadecane

No	Pressure, MPa	Y_1, Mole Fraction	Y_2, Mole Fraction	Y_3, Mole Fraction	Y_4, Mole Fraction	Y_5, Mole Fraction	Vapour Density, gm/cc
1	30.42	0.8330	0.0868	0.0479	0.0169	0.0153	0.3700
2	29.04	0.8486	0.0836	0.0442	0.0134	0.0102	0.3430
3	27.66	0.8585	0.0815	0.0417	0.0112	0.0072	0.3250
4	26.29	0.8659	0.0799	0.0396	0.0094	0.0052	0.3040
5	24.91	0.8721	0.0785	0.0378	0.0079	0.0037	0.2900

Table 5.2.3 (a) - Liquid Phase Compositions and Densities at 40°C for a Five Component Mixture (Fluid A), (Predicted Compositional Data and Measured Density Data).

1.- > Methane 2.- > Propane 3.- > n - Pentane 4.- > n - Decane 5.- > n - Hexadecane

No	Pressure, MPa	X_1, Mole Fraction	X_2, Mole Fraction	X_3, Mole Fraction	X_4, Mole Fraction	X_5, Mole Fraction	Liquid Density, gm/cc
1	31.11	0.7666	0.0997	0.0625	0.0316	0.0395	0.4720
2	30.94	0.7640	0.1003	0.0631	0.0322	0.0403	0.4735
3	30.77	0.7512	0.1009	0.0638	0.0328	0.0412	0.4816
4	30.42	0.7555	0.1021	0.0652	0.0341	0.0430	0.4876
5	29.73	0.7440	0.1045	0.0681	0.0367	0.0466	0.4983
6	29.04	0.7326	0.1069	0.0709	0.0393	0.0501	0.5072
7	28.35	0.7215	0.1092	0.0738	0.0419	0.0535	0.5171
8	27.66	0.7106	0.1114	0.0767	0.0445	0.0567	0.5203
9	26.29	0.6894	0.1158	0.0825	0.0496	0.0626	0.5326
10	24.91	0.6683	0.1203	0.0886	0.0547	0.0681	0.5430
11	23.53	0.6470	0.1248	0.0951	0.0599	0.0731	0.5509
12	20.77	0.6039	0.1345	0.1096	0.0702	0.0817	0.5648
13	18.02	0.5547	0.1456	0.1278	0.0813	0.0905	0.5765
14	15.26	0.4993	0.1583	0.1503	0.0927	0.0994	0.5890
15	12.50	0.4354	0.1719	0.1778	0.1050	0.1097	0.6026

Table 5.2.3 (b) - Vapour Phase Compositions and Densities at 40°C for a Five Component Mixture (Fluid A), (Predicted Compositional Data and Measured Density Data).

1.- > Methane 2.- > Propane 3.- > n - Pentane 4.- > n - Decane 5.- > n - Hexadecane

No	Pressure, MPa	Y_1, Mole Fraction	Y_2, Mole Fraction	Y_3, Mole Fraction	Y_4, Mole Fraction	Y_5, Mole Fraction	Vapour Density, gm/cc
1	31.11	0.8261	0.0882	0.0495	0.0185	0.0177	0.3629
2	30.94	0.8290	0.0877	0.0488	0.0178	0.0167	0.3609
3	30.77	0.8317	0.0871	0.0482	0.0172	0.0157	0.3582
4	30.42	0.8365	0.0862	0.0471	0.0162	0.0141	0.3469
5	29.73	0.8441	0.0846	0.0453	0.0144	0.0115	0.3371
6	29.04	0.8500	0.0834	0.0439	0.0131	0.0096	0.3227
7	28.35	0.8547	0.0824	0.0427	0.0120	0.0081	0.3167
8	27.66	0.8589	0.0816	0.0416	0.0110	0.0069	0.3080
9	26.29	0.8658	0.0801	0.0397	0.0093	0.0050	0.2877
10	24.91	0.8716	0.0789	0.0379	0.0079	0.0036	0.2733
11	23.53	0.8767	0.0778	0.0363	0.0067	0.0025	0.2601
12	20.77	0.8856	0.0757	0.0329	0.0045	0.0012	0.2276
13	18.02	0.8933	0.0739	0.0295	0.0028	0.0005	0.1973
14	15.26	0.9000	0.0722	0.0259	0.0016	0.0002	0.1626
15	12.50	0.9055	0.0710	0.0225	0.0008	0.0000	0.1279

Table 5.2.4 (a) - Liquid Phase Compositions and Densities at 80°C for a Five Component Mixture (Fluid A).

1.- > Methane 2.- > Propane 3.- > n - Pentane 4.- > n - Decane 5.- > n - Hexadecane

No	Pressure, MPa	X_1, Mole Fraction	X_2, Mole Fraction	X_3, Mole Fraction	X_4, Mole Fraction	X_5, Mole Fraction	Liquid Density, gm/cc
1	30.42	0.6880	0.1073	0.0772	0.0501	0.0774	0.4800
2	29.04	0.6640	0.1115	0.0827	0.0564	0.0854	0.4970
3	27.66	0.6414	0.1133	0.0886	0.0634	0.0933	0.5130
4	26.29	0.6187	0.1186	0.0940	0.0689	0.0998	0.5240
5	24.91	0.6003	0.1208	0.1001	0.0743	0.1045	0.5350

Table 5.2.4 (b) - Vapour Phase Compositions and Densities at 80°C for a Five Component Mixture (Fluid A).

1.- > Methane 2.- > Propane 3.- > n - Pentane 4.- > n - Decane 5.- > n - Hexadecane

No	Pressure, MPa	Y_1, Mole Fraction	Y_2, Mole Fraction	Y_3, Mole Fraction	Y_4, Mole Fraction	Y_5, Mole Fraction	Vapour Density, gm/cc
1	30.42	0.8362	0.0869	0.0465	0.0167	0.0137	0.2980
2	29.04	0.8448	0.0863	0.0445	0.0145	0.0099	0.2780
3	27.66	0.8512	0.0857	0.0431	0.0127	0.0073	0.2610
4	26.29	0.8580	0.0844	0.0414	0.0108	0.0054	0.2460
5	24.91	0.8625	0.0841	0.0398	0.0095	0.0041	0.2310

Table 5.2.5 - Phase Compositions and Densities at 65.5°C for a Twenty Component Mixture (Fluid C).

Component	35.93 MPa		34.56 MPa		33.18 MPa	
	X (m.f)	Y (m.f)	X (m.f)	Y (m.f)	X (m.f)	Y (m.f)
methane	0.7102	0.8261	0.6924	0.8338	0.6717	0.8441
ethane	0.0856	0.0815	0.0851	0.0801	0.0846	0.0798
propane	0.0242	0.0211	0.0244	0.0203	0.0260	0.0209
n - butane	0.0139	0.0107	0.0139	0.0098	0.0131	0.0091
n - pentane	0.0121	0.0071	0.0130	0.0076	0.0129	0.0073
n - hexane	0.0173	0.0097	0.0199	0.0102	0.0204	0.0096
n - heptane	0.0153	0.0082	0.0161	0.0078	0.0182	0.0069
n - octane	0.0093	0.0045	0.0099	0.0043	0.0123	0.0034
n - nonane	0.0092	0.0039	0.0098	0.0035	0.0115	0.0029
n - decane	0.0090	0.0036	0.0104	0.0028	0.0110	0.0027
n - undecane	0.0088	0.0030	0.0100	0.0029	0.0115	0.0022
n - dodecane	0.0089	0.0030	0.0101	0.0026	0.0111	0.0019
n - tridecane	0.0091	0.0029	0.0103	0.0024	0.0117	0.0019
n - tetradecane	0.0091	0.0025	0.0100	0.0020	0.0112	0.0015
n - pentadecane	0.0100	0.0025	0.0112	0.0021	0.0124	0.0016
n - hexadecane	0.0096	0.0021	0.0106	0.0016	0.0121	0.0012
n - heptadecane	0.0098	0.0023	0.0109	0.0018	0.0123	0.0012
n - octadecane	0.0097	0.0017	0.0106	0.0014	0.0119	0.0009
n - nonadecane	0.0106	0.0018	0.0117	0.0014	0.0127	0.0009
n - eicosane	0.0083	0.0017	0.0095	0.0015	0.0113	0.0000
Density, gm/cc	0.4977	0.3324	0.5146	0.3121	0.5284	0.2957

Table 5.2.6 - Phase Compositions and Densities at 93.3°C for a Twenty Component Mixture (Fluid C).

Component	35.93 MPa		34.56 MPa		33.18 MPa	
	X (m.f)	Y (m.f)	X (m.f)	Y (m.f)	X (m.f)	Y (m.f)
methane	0.7149	0.8230	0.6847	0.8304	0.6693	0.8399
ethane	0.0845	0.0809	0.0855	0.0821	0.0845	0.0822
propane	0.0244	0.0205	0.0259	0.0210	0.0260	0.0201
n - butane	0.0119	0.0120	0.0152	0.0112	0.0141	0.0087
n - pentane	0.0120	0.0077	0.0126	0.0075	0.0140	0.0070
n - hexane	0.0179	0.0108	0.0198	0.0101	0.0205	0.0093
n - heptane	0.0149	0.0081	0.0169	0.0077	0.0184	0.0071
n - octane	0.0091	0.0044	0.0111	0.0041	0.0122	0.0044
n - nonane	0.0091	0.0038	0.0105	0.0034	0.0112	0.0033
n - decane	0.0088	0.0036	0.0103	0.0032	0.0114	0.0028
n - undecane	0.0089	0.0033	0.0104	0.0026	0.0114	0.0027
n - dodecane	0.0093	0.0031	0.0103	0.0026	0.0115	0.0022
n - tridecane	0.0096	0.0030	0.0111	0.0024	0.0121	0.0020
n - tetradecane	0.0093	0.0027	0.0109	0.0022	0.0122	0.0016
n - pentadecane	0.0105	0.0027	0.0123	0.0021	0.0134	0.0018
n - hexadecane	0.0103	0.0024	0.0116	0.0016	0.0127	0.0014
n - heptadecane	0.0104	0.0023	0.0120	0.0016	0.0134	0.0013
n - octadecane	0.0106	0.0020	0.0117	0.0011	0.0129	0.0010
n - nonadecane	0.0104	0.0021	0.0120	0.0014	0.0132	0.0010
n - eicosane	0.0031	0.0013	0.0049	0.0014	0.0055	0.0000
Density, gm/cc	0.4505	0.3091	0.4605	0.2869	0.4682	0.2704

Table 5.2.7 - Phase Compositions and Densities at 121.1°C for a Twenty Component Mixture (Fluid C).

Component	35.25 MPa		33.87 MPa		32.49 MPa	
	X (m.f)	Y (m.f)	X (m.f)	Y (m.f)	X (m.f)	Y (m.f)
methane	0.7091	0.8236	0.6723	0.8378	0.6545	0.8441
ethane	0.0854	0.0823	0.0836	0.0796	0.0834	0.0802
propane	0.0240	0.0195	0.0254	0.0200	0.0249	0.0193
n - butane	0.0126	0.0105	0.0148	0.0098	0.0142	0.0094
n - pentane	0.0112	0.0082	0.0124	0.0072	0.0131	0.0072
n - hexane	0.0172	0.0108	0.0194	0.0100	0.0209	0.0101
n - heptane	0.0147	0.0083	0.0172	0.0075	0.0184	0.0069
n - octane	0.0092	0.0048	0.0111	0.0042	0.0114	0.0036
n - nonane	0.0090	0.0037	0.0104	0.0034	0.0116	0.0031
n - decane	0.0091	0.0038	0.0108	0.0029	0.0119	0.0025
n - undecane	0.0086	0.0032	0.0109	0.0025	0.0121	0.0022
n - dodecane	0.0088	0.0029	0.0110	0.0023	0.0119	0.0026
n - tridecane	0.0092	0.0027	0.0114	0.0022	0.0126	0.0018
n - tetradecane	0.0093	0.0025	0.0118	0.0021	0.0128	0.0015
n - pentadecane	0.0103	0.0027	0.0129	0.0019	0.0144	0.0015
n - hexadecane	0.0098	0.0022	0.0126	0.0016	0.0139	0.0012
n - heptadecane	0.0104	0.0022	0.0133	0.0015	0.0143	0.0011
n - octadecane	0.0101	0.0021	0.0131	0.0013	0.0143	0.0008
n - nonadecane	0.0113	0.0020	0.0141	0.0012	0.0155	0.0007
n - eicosane	0.0103	0.0019	0.0115	0.0012	0.0135	0.0000
Density, gm/cc	0.4395	0.2899	0.4676	0.2674	0.4897	0.2484

Table 5.2.8 - Interfacial Tension Data for a Five Component Mixture at 30°C (Fluid B) Using the Original Scaling Law and Parachor Method and the Hough - Stegemeier's Parachor Method.

No	Pressure, MPa	Measured, mN/m	Scaling Law, mN/m	Parachor Method, mN/m	Hough - Stegemeier's Parachor Method, mN/m
1	30.42	0.026	0.012	0.011	0.016
2	29.04	0.083	0.058	0.062	0.080
3	27.66	0.185	0.130	0.140	0.165
4	26.29	0.321	0.227	0.245	0.275
5	23.53	0.607	0.585	0.642	0.665
6	19.39	1.255	1.500	1.680	1.600

Table 5.2.9 - Interfacial Tension Data for a Five Component Mixture at 35°C (Fluid B) Using the Original Scaling Law and Parachor Method and the Hough - Stegemeier's Parachor Method.

No	Pressure, MPa	Measured, mN/m	Scaling Law, mN/m	Parachor Method, mN/m	Hough - Stegemeier's Parachor Method, mN/m
1	30.42	0.031	0.029	0.029	0.039
2	29.04	0.116	0.097	0.099	0.119
3	27.66	0.192	0.174	0.181	0.208
4	26.29	0.320	0.295	0.312	0.343
5	24.91	0.450	0.434	0.464	0.494

Table 5.2.10 - Interfacial Tension Data for a Five Component Mixture at 40°C (Fluid A) Using the Original Scaling Law and Parachor Method and the Hough - Stegemeier's Parachor Method.

No	Pressure, MPa	Measured, mN/m	Scaling Law, mN/m	Parachor Method, mN/m	Hough - Stegemeier's Parachor Method, mN/m
1	31.11	0.019	0.015	0.014	0.020
2	30.94	0.030	0.016	0.016	0.021
3	30.77	0.039	0.023	0.023	0.031
4	30.42	0.056	0.039	0.039	0.051
5	29.73	0.097	0.063	0.063	0.080
6	29.04	0.150	0.110	0.110	0.132
7	28.35	0.220	0.150	0.150	0.175
8	27.66	0.290	0.180	0.180	0.210
9	26.29	0.450	0.310	0.320	0.351
10	24.91	0.630	0.445	0.470	0.500
11	23.53	0.830	0.600	0.640	0.664
12	20.77	1.380	1.100	1.200	1.182
13	18.02	2.090	1.800	2.000	1.890
14	15.26	3.180	3.010	3.340	3.023
15	12.50	4.200	4.800	5.400	4.700

Table 5.2.11 - Interfacial Tension Data for a Five Component Mixture at 80°C (Fluid A) Using the Original Scaling Law and Parachor Method and the Hough - Stegemeier's Parachor Method.

No	Pressure, MPa	Measured, mN/m	Scaling Law, mN/m	Parachor Method, mN/m	Hough - Stegemeier's Parachor Method, mN/m
1	30.42	0.118	0.090	0.090	0.109
2	29.04	0.229	0.185	0.189	0.216
3	27.66	0.390	0.330	0.341	0.373
4	26.29	0.536	0.490	0.512	0.541
5	24.91	0.738	0.716	0.753	0.770

Table 5.2.12 - Interfacial Tension Data for a Twenty Component Mixture at 65.5°C (Fluid C) Using the Original Scaling Law and Parachor Method and the Hough - Stegemeier's Parachor Method.

No	Pressure, MPa	Measured, mN/m	Scaling Law, mN/m	Parachor Method, mN/m	Hough - Stegemeier's Parachor Method, mN/m
1	35.93	0.073	0.053	0.054	0.069
2	34.56	0.159	0.128	0.126	0.155
3	33.18	0.246	0.200	0.210	0.234

Table 5.2.13 - Interfacial Tension Data for a Twenty Component Mixture at 93.3°C (Fluid C) Using the Original Scaling Law and Parachor Method and the Hough - Stegemeier's Parachor Method.

No	Pressure, MPa	Measured, mN/m	Scaling Law, mN/m	Parachor Method, mN/m	Hough - Stegemeier's Parachor Method, mN/m
1	35.93	0.040	0.029	0.029	0.038
2	34.56	0.120	0.062	0.063	0.079
3	33.18	0.210	0.103	0.107	0.128

Table 5.2.14 - Interfacial Tension Data for a Twenty Component Mixture at 121.1°C (Fluid C) Using the Original Scaling Law and Parachor Method and the Hough - Stegemeier's Parachor Method

No	Pressure, MPa	Measured, mN/m	Scaling Law, mN/m	Parachor Method, mN/m	Hough - Stegemeier's Parachor Method, mN/m
1	35.25	0.053	0.037	0.037	0.048
2	33.87	0.159	0.114	0.117	0.140
3	32.49	0.294	0.252	0.262	0.293

5.4). The interfacial tension data measured and predicted[1,2] has been tabulated through Table (5.2.8) to Table (5.2.14), for these mixtures studied at various conditions. The tables also show a column of the IFTs predicted by using the Hough and Stegemeier's[3], method (Section 4.2.1, Chapter 4). This method basically uses the same principle as the parachor method[2], except that the exponent value used in this approach[3], is, E=3.67, instead of, E=4.

From, the presented IFT data, Table (5.2.8) to Table (5.2.14), it can be seen that the IFTs predicted by using the Hough and Stegmeiers[3], method (E=3.67) are in reasonable agreement with the values measured by us (the reliability of which has already been established[4]). Whereas the original scaling law and parachor methods[1,2], seem to underestimate the IFTs at high pressure conditions or at low IFTs, and overestimate the IFTs at low pressure conditions or high IFT conditions. The predictions agree, however, in some cases for the intermediate range, i.e., 0.5 - 1 mN/m. Hence, one can conclude from the presented IFT data that the exponents suggested in the scaling law (E=3.911111...)[1], and that suggested in the parachor method (E=4)[2], do not represent a universal value of exponent for the entire range of IFTs.

5.3 : PROPOSED MODIFICATION OF SCALING LAW AND PARACHOR METHOD

In this section a modification based on the molar and mass density difference dependence of the exponents for the scaling law[1] and parachor method[2] has been proposed. For this purpose reliable literature data on measured IFTs for seven binaries were collected for the analysis. The binaries were, C_1-C_3[2], C_1-nC_4[5], C_1-nC_5[6], C_1-nC_{10}[7], CO_2-nC_4[8], CO_2-nC_{10}[9] & CO_2-nC_{14}[10]. Interfacial tensions ranging from 0.001 - 10 mN/m comprised the data set of 213 points (Table 5.3.1), so that a wide ranging modification could be proposed. All the IFT data[5,6,7,8,9,10], had been measured by the conventional pendant drop method, only for the C_1-C_3[2], binary the IFTs were measured by the capillary rise method.

Table 5.3.1 - Literature IFT Data Used in the Modification.

No	System	No of Data Points	Temperature Range (°C)	Pressure Range (MPa)	IFT Range (mN/m)	Ref. No
1	C_1-C_3	47	-15-90	0.29-8.48	0.19-12.13	2
2	C_1-nC_4	25	38-88	9.6-13.09	0.003-1.64	5
3	C_1-nC_5	10	38-71	6.89-15.51	0.059-6.16	6
4	C_1-nC_{10}	30	38-71	10.34-36.19	0.002-9.77	7
5	CO_2-nC_4	42	46-104.5	2.18-7.96	0.026-5.75	8
6	CO_2-nC_{10}	41	71-104.5	6.94-16.45	0.008-7.81	9
7	CO_2-nC_{14}	18	71	11.03-16.27	0.016-4.03	10
	Total	213				

For all the IFT data points under consideration the molar and mass density differences were evaluated from the data sources[2,5,6,7,8,9,10]. The interfacial tensions were also predicted by using the Lee-Chien scaling law[1] and Weinaug-Katz parachor method[2] by employing the compositional and density data available from the same IFT data source. The percentage deviations [$100(\sigma_{pred}-\sigma_{exp})/\sigma_{exp}$] of predicted results by the scaling law and parachor method for all the binary systems are shown in Figures 5.3.1 and 5.3.2 respectively. Note that the performances of both methods are quite similar. The scaling law, however, shows more scatter particularly at low IFT.

Although the scaling law provides a value for the exponent E based on a mainly theoretical approach, the exponent has been generally treated as an empirical parameter. The results shown in Figures 5.3.1 and 5.3.2 indicate the performance of both methods can be significantly improved by relating E to the IFT[13].

Subsequently the values of exponents were evaluated for both the scaling law[1], and parachor method[2], by matching the predictions with the measured IFT data. A considerable scatter in the values of exponents was observed, however majority of the values lied between 3 & 4. This supports the conclusion that the exponents proposed in the original predictive techniques fail to represent the universal values of E. The value of E in this work was considered to be a function of the liquid-vapour molar density difference. The relation was determined for both methods by regressing E to minimise the deviations of the predicted results. The developed correlations of this work are :

Modified Lee-Chien Method :

$$E = 3.535 + 17.76\ (\rho_{lm}-\rho_{vm}) \qquad (5.3.1)$$

Modified Weinaug-Katz Method :

$$E = 3.583 + 0.16\ (\rho_{lm}-\rho_{vm}) \qquad (5.3.2)$$

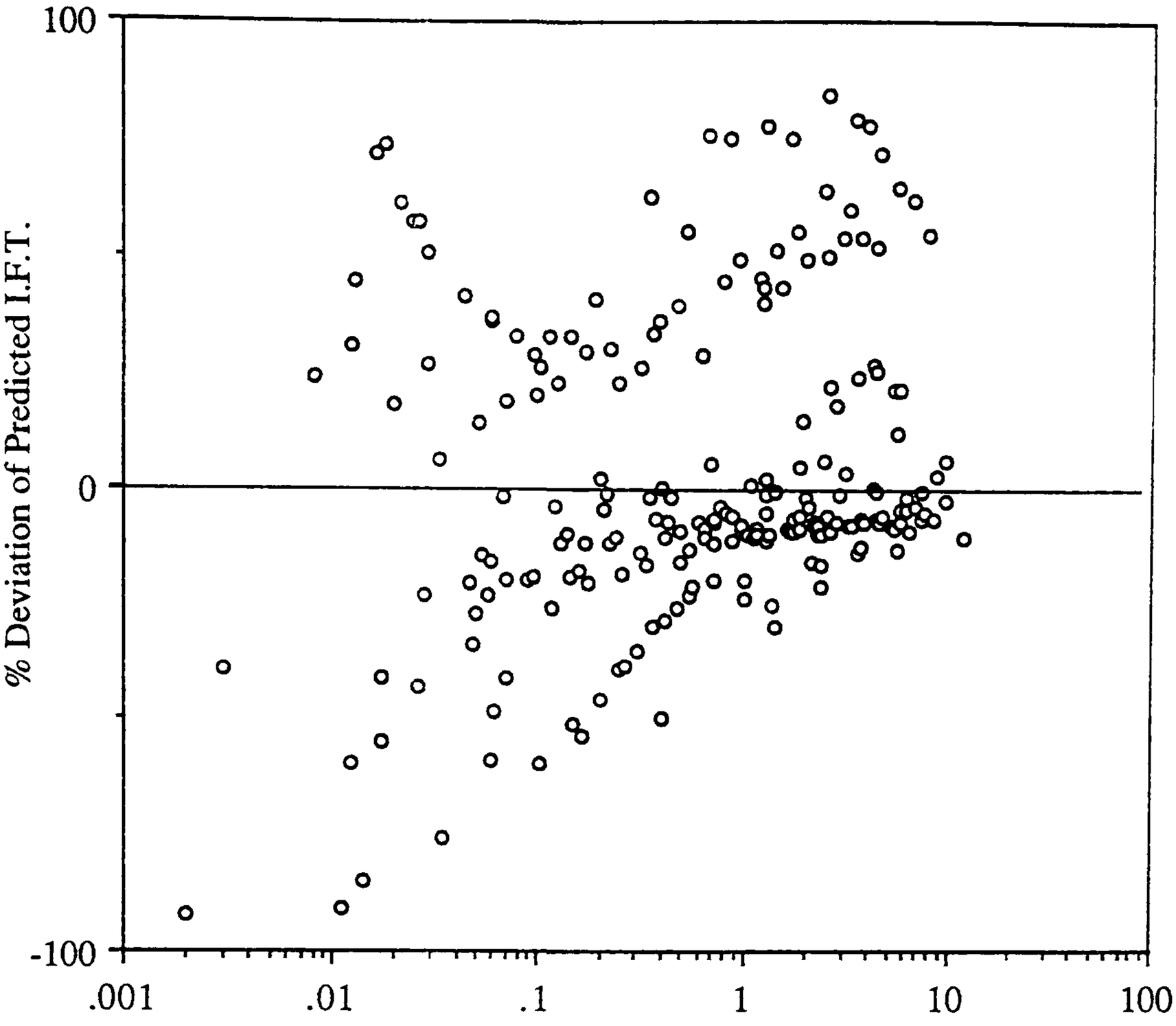

Figure 5.3.1 - Deviations of Predicted I.F.T. by Scaling Law for Binary Systems.

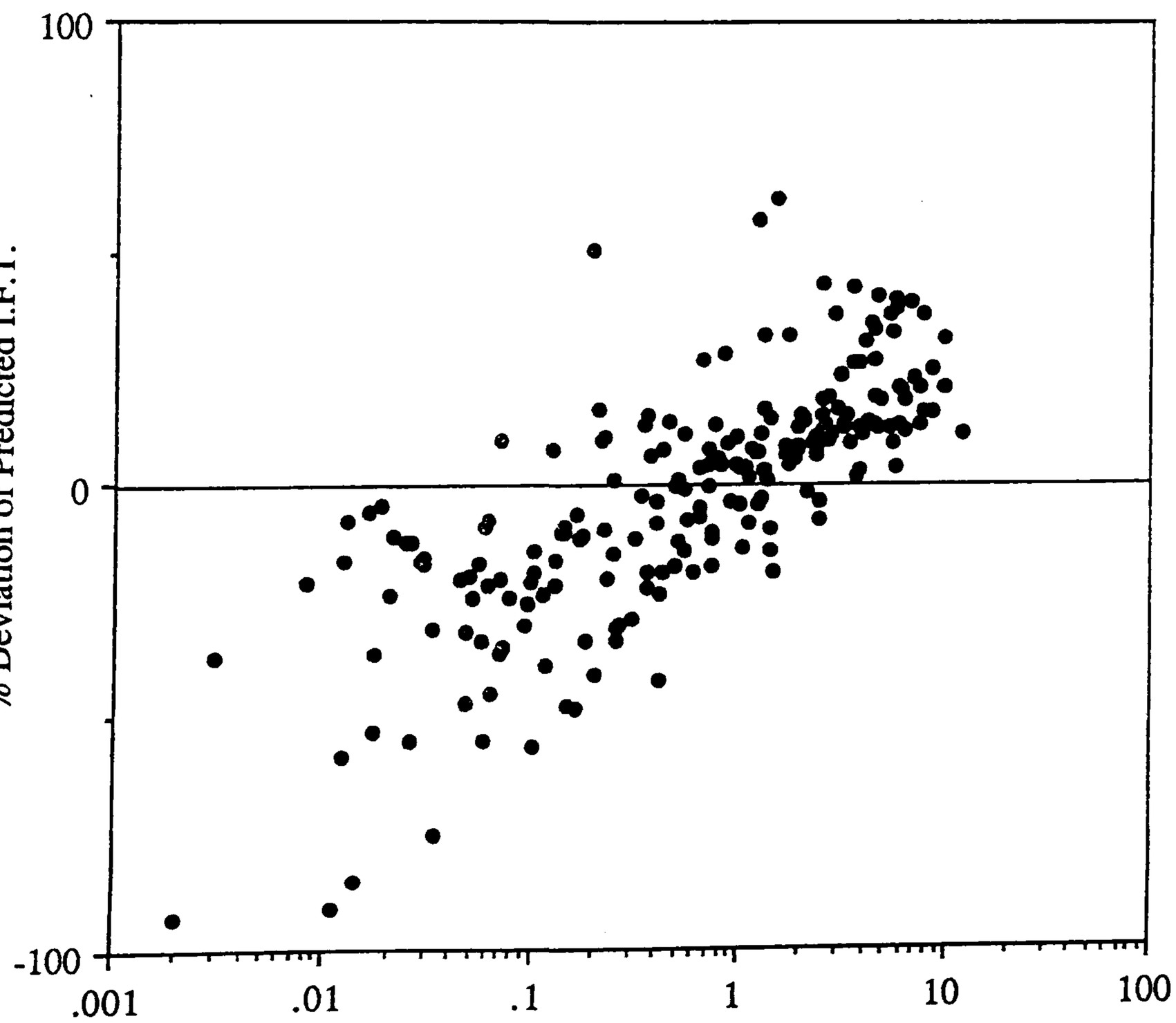

Figure 5.3.2 - Deviations of Predicted I.F.T. by Parachor Method for Binary Systems.

The constants 17.76 (Eq. 5.3.1) and 0.16 (Eq. 5.3.2) are dependent on the units used for ρ_{lm} (liquid molar density) and ρ_{vm} (vapour molar density). Since the unit for ρ_{lm} and ρ_{vm} used in this work is gm-mole/cc, the unit for the above constants is cc/gm-mole; thereby rendering the exponent E dimensionless.

The above modifications to the two methods were evaluated by comparing their predictions against experimental data of two multicomponent gas-condensate systems (Five and Twenty component) generated in this laboratory[13]. Since the completion of the above work, more data on interfacial tension was available for various other synthetic and real fluid systems. The following sections describe the experimental results on all these systems.

5.4 : EXPERIMENTAL RESULTS

Five and twenty component mixtures were selected and prepared to model real gas condensate fluids. The original single phase compositions of the tested fluids are given in Table 5.4.1. The two five-component mixtures A and B had similar compositions and were tested at 40 and 80°C; and 30 and 35°C respectively. The two phase compositions at 40 and 35°C were predicted using the three parameter Peng Robinson (PR) equations of state (EOS) as these data had not been measured. The two phase compositions and densities for these fluids are available in Tables 5.2.1-5.2.7 of Section 5.2. The values of IFT were measured at various pressure stages below the dew point at each temperature. The variation of IFT for the five component mixtures (Fluids A & B) at various isotherms is illustrated in Figure 5.4.1. The interfacial tension values predicted using both the modifications for Fluid A and B are presented in Table 5.4.2 and 5.4.3 respectively. For Fluid C the data has been furnished in Table 5.4.4.

After carrying out this preliminary study the deviations in prediction of interfacial tension were found to be reduced by half[13] when the modified exponents (Eq. 5.3.1 and 5.3.2) were applied. The effect was even more pronounced when the measured phase compositions and density data were applied. Also there is very little difference between accuracy of predicted

Table 5.4.1 - Compositions of Tested Fluids.

Component	Fluid A Mole(%)	Fluid B Mole (%)	Fluid D Mole (%)
CO_2	0.00	0.00	21.55
C_1	82.05	82.32	64.55
C_3	8.95	8.71	6.96
nC_5	5.00	5.05	3.63
nC_{10}	1.99	1.98	1.66
nC_{16}	2.01	1.94	1.65

Fluid C (20-Component System)

Component	Mole (%)
C_1	80.11
C_2	8.23
C_3	2.11
nC_4	1.07
nC_5	0.80
nC_6	1.20
nC_7	0.96
nC_8	0.55
nC_9	0.49
nC_{10}	0.48
nC_{11}	0.45
nC_{12}	0.44
nC_{13}	0.44
nC_{14}	0.41
nC_{15}	0.41
nC_{16}	0.39
nC_{17}	0.38
nC_{18}	0.37
nC_{19}	0.36
nC_{20}	0.35

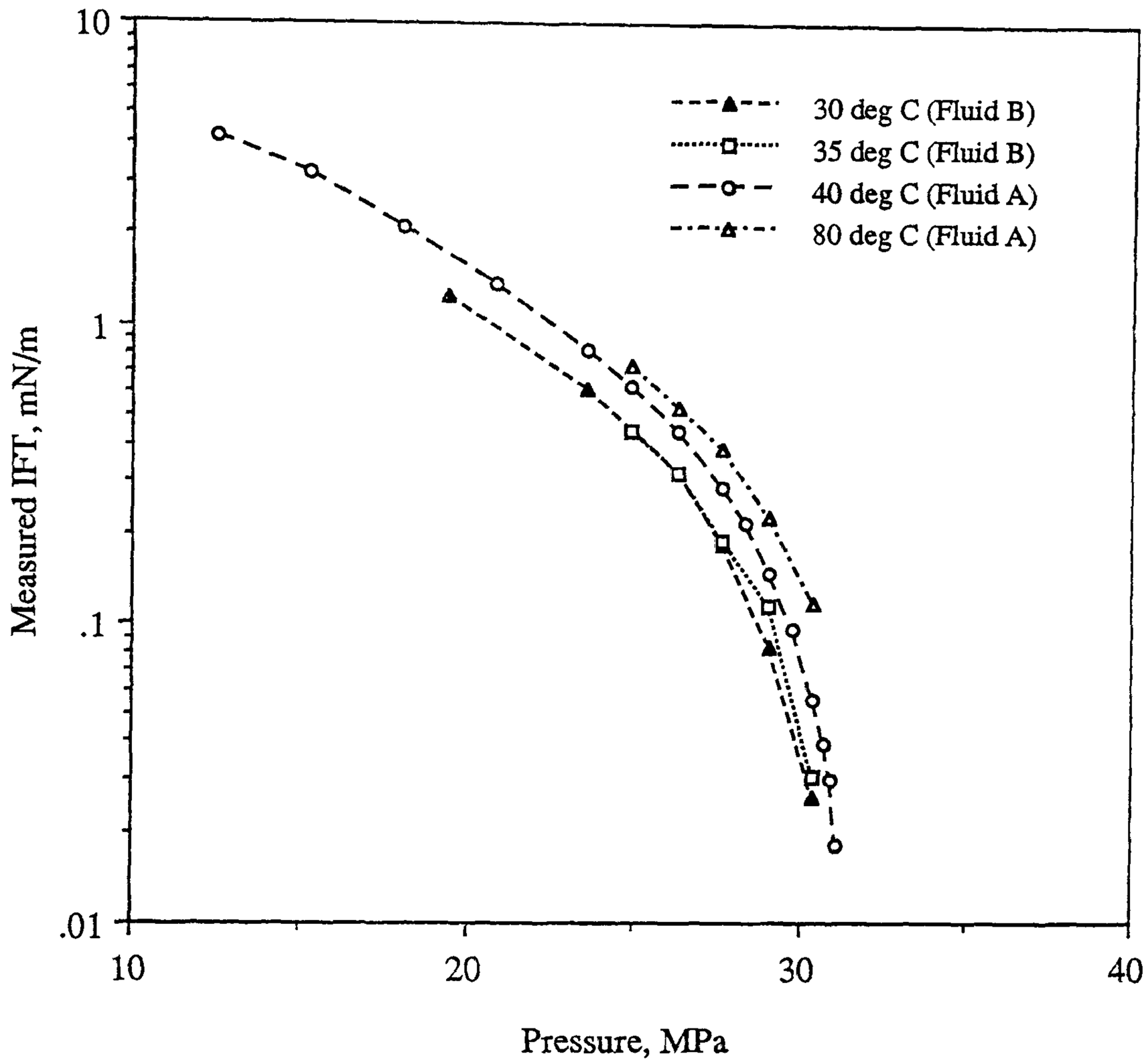

Figure 5.4.1 - Variations of IFT with Pressure for Five-Component Gas Condensate.

Table 5.4.2 - Interfacial Tension Data for Fluid A* Using Original and Modified Scaling Law and Parachor Methods.

No	Pressure MPa	Measured mN/m	Scaling Law, mN/m		Parachor Method, mN/m	
			Original	Modified	Original	Modified
			Temperature = 40°C			
1	31.11	0.019	0.015	0.022	0.014	0.022
2	30.94	0.030	0.016	0.025	0.016	0.025
3	30.77	0.039	0.023	0.034	0.023	0.034
4	30.42	0.056	0.039	0.054	0.039	0.054
5	29.73	0.097	0.063	0.083	0.063	0.085
6	29.04	0.150	0.110	0.133	0.110	0.137
7	28.35	0.220	0.150	0.173	0.150	0.179
8	27.66	0.290	0.180	0.207	0.180	0.216
9	26.29	0.450	0.310	0.343	0.320	0.360
10	24.91	0.630	0.445	0.484	0.470	0.512
11	23.53	0.830	0.600	0.629	0.640	0.669
12	20.77	1.380	1.100	1.099	1.200	1.178
13	18.02	2.090	1.800	1.716	2.000	1.850
14	15.26	3.180	3.010	2.736	3.340	2.950
15	12.50	4.200	4.800	4.215	5.400	4.516
		AAD** %	27.5	16.6	26.9	14.2
		STDEV %	14.7	11.0	18.9	10.5
			Temperature = 80°C			
1	30.42	0.118	0.090	0.114	0.090	0.115
2	29.04	0.229	0.185	0.220	0.189	0.225
3	27.66	0.390	0.330	0.371	0.341	0.382
4	26.29	0.536	0.490	0.529	0.512	0.549
5	24.91	0.738	0.716	0.744	0.753	0.776
		AAD %	14.0	2.9	12.1	2.8
		STDEV %	7.4	2.0	9.1	3.0

* The single phase composition of this fluid is provided in Table 5.4.1, and the two phase compositions are available in Tables 5.2.3 and 5.2.4 respectively.

** Average Absolute Deviation (AAD) and Standard Deviation (STDEV) are defined in Table 5.4.9.

Table 5.4.3 - Interfacial Tension Data for Fluid B* Using Original and Modified Scaling Law and Parachor Method.

No	Pressure MPa	Measured mN/m	Scaling Law, mN/m		Parachor Method, mN/m	
			Original	Modified	Original	Modified
			Temperature = 30°C			
1	30.42	0.026	0.012	0.019	0.011	0.018
2	29.04	0.083	0.058	0.080	0.062	0.083
3	27.66	0.185	0.130	0.164	0.140	0.171
4	26.29	0.321	0.227	0.268	0.245	0.284
5	23.53	0.607	0.585	0.623	0.642	0.672
6	19.39	1.255	1.500	1.445	1.680	1.589
		AAD %	27.7	12.7	28.4	14.5
		STDEV %	23.3	13.5	28.6	18.0
			Temperature = 35°C			
1	30.42	0.031	0.029	0.041	0.029	0.041
2	29.04	0.116	0.097	0.122	0.099	0.126
3	27.66	0.192	0.174	0.207	0.181	0.216
4	26.29	0.320	0.295	0.335	0.312	0.352
5	24.91	0.450	0.434	0.474	0.464	0.503
		AAD %	8.7	11.1	6.5	15.0
		STDEV %	4.3	10.7	5.8	8.7

* The single phase composition of this fluid is provided in Table 5.4.1, and the two phase compositions are available in Tables 5.2.1 and 5.2.2 respectively.

Table 5.4.4 - Interfacial Tension Data for Fluid C* Using Original and Modified Scaling Law and Parachor Method.

Pressure MPa	Measured mN/m	Scaling Law, mN/m		Parachor Method, mN/m	
		Original	Modified	Original	Modified
		Temperature = 65.5°C			
35.93	0.073	0.053	0.072	0.054	0.073
34.56	0.159	0.128	0.153	0.126	0.158
33.18	0.246	0.200	0.238	0.210	0.247
	AAD %	21.9	2.8	20.5	0.3
	STDEV %	12.8	1.0	12.7	0.4
		Temperature = 93.3°C			
35.93	0.040	0.029	0.041	0.029	0.042
34.56	0.120	0.062	0.085	0.063	0.086
33.18	0.210	0.103	0.130	0.107	0.135
	AAD %	42.3	23.3	41.3	23.0
	STDEV %	25.1	16.0	24.5	15.3
		Temperature = 121.1°C			
35.25	0.053	0.037	0.052	0.037	0.052
33.87	0.159	0.114	0.143	0.117	0.147
32.49	0.294	0.252	0.291	0.262	0.301
	AAD %	24.3	4.3	22.5	3.9
	STDEV %	14.6	3.4	13.9	2.7

* The single phase composition of this fluid is provided in Table 5.4.1, and the two phase compositions are available in Tables 5.2.5, 5.2.6 and 5.2.7.

results by the scaling law and the parachor method both with the original and the modified correlations.

These modifications have also been applied to a further amount of data on synthetic mixtures. Table 5.4.5 shows the comparison of measured (during a CCE test) and predicted interfacial tension data for a six component synthetic gas condensate mixture, referred to as Fluid D in Table 5.4.1, at 100°C. The two phase compositions were predicted from the three parameter PR EOS whereas measured density data were used for IFT calculations. The constant composition expansion (CCE) experiment was carried out in the gas condensate cell and the IFT data was determined by the gas-liquid curvature technique. Figure 5.4.2 and Table 5.4.6 present the comparison of measured and predicted interfacial tension for a gas cycling study for a six component synthetic gas condensate mixture at 100°C and 22.75 MPa (Section 3.5.6). Liquid phase compositions predicted by the three parameter PR EOS were used along with measured vapour phase compositions and densities. Table 5.4.7 shows the comparison of IFT data for a multiple contact study carried out on a ternary mixture of CH_4-C_3-n-C_{10} (Section 3.5.5) with pure methane at 37.8°C. Two phase compositions were predicted from the three parameter PR EOS whereas measured density data were used for IFT calculations. Figure 5.4.3 and Table 5.4.8 shows interfacial tension values predicted for a ternary mixture of CO_2-n-C_4-n-C_{10}[14] at 71.1°C. The calculations were performed using the measured phase compositions and density data provided in the literature[14]. An overall statistical analysis for 65 data points was performed for the original and modified scaling law and parachor methods and is furnished in Table 5.4.9. Also shown in Table 5.4.9 gives the deviations for all the methods for various different ranges of interfacial tension. This clearly indicates the superiority of the proposed modifications and it can also be seen that the simple introduction of a density dependent exponent has significantly improved the prediction performance of the scaling law and the parachor method.

5.5 : INTERFACIAL TENSION PREDICTIONS OF REAL RESERVOIR FLUIDS

A comparative study for real reservoir fluids has also been carried out using the scaling law[1] and the parachor method[2]. The interfacial tension predictions were carried out for the real

Table 5.4.5 - Interfacial Tension Data for Fluid D* Using Original and Modified Scaling Law and Parachor Method.

No	Pressure MPa	Measured mN/m	Scaling Law, mN/m		Parachor Method, mN/m	
			Original	Modified	Original	Modified
1	28.34	0.078	0.115	0.142	0.087	0.113
2	25.61	0.362	0.450	0.486	0.364	0.404
3	18.73	1.622	2.000	1.877	1.797	1.690
		AAD %	31.7	44.0	7.6	20.2
		STDEV %	11.1	27.9	5.0	17.7

* See Table 5.4.1 for single phase composition.

Table 5.4.6 - Interfacial Tension data for a Gas Injection Study on a Six Component Synthetic Gas Condensate at 22.75 Mpa and 100°C Using Original and Modified Scaling Law and Parachor Method.**

No	Stage No.	Measured mN/m	Scaling Law, mN/m		Parachor Method, mN/m	
			Original	Modified	Original	Modified
1	0	0.853	1.300	1.260	1.202	1.180
2	1	1.359	1.742	1.653	1.681	1.593
3	2	1.742	2.249	2.090	2.260	2.080
4	3	2.123	2.744	2.514	2.799	2.514
5	4	2.347	3.004	2.732	3.086	2.744
		AAD %	33.4	24.8	31.5	22.1
		STDEV %	15.5	12.3	14.3	10.5

** Tests carried out on this fluid are discussed in Section 3.5.6, Chapter 3. The two phase densities and compositions are available in Table 3.5.6.1 and 3.5.6.2 respectively.

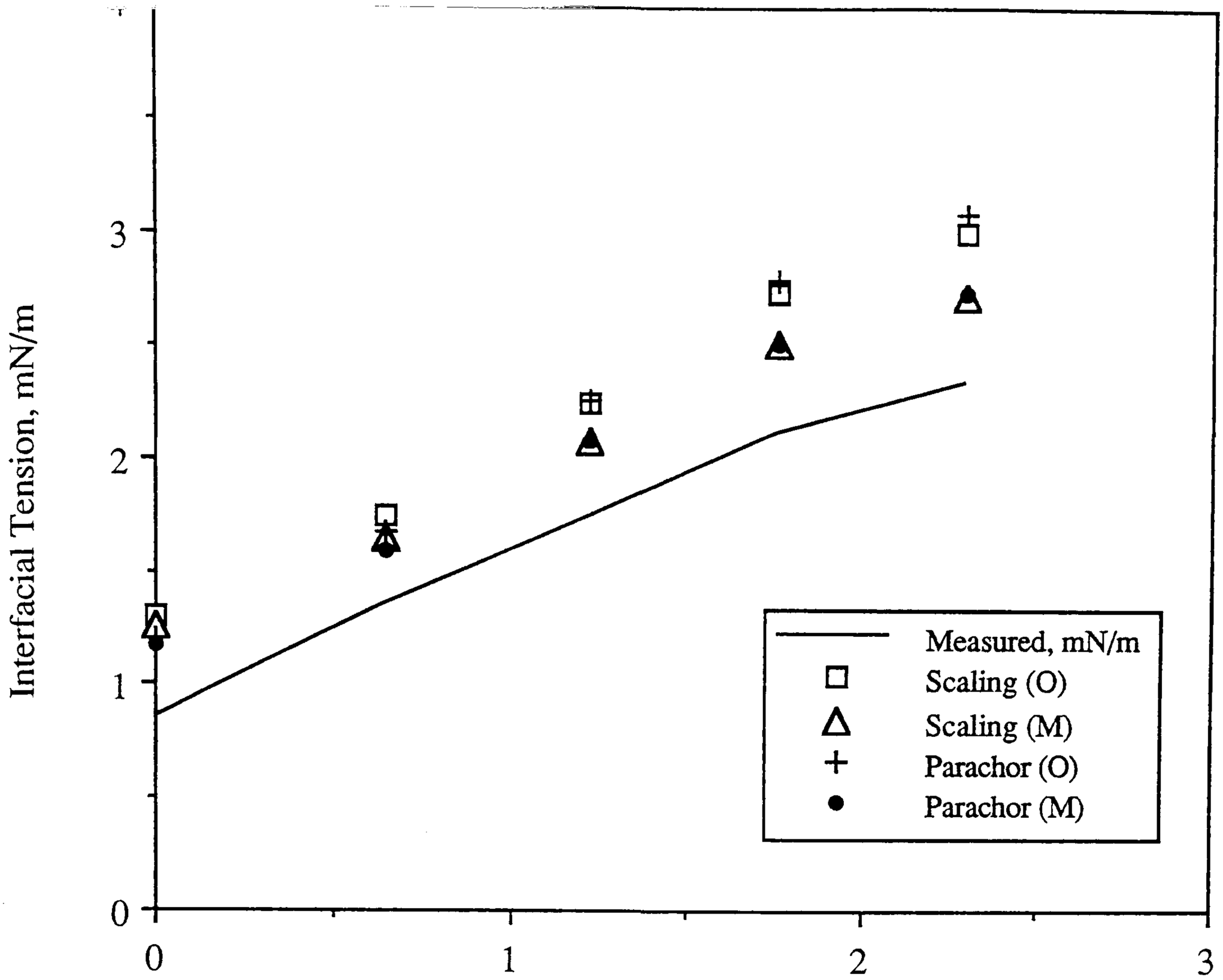

Figure 5.4.2 - IFT data for a Gas Cycling Study with CH4+CO2 on a Six Component Synthetic Gas Condensate at 22.75 MPa and 100 deg C.

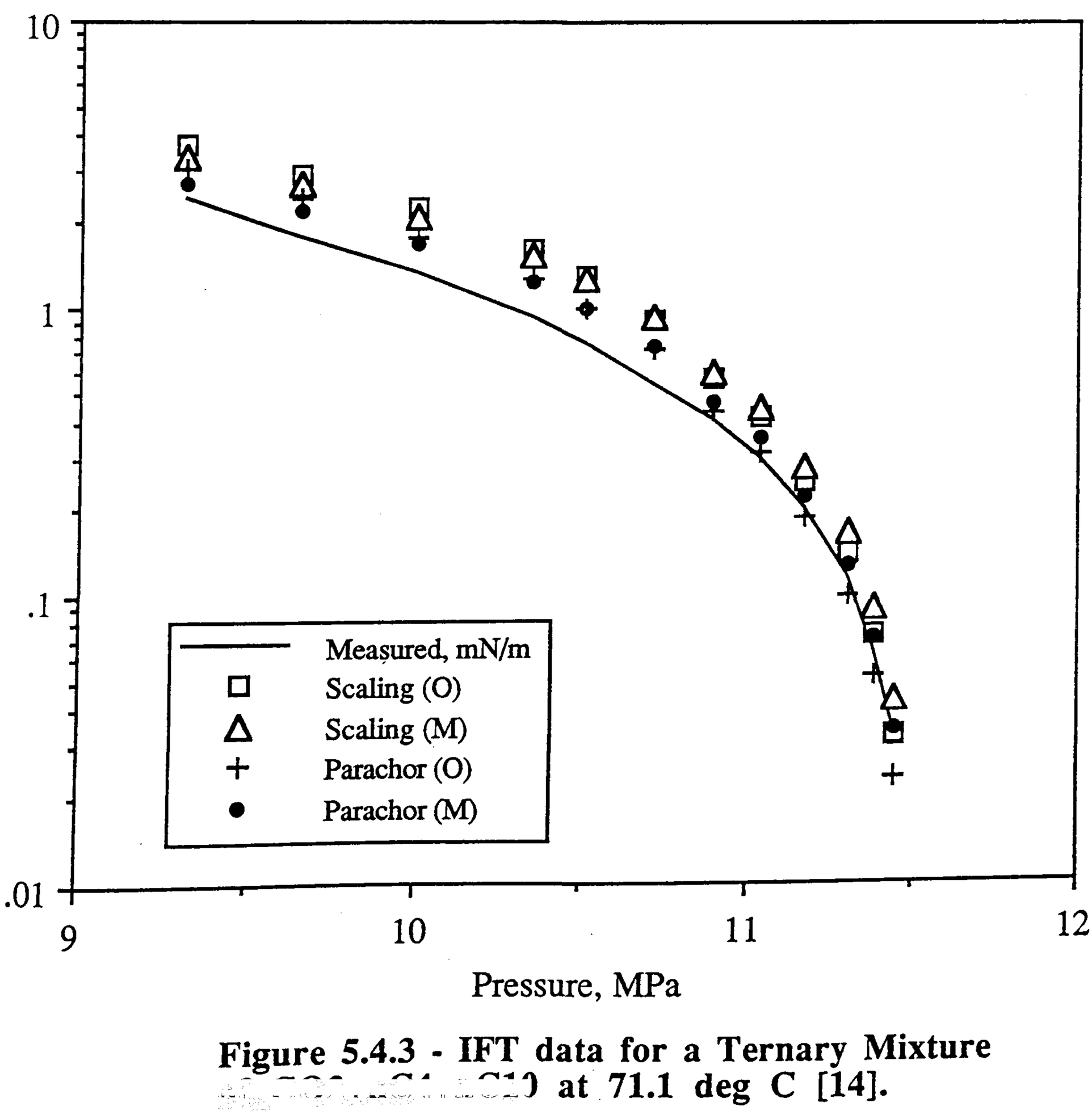

Figure 5.4.3 - IFT data for a Ternary Mixture [illegible] at 71.1 deg C [14].

Table 5.4.7 - Interfacial Tension data for a Forward Multiple Contact Study With CH_4 and a Ternary Mixture of CH_4-C_3-n-C_{10}* at 37.8°C Using Original and Modified Scaling Law and Parachor Method.

No	Stage No.	Measured mN/m	Scaling Law, mN/m		Parachor Method, mN/m	
			Original	Modified	Original	Modified
			Pressure = 20.68 MPa			
1	1	0.457	0.299	0.337	0.334	0.374
			Pressure = 13.79 MPa			
1	1	2.375	2.456	2.276	2.793	2.509
2	2	1.166	1.041	1.038	1.155	1.138
3	3	0.907	0.822	0.835	0.908	0.917
4	4	0.697	0.695	0.717	0.769	0.790
		AAD[1] %	11.7	10.4	11.1	8.1
		STDEV %	7.5	6.0	6.7	4.7

* See Table 3.5.5.1 and 3.5.5.2 for two phase densities and compositions respectively in Section 3.5.5 of Chapter 5.

1 Average absolute deviation and standard deviation is calculated for both pressures.

Table 5.4.8 - Interfacial Tension data for a Ternary Mixture of CO_2+n-C_4+n-C_{10} at 71.1°C[14] Using the Original and Modified Scaling Law and Parachor Method.

No	Pressure MPa	Measured mN/m	Scaling Law, mN/m		Parachor Method, mN/m	
			Original	Modified	Original	Modified
1	11.45	0.033	0.032	0.043	0.023	0.034
2	11.38	0.064	0.072	0.090	0.052	0.071
3	11.30	0.115	0.137	0.162	0.100	0.127
4	11.17	0.200	0.248	0.278	0.185	0.220
5	11.04	0.295	0.416	0.447	0.314	0.355
6	10.89	0.405	0.567	0.593	0.434	0.473
7	10.71	0.545	0.926	0.932	0.715	0.740
8	10.51	0.760	1.302	1.275	1.019	1.017
9	10.35	0.940	1.620	1.560	1.277	1.240
10	10.00	1.340	2.260	2.125	1.813	1.700
11	9.65	1.770	2.970	2.734	2.424	2.210
12	9.31	2.430	3.720	3.345	3.050	2.760
		AAD %	45.2	50.3	23.5	19.9
		STDEV %	14.8	15.0	7.6	6.5

Table 5.4.9 - Overall Statistical Analysis of IFT Prediction on Synthetic Hydrocarbon Mixtures.

No. of Data Points	Statistics	Scaling Law		Parachor Method	
		Original	Modified	Original	Modified
65	AAD	28	21	23	14
	STDEV	34	28	25	17
14 (I.F.T < 0.1 mN/m)	AAD	30	20	30	13
	STDEV	39	30	26	17
36 (0.1 < I.F.T < 1.0 mN/m)	AAD	28	22	20	14
	STDEV	33	29	22	15
15 (I.F.T > 1.0 mN/m)	AAD	28	22	22	14
	STDEV	27	24	16	14

$$\text{AAD \%} = \frac{100}{N} \sum_{i=1}^{N} \text{ABS}\left(\frac{\sigma_{pred} - \sigma_{exp}}{\sigma_{exp}}\right)$$

$$\text{STDEV \%} = \frac{100}{N} \text{SQRT}\left[\sum_{i=1}^{N}\left(\frac{\sigma_{pred} - \sigma_{exp}}{\sigma_{exp}}\right)^2\right]$$

gas condensate fluid C_3 (Section 3.6.1, Chapter 3), the real volatile oil (A) (Section 3.6.2, Chapter 3), the real black oil RFS-1 (Section 3.6.3, Chapter 3) and one data (named as Oil-C in Reference 15) set from the literature[15]. The parachor value and the B parameter used in the scaling law for the last fraction of each fluid was determined by matching to one measured IFT data point. This approach has been recommended by other investigators[15] as the generalised correlations for these parameters are not valid for the plus fraction of real reservoir fluids apparently due to the presence of heavy surface active compounds of asphaltic nature. These values were then applied to predict the IFT at other conditions for each mixture.

The predicted values of interfacial tension for the real gas condensate fluid C_3 are provided in Table 5.5.1 and Figures 5.5.1 and 5.5.2. The parameters of the last fraction were determined by matching the measured value of 0.622 mN/m for the constant volume depletion (CVD) test at 27.58 MPa and 140°C. These values were employed in calculating the IFT at other conditions for CCE, CVD and gas cycling tests. Measured phase densities and compositions were utilised in all calculations except for the gas cycling test where the liquid compositions were predicted as the liquid was not removed for sampling during the test. Information on two phase densities and compositions is available in Section 3.6.1 of Chapter 3.

Table 5.5.2 presents the comparison of predicted interfacial tension values with those measured by the pendant drop method for the real volatile oil (A) for the flash and four stage backward contact experiment at 100°C. The heavy end values were determined at an IFT value of 0.663 mN/m for the second stage of the four stage backward contact test. These values were then utilised in predicting the IFT for other conditions of the test and the flash experiment. Predicted phase compositions and measured density values were used for the IFT calculations for the four stage backward contact test. Measured phase compositions and densities were used for the flash test. Two phase densities and compositions are provided in Section 3.6.2 of Chapter 3.

A comparison between the measured and predicted interfacial tension data for the real black oil RFS-1 for various multiple contact tests at 34.58 MPa and 100°C has been presented in Table 5.5.3. Similar to the volatile oil the heavy end values were determined at an IFT value of

Table 5.5.1 - Prediction of IFT for Fluid C_3[1] Using Original and Modified Scaling Law and Parachor Method for CCE, CVD and Gas Cycling Tests.

No	Pressure/Stage No. MPa	Measured mN/m	Scaling Law, mN/m		Parachor Method, mN/m	
			Original	Modified	Original	Modified
			CCE*			
1	27.58	0.564	0.691	0.687	0.650	0.649
2	20.68	1.523	1.746	1.593	1.760	1.595
3	13.79	3.251	3.831	3.275	4.288	3.562
4	6.89	6.335	6.366	5.234	8.275	6.434
		AAD %	13.9	11.1	23.3	7.8
		STDEV %	8.1	7.1	12.3	4.6
			CVD**			
1	31.03	0.253	0.383	0.404	0.344	0.367
2	27.58	0.622	0.622	0.622	0.622	0.622
		AAD %	25.6	29.7	17.9	22.4
		STDEV %	18.1	29.7	17.9	22.4
			Gas Cycling***			
1	1	0.994	1.094	1.043	1.002	0.956
2	2	1.173	1.264	1.189	1.166	1.097
3	3	1.519	1.593	1.456	1.535	1.394
4	4	1.785	1.804	1.621	1.907	1.692
		AAD %	5.9	4.9	2.3	5.9
		STDEV %	3.4	2.8	1.7	3.1

1 See Table 3.6.1.1 for single phase compositions

* See Table 3.6.1.2 for compositions and Table 3.6.1.3 for densities

** See Table 3.6.1.4 compositions and Table 3.6.1.3 for densities

*** See Table 3.6.1.5 for compositions and Table 3.6.1.3 for densities

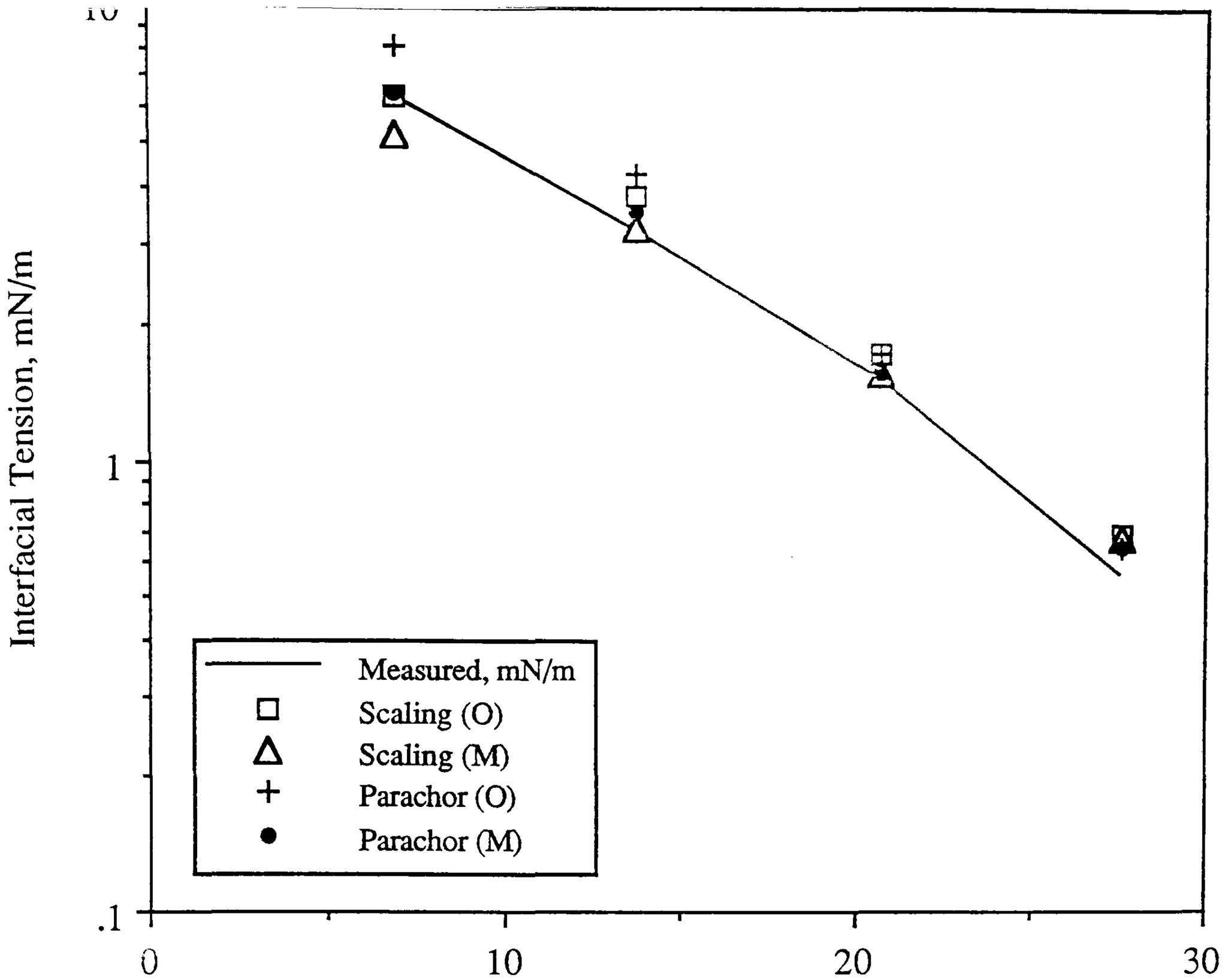

Figure 5.5.1 - IFT Data for Fluid C3 for a CCE Test at 140 deg C.

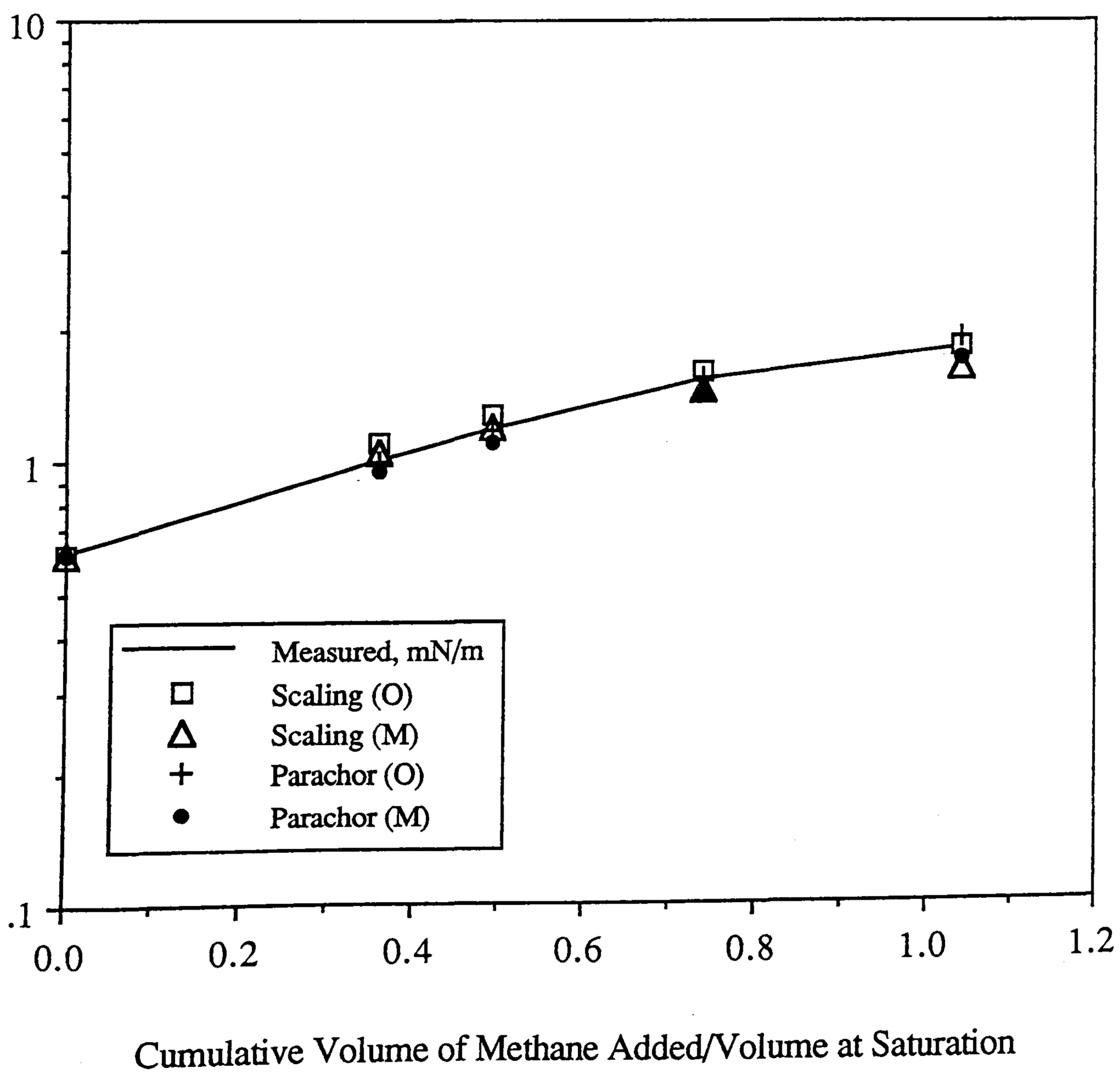

Figure 5.5.2 - IFT Data on Gas Cycling Test with Fluid C3 at 140 deg C.

Table 5.5.2 - Prediction of IFT for Real Volatile Oil (A)[1] Using Original and Modified Scaling Law and Parachor Method for CCE, and Four Stage Backward Contact Study.

No	Pressure/Stage No. MPa	Measured mN/m	Scaling Law, mN/m		Parachor Method, mN/m	
			Original	Modified	Original	Modified
			CCE*			
1	13.79	7.046	10.129	8.042	10.318	7.924
2	10.34	10.313	14.138	10.980	14.207	10.564
3	6.89	13.519	19.617	14.912	19.500	14.036
		AAD %	41.9	10.3	42.8	6.2
		STDEV %	24.3	6.2	24.8	4.4
			Multiple Contact**			
1	1	0.663	0.663	0.663	0.663	0.663
2	2	1.420	1.755	1.558	1.593	1.453
3	3	2.170	3.540	2.853	2.958	2.526
4	4	3.239	7.456	5.326	5.545	4.418
		AAD %	54.2	26.4	29.9	13.8
		STDEV %	36.6	18.1	20.2	10.0

1 See Table 3.6.2.1 for single phase compositions

* See Table 3.6.2.2 for compositions and Table 3.6.2.3 for densities

** See Table 3.6.2.5 for compositions and Table 3.6.2.4 for densities

Table 5.5.3 - Prediction of IFT for Real Black Oil, RFS - 1[11] Using Original and Modified Scaling Law and Parachor Method for Various Multiple Contact Tests.

No	Stage No.	Measured mN/m	Scaling Law, mN/m		Parachor Method, mN/m	
			Original	Modified	Original	Modified
			MBC[1] with Methane*			
1	2	2.189	2.880	2.581	2.710	2.440
2	3	3.319	4.727	4.022	4.380	3.751
3	4	4.515	6.127	5.036	5.581	4.660
		AAD %	36.6	16.9	26.5	9.2
		STDEV %	21.3	10.0	15.4	5.9
			MFC[2] with Methane**			
1	1	2.091	2.564	2.302	2.504	2.273
2	2	0.987	0.987	0.987	0.987	0.987
3	3	0.437	0.444	0.484	0.451	0.490
		AAD %	8.1	6.9	7.6	6.9
		STDEV %	7.6	4.9	6.7	5.0
			MFC with CH_4+CO_2***			
			CH_4 = 79.86 mole %			
			CO_2 = 20.16 mole %			
1	1	1.168	1.957	1.812	1.735	1.636
2	2	0.325	0.480	0.519	0.448	0.487
		AAD %	57.6	57.4	43.2	44.9
		STDEV %	41.3	40.6	30.8	32.0

1 MBC - Multiple Backward Contact

2 MFC - Multiple Forward Contact

11 See Table 3.6.3.1 for single phase compositions

* See Table 3.6.3.2 for compositions and Table 3.6.3.3 for densities

** See Table 3.6.3.4 for compositions and Table 3.6.3.5 for densities

*** See Table 3.6.3.6 for compositions and Table 3.6.37 for densities

Table 5.5.4 - Prediction of IFT for Oil - C[1] from Reference [15] Using Original and Modified Scaling Law and Parachor Method.

No	Pressure MPa	Measured mN/m	Scaling Law, mN/m		Parachor Method, mN/m	
			Original	Modified	Original	Modified
1	26.30	1.300	1.500	1.700	1.200	1.400
2	22.86	2.300	2.400	2.500	2.100	2.300
3	19.41	3.300	3.400	3.500	3.100	3.300
4	15.96	4.600	4.600	4.600	4.600	4.600
		AAD %	5.7	11.4	5.6	1.9
		STDEV %	4.1	8.1	3.3	1.9

1 Densities and phase compositions from Reference 15 employed for all calculations

Table 5.5.5 - Overall Statistical Analysis of IFT Prediction for 29 data Points on Real Reservoir Fluids.

No. of Data Points	Statistics	Scaling Law		Parachor Method	
		Original	Modified	Original	Modified
29	AAD	26	17	21	11
	STDEV	28	21	20	15

$$\text{AAD \%} = \frac{100}{N} \sum_{i=1}^{N} \text{ABS}\left(\frac{\sigma_{pred} - \sigma_{exp}}{\sigma_{exp}}\right)$$

$$\text{STDEV \%} = \frac{100}{N} \text{SQRT}\left[\sum_{i=1}^{N}\left(\frac{\sigma_{pred} - \sigma_{exp}}{\sigma_{exp}}\right)^2\right]$$

0.987 mN/m for the second stage of the multiple forward contact test using pure methane as an injection gas. Measured phase compositions and densities were employed for all IFT predictions. All the data on two phase densities and compositions is furnished in Section 3.6.3 of Chapter 3. These tuned parameters were subsequently employed to predict the IFT at other contact stages.

Table 5.5.4 shows the predictions for Oil-C at 82°C from Reference 15. The heavy end values were determined at an IFT value of 4.6 mN/m and were used in prediction at other conditions. Two phase compositions and densities provided in Reference 15 were employed for all the IFT calculations. The overall statistical analysis of all the data of Tables 5.5.1 to 5.5.4 for the original and modified scaling law and the parachor method has been provided in Table 5.5.5. The modified methods clearly show a better overall performance than the original methods.

References

1) Lee, S.T. and Chien, M.C.H.: "A New Multicomponent Surface Tension Correlation Based on Scaling Theory", Presented at the SPE/DOE Fourth Symposium on Enhanced Oil Recovery held in Tulsa, Oklahoma, SPE/DOE, 12643, April 15-18, (1984).

2) Weinaug, C.F. and Katz, D.L.:"Surface Tension of Methane - Propane Mixtures", *Industrial & Engineering Chemistry (I & EC)*, pp. 239-246, (1943).

3) Hough, E.W. and Stegemeier, G.L.: "Correlation of Surface Tension of Light Hydrocarbons in the Critical Region", *Society of Petroleum Engineers Journal (SPEJ)*, pp. 259-263, (Dec., 1961).

4) Danesh, A., Todd, A.C., Somerville, J. and Dandekar, A.: "Direct Measurement of Interfacial Tension, Density, Volume, and Compositions of Gas - Condensate System", *Trans IChem E*, Vol. 68, Part A, (Jul., 1990).

5) Pennington, B.F. and Hough, E.W.: "Interfacial Tension of the Methane - Normal Butane System", *Producers Monthly*, pp. 4, (Jul., 1965).

6) Stegemeier, G.L. and Hough, E.W.: "Interfacial Tension of the Methane - Normal Pentane System", *Producers Monthly*, pp. 6-9, (Nov., 1961).

7) Stegemeier, G.L., Pennington, B.F., Brauer, E.B. and Hough, E.W.: "Interfacial Tension of the Methane - Normal Decane System", *Society of Petroleum Engineers Journal (SPEJ)*, pp. 257-260, (Sep., 1962).

8) Hsu, Jack, J.C, Nagarajan, N. and Robinson, R.L.Jr.: "Equilibrium Phase Compositions, Phase Densities, and Interfacial Tensions for CO_2 + Hydrocarbon Systems. 1. CO_2 + n - Butane", *J. Chem. & Engg. Data.*, Vol. 30, No.4, pp. 485-491, (1985).

9) Nagarajan, N. and Robinson, R.L.Jr.: "Equilibrium Phase Compositions, Phase Densities, and Interfacial Tensions for CO_2 + Hydrocarbon Systems. 2. CO_2 + n - Decane", *J. Chem. & Engg. Data.*, Vol. 31, No. 2, pp. 168-171, (1986).

10) Gasem, K.A.M., Dickson, K.B., Dulcamara, P.B., Nagarajan, N. and Robinson, R.L.Jr.: "Equilibrium Phase Compositions, Phase Densities, and Interfacial Tensions for CO_2 + Hydrocarbon Systems. 5. CO_2 + n - Tetradecane", *J. Chem. & Engg. Data.*, Vol. 34, No. 2, pp. 191-195, (1989).

11) Sage, B.H. and Lacey, W.N.: "Thermodynamic Properties of the Lighter Paraffin Hydrocarbons and Nitrogen", New York, API, (1950).

12) Reid, R.C. and Sherwood, T.K.: "The Properties of Gases and Liquids", Second Edition, McGraw Hill Book Co., New York (1973).

13) Danesh, A.S., Dandekar, A.Y., Todd, A.C. and Sarkar, R.:"A Modified Scaling Law and Parachor Method Approach for Improved Prediction of Interfacial Tension of Gas-Condensate Systems", Presented at the 66th Annual Technical Conference and Exhibition of the Society of Petroleum Engineers held in Dallas, Texas, October 6-9, SPE 22710, (1991).

14) Nagarajan, N., Gasem, K.A.M. and Robinson, R.L.:"Equilibrium Phase Compositions, Phase Densities, and Interfacial Tensions for

CO_2+Hydrocarbon Systems. 6. CO_2+n-Butane+n-Decane", *J. Chem. Eng. Data*, Vol. 35, No. 35, pp. 228-231, (1990).

15) Firoozabadi, A., Katz, D.L., Soroosh, H. and Sajjadian, V.A.:"Surface Tension of Reservoir Crude-Oil/Gas Systems Recognising the Asphalt in the Heavy Fraction", *Society of Petroleum Engineers Journal (Reservoir Engineering)*, pp. 265-272, (Feb., 1988).

CHAPTER 6 : CONCLUSIONS AND RECOMMENDATIONS

6.1 : CONCLUSIONS

Various techniques for measuring the interfacial tension between hydrocarbon vapour and liquid phases have been evaluated in this work. It has been shown that the pendant drop method which is widely used in the petroleum industry for measuring IFT, proves to be a useful technique for measuring IFT at high values or low pressures but it is rather inaccurate for measuring IFT at low values or high pressure conditions. A novel technique based on the liquid-vapour interface curvature is introduced in this work to measure the interfacial tension of hydrocarbon fluids along with other properties with a minimum effort. The IFT values measured by the above technique have been compared with literature data wherever possible and their reliability demonstrated. The following main conclusions can be drawn from the work carried out on IFT measurements :

1. A large amount of accurate and highly valuable data on interfacial tension, of synthetic hydrocarbon mixtures and real reservoir fluids, at high pressure and high temperature conditions has been generated in this work along with the commonly available data on phase compositions, densities and volumes.

2. The measurement of gas-liquid interface curvature provides accurate interfacial tension data with almost no extra effort if one has access to the equipment. The relationship is rigorous and does not involve any empiricism and hence no need for calibration. The simultaneous measurement of IFT, density and composition is highly advantageous. It provides accurate IFT values and all the information required to evaluate and improve IFT prediction methods.

3. The gas-liquid curvature technique developed in this work is now routinely employed in the gas condensate PVT cell for measuring the IFT data for gas condensate type

fluids. Similarly the pendant drop method is now trivially used in the VLE cell to measure the IFT data for volatile oil and black oil systems.

4. Interfacial tension varies with density difference between liquid and gas phases in direct proportion, and hence accurate density data is essential for a reliable measurement of interfacial tension, especially at high pressure conditions.

The two most widely used methods of predicting the interfacial tension in the petroleum industry i.e. the scaling law and the parachor methods have been evaluated in this work. It has been shown that the exponent in the interfacial tension correlations is not a universal constant as commonly assumed in the prediction methods. The methods have been modified by relating the exponent value to the liquid-vapour density difference and the relevant correlations have been developed. The following main conclusions can be drawn from this study.

1. The Weinaug-Katz (parachor method) and the Lee-Chien (scaling law) correlations predict the IFT of high pressure hydrocarbon systems with a comparable accuracy. The first method is, however, superior particularly at low IFT conditions.

2. Both methods generally underpredict at low IFT and overpredict at high IFT ranges, with relatively accurate results around 1 mN/m.

3. The modification proposed in this work, which can be simply applied to both methods has improved the predicted IFT.

4. The comparative study carried out on the original and modified scaling law and parachor method using interfacial tension data measured in-house and from literature on synthetic mixtures and real reservoir fluids has clearly demonstrated the superiority of the proposed modifications.

6.2 : RECOMMENDATIONS

The proposed measurement technique for IFT should further be used for more real gas - condensate fluids, at a wide range of temperature and pressure conditions, in order to obtain more of reliable data on interfacial tension.

The modifications proposed in the predictive techniques namely the scaling law and the parachor method are recommended for estimation of interfacial tension of synthetic hydrocarbon mixtures and real reservoir fluids instead of the original ones.

PART B - VISCOSITY

ABSTRACT

Viscosity is an important property required in various reservoir engineering calculations. It is commonly predicted by either, the residual viscosity method or the principle of corresponding states method. Various correlations available for estimation of viscosity are reviewed in this part of the thesis. Also discussed are the various density correlations which are generally used for density dependent viscosity correlations.

A comparative study for pure hydrocarbon components and their mixtures by using various viscosity prediction methods is presented. Also presented is a tuning study on various real reservoir fluids by employing the popularly used residual viscosity and corresponding states methods respectively. The drawbacks of these techniques have been highlighted.

The residual viscosity method is critically evaluated and it has been proved that the variation of residual viscosity with respect to reduced density is not uniform for all fluids, particularly in the dense fluid phase. Based on a large number of data on pure hydrocarbon compounds in the dense fluid phase from literature, the residual method is modified by relating the residual viscosity of a fluid to its molecular weight along with its reduced density in dense fluid phase conditions. The modified method has been applied to various pure hydrocarbon compounds and their mixtures, and real reservoir fluids. The superiority of the new method has been demonstrated by comparing the results with those of the original methods and those based on the principle of corresponding states.

TABLE OF CONTENTS

LIST OF SYMBOLS

Nomenclature

A,a	=	Equations of State Constants
B,b	=	Equations of State Constants
E,r,s	=	Constants in Alani-Kennedy Equations of State
f,h	=	Substance Reducing Ratios in the TRAPP Method
F_η	=	Parameter in the TRAPP Method
L,l	=	Liquid Phase
M,MW	=	Molecular Weight
P	=	Pressure
R	=	Universal Gas Constant
T	=	Temperature
V	=	Volume
v	=	Vapour Phase
X,x	=	Liquid Phase Mole Fraction
Y,y	=	Vapour Phase Mole Fraction
Z	=	Compressibility Factor
z	=	Mole Fraction of the ith Component in a Mixture

Greek

α	=	Rotational Coupling Effect
η	=	Dynamic Viscosity
η^*	=	Low Pressure Gas Phase Viscosity
θ,ϕ	=	Shape Factors in the TRAPP Method
ρ	=	Density

σ	=	Interfacial Tension
ω	=	Acentric Factor
ξ,λ	=	Inverse of Critical Viscosity

Subscripts

c	=	Critical Value
C7+	=	Plus Fraction of a Real Reservoir Fluid
i,j	=	Component Index
l	=	Liquid
m	=	Molar/Mixture
mix	=	Mixture
n	=	Number of Components
o	=	Reference Component Indicator
r	=	Reduced Value
v	=	Vapour

Abbreviations

AAD	=	Average Absolute Deviation
ABS	=	Absolute Value
BIAS	=	Arithmetic Average of Percentage Deviations
EOR	=	Enhanced Oil Recovery
EOS	=	Equations of State
FPE	=	Fluid Phase Equilibria
J-S-T	=	Jossi-Stiel-Thodod
L-B-C	=	Lohrenz-Bray-Clark

PCS	=	Principle of Corresponding States
RV	=	Residual Viscosity
SG	=	Specific Gravity
STDEV	=	Standard Deviation
TRAPP	=	Transport Properties Prediction Program
VLE	=	Vapour-Liquid Equilibria

LIST OF TABLES

LIST OF FIGURES

CHAPTER 1 : INTRODUCTION - VISCOSITY

1.1 : DEFINITIONS

When a shearing force is applied to a fluid at rest it causes the fluid to deform. The deformation takes place in the form of one layer of fluid sliding over an adjacent one with a different velocity. All fluids in nature are known to offer some resistance to such a movement of one layer over another. This resistance is attributed to a property of the fluid called *viscosity*. Therefore, viscosity is the property of a fluid which is a measure of its internal resistance to relative motion between adjacent layers. The dynamic viscosity, η, of a Newtonian fluid is defined as the ratio of shear stress to shear rate :

$$\eta = \frac{\varsigma_{xy}}{\frac{dV_x}{dY}} \qquad (1.1.1)$$

the quantity in the numerator is the shear stress, and V_x is the velocity of the fluid in the x - direction (the direction of the applied stress), and the denominator is the gradient of the velocity in y - direction (perpendicular to flow (x) - direction). Viscosity can also be described as the physical property which describes the shear force in flow phenomenon. In fluids subjected to shear deformation, the deformation rate varies linearly with shear for Newtonian fluids, where the proportionality is dynamic viscosity. Although the viscosity is not an equilibrium property, it is determined by the state of temperature, pressure and composition of a fluid.

The phenomenon of viscosity can be further investigated by the following experiment. In Figure 1.1.1 two adjacent layers of area A within a fluid separated by a small distance dy are shown to be in motion. The top layer is moving at a velocity of V + dV, and the lower layer with a velocity V. In order to maintain a difference in velocity dV between the layers, a force F is required in the upper layer in order to counteract the friction between the molecules of the fluid. According to experimental observations :

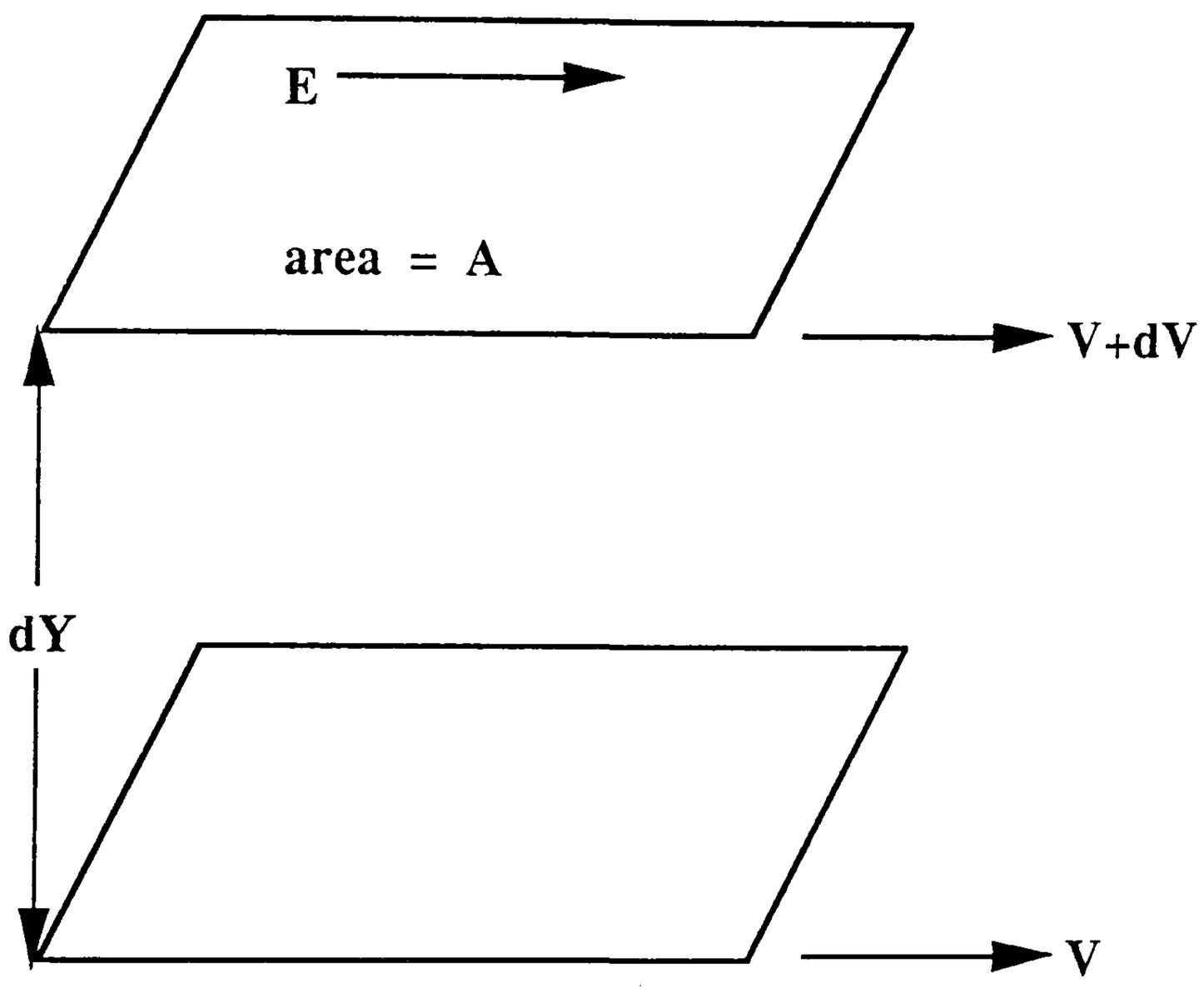

Figure 1.1.1 - Two Layers of a Fluid in Relative Motion.

$$\frac{F}{A} \sim \frac{dV}{dY}$$

or,

$$\frac{F}{A} = \eta \frac{dV}{dY} \qquad (1.1.2)$$

Where η is generally constant for a given (Newtonian) fluid at a given set of pressure and temperature. Hence, another definition of viscosity is:

$$\eta = \frac{\frac{F}{A}}{\frac{dV}{dY}} \qquad (1.1.3)$$

However, a wide range of industrially important liquids, such as solutions of high molecular weight polymers, colloids, suspensions, and emulsions, exhibit more complex behaviour, which is termed non-Newtonian in which case the ratio of shear stress to shear rate is not constant. This work is limited to Newtonian fluids, i.e., fluids in which the viscosity, η, is constant and is independent of either the magnitude of the shearing stress or velocity gradient (rate of change in shear).

In the CGS system of units, force F is in dynes, area A is in sq. cm, differential velocity dV is in cm/sec and the distance between the two layers dY is in cm, which gives :

$$\eta = \frac{\text{dyne/cm}^2}{\text{(cm/sec)/cm}} \qquad (1.1.4)$$

but, 1 dyne = $\frac{\text{gm cm}}{\text{sec}^2}$ therefore we get :

$$\eta = \frac{\text{gm}}{\text{cm sec}}$$

$$= \text{poise} \quad (ML^{-1}T^{-1})$$

Viscosity is commonly expressed in centipoise, in the oil industry.

In the SI units it is denoted in $\frac{Ns}{m^2}$ which is:

$$1\ \frac{Ns}{m^2} = 0.1\ \text{Poise}$$

The kinematic viscosity is defined as the ratio of the dynamic viscosity to the density, with viscosity in centipoise and the density in gram per cubic centimetre, and its unit is called centistoke.

1.2 : SIGNIFICANCE OF VISCOSITY IN RESERVOIR ENGINEERING

As mentioned earlier viscosity can be loosely defined as the internal resistance to the flow of fluid. Since pressure drop due to flow of fluids in porous media and in pipes is directly related to the fluid viscosity, its determination for high pressure multicomponent hydrocarbon fluids is of considerable interest at reservoir and flow line conditions. In this section a brief discussion is presented regarding the importance of this property in recovery of petroleum fluids.

The viscosity of hydrocarbon mixtures is of particular interest in various reservoir engineering calculations and mathematical simulations. It also plays a significant role in chemical engineering design calculations for process equipments. In dealing with condensate fluids and volatile and black oils the compositional effects resulting from changing pressure materially affect the viscosity. The effect of compositional changes is very significant in certain secondary recovery or pressure maintenance processes, notably miscible displacement or gas injection.

In compositional material balance computations, the compositions of the reservoir gases and oils is available. The calculation of the viscosities of these fluids using this composition

information is required for calculation of flowrates or pressure drops in reservoir due to flow of these fluids.

Viscosity is of paramount importance as far as the processes of enhanced oil recovery (EOR) are concerned, its significance is demonstrated in the following paragraphs. The mobility of a fluid can be defined by the following simple equation:

$$\lambda = \frac{k_r}{\mu} \qquad (1.2.1)$$

where

λ = fluid mobility

k_r = relative permeability and

μ = fluid viscosity

In the process of enhanced oil recovery, the mobility ratio in terms of the ratio of the mobility of the displacing fluid to the mobility of the displaced fluid can be defined by :

$$M = \frac{\lambda_1}{\lambda_2} \qquad (1.2.2)$$

where

M = the mobility ratio

λ_1 = mobility of the displacing fluid and

λ_2 = mobility of the displaced fluid

The higher the viscosity of the displacing fluid the lower will be its mobility and it will provide a piston type and very efficient displacement mechanism (rather than fingering through the displaced fluid). In polymer flooding the viscosity of the injected water is expressly increased (by addition of polymers) to improve the displacement efficiency and increase recovery.

In high viscosity oil reservoirs where the viscosity of oil is many fold that of water, waterflooding is not efficient because of poor mobility ratio. Either the viscosity of oil is reduced by injecting steam or viscosity of water is increased by addition of polymers. Since steam has itself low viscosity, surfactants are used to create foam ahead of steam, to increase the displacing fluid viscosity (hence reduce its mobility) and improve the displacement (and recovery) efficiency. Reference[1], gives more detailed information on the significance of viscosity in enhanced oil recovery (EOR), processes.

1.3 : EFFECT OF TEMPERATURE AND PRESSURE ON VISCOSITY OF PURE COMPONENTS

Viscosity of gases and liquids is a function of pressure and temperature as illustrated in Figures 1.3.1 through 1.3.5[2]. In Figure 1.3.1, the viscosity of carbon dioxide is plotted as a function of temperature with isobars. However, if the viscosity were plotted as a function of pressure with isotherms, one would have a phase diagram as illustrated in Figure 1.3.2 for nitrogen. Lucas[2] has generalised the viscosity phase diagram (for non-polar gases) as shown in Figure 1.3.3. In this case the ordinate $\eta\xi$ and the temperatures and pressures are reduced values. η is the viscosity and ξ is the inverse reduced viscosity defined by:

$$\xi = \frac{T_c^{1/6}}{M^{1/2}\, P_c^{2/3}} \qquad (1.3.1)$$

where,

T_c = critical temperature

M = molecular weight and

P_c = critical pressure

In Figure 1.3.3, the lower limit of the P_r curves would be indicative of the dilute gas state (low pressure conditions). In such a state, η increases with temperature. At high reduced pressures, there is a wide range of temperatures where η decreases with temperature. In this region the viscosity behaviour more closely simulates a liquid state, and, as will be discussed

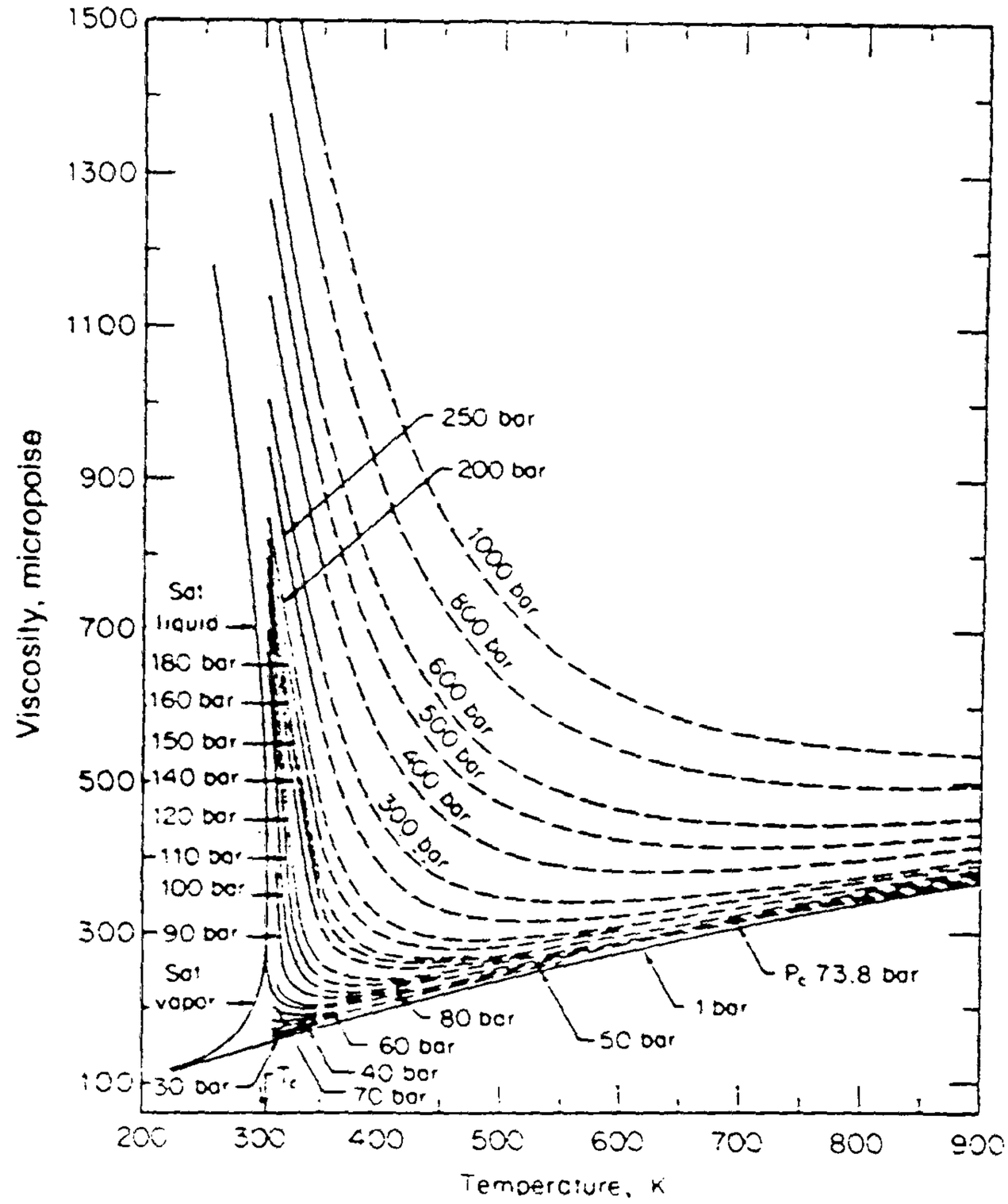

Figure 1.3.1 - Viscosity of Carbon Dioxide (from Reference 2).

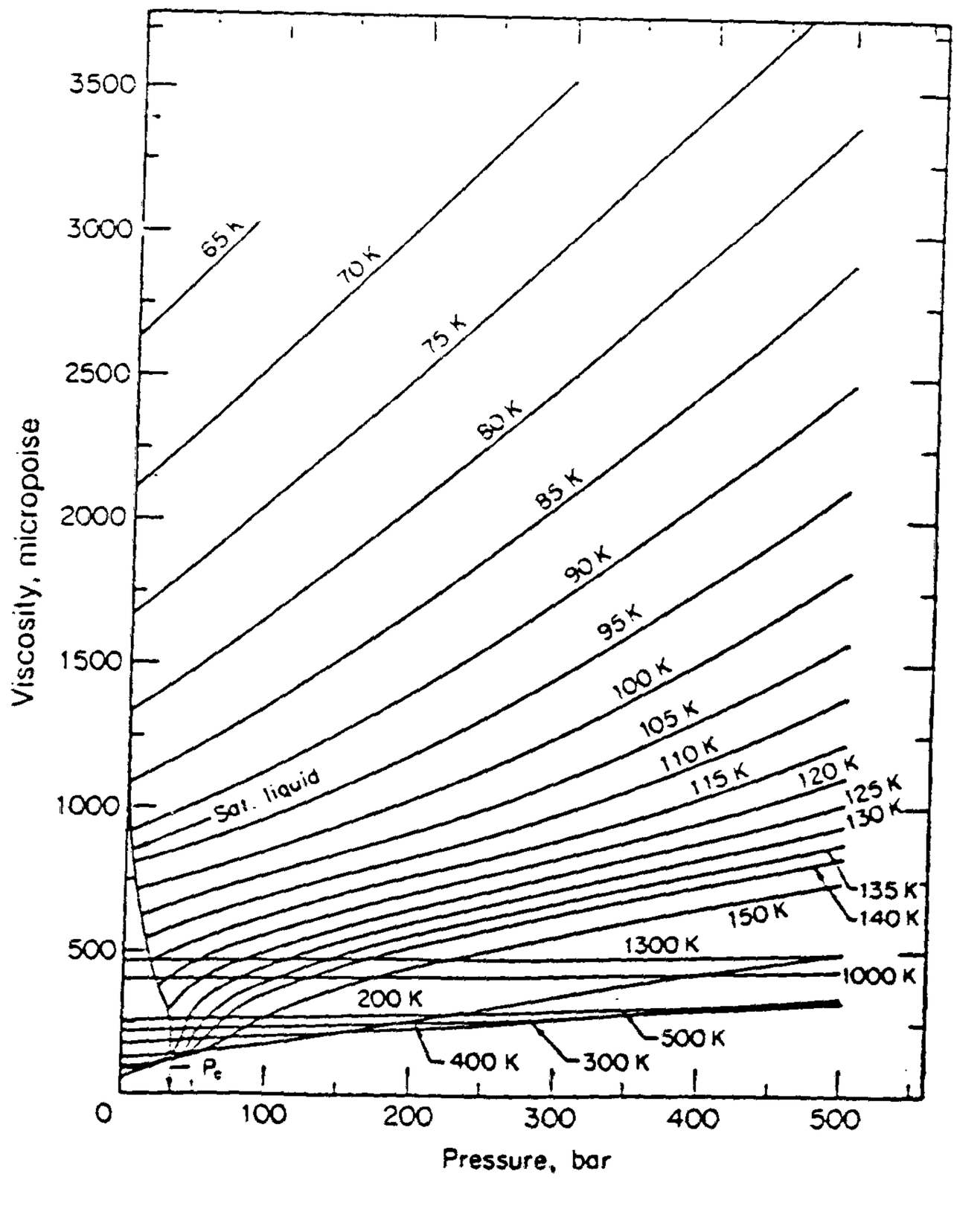

Figure 1.3.2 - Viscosity of Nitrogen (from Reference 2).

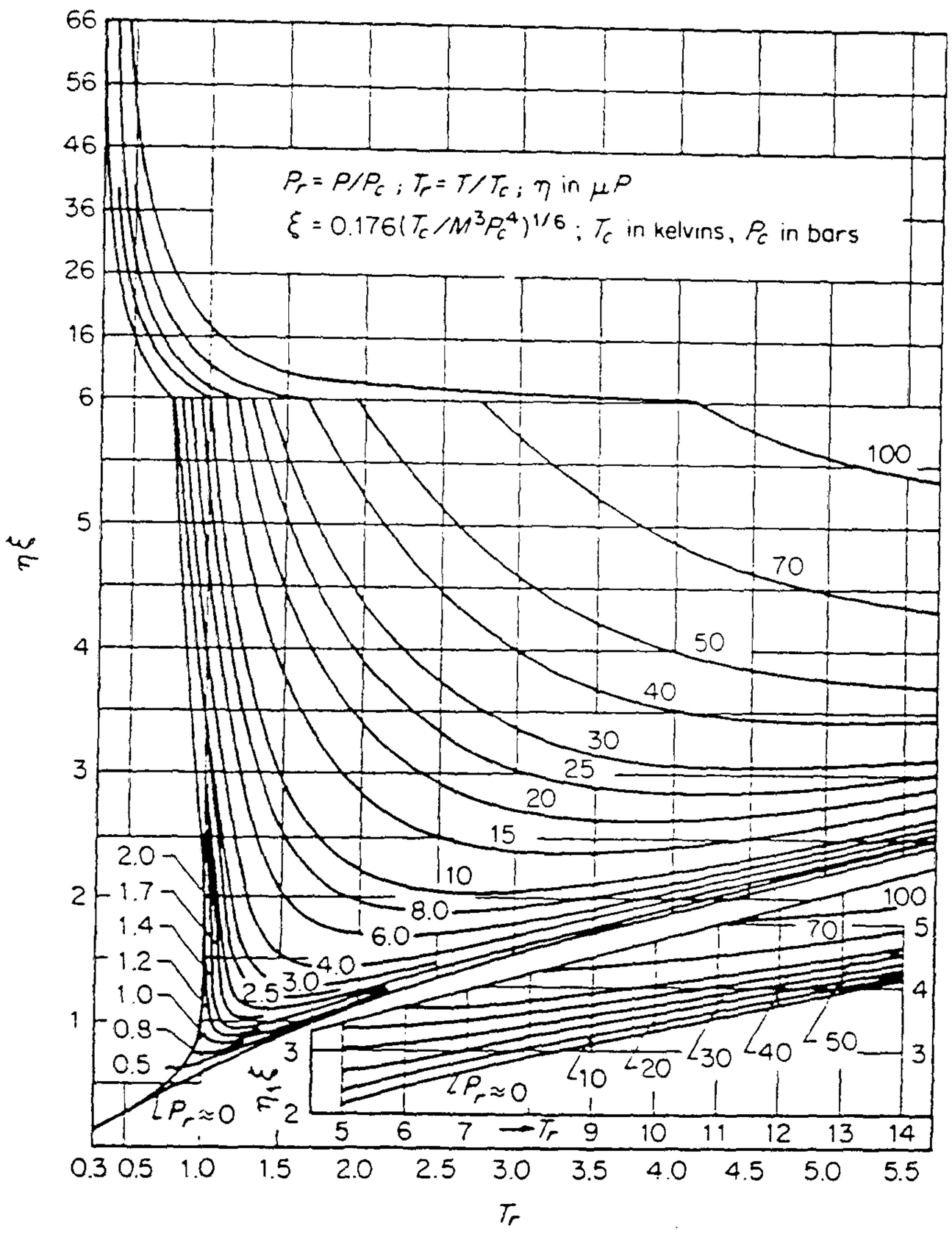

Figure 1.3.3 - Generalized Phase Diagram for Gas Viscosity (from Reference 2).

in the following paragraph, an increase in temperature results in a decrease in viscosity. Finally, at very high reduced temperatures, there again results a condition in which pressure has little effect and viscosities increase with temperature.

The effect of increasing temperature on liquid viscosities is exactly opposite to that of the effects on the gas viscosities at low values of pressure and high values of temperature (Figure 1.3.3). The rise in temperature of the liquid reduces its viscosity. Since liquids have more compact molecules, with very low compressibility as compared to the gases, when the temperature is raised, the molecules of the liquid start slowly moving away from each other, thus reducing the affinity between them, which results in the reduction of viscosity. Conversely, a reduction in temperature brings the liquid molecules closer and thus increases the affinity which results in an increase in the viscosity. Simple expressions have been formulated to show the effects of temperature on liquid viscosities[2]. For example Eq. 1.3.2, given below describes the viscosity of a liquid as a function of two constant parameters A & B :

$$\ln \eta_L = A + \frac{B}{T} \qquad (1.3.2)$$

similarly equations involving three parameters are given as :

$$\ln \eta_L = A + \frac{B}{T+C} \qquad (1.3.3)$$

values of constants A, B & C are calculated using experimental data and are tabulated in Reference[2] for some pure compounds, which can be used for their viscosity prediction.

An increasing pressure causes an increase in viscosity for liquids and vice - versa. But this effect on changes in pressure is only true when the composition of the liquid remains constant. The effect of temperature and pressure on a liquid viscosity is shown in Figures (1.3.4) and (1.3.5) respectively.

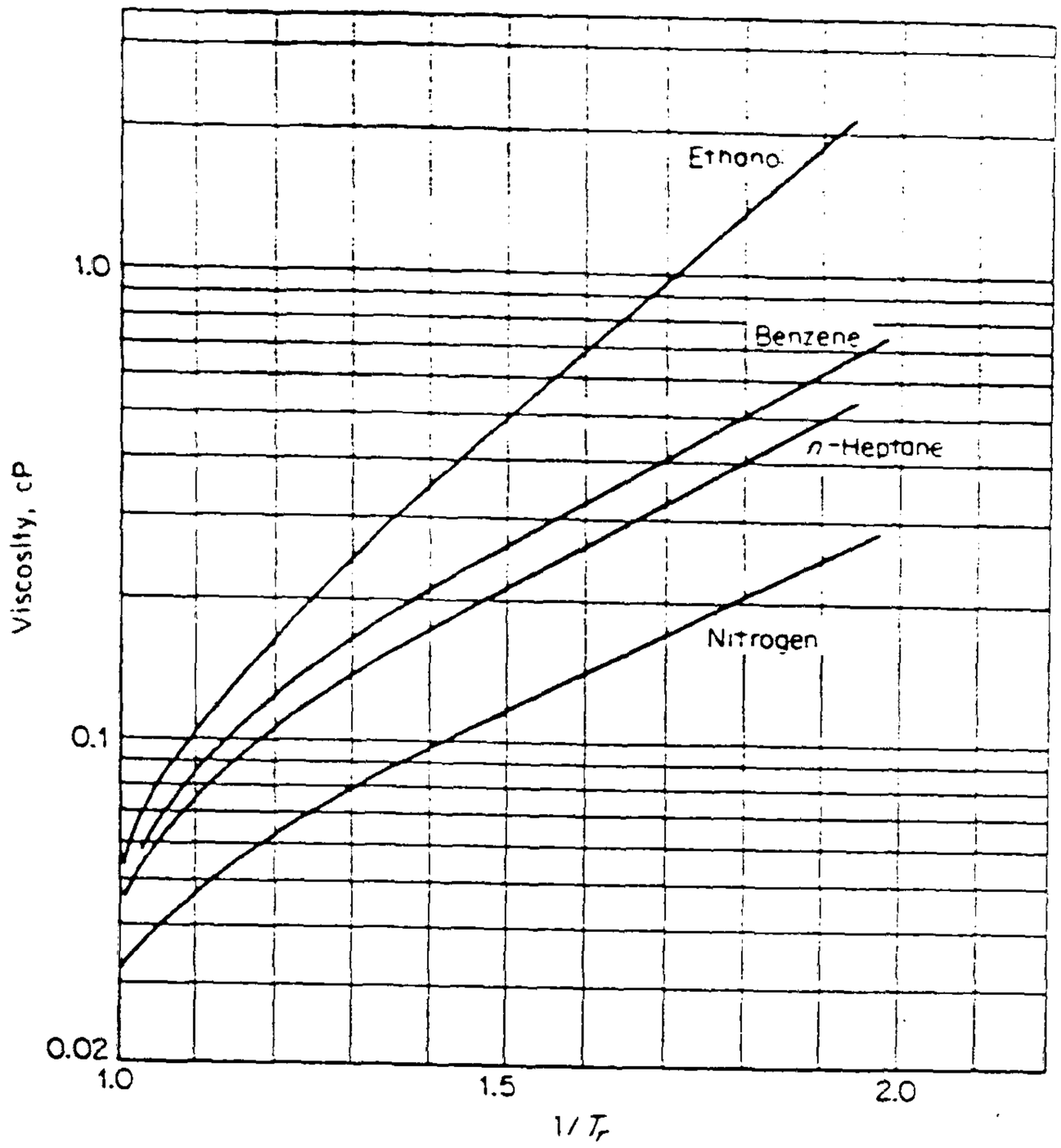

Figure 1.3.4 - Viscosities of Various Liquids as Functions of Temperature (from Reference 2).

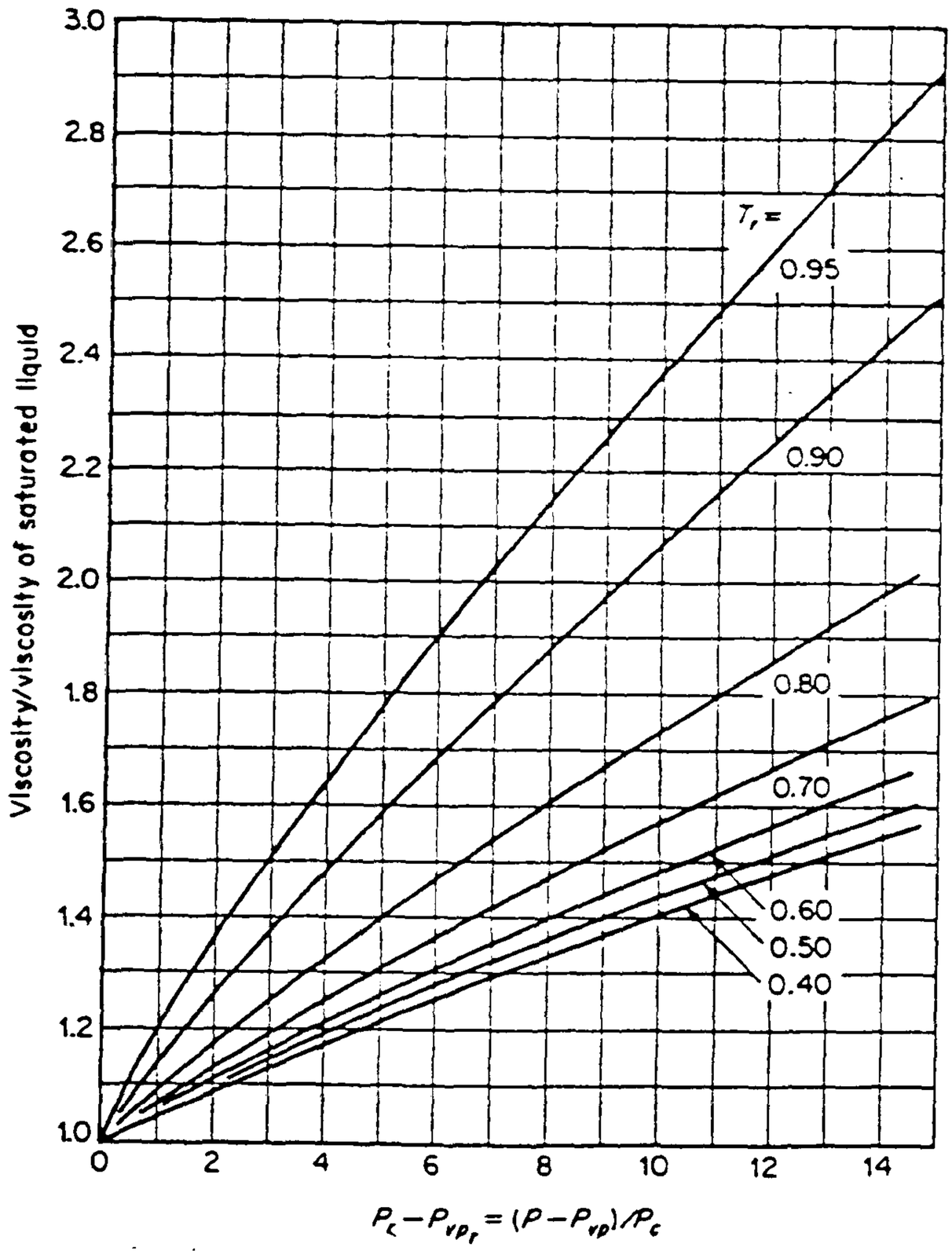

Figure 1.3.5 - Effect of Pressure on the Viscosity of Liquids (from Reference 2).

1.4 : EFFECT OF TEMPERATURE, PRESSURE, AND COMPOSITION ON VISCOSITY OF REAL RESERVOIR FLUIDS

Figure 1.4.1 shows the effect of temperature on a typical North Sea crude oil[4] at a constant composition and constant pressure. As expected, the plot indicates a decrease in the viscosity as temperature increases. Figure 1.4.2 illustrates the effect of pressure on the viscosity of another typical North Sea oil[5], at a constant temperature and constant composition. The plot clearly shows the decrease in oil viscosity as pressure reduces.

However, the phenomenon observed in Figure 1.4.2 is not always valid when pressure drops below the saturation pressure and as a result compositional changes take place which significantly increase the oil viscosity despite reduction in pressure. Figure 1.4.3, shows the effect of reduction in pressure on viscosity of a synthetic near critical gas - condensate in a retrograde region. A decrease in pressure for a retrograde liquid in the retrograde region, the reduction in pressure increases its viscosity. This is entirely because of the effect of changes in the liquid phase composition and hence density as the pressure starts falling further and further below the dew - point. For a retrograde mixture the mole fraction of heavier components in the liquid phase increases by reduction in pressure below the dew - point. Volatile oils and black oils exhibit similar behaviour, as observed in Figure 1.4.3, when pressure falls below their bubble point pressure; i.e. the viscosity of the liberated gas keeps decreasing with decrease in pressure whereas the viscosity of the remaining liquid keeps increasing with decrease in pressure. The liberation of gas normally results in heavier and more viscous liquid. Figure 1.4.4 shows the viscosity of a typical North Sea oil[5] graphed against pressure at a constant temperature. The viscosity smoothly decreases as pressure is reduced and approaches the bubble point and then suddenly increases inspite of reduction in pressure and reaches a maximum value at atmospheric conditions. During the stages below the bubble point pressure, significant changes in the liquid phase compositions occur (increasing concentration of heavy components) which are responsible for the increasing viscosity.

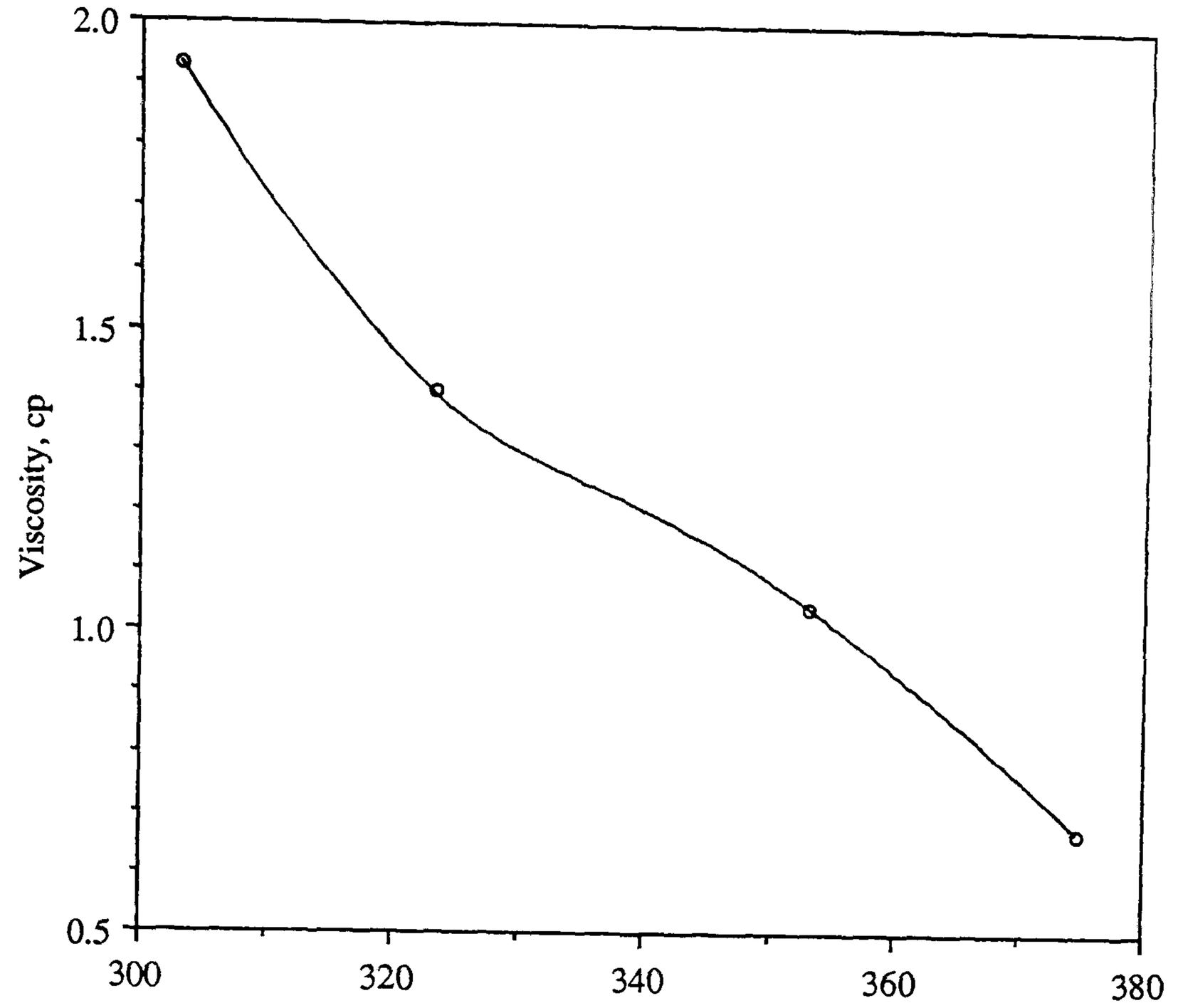

Figure 1.4.1 - Effect of Temperature on the Viscosity of a North Sea Oil at Constant Pressure (27.76 MPa) and Constant Composition (from Reference 4).

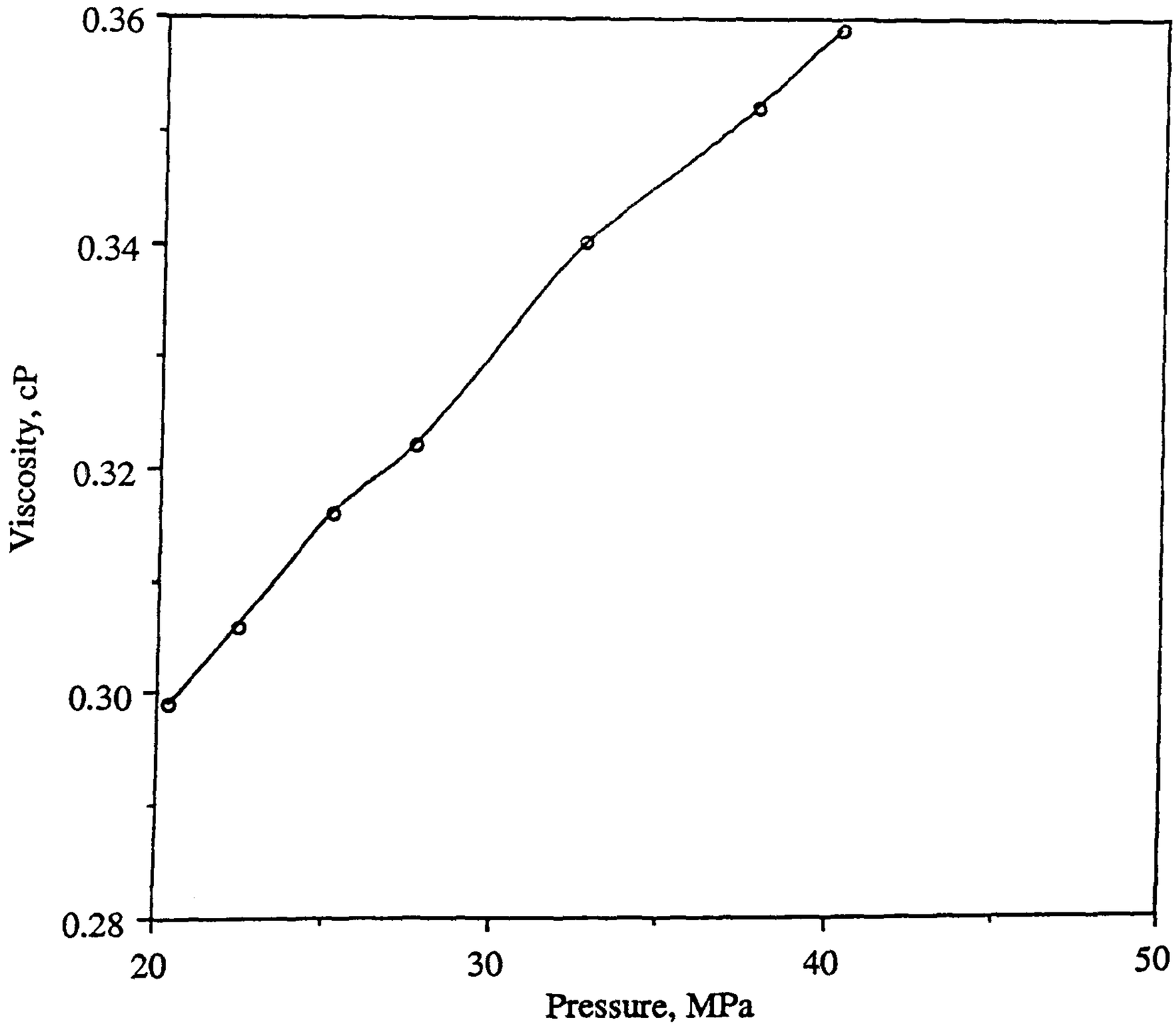

Figure 1.4.2 - Effect of Pressure on the Viscosity of a North Sea Oil at Constant Temperature (97.8 deg C) and Constant Composition (from Reference 5).

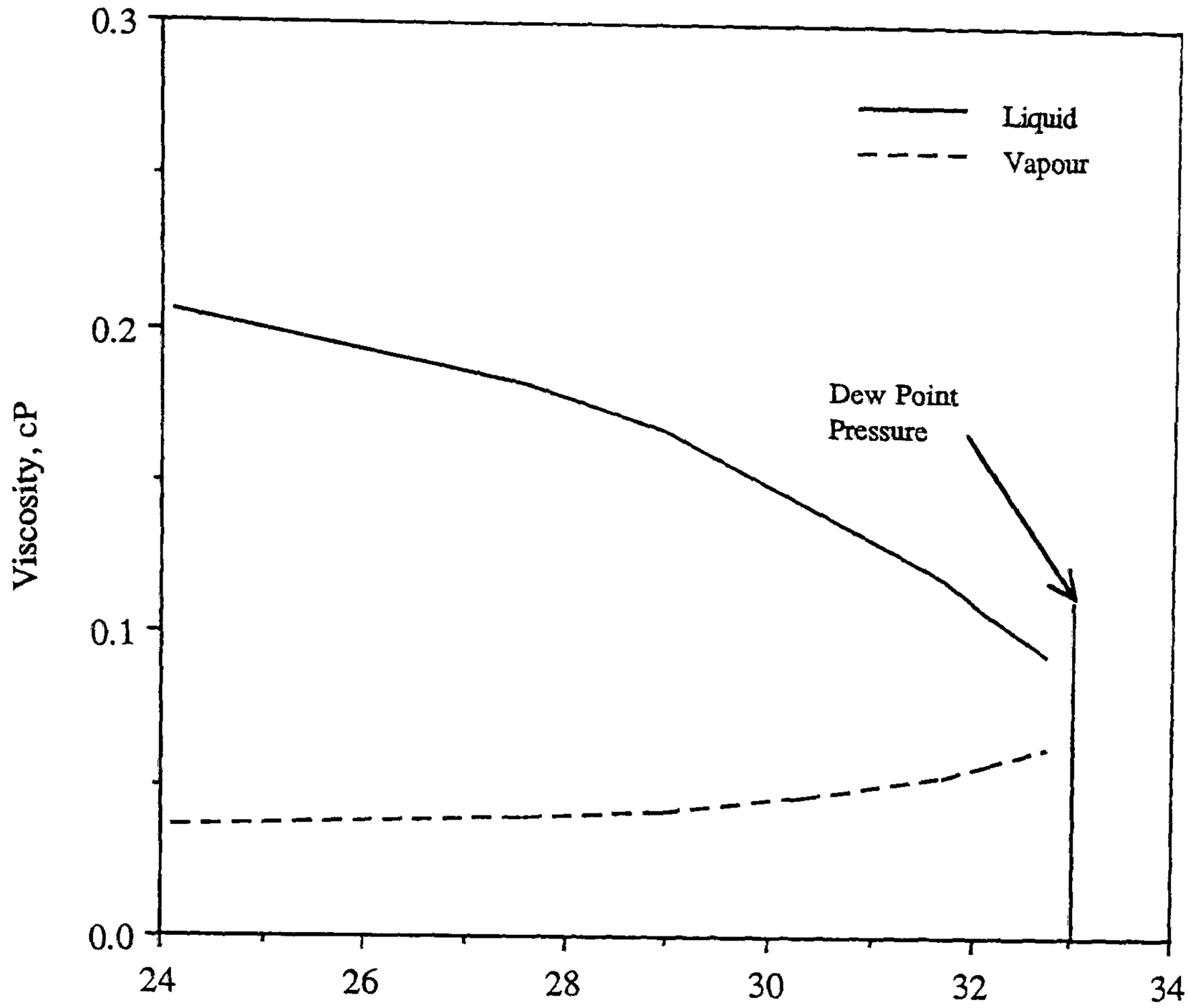

Figure 1.4.3 - Effect of Pressure and Composition on Viscosity of a Synthetic Near Critical Fluid at 38 deg C (from Section 3.5.7, Chapter 3, Part-A).

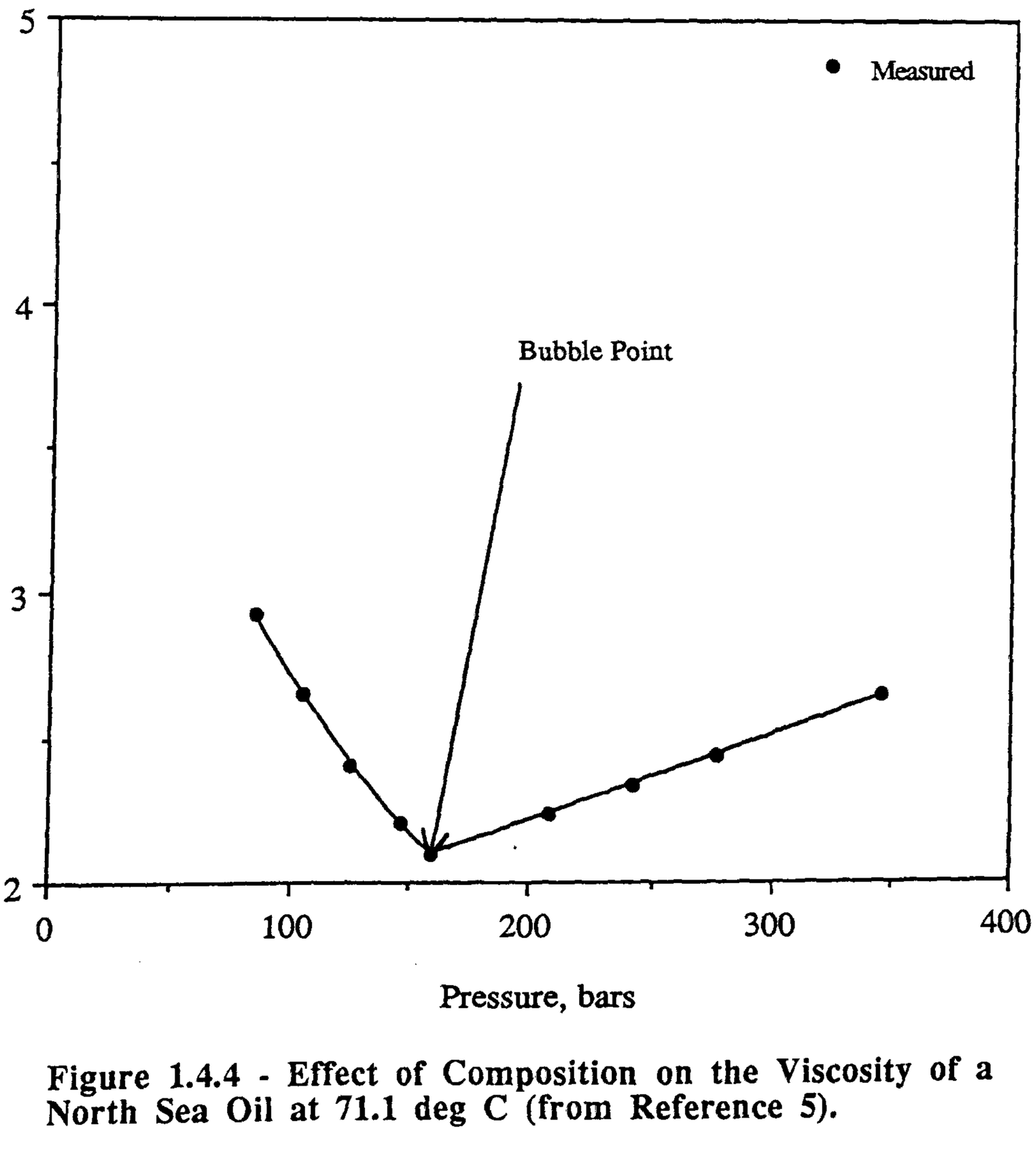

Figure 1.4.4 - Effect of Composition on the Viscosity of a North Sea Oil at 71.1 deg C (from Reference 5).

References

1) Stewart, G. : "Enhanced Oil Recovery : A Technological Achievement in the United States and Potential Application in the North Sea", Department of Petroleum Engineering, Heriot - Watt University, (Jul., 1977).

2) Reid, R.C., Prausnitz, J.M. and Poling, B.E.: "The Properties of Gases and Liquids", Fourth Edition, McGraw Hill Book Company, New York, (1987)

3) Ahrabi, F., Ashcroft, S.J. and Shearn, R.B.: "High Pressure Volumetric, Phase Composition and Viscosity data for a North Sea Crude Oil and NGL", *Chem Eng. Res. Des*, Vol. 65, pp. 63-73, (Jan., 1987).

4) Pedersen, K.S., Fredenslund, Aa. and Thomassen, P.: "Properties of Oils and Natural Gases", Contributions in Petroleum Geology & Engineering, 5, Gulf Publishing Company, (1989).

CHAPTER 2 : THE AVAILABLE VISCOSITY CORRELATIONS

2.1 : INTRODUCTION

As mentioned previously viscosity is an important transport property required in various reservoir engineering flow calculations and mathematical simulations. This parameter, however, is impossible to measure for mixtures of all hydrocarbon fluids for all the relevant conditions. Even if it were possible to measure the viscosities of all hydrocarbon mixtures, the cost of obtaining sufficient experimental data on mixtures containing all the components of interest in all proportions of interest would be prohibitive. Therefore there is a considerable current interest in accurate and reliable prediction of transport properties for different type of hydrocarbon mixtures over wide ranges of temperatures and pressures pertinent to reservoir conditions.

The literature contains many correlations for estimating the viscosities of fluids. However, the applicability of a majority of these correlations is limited to single component fluids and low pressures. And, most of them, when applied to complex hydrocarbon systems, are of little value. The lack of utility of the majority of viscosity correlations results from the fact that they were developed to show the separate effect of temperature, pressure or composition on viscosity, but not to estimate the viscosity as a function of all variables. And with a few exceptions, they were developed for application to much simpler systems than hydrocarbon mixtures in petroleum reservoirs.

In the simulation of processes related to oil and gas production, however, viscosity correlations simultaneously applied to both phases are needed that are applicable to a wide range of hydrocarbon mixtures at reservoir and surface conditions. During the last 50 - 60 years several attempts have been made in this direction[1,2,3,4,5] for predicting this property, based on different theories. Some of these correlations have been reviewed in reference[6]. In this chapter popular correlations used for prediction of viscosity of petroleum reservoir

fluids are reviewed in details. A comparative study for these methods is presented in Chapter 4. Greater emphasis is put on correlations applicable for predicting viscosities of both oil and gas phases. Correlations reviewed in this chapter are, Lohrenz - Bray - Clark's residual viscosity correlation, the principle of corresponding states (one reference component), the extended principle of corresponding states (TRAPP), principle of corresponding states (two reference components), Lee's method for viscosity of gases, and the Little & Kennedy's method for the viscosity of oils.

2.2 : RESIDUAL VISCOSITY CORRELATION

The viscosity correlation that has probably the most widespread use in flow models for petroleum mixtures is the correlation of Jossi et. al[7], in the form suggested by Lohrenz et. al[8], in which gas and liquid viscosities are related to a fourth - degree polynomial of the reduced density. Jossi et. al[7], correlated viscosities of nitrogen, argon, carbon dioxide, sulphur dioxide, methane, ethane, propane, i - butane, n - butane, and n - pentane in gaseous and liquid phases, with reduced density by the use of dimensional analysis and the Abas - Zade[9] equation for residual viscosity to produce a single generalised relationship which can be used both graphically and analytically for single pure compounds.

Recent studies on the prediction of the transport properties of pure substances have been primarily concerned with the viscosity and thermal conductivity of gases at normal pressures[10]. Using a dimensional analysis approach and viscosity data reported in the literature data for fifty-two non - polar gases and fifty-three polar gases, gave the relationships which were developed for the viscosity, η^* of any pure gas at moderate pressures (0.01013 MPa to 0.50 MPa). For non - polar gases the following relationships resulted :

$$\eta^*\lambda = 34.0\ E^{-05}T_r^{0.94} \qquad \text{for } T_r \leq 1.5 \qquad (2.2.1)$$

and

$$\eta^*\lambda = 17.78\ E^{-05}[4.58T_r - 1.67]^{5/8} \quad \text{for } T_r > 1.5 \tag{2.2.2}$$

where

$$\lambda = \frac{T_c^{1/6}}{M^{1/2}P_c^{2/3}} \tag{2.2.2 a}$$

A relationship for polar gases is not given here, since most of the petroleum reservoir fluids exhibit non - polar behaviour. Critical properties and molecular weight of each compound were used to calculate the viscosity reducing parameter, λ. The residual viscosity (RV) function, $(\eta-\eta^*)\lambda$, was evaluated using the experimental viscosity data in the dense gaseous and liquid phase regions together with the viscosity data (η^*) at low pressure conditions or at 1 atm. The density data of these components in different thermodynamic regions were obtained from the PVT data and were used to calculate the reduced density[7]. In Figure (2.2.1) the group $(\eta-\eta^*)\lambda$ is plotted against the reduced density on log-log co-ordinates. Precise details about the development of these correlations and the sources of the PVT and viscosity data are given in Reference[7]. The following fourth degree polynomial was found to represent accurately the relationship over the entire range of reduced densities :

$$[(\eta-\eta^*)\lambda+10^{-4}]^{1/4} = 0.1023+0.023364\rho_r+0.058533\rho_r^2-0.040758\rho_r^3+0.0093324\rho_r^4 \tag{2.2.3}$$

Where,

η = viscosity of the fluid in centipoise

η^* = gas phase viscosity of the same fluid at moderate pressure (e.g. 1 atm), in centipoise

λ = inverse of the critical viscosity or viscosity reducing parameter, as defined by Eq. 2.2.2 a

ρ = density of the fluid, in gm/cc

ρ_c = critical density of the fluid, in gm/cc

$\rho_r = \frac{\rho}{\rho_c}$ the reduced density

T_c = critical temperature in Kelvin

T_r = reduced temperature

M = molecular weight of the fluid

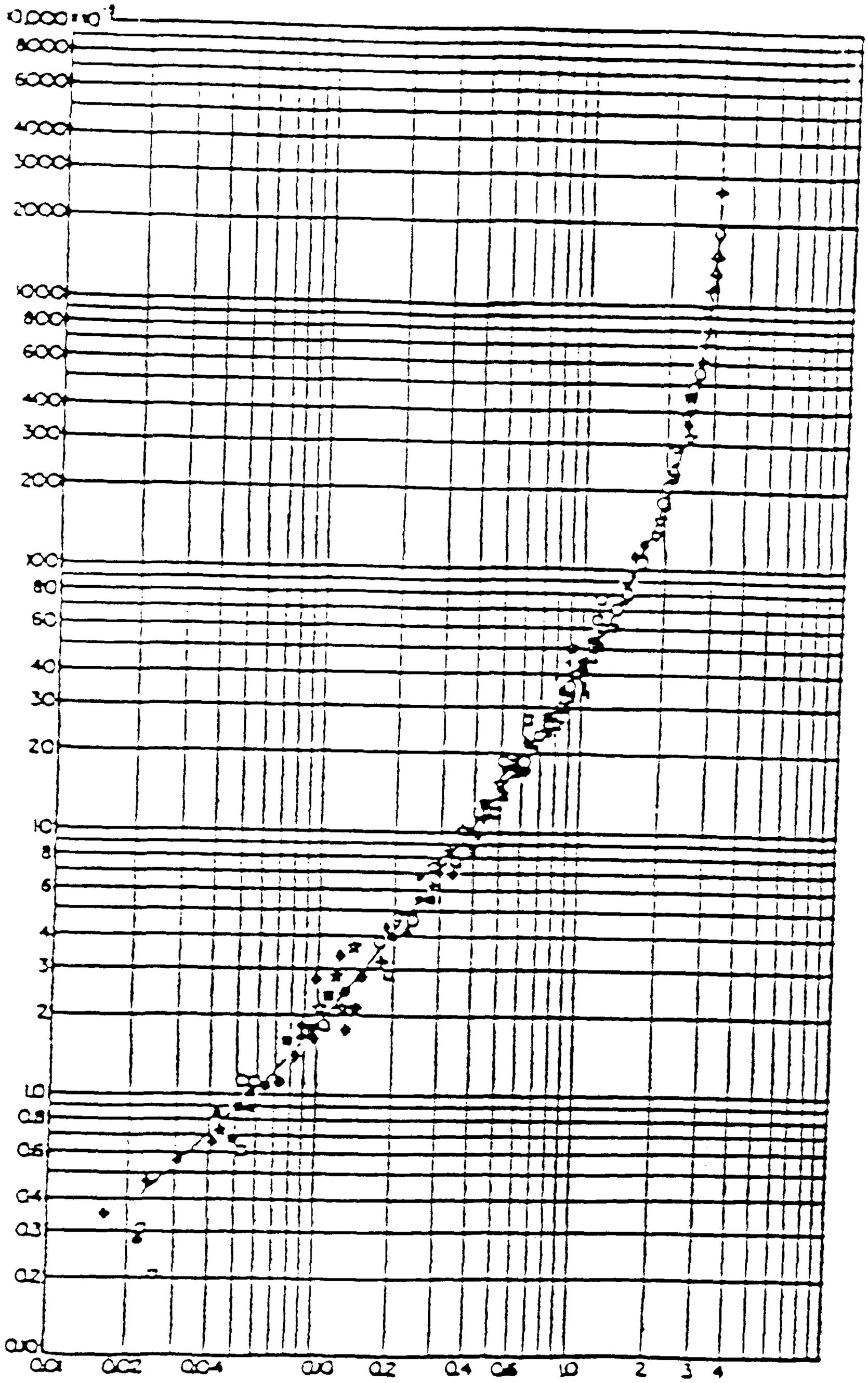

Figure 2.2.1 - Relationship Between Residual Viscosity Function and Reduced Density (from Reference 7).

Eq. 2.2.3, is however applicable only to all the pure single components investigated by Jossi et. al[7], except hydrogen due to its quantum deviations, water and ammonia due to hydrogen bonding which follow different trends compared to the normally behaving substances.

It was the effort of Lohrenz - Bray - Clark[8] in 1964 which made the application of Eq. 2.2.3 feasible for the prediction of viscosity of reservoir oils and gases. It in fact represented the first attempt to relate viscosities of liquids and gases to composition, and was principally designed for application to flow calculations. Lohrenz et. al[8] basically introduced several mixing rules in the pure component viscosity correlations proposed by Jossi et. al[7], discussed earlier, to make the method applicable for calculation of gas and liquid mixture viscosities. According to Lohrenz et. al[8], Eq. 2.2.1 & 2.2.2 for a component, i, in the mixture can be written as :

$$\eta_i^*\lambda_i = 34.0\ E^{-05}T_{ri}^{0.94},\ (T_{ri} \leq 1.5) \qquad (2.2.4)$$

$$\eta_i^*\lambda_i = 17.78\ E^{-05}[4.58T_{ri} - 1.67]^{5/8},\ (T_{ri} > 1.5) \qquad (2.2.5)$$

where

$$T_{ri} = \frac{T}{T_{ci}} \quad \text{and} \quad \lambda_i = \frac{T_{ci}^{1/6}}{M_i^{1/2}P_{ci}^{2/3}} \qquad (2.2.6\ a\ \&\ 2.2.6\ b)$$

hence for a mixture containing, n components, for i^{th} component, Eq. 2.2.4, 2.2.5, 2.2.6 a & 2.2.6 b should be used to calculate the reduced low pressure viscosity (η_i^*), reduced temperature (T_{ri}) and the viscosity reducing parameter (λ_i). Temperature is in Kelvins and pressure is in atmospheres and viscosity is in centipoise. Now using the information obtained from the above equations, the low pressure viscosity of **gas mixtures** should be calculated, the following simple molar mixing rules are used[11] :

$$\eta^* = \frac{\sum_{i=1}^{n} X_i \eta_i^* \sqrt{M_i}}{\sum_{i=1}^{n} X_i \sqrt{M_i}} \qquad (2.2.7)$$

whereas the reduced density of the mixture is calculated from:

$$\rho_r = \frac{\rho}{\rho_c'} \tag{2.2.8}$$

and $$\frac{1}{\rho_c'} = \sum_{\substack{i=1 \\ i \neq C_{7+}}}^{n} X_i V_{ci} + X_{C7+} V_{C7+} \tag{2.2.8 a}$$

M_i and V_{ci} are the molecular weight and critical molar volume of the i^{th} component in the mixture. Critical volume for a pseudo fraction, C_{7+} is estimated by the expression suggested by Lohrenz et. al[8] :

$$V_{c7+} = 21.573 + 0.015122\, M_{c7+} - 27.656\, SG_{c7+} + 0.070615\, M_{c7+}\, SG_{c7+} \tag{2.2.9}$$

Where,

V_{c7+} = critical molar volume of the plus fraction

M_{c7+} = molecular weight of the plus fraction and

SG_{c7+} = specific gravity of the plus fraction

viscosity reducing parameter, λ, of the mixture is calculated by introducing simple molar mixing rules into Eq. 2.2.6 b:

$$\lambda = \frac{[\sum_{i=1}^{n} X_i T_{ci}]^{\frac{1}{6}}}{[\sum_{i=1}^{n} X_i M_i]^{\frac{1}{2}} [\sum_{i=1}^{n} X_i P_{ci}]^{\frac{2}{3}}} \tag{2.2.10}$$

Hence, calculation of gas or liquid mixture viscosity is accomplished by applying Eq. 2.2.4 - 2.2.10 to Eq. 2.2.3. The typical input data required to accomplish the viscosity calculation is, compositions of gas or liquid phase, reliable density data of each phase, molecular weights of each component in the mixture and the critical properties of each component in the mixture,

similar data for the pseudo fractions are also required for mixtures containing plus fractions. Critical property data and other data for a majority of the pure hydrocarbon components and organic compounds is listed in Reference 6, various methods for estimating the critical temperature and pressure of the C_{7+} fraction are given in Reference 30.

The method is simple and fast in application and is easily tuned to experimental data. However, it relies significantly on the density data of the fluid. Hence, it should always be used in conjunction with an EOS known to predict the densities reliably, where measured density data is not available. The weaknesses and strengths of this method compared with other viscosity prediction techniques are given in Chapter 4.

2.3 : PRINCIPLE OF CORRESPONDING STATES (ONE REFERENCE COMPONENT)

This is one of the recent methods published for predicting viscosities of gas and liquid phases using the principle of corresponding states. The basic assumption behind the principle of corresponding states is that any reduced property of a mixture or a pure component can be expressed in terms of other reduced properties. For example, the reduced viscosity (η/η_c) can be expressed in terms of reduced pressure (P/P_c), reduced temperature (T/T_c) and reduced density (ρ/ρ_c). Moreover, to improve such correlations a reference component (generally methane) is used as a pivot point.

In the principle of corresponding states (PCS), the reduced viscosity may be related to any two reduced state properties such as reduced pressure, reduced temperature, reduced density, or reduced volume. Hydrocarbon fluids, particularly complex mixtures, cannot be accurately modelled by the above simple (PCS), hence correlations based on this approach include some correction factors generally evaluated by matching the predicted and experimental data[12-15].

It was the work of Tham and Gubbins[16] in which they proposed the viscosity of a component in terms of a correction factor in order to express the deviation from the simple

corresponding states principle, called as a rotational coupling effect, α_{TG}, entering the viscosity correlation as :

$$\eta_x(P,T) = \left(\frac{Tcx}{Tco}\right)^{1/6}\left(\frac{Pcx}{Pco}\right)^{2/3}\left(\frac{MWx}{MWo}\right)^{1/2}\left(\frac{\alpha_{TGx}}{\alpha_{TGo}}\right)\eta_o\left[\frac{PPco\alpha_{TGo}}{Pcx\alpha_{TGx}}, \frac{TTco\alpha_{TGo}}{T_{cx}\alpha_{TGx}}\right] \qquad (2.3.1)$$

Where,

$\eta_x(P,T)$ = viscosity of fluid 'x' at pressure P and temperature T

T_{cx}, T_{co} = critical temperature of the fluid 'x' and reference component 'o' respectively

P_{cx}, P_{co} = critical pressure of the fluid 'x' and reference component 'o' respectively

MW_x, MW_o = molecular weight of the fluid 'x' and reference component 'o' respectively

α_{TGx}, α_{TGo}= rotational coupling effect for fluid 'x' and reference component 'o' respectively

η_o = viscosity of the reference component at $P = \frac{PPco\alpha_{TGo}}{Pcx\alpha_{TGx}}$ and $T = \frac{TTco\alpha_{TGo}}{T_{cx}\alpha_{TGx}}$

Although Eq. 2.3.1, was first proposed by Tham and Gubbins[16] for liquids only, it was the work of Christensen and Fredenslund[17], who extended it to a model applicable for prediction of viscosities of both gaseous and liquid mixtures. The basic step in calculating the viscosity from this principle involves the evaluation of critical properties of the mixture, namely $T_{c,mix}$ and $P_{c,mix}$ which are evaluated using the following mixing rules :

$$T_{c,mix} = \frac{\sum_i\sum_j X_i X_j \left[\left(\frac{T_{ci}}{P_{ci}}\right)^{\frac{1}{3}} + \left(\frac{T_{cj}}{P_{cj}}\right)^{\frac{1}{3}}\right]^3 \left[T_{ci}T_{cj}\right]^{\frac{1}{2}}}{\sum_i\sum_j X_i X_j \left[\left(\frac{T_{ci}}{P_{ci}}\right)^{\frac{1}{3}} + \left(\frac{T_{cj}}{P_{cj}}\right)^{\frac{1}{3}}\right]^3} \qquad (2.3.2)$$

and

$$P_{c,mix} = \frac{8\sum_i\sum_j X_i X_j \left[\left(\frac{T_{ci}}{P_{ci}}\right)^{\frac{1}{3}} + \left(\frac{T_{cj}}{P_{cj}}\right)^{\frac{1}{3}}\right]^3 \left[T_{ci}T_{cj}\right]^{\frac{1}{2}}}{\left[\sum_i\sum_j X_i X_j \left[\left(\frac{T_{ci}}{P_{ci}}\right)^{\frac{1}{3}} + \left(\frac{T_{cj}}{P_{cj}}\right)^{\frac{1}{3}}\right]^3\right]^2} \qquad (2.3.3)$$

the next step is the calculation of the relevant temperatures and pressures using the mixture critical properties calculated by Eq. 2.3.2 & 2.3.3, to calculate the density of reference component and subsequently the viscosity of the reference component. The density of the reference component methane is extracted from the 33 - parameter Benedict-Webb-Rubin (BWR) Equation of State[18]. The next step involves the calculation of molecular weight of the mixture, which is obtained by applying the following mixing rules, suggested in[17] :

$$MW_{mix} = 1.304E^{-4}\left(\overline{MW}_w^{\,2.303} - \overline{MW}_n^{\,2.303}\right) + \overline{MW}_n \qquad (2.3.4)$$

where,

$$\overline{MW}_n = \sum_i X_i MW_i \qquad (2.3.4\ a)$$

$$\overline{MW}_w = \frac{\sum_i X_i MW_i^{\,2}}{\sum_i X_i MW_i} \qquad (2.3.4\ b)$$

Where,

X_i = mole fraction of the ith component in a mixture and

MW_i= molecular weight of the ith component in the mixture

the mixture critical properties $T_{c,mix}$ and $P_{c,mix}$ are used to calculate a separate set of temperature and pressure at which the reference component density is evaluated as mentioned earlier, these conditions are defined by the ratios $(T.T_{co}/T_{c,mix})$ and $(P.P_{co}/P_{c,mix})$, where T

and P are the temperature and pressure at which the viscosity of a given fluid is desired. T_{co} and P_{co} are the critical temperature and pressure respectively of the reference component (methane).

Employing the calculated molecular weights and the reference component density (evaluated at the above defined temperature and pressure by the 33 - parameter EOS), the rotational coupling effects for the given fluid and the reference component are calculated, as given below :

$$\alpha_{TG,mix} = 1.000 + 7.378E^{-3}\rho_r^{1.847}\, MW_{mix}^{0.5173} \qquad (2.3.5\ a)$$

$$\alpha_{TG,o} = 1.000 + 0.031\rho_r^{1.847} \qquad (2.3.5\ b)$$

The constants and exponents in Eq. 2.3.5 a and 2.3.5 b are estimated on the basis of experimental viscosity data. In Eq. 2.3.5 a and 2.3.5 b:

$$\rho_r = \frac{\rho_o}{\rho_{co}} \qquad (2.3.5\ c)$$

and the density of the reference component, ρ_o, is determined at the temperature and pressure defined by $\frac{T\,T_{co}}{T_{cmix}}$ and $\frac{P\,P_{co}}{P_{cmix}}$, ρ_{co} denotes the critical density of the reference component.

As given in Eq. 2.3.1, the viscosity of the reference component methane is required at the temperature and pressure conditions calculated after incorporating the rotational coupling effects.

A set of correlations proposed by Hanley[19] is used for evaluation of the reference component viscosity, η_o at a given temperature, T and density, ρ_o :

$$\eta_o(\rho,T) = \eta_1(T) + \eta_2(T)\rho_o + F_1\Delta\eta^1(\rho,T) + F_2\Delta\eta''(\rho,T) \qquad (2.3.6)$$

where

$$\eta_1(T) = A + B\,[C - \log_e(\frac{T}{F})]^2 \qquad (2.3.6\ a)$$

constants A, B, C and F are :

$A = 1.696985927$

$B = -\ 0.133372346$

$C = 1.4$

$F = 168.0$

the second function of Eq. 2.3.6 is given by :

$$\eta_2(T) = \exp\left[j_1 + \frac{j_4}{T}\right]\left[\exp\left[\rho^{0.1}\left(j_2 + \frac{j_3}{T^{3/2}}\right) + \theta\rho^{0.5}\left(j_5 + \frac{j_6}{T} + \frac{j_7}{T^2}\right)\right] - 1.0\right] \qquad (2.3.6\ b)$$

constants j_1 to j_7 have values :

$j_1 = -10.3506$

$j_2 = 17.5716$

$j_3 = -3019.39$

$j_4 = 188.7300$

$j_5 = 0.0429036$

$j_6 = 145.290$

$j_7 = 6127.68$

whereas, θ, is defined as :

$$\theta = \left(\frac{\rho_o - \rho_{co}}{\rho_{co}}\right) \qquad (2.3.6\ c)$$

and the third function, $\Delta\eta^1(\rho,T)$, in Eq. 2.3.6 is defined as :

$$\Delta\eta^1(\rho,T) = GV(1)T^{-1} + GV(2)T^{-2/3} + GV(3)T^{-1/3} + GV(4) + GV(5)T^{1/3} + GV(6)T^{2/3} + GV(7)T + GV(8)T^{4/3} + GV(9)T^{5/3} \quad (2.3.6\ d)$$

constants GV(1) to GV(9) are :

$GV(1) = -2.090975\ E^{05}$

$GV(2) = 2.647269\ E^{05}$

$GV(3) = -1.472818\ E^{05}$

$GV(4) = 4.716740\ E^{04}$

$GV(5) = -9.491872\ E^{03}$

$GV(6) = 1.219979\ E^{03}$

$GV(7) = -9.627993\ E^{01}$

$GV(8) = 4.2741520\ E^{00}$

$GV(9) = -8.141531\ E^{-02}$

Pedersen and Fredenslund[15], have estimated an additional set of coefficients for the term, $\Delta\eta''(\rho,T)$, in Eq. 2.3.6 using viscosity data measured at reduced temperatures below 0.4, i.e., corresponding to a methane reference state where methane is in a solid form:

$$\Delta\eta''(\rho,T) = \exp\left[k_1 + \frac{k_4}{T}\right]\left[\exp\left[\rho^{0.1}\left(k_2 + \frac{k_3}{T^{3/2}}\right) + \theta\rho^{0.5}\left(k_5 + \frac{k_6}{T} + \frac{k_7}{T^2}\right)\right] - 1.0\right] \quad (2.3.6\ e)$$

where constants k_1 to k_7 have values :

$k_1 = -9.74602$

$k_2 = 18.0834$

$k_3 = -4126.66$

$k_4 = 44.6055$

$k_5 = 0.976544$

$k_6 = 81.8134$

$k_7 = 15649.9$

The constants F_1 and F_2 in Eq. 2.3.6 are defined by :

$$F_1 = \frac{HTAN + 1}{2}$$

$$F_2 = \frac{1 - HTAN}{2}$$

where,

$$HTAN = \frac{\exp(\Delta T) - \exp(-\Delta T)}{\exp(\Delta T) + \exp(-\Delta T)}$$

with $\Delta T = T - T_F$, where T_F is the freezing point of the reference component (methane)

After calculating all the required parameters, Eq. 2.3.1 would be employed to calculate the viscosity of the desired fluid.

The method does not rely on the density of either gas or liquid phases, and can be simultaneously applied to the prediction of both gas and liquid phase viscosities. Typical input data required for the method are compositions of both phases, critical properties of the mixture components, temperature, pressure and molecular weights of each component. The method can be employed in a reservoir pressure depletion process in which it can simultaneously predict the viscosities of both oil and gas phases.

2.4 : EXTENDED PRINCIPLE OF CORRESPONDING STATES METHOD (TRAPP)

The method is somewhat similar to the principle of corresponding states reviewed in Section 2.3. In the previous method Pedersen et. al[14,15], introduced rotational coupling effect, (α), for mixtures and the reference component in the functional forms to account for the

deviations from the simple corresponding states principle when it is applied to complex hydrocarbon mixtures. Ely and Hanley[12,21] have suggested expressing the deviations from the simple corresponding states principle in terms of shape factors, $\theta(T_r,V_r,w)$, and $\phi(T_r,V_r,w)$, which are functions of reduced volume, reduced temperature and the Pitzer's acentric factor. The proposed shape factors enter into the functional form as :

$$\eta_x(\rho,T) = \left(\frac{\theta T_{cx}}{T_{co}}\right)^{1/2}\left(\frac{\phi V_{cx}}{V_{co}}\right)^{-2/3}\left(\frac{MW_x}{MW_o}\right)^{1/2}\eta_o(\rho_o\phi,T_o/\theta) \qquad (2.4.1)$$

In Eq. 2.4.1:

$\eta_x(\rho,T)$ = the viscosity of a given fluid at density ρ and temperature T

θ,ϕ = the shape factors

T_{cx},T_{co} = critical temperature of the given fluid and reference component respectively

V_{cx},V_{co} = critical molar volume of the given fluid and reference component respectively

MW_x,MW_o = molecular weight of the given fluid and reference component respectively and

η_o = the viscosity of the reference component

The basic assumption in this procedure is that, the mixture is considered as one single fluid consisting of one hypothetical pure component with a given set of critical temperature, pressure and molecular weight. The method is solved iteratively for calculation of the shape factors. Since the density of the fluid for which the viscosity is desired, is unknown, the first step is to assign to the ith component in a mixture an initial value of $V_{ri} = 2.0$ for vapour phase and $V_{ri} = 0.5$ for the liquid phase, whereas T_{ri} for each component of the mixture is calculated from $T_{ri} = T/T_{cx}$ which is followed by first estimate of the shape factors from :

$$\theta_i = 1 + (\omega_i-\omega_o)F(T_{ri},V_{ri}) \qquad (2.4.2\ a)$$

$$\phi_i = [1 + (\omega_i-\omega_o)G(T_{ri},V_{ri})]\frac{Z_{co}}{Z_{ci}} \qquad (2.4.2\ b)$$

where

$$F(T_{ri},V_{ri}) = a_1 + b_1\ln(T_{ri}) + \left(c_1 + \frac{d_1}{T_\alpha+}\right)(V_{ri} - 0.5) \qquad (2.4.3\ a)$$

$$G(T_{ri}, V_{ri}) = a_2(V_{ri} + b_2) + c_2(V_{ri} + d_2)\ln(T_{ri}) \qquad (2.4.3\ b)$$

and the constants have the following values :

$a_1 = 0.090569$	$a_2 = 0.394901$
$b_1 = -0.862762$	$b_2 = -1.023545$
$c_1 = 0.316636$	$c_2 = -0.932813$
$d_1 = -0.465684$	$d_2 = -0.754639$

ω_i and ω_o are the acentric factors for ith component of the fluid and reference component 'o' respectively, whereas Z_{ci} and Z_o are the critical compressibility factors of the ith component of the fluid and the reference component respectively.

The next step is to calculate the substance reducing ratios, f_i and h_i using the following equations and values obtained from Eq. 2.4.2 a and 2.4.2 b:

$$f_i = \left[\frac{T_{ci}}{T_{co}}\right] \theta_i \qquad (2.4.4\ a)$$

$$h_i = \left[\frac{V_{ci}}{V_{co}}\right] \phi_i \qquad (2.4.4\ b)$$

where T_{ci} is the critical temperature of the ith component in the mixture and V_{ci} is the critical volume of the ith component in the mixture. All the above expressions are proposed by Leach and Leland[22,23].

The following mixing rules are employed for calculating the equivalent substance reducing ratios for the mixture :

$$f_x = h_x^{-1} \sum_i \sum_j X_i X_j f_{ij} h_{ij} \qquad (2.4.5\ a)$$

$$h_x = \sum_i \sum_j X_i X_j h_{ij} \qquad (2.4.5\ b)$$

where f_{ij} and h_{ij} are calculated from:

$$f_{ij} = (f_i f_j)^{1/2} \qquad (2.4.6\ a)$$

$$h_{ij} = \frac{1}{8}\ [h_i^{1/3} + h_j^{1/3}]^3 \qquad (2.4.6\ b)$$

f_x and h_x values calculated from Eq. 2.4.5 a and 2.4.5 b are used to calculate the equivalent temperature, $T_{eq} = \frac{T}{f_x}$, and pressure, $P_{eq} = \frac{P\ h_x}{f_x}$ at which the reference component density (ρ_o) is calculated for the first guess, here P and T represent the pressure and temperature at which the viscosity of the given fluid is desired. Again the 33-parameter Benedict-Webb-Rubin (BWR) EOS[18] is used to calculate the methane density. This calculated methane density is then converted into the density of the fluid for which the viscosity is desired from the following:

$$\rho_x = \frac{\rho_o(T_{eq}, P_{eq})}{h_x} \quad \left(V_x = \frac{MW_x}{\rho_x}\right) \qquad (2.4.7)$$

where,

$$MW_x = \sum_i X_i MW_i \qquad (2.4.8)$$

here MW_x is the molecular weight of the mixture, MW_i is the molecular weight of the ith component in the mixture and X_i is the mole fraction of the ith component in the mixture. The reduced temperature and the reduced volume are then recalculated and steps through Eq. 2.4.2 to 2.4.5 until convergence is achieved for f_x and h_x.

The density of methane at which the shape factor iteration loop converges is then used to calculate the methane viscosity using correlations similar to those described in Section 2.3

with different set of parameters[12,21]. The viscosity of a given component or a mixture is then calculated via[12] :

$$\eta_x(\rho_x,T) = \eta_o(\rho_o,T)\, F_\eta \qquad (2.4.9)$$

where

$$F\eta = \left(\frac{Mx\eta}{Mo}\right)^{1/2} f_x^{1/2}\, h_x^{-2/3} \qquad (2.4.10)$$

$M_{x\eta}$ is the molecular weight of the mixture which is calculated from the following mixing rules, M_o represents molecular weight of the reference component methane :

$$M_{x\eta} = \left(\sum_i \sum_j X_i X_j h_{ij}^{\frac{4}{3}} f_{ij}^{\frac{1}{2}} M_{ij}^{\frac{1}{2}}\right)^2 f_x^{-1} h_x^{-\frac{8}{3}} \qquad (2.4.11)$$

where M_{ij} is given by :

$$M_{ij} = \frac{2M_iM_j}{(M_i+M_j)} \qquad (2.4.12)$$

Typical input data required for the calculation procedure are temperature, pressure, composition, critical properties, molecular weight and acentric factor of all the constituents of the mixture. The method also predicts the fluid density ($\rho_x = \rho_o/h_x$) from the iterative procedure as explained above. Ely and Hanley[12,21], have quoted average absolute deviation of 8.4 % for 1869 pure component data points and 6.95 % for 455 mixture data points, the same authors have developed a computer program based on this method called 'TRAPP' (Transport Properties Prediction Program) and can be acquired from the Gas Processors Association (GPA) at a nominal cost.

2.5 : PRINCIPLE OF CORRESPONDING STATES (TWO REFERENCE COMPONENTS)

It was seen that reliable predictions for mixtures similar to the prediction of the viscosity of the reference component (methane) are usually obtained using the one reference, principle of corresponding states method. However, for systems with components considerably different in size and shape, substantial deviations may occur. Considering these implications, Petersen et. al.[27] presented a method in 1991 based on the principle of corresponding states using two reference components. The reduced viscosity (η_{rx}) of a given component (denoted by x) is calculated using the following expression :

$$\ln \eta_{rx} = \ln \eta_{r1} + \frac{MW_x - MW_1}{MW_2 - MW_1} \ln \frac{\eta_{r2}}{\eta_{r1}} \qquad (2.5.1)$$

MW stands for molecular weight and subscripts 1 and 2 refer to the two reference components. The functional form for Eq. 2.5.1 was originally suggested by Teja and Rice[28] using the acentric factor instead of molecular weight. The reduced properties are determined from :

$$E_r = \frac{E}{E_c} \qquad E = T, P, \eta \qquad (2.5.2)$$

Subscripts r and c indicate reduced and critical properties respectively. The critical viscosity, η_c is calculated from :

$$\eta_c = C\, MW^{1/2} P_c^{2/3} T_c^{-1/6} \qquad (2.5.3)$$

Where, C is a constant, MW is the molecular weight, P_c is the critical pressure and T_c is the critical temperature. The final form of the correlation can be derived by rearranging Eq. 2.5.1 and utilising Eq. 2.5.2 :

$$\eta = \frac{\eta_{cx}\eta_1(T_1,P_1)}{\eta_{c1}} \left[\frac{\eta_2(T_2,P_2)\eta_{c1}}{\eta_1(T_1,P_1)\eta_{c2}} \right]^K \qquad (2.5.4)$$

The constant 'C' in Eq. 2.5.3 will cancel out on obtaining Eq. 2.5.4, where K represents the slope of the straight line, in terms of molecular weight :

$$K = \frac{MW_x - MW_1}{MW_2 - MW_1} \qquad (2.5.5)$$

η_1 and η_2, are viscosities of the first and the second reference component and are evaluated at conditions defined by :

$$T_i = T \frac{T_{ci}}{T_{cx}} \qquad i = 1, 2 \qquad (2.5.6)$$

and

$$P_i = P \frac{P_{ci}}{P_{cx}} \qquad i = 1, 2 \qquad (2.5.7)$$

Where, T and P are the temperature and pressure at which viscosity calculations are desired. The mixing rules employed to calculate the critical temperature (T_{cx}) and pressure (P_{cx}) of the mixture are identical to those employed in the one reference method (Section 2.3). The expressions for calculating the molecular weight are similar to those used in the one reference method with a different set of parameters :

$$MW_{mix} = MW_n + 0.00867358\ (MW_w^{1.56079} - MW_n^{1.56079}) \qquad (2.5.8)$$

$$MW_w = \frac{\Sigma z_i MW_i^2}{\Sigma z_i MW_i} \qquad (2.5.9)$$

and

$$MW_n = \Sigma z_i MW_i \qquad (2.5.10)$$

here z_i is the mole fraction of the ith component in the mixture and MW_i is the molecular weight of the ith component in the mixture.

The two reference components chosen are methane and n-decane. Decane is chosen as the second reference due to the fact that it is the largest alkane for which sufficient amount of transport and PVT data exists in the literature.

The reference component viscosities are calculated from the expressions similar to those in the one reference method with different set of parameters[27]. The reference component densities are however, calculated from the new correlation developed by Petersen et. al[27] which is based on the cubic Adachi-Lu-Sugie (ALS) equation of state in the form given by Jensen[29].

Typical input data required are critical temperature, pressure, molecular weight and composition. The method is computationally much faster and superior compared to other corresponding states methods. It, however, is not very accurate and reliable for fluids having molecular weight more than decane due to that fact that the straight line functional form cannot be successfully extrapolated beyond n-decane.

2.6 : LEE'S METHOD FOR VISCOSITY OF GASES

The methods discussed earlier were applicable for the simultaneous prediction of viscosity of both gas and liquid phases, and thus were very self consistent in their predictive capabilities. Apart from these methods there are certain methods which are specifically applicable for estimating either the viscosity of gases or liquids only. In this section another widely used method for predicting the viscosity of gases is reviewed.

In 1966 Lee et. al[1], developed a method for estimating viscosity of natural gases, the method is based on experimental viscosity data of pure hydrocarbon gases and one binary gas mixture. Viscosity is basically expressed in terms of the molecular weight, temperature and the density. The original equation of Starling and Ellington[25], is used as a starting point:

$$\eta = \eta_o \exp[X(T)\rho^{Y(T)}] \qquad (2.6.1)$$

Eq. 2.6.1, was modified by Lee et. al[26], to represent a mixture and pure component data simultaneously, which had the modified form as :

$$\eta = K\exp[X\rho^{Y}] \tag{2.6.2}$$

where

$$K = \frac{(7.77+0.0063M)T^{1.5}}{122.4+12.9M+T} \tag{2.6.3}$$

$$X = 2.57 + \frac{1914.5}{T} + 0.0095M \tag{2.6.4}$$

$$Y = 1.11 + 0.04X \tag{2.6.5}$$

Where,

η = viscosity in micropoise

K,X, and Y = parameters defined by Eqs. 2.6.3 to 2.6.5

M = molecular weight

T = temperature in °Rankine

ρ = gas density in gm/cc

the coefficients and constants in the above set of equations were obtained by fitting the viscosity data of methane, ethane, propane, n - butane and four methane-n-butane mixtures. The density data used were from Sage and Lacey[24]. The measured viscosities of four natural gas mixtures were compared with those calculated from Eq. 2.6.2 which reproduced the experimental data within ± 5 %. Although the proposed method gives reasonably accurate results for hydrocarbon gases and their mixtures, it fails to predict the viscosity of non - hydrocarbons, like, CO_2, O_2, N_2 and CO giving unreliable viscosity figures, the same problem occurs in a gas mixture consisting of high concentration of one of these gases. The method is very simple to apply. For mixtures the density used is either measured or calculated by reliable equations of state (EOS), the molecular weight of the mixture can be calculated by the simple molar mixing rules :

$$MW_{mix} = \sum_{i=1}^{n} X_i M_i \qquad (2.6.6)$$

the method is very widely used in the compositional reservoir simulators.

2.7 : LITTLE AND KENNEDY'S METHOD FOR VISCOSITY OF LIQUIDS

Little and Kennedy's[2] correlation is based on the analogy between viscosity-temperature at constant pressure and specific volume-temperature at constant pressure. This enabled them to formulate a viscosity-temperature-pressure correlation similar to that of van der Waal's fundamental equation of state for volume, which is:

$$\left(P+\frac{A}{V^2}\right)(V-B) = RT \qquad (2.7.1)$$

where,

P = pressure

A,B = EOS constants

V = volume

R = universal gas constant and

T = temperature

This formed the groundwork of Little and Kennedy's correlation[2]. In their work the above equation was reconstructed in terms of viscosity to give the form :

$$\left(T+\frac{a}{\eta^2}\right)(\eta-b) = cP \qquad (2.7.2)$$

a, b and c are empirical constants for each pure material and η is the viscosity. They applied Eq. 2.7.2 to nitrogen and the normal hydrocarbons, methane through hexane which resulted in the following correlations for a, b, and c :

$$a = re^{-k/P} \tag{2.7.3}$$

$$b = sP^{m} \tag{2.7.4}$$

$$c = tP^{-n} \tag{2.7.5}$$

where,

r, k, s, m, t, and n = empirical constants for each pure component
(obtained from the data on nitrogen and methane through n-hexane)

P = pressure in psia

η = viscosity in centipoise

Rearrangement of Eq. 2.7.2 - 2.7.5 gives :

$$\left(T+\frac{re^{-k/P}}{\eta^2}\right)(\eta - sP^{m}) = (tP^{-n})P \tag{2.7.6}$$

or in a more convenient form :

$$\eta^3 - \eta^2\left(sP^{m} + \frac{tP^{-n+1}}{T}\right) + \eta\left(\frac{re^{-k/P}}{T}\right) - \frac{(re^{-k/P})(sP^{m})}{T} = 0 \tag{2.7.7}$$

The above cubic equation has three real roots π_1,π_2 and π_3 to satisfy the criteria such that :

$$(\eta - \pi_1)(\eta - \pi_2)(\eta - \pi_3) = 0$$

The following set of rules are followed to calculate the viscosity of a pure hydrocarbon.

1. In the single phase gas region the minimum of the roots π_1, π_2 and π_3 is used if three real, unequal roots are obtained.
2. In the liquid or dense gas phase region, the maximum of the roots π_1, π_2 and π_3 is used when three real, unequal roots are obtained.
3. Imaginary roots obtained in either region have no significance and should be neglected.

The values of various pure component empirical constants in Eq. 2.7.7 are available in Table 2.7.1. The above correlations were tested by the above authors for 1006 data points on pure hydrocarbons with an average absolute deviation of 1.9 %.

Little and Kennedy extended Eq. 2.7.2 to predict viscosities of complex hydrocarbon mixtures, for a mixture Eq. 2.7.2 would therefore be :

$$\left(T+\frac{a_m}{\eta^2} \right) (\eta - b_m) = c_m P \qquad (2.7.8)$$

where

η = viscosity of a mixture

a_m, b_m and c_m are functions of composition for each mixture.

The following relations resulted for the parameters a_m, b_m and c_m using 3349 data points on viscosity measurements on real reservoir fluids :

$$a_m = \exp (\log_e A) \qquad (2.7.9)$$

$$b_m = \exp (\log_e B) \qquad (2.7.10)$$

where

$$\log_e(A) = A_0 + A_1\left(\frac{1}{T}\right) + A_2(M)_{C7+} + A_3\left(\frac{M}{SG}\right)_{C7+} + A_4\left(\frac{\rho_m}{T}\right) + A_5\left(\frac{\rho_m}{T}\right)^2 + A_6(\bar{M}) + A_7(\bar{M})^3 + A_8(\bar{M}\rho_m) + A_9(\bar{M}\rho_m)^3 + A_{10}(\rho_m)^2 \qquad (2.7.11)$$

$$\log_e(B) = B_0 + B_1\left(\frac{1}{T}\right) + B_2\left(\frac{1}{T}\right)^4 + B_3(SG)^3_{C7+} + B_4(SG)^4_{C7+} + B_5\left(\frac{M}{SG}\right)^4_{C7+} + B_6\left(\frac{\rho_m}{T}\right)^4 + B_7(\bar{M}) + B_8(\bar{M}\rho_m) + B_9(\bar{M}\rho_m)^4 + B_{10}(\rho_m)^3 + B_{11}(\rho_m)^4 \qquad (2.7.12)$$

Where,

$(M)_{C7+}$ = molecular weight of the C7+ fraction

Table 2.7.1 - Empirical Constants in Eq. 2.7.7 for Pure Components for the Little and Kennedy Method (from Reference 2).

Material	Pressure Range psia Min.	Max.	r	k	Pressure Range psia Min.	Max.	s	m	Pressure Range psia Min.	Max.	t	n
Nitrogen												
	100	865	3.6410767	422.84326	100	1938	.29544804	$.49401475\times10^{-1}$	100	1898	-60.638538	.87402138
	865	2002	27.610946	2176.0624	1938	5999	$.18693206\times10^{-7}$	2.2391550	1898	8000	$-.41089473\times10^{-11}$	-3.1447446
	2002	4400	650.32531	8500.8332	5999	8000	$.27678598\times10^{-6}$	1.9031151	-	-	-	-
	4400	8000	16718.530	22786.676	-	-	-	-	-	-	-	-
Methane												
	14.7	140	1.0846747	-6.7376911	14.7	132	.33952795	$-.42355657\times10^{-1}$	14.7	140	-170.02510	1.1046515
	140	920	2.6660956	155.66976	132	1170	.20769226	$.58198018\times10^{-1}$	140	1115	-49.268990	.85333647
	920	2500	330.12035	4589.5077	1170	2500	$.59758720\times10^{-20}$	6.4260185	1115	2500	$-.31870264\times10^{-23}$	-7.4154938
	2500	5000	-40.958106	2406.3575	2500	5000	-.10330795	.86563179	2500	5000	67.799253	.35440274
	5000	8000	-94.026998	6503.3884	5000	8000	-39305707.	-1.4570222	5000	8000	23442.651	1.0411081
Ethane												
gas	14.7	154	.80785003	-12.516490	14.7	105	.50941515	-.14638282	14.7	105	-421.42381	1.2998807
	154	533	2.7983501	179.27398	105	-	.15599491	.10759939	105	600	-38.945001	.78839133
	533	1000	47.034833	1683.2323	-	-	-	-	600	-	-4.1583434	.43909889
liquid	-	1000	$.20853505\times10^{-3}$	-7332.5773	-	1500	$-.46160060\times10^{-1}$	.56547032	-	1500	77.045189	.57175811
	1000	2140	-7.4989064	976.91412	1500	6650	-8.9414509	-.22802507	1500	10,000	1967.6077	1.0726470
	2140	10,000	-82.033356	6090.6307	6650	10,000	-572.67565	-.70063633	-	-	-	-
Propane												
gas	14.7	100	.36192305	-9.6155439	14.7	300	.24701995	$-.25686867\times10^{-1}$	14.7	300	-121.19586	1.0860752
	100	300	.26384144	-40.947778	300	-	2.2109213	-.40956858	300	-	-113959.35	2.2886764
	300	617.5	$.15226247\times10^{-3}$	-2280.6819	-	-	-	-	-	-	-	-
liquid	-	887	3.9189138	-335.87861	-	1335	-1.3460621	$.40089160\times10^{-1}$	-	3475	1174.4216	.96089292
	887	1250	$.32790000\times10^{-2}$	-6630.1433	1335	3410	-2.2244542	$-.29738480\times10^{-1}$	3475	8000	141.43449	.70128307
	1250	3239	-99.499079	5555.7898	3410	8000	$-.88997090\times10^{-1}$	.36594389	-	-	-	-
	3239	8000	-356.20085	9686.5520	-	-	-	-	-	-	-	-
n-Butane												
	100	1000	-.91862520	-219.89138	100	1500	-3.8437204	$-.80620090\times10^{-1}$	100	1500	2677.3515	1.0373570
	1000	5000	-256.34733	5470.1402	1500	6000	-.50774903	.19733166	1500	10,000	564.07984	.82222409
	5000	10,000	-408.34176	7681.1240	6000	10,000	-1.8684646	$.47111960\times10^{-2}$	-	-	-	-
n-Pentane												
	147	688	-2.5895703	-385.77133	147	686	-8.5218112	-.18612526	147	699	4761.1950	1.0959771
	688	4081	-287.85052	2855.4427	686	4465	-.38708680	.28729981	699	4310	687.70260	.80058171
	4081	7348	-1223.5605	8760.3749	4465	7348	$-.15460000\times10^{-3}$	.94447999	4310	7348	11.989817	.31732360
n-Hexane												
	600	1750	40.531074	-288.33964	600	1500	-3.1567826	$-.17899854\times10^{-1}$	600	1536	3121.8378	.99549948
	1750	3000	-8322.2662	14191.145	1500	5000	-.43352526	.25563756	1536	5007	983.37496	.83804706
	3000	4738	-411.69984	5281.1149	5000	10,000	$-.16250329\times10^{-2}$	.90991092	5007	10,000	28.319913	.42161610
	4738	10,000	-2137.1803	13083.760	-	-	-	-	-	-	-	-

$(SG)_{C7+}$ = specific gravity of the C7+ fraction

ρ_m = density of the mixture at reservoir conditions in gm/cc

T = temperature in °Rankine

$\overline{M}$ = average molecular weight of the mixture given by:

$$\overline{M} = \Sigma x_i M_i \qquad (2.7.13)$$

x_i is the mole fraction of the ith component in the mixture and M_i is the molecular weight of the ith component in the mixture.

values for constants A_0 to A_{10} and B_0 to B_{11} are :

i	A	B
0	21.918581	-2.6941621
1	-16815.621	3757.4919
2	0.023315983	$-0.31409829E^{12}$
3	-0.019218951	-33.744827
4	29938.501	31.333913
5	-2802762.9	$0.24400196E^{-10}$
6	-0.096858449	$0.70237064E^{12}$
7	$0.54324554E^{-06}$	-0.037022195
8	0.13129082	0.070811794
9	$-0.10526154E^{-05}$	$-0.83033554E^{-09}$
10	-31.680427	21.710610
11	-	-31.083544

The authors claim that the best results are obtained using the minimum real root of Eq. 2.7.8 for $c_m = 1.0$. Typical input data needed to accomplish calculations are fluid composition, molecular weight, fluid density and properties of the C_{7+} fraction. A better accuracy has been

claimed by the authors compared to the Lohrenz-Bray-Clark correlation[8]. The method is known to be best suited for black oil applications.

References

1) Lee, A.L., Gonzalez, M.H. and Eakin, B.E.: "The Viscosity of Natural Gases", *Journal of Petroleum Technology*, pp. 997 - 1000, (Aug., 1966).

2) Little, J.E. and Kennedy, H.T.: "A Correlation of the Viscosity of Hydrocarbon Systems with Pressures, Temperature and Composition", *Society of Petroleum Engineers Journal (SPEJ)*, pp. 157 - 162, (Jun., 1968).

3) Eakin, B.E. and Ellington, R.T.: "Predicting the Viscosity of Pure Light Hydrocarbons", *Journal of Petroleum Technology*, pp. 210 - 214, (Feb., 1963).

4) Giddings, J.G. and Kobayashi, R.: "Correlation of the Viscosity of Light Paraffin Hydrocarbons and Their Mixtures in the Liquid and Gaseous Regions", *Journal of Petroleum Technology*, pp. 679 - 682, (Jun., 1964).

5) Twu, C.H.: "Generalised Methods for Predicting Viscosities of Petroleum Fractions", *AIChEJ*, Vol. 32, No. 12, pp. 2091 - 2094, (Dec., 1986).

6) Reid, R.C., Prausnitz, J.M. and Poling, B.E.: "The Properties of Gases and Liquids", Fourth Edition, McGraw Hill Book Company, New York (1989).

7) Jossi, J.A., Stiel, L.I. and Thodos, G.: "The Viscosity of Pure Substances in the Dense Gaseous and Liquid Phases", *AIChEJ*, Vol. 8, pp. 59 - 63, (1962).

8) Lohrenz, J., Bray, B.G. and Clark, C.R.: "Calculating Viscosities of Reservoir Fluids from Their Compositions", *Journal of Petroleum Technology*, pp. 1171-1176, (Oct., 1964).

9) Abas - Zade, A.K., *Zhur. Ekspl. i, Teoret. Fiz.*, 23, 60, (1952).

10) Misic, Dragoslav, and George Thodos, *AIChEJ*, Vol. 7, pp. 264, (1961).

11) Herning, F. and Zipperer, L.: "Calculation of the Viscosity of Technical Gas Mixtures from the Viscosity of Individual Gases", *Gas U. Wasserfach*, No. 49, (1936).

12) Ely, J.F. and Hanley, H.J.M.: "Prediction of Transport Properties 1, Viscosity of Fluids and Their Mixtures", *Industrial & Engineering Chemistry (I & EC) Fundamentals*, Vol. 20, pp. 323-332, (1981).

13) Baltatu, M.E.: "Prediction of the Liquid Viscosity for Petroleum Fractions", *Industrial & Engineering Chemistry (I & EC) Process Design & Development*, Vol. 21, pp. 192-195, (1982).

14) Pedersen, K.S. et. al : "Viscosity of Crude Oils", *Chemical Engineering Science*, Vol. 39, pp. 1011-1016, (1984).

15) Pedersen, K.S. and Fredenslund, Aa.: "An Improved Corresponding States Model for Prediction of Oil and Gas Viscosities and Thermal Conductivities", *Chemical Engineering Science*, Vol. 42, pp. 182-186, (1987).

16) Tham, M.J. and Gubbins, K.E., *Industrial & Engineering Chemistry (I & EC) Fundamentals*, Vol. 9, pp. 63, (1970).

17) Christensen, P.L. and Fredenslund, Aa., *Chemical Engineering Science*, Vol. 35, pp. 871, (1980).

18) McCarty, R.D.: "A Modified Benedict - Webb - Rubin Equation of State for Methane Using Recent Experimental Data", *Cryogenics*, (May, 1974).

19) Hanley, H.J.M., McCarty, R.D. and Haynes, W.M.: "Equations for the Viscosity and Thermal Conductivity Coefficients of Methane", *Cryogenics*, (Jul., 1975).

20) Baltatu, M.E.: "Prediction of the Transport Properties of Petroleum Fractions", Paper Presented at the 1984 Winter National Meeting of AIChE, Atlanta, Georgia, (1984).

21) Ely, J.F. and. Hanley, H.J.M.: "Prediction of the Viscosity and Thermal Conductivity in Hydrocarbon Mixtures - Computer Program, TRAPP", Proceedings of the Sixtieth Annual Convention of Gas Processors Association, pp. 20-29, (Mar., 1981).

22) Leach, J.W.: "Molecular Structure Corrections for Application of the Theory of Corresponding States to Non - Spherical Pure Fluids and Mixtures", PhD Thesis, Rice University, (1967).

23) Leach, J.W., Chappelear, P.S. and Leland, T.W., *AIChEJ*, Vol. 14, pp. 568, (1968).

24) Sage, B.H. and Lacey, W.N.: "Thermodynamic Properties of the Lighter Paraffin Hydrocarbons and Nitrogen", API, New York, N.Y. (1950).

25) Starling, K.E. and Ellington, R.T.: "Viscosity Correlations for Non polar Fluids", *AIChEJ*, pp. 11-15, (Jan., 1964).

26) Lee, A.L., Starling, K.E., Dolan, J.P. and Ellington, R.T.: "Viscosity Correlation for Light Hydrocarbon Systems", *AIChEJ*, pp. 694-697, (Sep., 1964).

27) Aasberg-Petersen, K., Knudsen, K. and Fredenslund, A.: "Prediction of Viscosities of Hydrocarbon Mixtures", *Fluid Phase Equilibria*, Vol. 70, pp. 293-308, (1991).

28) Teja, A.S. and Rice, P.: "Generalised Corresponding States Method for the Viscosities of Liquid Mixtures", *Industrial & Engineering Chemistry (I & EC) Fundamentals*, Vol. 20, pp. 77 (1981).

29) Jensen, B.H.: "Densities, Viscosities, and Phase Equilibria in Enhanced Oil Recovery", PhD Thesis, Institut for Kemiteknik, the Technical University of Denmark, (1987).

30) Pedersen, K.S., Fredenslund, Aa. and Thomassen, P.: "Properties of Oils and Natural Gases", Contributions in Petroleum Geology & Engineering, 5, Gulf Publishing Company, (1989).

CHAPTER 3 : REVIEW OF CORRELATIONS FOR DENSITY OF GASES AND LIQUIDS

3.1 : INTRODUCTION

In the last chapter various viscosity correlations used for predicting oil and gas viscosities were reviewed. Some of these correlations, such as, the Lohrenz - Bray - Clark[7], the Little and Kennedy[10] and the Lee's[8] method require oil and gas phase densities to predict their viscosities. Hence, density correlations or equation of state models are required to be used in conjunction with these viscosity correlations in the absence of experimentally measured densities. Hence in this chapter two commonly used density correlations are reviewed for prediction of oil and gas phase densities in order to compliment the review of various viscosity correlations presented in the previous chapter. The Alani and Kennedy[1] method is used for liquid phase densities and the Soave - Redlich - Kwong[2] method is used for the densities of gas phase. These correlations are considered to accurately predict the oil and gas phase densities at high temperature and pressure conditions and are recommended for use in the viscosity correlations.

3.1.1 : Significance of Density in the Residual Viscosity Correlation

As mentioned in the previous section, the residual viscosity method requires accurate density data of the gas and liquid phases in order to have reliable estimates of viscosities. In a comparative study recently published by Ali[9], he has highlighted the importance of accurate density data for reliable estimation of viscosity using the Lohrenz-Bray-Clark (L-B-C)[7] correlation.

In general, for the vapour phase, the error in the viscosity estimate is in direct proportion to the error for density errors up to 20%. For the liquid phase, however, the error in viscosity varies from an average of 50% for 5% error in density to over 500% for 20% error in density.

Table 3.1.1.1 - Effect of Density Inaccuracy on the Estimated Viscosity Using the Lohrenz-Bray-Clark (LBC)[7] correlation (from Reference 9).

Measured density (g/cm^3)	Measured viscosity (μP)	% Dev in viscosity for given percent error in density							
		5%		10%		15%		20%	
		−	+	−	+	−	+	−	+
Mix no. 1									
0.0543	162.6	1.0	1.6	0.8	2.0	0.5	2.3	0.2	2.6
0.1254	180.1	−0.1	2.0	−1.1	3.1	−2.0	4.2	−2.9	5.4
0.3370	279.1	−1.2	7.2	−5.2	11.7	−8.9	16.3	−12.5	21.2
0.5126	419.8	−2.2	9.9	−7.8	16.3	−13.2	23.1	−18.3	30.4
0.6055	532.3	−5.9	7.7	−12.0	15.4	−17.8	23.9	−23.3	33.5
0.6609	613.6	−8.2	6.9	−14.7	15.9	−20.8	26.4	−26.4	38.8
0.7000	675.8	−9.3	7.4	−16.3	18.0	−22.6	30.6	−28.3	46.1
0.7298	726.1	−9.8	8.7	−17.2	20.7	−23.7	35.6	−29.7	54.3
0.7562	781.1	−10.9	9.3	−18.7	23.0	−25.4	40.2	−31.5	62.5
0.7763	821.6	−11.1	10.8	−19.3	26.0	−26.3	45.6	−32.5	71.3
0.7908	855.6	−11.4	11.7	−20.0	28.1	−27.2	49.6	−33.5	78.0
Mix no. 4									
0.6838	5444.9	−43.9	39.5	−61.8	133.4	−72.8	302.5	−79.6	610.7
0.6874	5607.1	−43.2	43.1	−61.6	141.0	−72.8	318.3	−79.7	642.4
0.6911	5789.1	−42.6	46.8	−61.5	148.9	−72.9	334.5	−79.9	675.4
0.6943	5892.8	−41.4	51.6	−61.0	158.4	−72.6	353.6	−79.9	713.3
0.6975	6110.1	−41.3	53.7	−61.1	163.6	−72.9	365.0	−80.2	747.3
0.7001	6315.5	−41.4	54.9	−61.4	166.9	−73.2	372.8	−80.5	754.7
0.7031	6597.2	−41.9	55.5	−62.0	169.4	−73.7	380.0	−80.9	770.3
0.7052	6730.1	−41.6	57.7	−61.9	174.0	−73.8	389.4	−81.0	790.9

− underestimated; + overestimated.

Mix 1 - CH_4+CO_2

Mix 4 - CH_4+n-C_{10}

The data presented in Table (3.1.1.1) proves that the results obtained from the L-B-C correlation are highly sensitive to the accuracy of the density values. In general the errors associated with overestimated (+) densities are greater than the errors obtained from underestimated (-) densities for both the liquid and vapour phases.

In all the compositional reservoir simulators an equation of state would normally be required to obtain the necessary volumetric data if these are not directly available. Near the critical point and in regions where the fluid density is approaching that of a liquid, larger errors are encountered. However, the computation of density for simple hydrocarbons and real reservoir fluid systems, despite the important advances achieved by cubic equation of state, still remains the weak point of density dependent viscosity correlations.

3.2 : ALANI AND KENNEDY METHOD FOR DENSITY OF LIQUIDS

Alani and Kennedy[1], used the van der Waals equation of state as a basis for their work. The original van der Waal's equation of state (EOS) is :

$$\left(P+\frac{a}{V^2} \right) (V-b) = RT \qquad (3.2.1)$$

where,

P = absolute pressure

V = molar volume

a & b = EOS constants

R = universal gas constant, and

T = absolute temperature

Alani and Kennedy[1], used the known values of gas constant-R, temperature-T, pressure-P and volume-V in Eq. 3.2.1, for each pure hydrocarbon on which accurate data were available. The parameters a and b were made functions of temperature. They used 647 experimental measurements of volume on 47 bottom hole samples in a temperature range of 72 to 250°F

and a pressure range from bubble point to 5000 psig for developing correlations for mixtures. The relationships for a and b are :

$$a = Ke^{n/T} \tag{3.2.2}$$

$$b = mT + C \tag{3.2.3}$$

k, n, m and C are constants for each hydrocarbon listed in Table (3.2.1)[3]. After recasting Eq. 3.2.1 with the help of Eq. 3.2.2 and 3.2.3 :

$$RT = \left(P + \frac{Ke^{n/T}}{V^2} \right) \left(V - mT - C \right) \tag{3.2.4}$$

Eq. 3.2.4 may also be written in terms of volume as :

$$V^3 - \left(\frac{RT}{P} + mT + C \right) V^2 + \left(\frac{Ke^{n/T}}{P} \right) V - \left(\frac{Ke^{n/T}}{P} \right) (mT + C) = 0 \tag{3.2.5}$$

Eq. 3.2.5 has three roots, at least one of which is real under all temperatures and pressures. The real root is :

$$V = A + B + \frac{1}{3} \left(\frac{RT}{P} + mT + C \right) \tag{3.2.6}$$

where, A and B are defined as :

$$A = [sqrt(-\frac{r}{2}) + sqrt(\frac{r^2}{4} + \frac{s^3}{27})]^{1/3} \tag{3.2.7}$$

$$B = [sqrt(-\frac{r}{2}) - sqrt(\frac{r^2}{4} + \frac{s^3}{27})]^{1/3} \tag{3.2.8}$$

and constants, r and s are defined by :

$$r = \frac{1}{27} \left[-2 \left(\frac{RT}{P} + mT + C \right)^3 + 9 \frac{Ke^{n/T}}{P} \left(\frac{RT}{P} + mT + C \right) - 27 \left(\frac{Ke^{n/T}}{P} \right) \left(mT + C \right) \right] \tag{3.2.9}$$

Table 3.2.1 - Constants of Individual Pure Components for Alani and Kennedy Correlation (from Reference 3).

Hydrocarbon	k	n	m E^{04}	c
Methane				
21 - 149°C	9160.64	61.8932	3.31625	0.508743
149.5 - 238°C	147.473	3247.45	-14.0726	1.83267
Ethane				
37.8 - 120.5°C	46709.6	-404.488	5.15210	0.522397
121.1 - 237.8°C	17495.3	34.1636	2.82017	0.623099
Propane	20247.8	190.244	2.15864	0.908325
i - Butane	3220.4	131.632	3.38623	1.10138
n - Butane	33016.2	146.154	2.90216	1.11681
n - Pentane	37046.2	299.626	2.19548	1.43643
n - Hexane	52093.0	254.561	3.69619	1.59294
n - Heptane	82295.5	64.3801	5.25780	1.72999
n - Octane	89185.4	149.390	5.98975	1.93110
n - Nonane	124062	37.9172	6.72999	2.15200
n - Decane	146643	26.5241	7.85618	2.33299
Hydrogen Sulphide	13200	0.0	17.9	0.3945
Carbon Dioxide	8166	126.0	1.818	0.3872
Nitrogen	4300	2.293	4.49	0.3853

Units : P = psia, T = °R, V = ft^3/lb-mole, R = 10.7335 $lbft^3/°R$ lb-mole

$$s = \frac{1}{3}\left[3\,\frac{Ke^{n/T}}{P} - \left(\frac{RT}{P} + mT + C\right)^2\right] \qquad (3.2.10)$$

The solution for the above root is obtained only if $\frac{r^2}{4} + \frac{s^3}{27} > 0$. The other two roots are then imaginary and have no significance in determining liquid volumes.

Similarly, Eq. 3.2.5 has three real and unequal roots if $\frac{r^2}{4} + \frac{s^3}{27} < 0$. The minimum real root in this case represents the volume as :

$$V = 2E^{1/3}\,\mathrm{Cos}\left(\frac{\theta + 2\pi}{3}\right) + \left(\frac{RT}{P} + mT + C\right) \qquad (3.2.11)$$

where, E and Cos (θ), are defined by :

$$E = \mathrm{sqrt}\left[-\frac{1}{27}\left(\frac{Ke^{n/T}}{P} - \frac{1}{3}\left(\frac{RT}{P} + mT + C\right)^2\right)^3\right] \qquad (3.2.12)$$

$$\cos(\theta) = \frac{\frac{1}{2}\,\frac{Ke^{n/T}}{P}\,(mT+C) - \frac{1}{6}\,\frac{Ke^{n/T}}{P}\left(\frac{RT}{P} + mT + C\right) + \frac{1}{27}\left(\frac{RT}{P} + mT + C\right)^3}{\mathrm{sqrt}\left[-27\left(\frac{Ke^{n/T}}{P} - \frac{1}{3}\left(\frac{RT}{P} + mT + C\right)^2\right)^3\right]} \qquad (3.2.13)$$

Eq. 3.2.5 can be applied to pure components in its form given above and the liquid specific volume can be obtained by solving the cubic equation for its minimum real root, among the three roots obtained.

For a hydrocarbon mixture containing, n, number of components, the constants a and b can be defined as :

$$a_m = \sum_{i=1}^{n} X_i a_i \qquad (3.2.14)$$

$$b_m = \sum_{i=1}^{n} X_i b_i \qquad (3.2.15)$$

for plus fractions Alani and Kennedy[1], have suggested the following relationships for calculating the constants 'a' and 'b':

$$\log_e(a_{C7+}) = 3.8405985E^{-3}M_{C7+} - 9.5638281E^{-4}\left(\frac{M_{C7+}}{SG_{C7+}}\right) + \frac{2.6180818E^2}{T} + 7.3104464E^{-6}(M_{C7+})^2 + 10.753517 \quad (3.2.16)$$

$$b_{C7+} = 3.4992740E^{-2}M_{C7+} - 7.2725403SG_{C7+} + 2.2323950E^{-4}T - 1.6322572E^{-2}\left(\frac{M_{C7+}}{SG_{C7+}}\right) + 6.2256545 \quad (3.2.17)$$

where,

M_{C7+} = molecular weight of the C7+ fraction and

SG_{C7+} = specific gravity of the plus fraction

(see Table 3.2.1 for units)

After calculating the values of a_m and b_m for a mixture the molar volume can be computed by a method similar to that of a pure component (Eq. 3.2.6 - 3.2.13).

Alani and Kennedy have quoted an average absolute deviation (AAD) of 0.33 % for any pure hydrocarbon studied after comparing the calculated and experimental values in the range of 30 to 250°F, and bubble point to 68.95 MPa. The AAD for 647 experimental measurements on 47 bottom hole samples covering a temperature range of 22 to 121°C, and bubble point to 34.45 MPa, was 1.6 %. In the work presented in this study, in all the viscosity calculations measured density data were used wherever possible to maintain the consistency between predicted viscosities. A comparison of densities calculated and measured for liquid phase mixtures of methane - n - butane[4] and carbon dioxide synthetic oil[5] are presented in Table (3.2.2) & (3.2.3).

Table 3.2.2 - Comparison of Predicted Densities and Measured Densities for a Binary Liquid Phase Mixture of Methane - n - Butane at 80°C.

No	Pressure, MPa	Experimental[4], Density, gm/cc	Predicted by Alani & Kennedy, gm/cc	% Deviation
1	10.78	0.3500	0.3930	-12.30
2	10.34	0.3620	0.4020	-11.05
3	9.75	0.3800	0.4121	-8.45
4	9.06	0.3950	0.4225	-6.96
5	7.68	0.4212	0.4398	-4.41
6	6.30	0.4424	0.4544	-2.71
7	4.92	0.4614	0.4675	-1.32
8	4.23	0.4702	0.4737	-0.74
			AAD	6.0 %

Table 3.2.3 - Comparison of Predicted Densities and Measured Densities for a Carbon Dioxide and Synthetic Oil Mixture[5].

No	Pressure, MPa	Experimental[5] Density, gm/cc	Predicted by Alani & Kennedy, gm/cc	% Deviations
1	8.96, 37.8°C	0.7545	0.7976	-5.70
2	8.96, 37.8°C	0.7599	0.7977	-4.90
3	8.96, 37.8°C	0.7848	0.8040	-2.45
4	8.96, 37.8°C	0.7978	0.7999	-0.26
5	13.79, 37.8°C	0.8017	0.8018	-0.01
6	13.79, 37.8°C	0.8053	0.7994	0.73
7	13.79, 37.8°C	0.8080	0.7916	2.00
8	13.79, 37.8°C	0.8096	0.7768	4.00
9	13.79, 87.8°C	0.7160	0.7798	-8.90
10	13.79, 87.8°C	0.7253	0.7729	-6.60
11	13.79, 87.8°C	0.7243	0.7851	-8.40
12	13.79, 87.8°C	0.7340	0.7778	-5.97
			AAD	4.0 %

3.3 : SOAVE - REDLICH - KWONG EOS FOR PREDICTION OF GAS DENSITY

The original Redlich-Kwong[6] equation of state is :

$$P = \frac{RT}{v-b} - \frac{a/T^{0.5}}{v(v+b)} \qquad (3.3.1)$$

where,

P = pressure

T = temperature

v = volume

R = universal gas constant and

a & b = EOS constants

Soave[2] modified the term, $a/T^{0.5}$ with a more general temperature dependent term a(T) :

$$P = \frac{RT}{v-b} - \frac{a(T)}{v(v+b)} \qquad (3.3.2)$$

substituting $v = z\frac{RT}{P}$, where z is compressibility factor, and letting,

$$\frac{aP}{R^2T^2} = A \qquad (3.3.3)$$

$$\frac{bP}{RT} = B \qquad (3.3.4)$$

Eq. 3.3.2, can also be written in terms of compressibility factor, Z, and using Eq. 3.3.3, and 3.3.4 :

$$Z^3 - Z^2 + Z(A-B-B^2) - AB = 0 \qquad (3.3.5)$$

at critical point, first and second derivatives of pressure with respect to volume are set to zero, to give :

$$a_i(T_{ci}) = a_{ci} = 0.42747 \frac{R^2 T_{ci}^2}{p_{ci}} \quad (3.3.6)$$

$$b_i = 0.08664 \frac{RT_{ci}}{p_{ci}} \quad (3.3.7)$$

at temperatures other than critical, by letting :

$$a_i(T) = a_{ci}\, \alpha_i(T) \quad (3.3.8)$$

$\alpha_i(T)$ is an adimensional factor which becomes unity at critical temperatures, using Eq. 3.3.6 - 3.3.8, Eq. 3.3.3 & 3.3.4 for pure components become :

$$A = 0.42747\, \alpha_i(T) \frac{P/P_{ci}}{(T/T_{ci})^2} \quad (3.3.9)$$

$$B = 0.08664\, \frac{P/P_{ci}}{T/T_{ci}} \quad (3.3.10)$$

A plot of $\alpha_i(T)$ vs. $T_{ri} = T/T_{ci}$ shows separate curves for pure compounds indicating similar trends[2]. By plotting $\alpha_i^{0.5}$ against $T_{ri}^{0.5}$ straight lines are obtained with a condition that all lines must pass through ($T_r = \alpha = 1$) :

$$\alpha_i^{0.5} = 1 + m_i(1 - T_{ri}^{0.5}) \quad (3.3.11)$$

where, m, is related directly to the acentric factor (ω) of the related compounds :

$$m_i = 0.480 + 1.574\omega_i - 0.176\omega_i^2 \quad (3.3.12)$$

The above equations can be applied for volumetric predictions of pure substances.

For mixtures the following mixing rules are proposed by Soave[2], for constants A and B:

$$A = 0.42747 \frac{P}{T^2} \left(\Sigma x_i \frac{T_{ci}\alpha_i^{0.5}}{P_{ci}^{0.5}}\right)^2 \quad (3.3.13)$$

Table 3.3.1 - Comparison of Predicted Densities and Measured Densities for a Binary Vapour Mixture of Methane - n - Butane at 80°C.

No	Pressure, MPa	Experimental[4], Density, gm/cc	Predicted by S - R - K, gm/cc	% Deviations
1	10.78	0.1683	0.1620	3.74
2	10.34	0.1557	0.1486	4.56
3	9.75	0.1404	0.1338	4.70
4	9.06	0.1252	0.1197	4.39
5	7.68	0.1015	0.0965	4.90
6	6.30	0.0823	0.0769	6.60
7	4.92	0.0649	0.0602	7.24
8	4.23	0.0569	0.0529	7.03
			AAD	5.4 %

Table 3.3.2 - Comparison of Predicted Densities and Measured Densities for a Low Ethane Natural Gas at 29.5°C.

No	Pressure, MPa	Experimental[8], Density, gm/cc	Predicted by S - R - K, gm/cc	% Deviations
1	13.92	0.0991	0.1103	-11.30
2	27.69	0.2109	0.2006	4.90
3	31.18	0.2288	0.2167	5.30
4	34.61	0.2385	0.2307	3.27
5	41.52	0.2602	0.2543	2.27
6	48.38	0.2761	0.2734	0.98
7	55.36	0.2870	0.2897	-0.94
8	58.33	0.2941	0.2959	-0.61
			AAD	3.7 %

Table 3.3.3 - Comparison of Predicted Densities and Measured Densities for a Low Ethane Natural Gas at 104.4°C.

No	Pressure, MPa	Experimental[8], Density, gm/cc	Predicted by S - R - K, gm/cc	% Deviations
1	7.09	0.0396	0.0391	1.26
2	10.45	0.0582	0.0580	0.34
3	14.16	0.0747	0.0786	-5.22
4	20.85	0.1178	0.1137	3.48
5	27.68	0.1508	0.1455	3.51
6	38.09	0.1893	0.1857	1.90
7	44.78	0.2102	0.2070	1.52
			AAD	2.5 %

Table 3.3.4 - Comparison of Predicted Densities and Measured Densities for a High Ethane Natural Gas at 25.9°C.

No	Pressure, MPa	Experimental[8], Density, gm/cc	Predicted by S - R - K, gm/cc	% Deviations
1	27.68	0.2746	0.2590	5.68
2	32.89	0.2976	0.2818	5.30
3	38.09	0.3172	0.3001	5.39
4	44.99	0.3384	0.3199	5.47
5	48.37	0.2474	0.3283	5.49
6	51.90	0.2554	0.3363	5.37
7	55.45	0.3642	0.3436	5.65
8	58.82	0.3741	0.3500	6.44
9	62.20	0.3791	0.3561	6.07
10	69.12	0.3906	0.3672	5.99
			AAD	5.7

Table 3.3.5 - Comparison of Predicted Densities and Measured Densities for a High Ethane Natural Gas at 65.7°C.

No	Pressure, MPa	Experimental[8], Density, gm/cc	Predicted by S - R - K, gm/cc	% Deviations
1	8.71	0.0714	0.0703	1.54
2	10.47	0.0887	0.0861	2.93
3	12.14	0.1050	0.1011	3.71
4	15.61	0.1423	0.1313	7.73
5	19.09	0.1719	0.1591	7.44
6	24.21	0.2070	0.1937	6.42
7	27.69	0.2270	0.2135	5.95
8	34.61	0.2615	0.2456	6.08
			AAD	5.2 %

$$B = 0.08664 \frac{P}{T} (\Sigma x_i \frac{T_{ci}}{P_{ci}}) \qquad (3.3.14)$$

Here, x_i is the mole fraction of ith component in the mixture, T_{ci} is the critical temperature of the ith component in the mixture and P_{ci} is the critical pressure of the ith component in the mixture, whereas P and T represent the absolute temperature and absolute pressure at which volumes are desired. Hence after calculating the value of α_i for each component of the mixture, constants A and B can be computed which can then be substituted in Eq. 3.3.5 to give the compressibility factor. The maximum real root for Z can then be used for vapour phase and minimum real root for Z can be used for the liquid phase. Comparison of predicted and measured densities by the S-R-K[2] equation of state for the vapour phase of a methane - n - butane binary mixture[4], and natural gas mixtures[8], is presented through Table (3.3.1) to Table (3.3.5).

References

1) Alani, G.H. and Kennedy, H.T.: "Volumes of Liquid Hydrocarbons at High Temperatures and Pressures", *Petroleum Transactions of AIME*, Vol. 219, pp. 288-292, (1960).

2) Soave, G.: "Equilibrium Constants from a Modified Redlich - Kwong Equation of State", *Chemical Engineering Science*, Vol. 27, pp. 1197-1203, (1972).

3) Pedersen, et. al : "Properties of Oils and Natural Gases", (Contrib. Petrol. Geol. & Eng., Vol. 5), Gulf Publishing Co., (1989).

4) Sage, B.H., Hicks, B.L. and Lacey, W.N: "Phase Equilibria in Hydrocarbon Systems, The Methane - n - Butane System in the Two Phase Region", *Industrial & Engineering Chemistry (I & EC)*, Vol. 32, No. 8, pp. 1088-1091.

5) Kovarik, F.S. and Taylor, M.A.: "Viscosity Measurements of High Pressure CO_2/Hydrocarbon Mixtures", AIChE Annual Meeting, New York, (Nov., 15-20, 1987).

6) Redlich - Kwong, *Chemical Review*, Vol. 44, pp. 23, (1949).

7) Lohrenz, J., Bray, B.G. and Clark, C.R.: "Calculating Viscosities of Reservoir Fluids from Their Compositions", *Journal of Petroleum Technology*, pp. 1171-1176, (Oct., 1964).

8) Lee, A.L.: "Viscosity of Light Hydrocarbons", Monograph on API Research Project 65, Published by API, New York, (1965).

9) Ali, J.K: "Evaluation of Correlations for Estimating the Viscosities of Hydrocarbon Fluids", *J. of Petroleum Science and Engineering*, Vol. 5, pp. 351-369, (1991).

10) Little, J.E. and Kennedy, H.T.: "A Correlation of the Viscosity of Hydrocarbon Systems with Pressures, Temperature and Composition", *Society of Petroleum Engineers Journal (SPEJ)*, pp. 157 - 162, (Jun., 1968).

CHAPTER 4 : COMPARATIVE STUDY OF PREDICTIVE TECHNIQUES FOR VISCOSITY

4.1 : INTRODUCTION

In this chapter a study conducted on evaluating the reliability and accuracy of the widely used correlations is presented. Only viscosity correlations applicable to both the oil and gas phases were considered for the study, namely, the Lohrenz - Bray - Clark[1] (Jossi-Stiel-Thodos[18] for pure components) method, principle of corresponding states (one reference method)[2] and the extended principle of corresponding states[3]. The Lee's method[4], although was reviewed in this study, the results are not presented here because of two reasons, first, the method is only applicable to gases and the viscosities predicted by it are almost identical to those predicted by the other methods[1,2,3], secondly, the method was found inapplicable to pure non - hydrocarbons, or mixtures of hydrocarbons with significantly large concentration of non - hydrocarbons. The study has been conducted on both pure hydrocarbons and non - hydrocarbons, and their mixtures at wide ranging temperature and pressure conditions. However, a more complete study is presented in the next chapter which provides the modification of the residual viscosity method, proposed in this work, for high reduced density conditions. The comparative study recently carried out by Ali[16] is briefly discussed. A brief study on the tuning of viscosity correlations for real reservoir fluids is also presented.

4.2 : VISCOSITY OF PURE COMPONENTS

Pure normal paraffins ranging from methane to normal decane and non - hydrocarbons, namely, carbon dioxide and nitrogen in both gaseous and liquid phases were considered for the study. The data published by Stephan and Lucas[5], for the work of several researchers was considered for comparing the measured and predicted values. Viscosity data presented in Reference[5], is measured by a variety of conventional viscosity measurement equipment

such as the capillary tube viscometer, oscillating disc, falling body, rotating cylinder, rolling ball and the torsional crystal viscometer. A total number of 1041 viscosity measurements at different temperature and pressure conditions were considered. A FORTRAN 77 program was developed during the course of this study to perform the calculations. The input data for running the program requires, name of the component, temperature, pressure, the density which can either be supplied or can be predicted by the EOS available in the program.

A typical program output for a pure component is given in Table (4.2.1). The output lists the temperature and pressure conditions and writes the corresponding viscosities predicted by different methods and outputs a separate table giving absolute percentage deviations, and at the end writes the average absolute deviations (AAD) for each method. Table (4.2.1), lists viscosity calculations for n-pentane in gas and liquid phases.

The overall AADs for all the pure components considered in the study is presented in Table (4.2.2). It can be seen from the table that the extended principle of corresponding states method by Ely and Hanley[3], gave the lowest AAD of 4.9 % compared to 13.7 % for the residual viscosity method[17] and 17 % for the principle of corresponding states method of Pedersen and Fredenslund[2]. The residual viscosity method was found to be reasonably accurate if the density data supplied were reliable. The principle of corresponding states method[2] was found to be most unreliable for high molecular weight components. This is attributed to the failure of the 33-parameter equation of states[6] which predicted the methane densities (reference component) at temperatures below its freezing point for high molecular weight components and mixtures.

4.3 : VISCOSITY OF MIXTURES

The comparative study for the mixtures ranged from simple binary mixtures, natural gas mixtures to synthetic oil and carbon dioxide mixtures at a variety of temperature and pressure conditions. The data included five natural gas mixtures, seven mixtures of methane with, ethane, propane, normal butane, carbon dioxide, nitrogen - hydrogen and normal decane,

Table 4.2.1 - Typical Program Output for Viscosity Prediction of a Pure Component.

Component
==========
n-Pentane

Viscosity Summary in cp

No	Press Bars	Temp K	Lee's[4] Method	JST[18] Model	TRAPP Progr[3]	PCS-1[2] Model	Exptl[5] Values
1	50.0	400.0	0.0000	0.0552	0.1015	0.1153	0.1010
2	60.0	400.0	0.0000	0.0560	0.1038	0.1181	0.1038
3	70.0	400.0	0.0000	0.0568	0.1060	0.1209	0.1061
4	80.0	400.0	0.0000	0.0576	0.1082	0.1236	0.1083
5	100.0	400.0	0.0000	0.0590	0.1123	0.1288	0.1124
6	110.0	400.0	0.0000	0.0597	0.1143	0.1313	0.1144
7	130.0	400.0	0.0000	0.0610	0.1182	0.1362	0.1184
8	150.0	400.0	0.0000	0.0623	0.1220	0.1409	0.1220
9	200.0	400.0	0.0000	0.0652	0.1310	0.1522	0.1310
10	300.0	400.0	0.0000	0.0703	0.1475	0.1733	0.1473
11	400.0	400.0	0.0000	0.0746	0.1627	0.1930	0.1639
12	500.0	400.0	0.0000	0.0785	0.1770	0.2116	0.1791
13	50.0	440.0	0.0000	0.0450	0.0729	0.0842	0.0715
14	60.0	440.0	0.0000	0.0462	0.0757	0.0875	0.0740
15	70.0	440.0	0.0000	0.0473	0.0783	0.0905	0.0767
16	80.0	440.0	0.0000	0.0483	0.0808	0.0933	0.0794
17	100.0	440.0	0.0000	0.0501	0.0853	0.0986	0.0838
18	110.0	440.0	0.0000	0.0509	0.0874	0.1011	0.0862
19	130.0	440.0	0.0000	0.0525	0.0914	0.1058	0.0904/
56	150.0	550.0	0.0423	0.0322	0.0501	0.0601	0.0487
57	200.0	550.0	0.0520	0.0368	0.0596	0.0704	0.0580
58	300.0	550.0	0.0680	0.0435	0.0739	0.0866	0.0730
59	400.0	550.0	0.0814	0.0485	0.0852	0.0999	0.0865
60	500.0	550.0	0.0931	0.0527	0.0951	0.1118	0.0990
61	50.0	600.0	0.0169	0.0158	0.0177	0.0176	0.0176
62	60.0	600.0	0.0182	0.0167	0.0190	0.0192	0.0197
63	70.0	600.0	0.0197	0.0177	0.0209	0.0215	0.0218
64	80.0	600.0	0.0214	0.0189	0.0230	0.0244	0.0240
65	100.0	600.0	0.0251	0.0215	0.0279	0.0315	0.0282
66	110.0	600.0	0.0271	0.0228	0.0304	0.0350	0.0301
67	130.0	600.0	0.0311	0.0254	0.0351	0.0411	0.0340
68	150.0	600.0	0.0349	0.0278	0.0394	0.0464	0.0378

cont'd...

Standard Deviation Summary in %

No	Press Bars	Temp K	Lee's Method	JST Model	TRAPP Progr	PCS Model
1	50.0	400.0	0.0000	45.3887	0.4862	14.1404
2	60.0	400.0	0.0000	46.0560	0.0115	13.8210
3	70.0	400.0	0.0000	46.4709	0.0826	13.9636
4	80.0	400.0	0.0000	46.8482	0.1171	14.1355
5	100.0	400.0	0.0000	47.4909	0.0597	14.5856
6	110.0	400.0	0.0000	47.8029	0.0498	14.7766
7	130.0	400.0	0.0000	48.4456	0.1306	15.0230
8	150.0	400.0	0.0000	48.9360	0.0107	15.5067
9	200.0	400.0	0.0000	50.2289	0.0248	16.2022
10	300.0	400.0	0.0000	52.3031	0.1208	17.6568
11	400.0	400.0	0.0000	54.4628	0.7162	17.7548
12	500.0	400.0	0.0000	56.1499	1.1479	18.1619
13	50.0	440.0	0.0000	37.0964	1.8909	17.7413
14	60.0	440.0	0.0000	37.5898	2.3272	18.1956
15	70.0	440.0	0.0000	38.3610	2.1152	17.9907
16	80.0	440.0	0.0000	39.1897	1.7128	17.5665
17	100.0	440.0	0.0000	40.2149	1.7466	17.7025
18	110.0	440.0	0.0000	40.9141	1.3564	17.3078
19	130.0	440.0	0.0000	41.9472	1.0554	17.0879/
56	150.0	550.0	13.1271	33.9643	2.8420	23.3521
57	200.0	550.0	10.4057	36.5077	2.7276	21.4581
58	300.0	550.0	6.9129	40.4432	1.2749	18.6269
59	400.0	550.0	5.9290	43.9317	1.4555	15.5417
60	500.0	550.0	5.9312	46.7591	3.9862	12.9484
61	50.0	600.0	3.7657	10.0869	0.3305	0.0960
62	60.0	600.0	7.6458	15.3922	3.5054	2.4286
63	70.0	600.0	9.7287	18.8438	4.3254	1.4892
64	80.0	600.0	10.9689	21.3596	4.1259	1.8600
65	100.0	600.0	10.8427	23.7388	1.0270	11.7864
66	110.0	600.0	9.9088	24.0888	1.0115	16.1861
67	130.0	600.0	8.6611	25.2294	3.2850	20.9576
68	150.0	600.0	7.7556	26.5525	4.1783	22.6882
Average Abs Dev %			10.4	39.7	1.8	17.9

Table 4.2.2 - Average Absolute Deviations in Pure Component Viscosity Predictions.

Fluid	N	J - S - T[17]	TRAPP[3]	PCS-1[2]
Methane (G)	97	1.86	1.68	1.98
Ethane (G)	88	4.29	2.99	2.51
Propane (G,L)	80	8.29	5.26	8.08
i - Butane (G,L)	59	10.49	8.93	11.56
n - Butane (G,L)	94	12.88	6.99	16.45
n - Pentane (G,L)	68	39.71	1.77	17.93
n - Hexane (L)	46	22.13	2.83	24.02
n - Heptane (L)	70	23.27	3.67	26.00
n - Octane (L)	48	17.17	5.67	33.61
n - Nonane (L)	94	13.38	2.62	36.11
n - Decane (L)	99	17.99	3.32	42.38
Nitrogen (G)	133	14.60	3.74	3.44
Carbon Dioxide (G)	65	5.46	9.51	10.33
OVERALL AADs (%)	1041	13.7	4.9	17.0

$$AAD\ (\%) = \sum_{ABS} \left(\frac{\eta_{pre} - \eta_{exp}}{\eta_{exp}} \right) * 100$$

η_{exp} - experimental viscosity

η_{pre} - predicted viscosity

N - number of data points

J-S-T : Jossi-Stiel-Thodos, residual viscosity correlation[17]
TRAPP : Transport properties prediction program of Ely and Hanley[3]
PCS -1 : Principle of corresponding states method (one reference component)[2]

Table 4.3.1 - Typical Program Output for Viscosity Prediction of Mixtures.

Number of Components - 4
Number of Pseudo Components - 0

Component	Vap. Compn.
Methane	$0.95600E^{+00}$
Ethane	$0.36000E^{-01}$
Propane	$0.50000E^{-02}$
Nitrogen	$0.30000E^{-02}$

Viscosity Summary in cp

No	Press Bars	Temp K	Lee's[4] Method	LBC[1] Model	TRAPP Progr[3]	PCS-1[2] Model	Exptl[7] Values
1	139.3	302.7	0.0148	0.0151	0.0162	0.0161	0.0161
2	277.0	302.7	0.0241	0.0261	0.0245	0.0244	0.0243
3	312.0	302.7	0.0263	0.0285	0.0265	0.0263	0.0261
4	346.3	302.7	0.0276	0.0298	0.0283	0.0281	0.0279
5	415.4	302.7	0.0309	0.0331	0.0316	0.0315	0.0312
6	484.1	302.7	0.0336	0.0358	0.0347	0.0345	0.0342
7	553.9	302.7	0.0356	0.0379	0.0375	0.0373	0.0370
8	583.6	302.7	0.0370	0.0393	0.0387	0.0384	0.0382
9	8.4	377.6	0.0138	0.0139	0.0138	0.0136	0.0136
10	35.8	377.6	0.0141	0.0142	0.0142	0.0141	0.0139
11	70.9	377.6	0.0148	0.0147	0.0149	0.0148	0.0146
12	104.5	377.6	0.0155	0.0154	0.0157	0.0156	0.0155
13	141.7	377.6	0.0163	0.0162	0.0167	0.0166	0.0166
14	208.6	377.6	0.0189	0.0190	0.0188	0.0188	0.0187
15	277.0	377.6	0.0214	0.0219	0.0212	0.0212	0.0211
16	381.1	377.6	0.0251	0.0260	0.0249	0.0248	0.0248
17	448.0	377.6	0.0275	0.0286	0.0272	0.0271	0.0273

cont'd...

Standard Deviation Summary in %

No	Press Bars	Temp K	Lee's Method	LBC Model	TRAPP Progr	PCS Model
1	139.3	302.7	7.4860	5.9364	0.9632	0.5276
2	277.0	302.7	0.8070	7.5306	1.0466	0.6439
3	312.0	302.7	0.7309	9.0495	1.4021	0.9884
4	346.3	302.7	1.0926	6.8554	1.2994	0.8687
5	415.4	302.7	1.1906	6.0425	1.2775	0.7920
6	484.1	302.7	1.9733	4.6629	1.2656	0.7157
7	553.9	302.7	3.8841	2.3436	1.3183	0.7036
8	583.6	302.7	3.2336	2.9239	1.1339	0.4940
9	8.4	377.6	1.0031	2.1570	1.3173	0.1664
10	35.8	377.6	1.4665	2.0766	2.1366	1.0340
11	70.9	377.6	0.9712	0.7499	1.7524	0.7918
12	104.5	377.6	0.4279	0.2514	1.3070	0.5227
13	141.7	377.6	1.8876	2.6018	0.2649	0.3196
14	208.6	377.6	0.8857	1.4597	0.4116	0.0644
15	277.0	377.6	1.4965	3.7692	0.4931	0.2023
16	381.1	377.6	1.1708	4.9226	0.4015	0.1243
17	448.0	377.6	0.5323	4.5455	0.5459	0.7838
Average Abs Dev %			1.8	4.0	1.1	0.6

Table 4.3.2 - Average Absolute Deviations in Mixture Viscosity Predictions.

Mixture	N	L - B - C[1]	TRAPP[3]	PCS-1[2]
Natural Gas 1[7]	17	3.99	1.08	0.57
Natural Gas 2[7]	15	7.54	3.44	3.29
Natural Gas 3[4]	19	1.61	0.98	0.65
Natural Gas 4[4]	23	3.05	2.22	2.28
Natural Gas 5[8]	94	6.16	4.24	4.06
C_1 - C_2 (G,L),[9]	41	2.80	0.73	2.34
C_1 - C_3 (G,L),[10]	154	10.62	2.69	4.41
C_1 - C_4 (G,L),[7]	16	8.67	3.79	4.29
C_1 - C_{10} (G,L),[7]	71	18.39	5.33	16.32
C_1 - N_2 (G,L),[11]	42	8.04	2.03	2.85
C_1 - CO_2 (G),[12]	102	3.59	3.10	8.18
C_2 - CO_2 (G,L),[13]	49	6.38	16.46	28.23
C_{10} - CO_2 (L),[14]	57	6.55	30.77	52.16
C_1 - N_2 - H_2 (G),[8]	50	8.74	3.39	4.41
CO_2 - n C_5 - n C_{10} - n C_{16} - n C_{30} (L),[15]	117	16.94	36.57	54.76
OVERALL AADs (%)	867	8.6	10.2	16.6

$$AAD\ (\%) = \sum_{ABS} \left(\frac{\eta_{pre} - \eta_{exp}}{\eta_{exp}} \right) * 100$$

η_{exp} - experimental viscosity

η_{pre} - predicted viscosity

N - number of data points

L-B-C : Lohrenz-Bray-Clark, residual viscosity correlation[1]
TRAPP : Transport properties prediction program of Ely and Hanley[3]
PCS -1 : Principle of corresponding states method (one reference component)[2]
[n] : References providing the source for the data

along with a synthetic mixture of carbon dioxide with n - pentane, n - decane, n - hexadecane and n - C_{30}. The viscosity predictions were performed in both gas and liquid phases. The sources of the experimental data have been referenced in Table (4.3.2), which shows the average absolute deviations (AADs). The typical program output for a mixture viscosity, showing predicted viscosity values and AADs is shown in Table (4.3.1), the table shows viscosity calculations for a natural gas mixture containing, 95.6 mole % methane, 3.6 mole % ethane, 0.5 mole % propane, and 0.3 mole % nitrogen. The AAD figures obtained for the mixtures studied are shown in Table (4.3.2).

From the study it was generally observed that the prediction of gas mixture viscosity was very accurate by almost all the three methods except for the Lohrenz - Bray - Clark[1] method for the Natural gas mixture 2 and Natural gas mixture 5. This might be attributed to the density of the gas mixture used, which in case of these two mixtures were predicted by the SRK EOS. Similarly the Lohrenz - Bray - Clark[1], method was found doing a uniformly better job for the entire data set except in cases which used predicted density data. Predictions of all the methods were found to be less accurate for liquid systems. The Lohrenz - Bray - Clark[1] method was however, found to be giving the minimum AADs for 867 data points which was 8.64 %.

The principle of corresponding states method[2] was again found to be unreliable for predicting viscosities of mixtures containing higher molecular weight fractions (as observed in cases of pure components). Due to the high critical temperatures of high molecular weight fractions, the temperature at which the reference component (methane) density is to be determined, gets significantly reduced, very often below the freezing point of methane. Because of this very low temperature the 33 - parameter EOS[6] fails to predict the density of methane accurately. This eventually affects the viscosity prediction and thus results in gross errors. The extended principle of corresponding states (TRAPP)[3] was however found to be most inaccurate for mixtures containing high concentration of carbon dioxide.

The AADs calculated for the system where measured density data was available, showed for 452 data points that the Lohrenz - Bray - Clark's method[1] gave the lowest AAD of 10.47 %

compared to 16.55 % in case of the extended principle of corresponding states method[3] and 27.17 % in case of the original principle of corresponding states method[2]. However, when the AADs were calculated for the systems where the reference component (methane) temperature remained above its freezing point showed for 471 data points that the principle of corresponding states method[2] gave an AAD of 4.4 % and the extended principle of corresponding states method[3] 2.82 %, whereas for the Lohrenz - Bray - Clark's[1] method the AAD figure was 6.80 %. Hence, it can be concluded that, if the density data available is reliable, the Lohrenz - Bray - Clark's method[1] should be used for viscosity predictions. In case of the lighter hydrocarbon mixtures the principle of corresponding states method[2], or the extended principle of corresponding states method[3], is recommendable in the absence of measured density data.

A comparative study recently carried out for evaluating the viscosity correlations by Ali[16] draws conclusions similar to those presented in this work. Table 7 of Reference[16] confirms that when accurate and reliable density data is available the residual viscosity method[1,17] proves to be a useful tool for estimation of viscosity. However it is interesting to note that the principle of corresponding states method[2] is also confirmed as a suitable model for estimation of viscosities. It has the advantage of eliminating the need for density and is found to combine the accuracy of extended principle of corresponding states method[3] and the simplicity of the residual viscosity method[1,17].

4.4 : TUNING OF VISCOSITY CORRELATIONS

A brief study on tuning of the viscosity correlations was also carried out to complete the comparative study on viscosity prediction methods. Each correlation was tuned (by altering an uncertain parameter) so as it could reproduce the viscosity of the desired fluid at its bubble point pressure. The various correlations were compared.

The methods studied were, the residual viscosity correlation of Lohrenz-Bray-Clark[1], the principle of corresponding states method[2] (one reference component) and the principle of

corresponding states method with two reference components[18]. A total of 106 viscosity measurements were considered for seven fluid samples; four North Sea oils[19] and three Malaysian crude oils[20].

All the methods were applied to the viscosity data to initially carry out the raw predictions. Oil densities calculated from the Alani-Kennedy[23] method were used in the Lohrenz-Bray-Clark correlation (L-B-C). The critical properties of the plus fractions were estimated from the Twu correlation[21]. Composition of the oil samples below the bubble point were estimated using the in-house Vapour Liquid Equilibrium (VLE) model[22]. The plots of untuned viscosity predictions and the experimental viscosity vs. pressure for all the samples are shown in Figures (4.4.1a to 4.4.7a). These plots (all labelled by 'a') clearly indicate inconsistent predictions for all the methods, none of the method is performing a particularly good job for all the data. The L-B-C method results in large overpredictions for all the samples. These correlations were later tuned at the bubble point viscosity of all the oil samples. The L-B-C correlation was tuned by changing the critical volume of the plus fraction whereas the other two principle of corresponding states methods (PCS 1 and PCS 2) were tuned by changing the critical temperature of the plus fractions. Figures (4.4.1b to 4.4.7b) show the plots of tuned viscosity predictions and experimental viscosities vs. pressure for all the samples. The L-B-C correlation was rather easily tuned to the bubble point viscosity due to the fact that it is highly sensitive to the reduced density, or critical volume, being a major parameter correlated to the fluid viscosity. All these plots indicate that for a majority of cases the L-B-C correlation and the one reference principle of corresponding states method perform well especially below the bubble point pressure, consistently responding to the major changes in the oil composition due to reduction in pressure.

The average absolute deviation (AAD) for the 106 data points are shown in Table (4.4.1). The AAD for the two reference principle of corresponding states method (PCS 2) is lowest among the group for untuned calculations whereas the L-B-C method has the lowest AAD among the group for tuned calculations. This study however confirms the usefulness of the L-B-C method as a reliable tool for viscosity estimations and also shows that it can be fairly easily tuned to the experimental data.

Table 4.4.1 - Average Absolute Deviations of Predicted Viscosities of Real Fluids.

Total No of Data Points = 106

Type of Fluids :

Four North Sea Oil Samples

Three Malaysian Oil Samples

UNTUNED	TUNED
L-B-C = 194 %	L-B-C = 7 %
PCS1 = 34 %	PCS1 = 8 %
PCS2 = 22 %	PCS2 = 13 %

L-B-C :

Lohrenz-Bray-Clark Residual Viscosity Correlation[1]

PCS1 :

Principle of Corresponding States Correlation with one Reference Component[2]

PCS2 :

Principle of Corresponding States Correlation with two Reference Components[18]

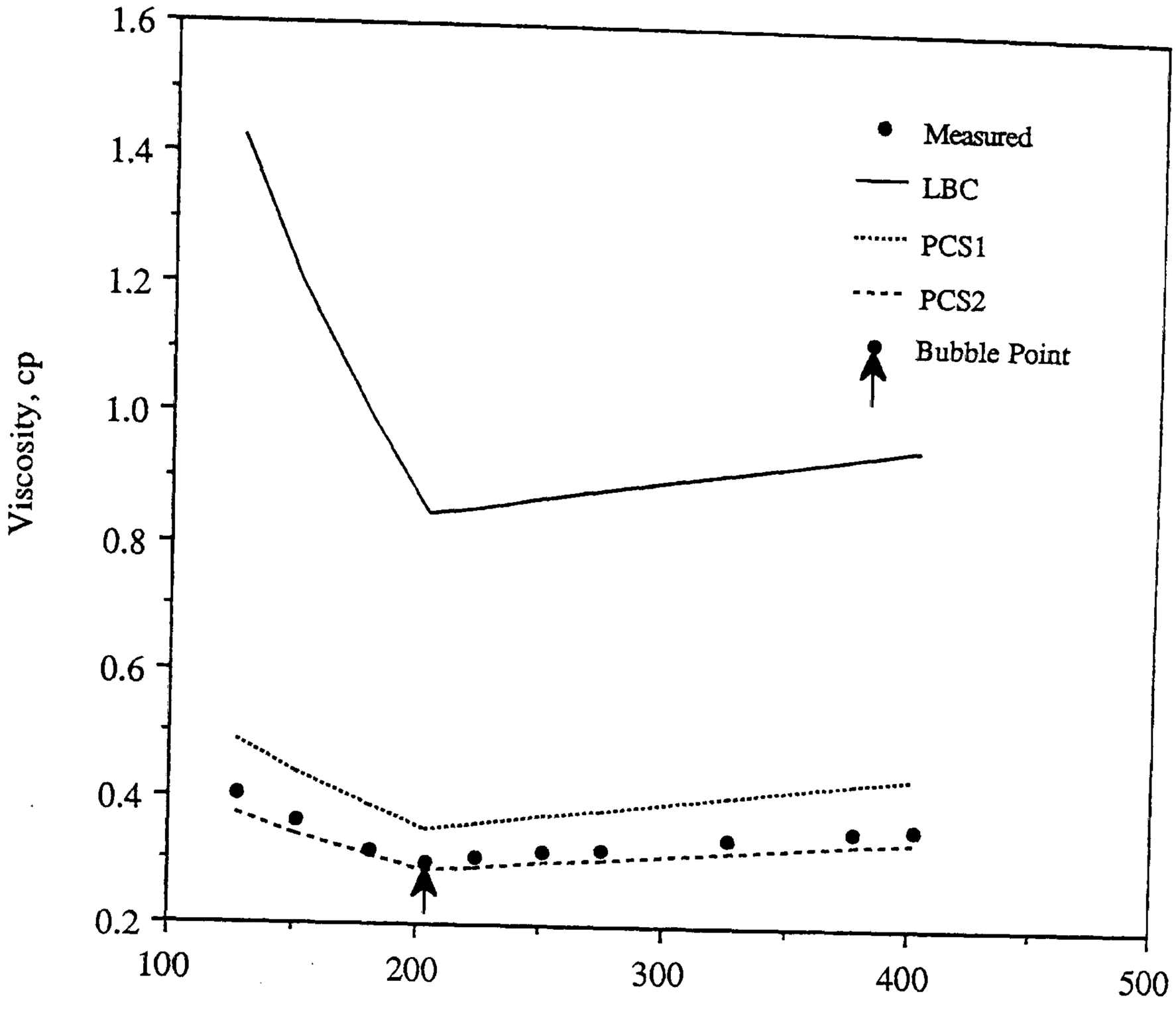

Figure 4.4.1a - Viscosity of North Sea Oil 1 at 97.8 deg C.

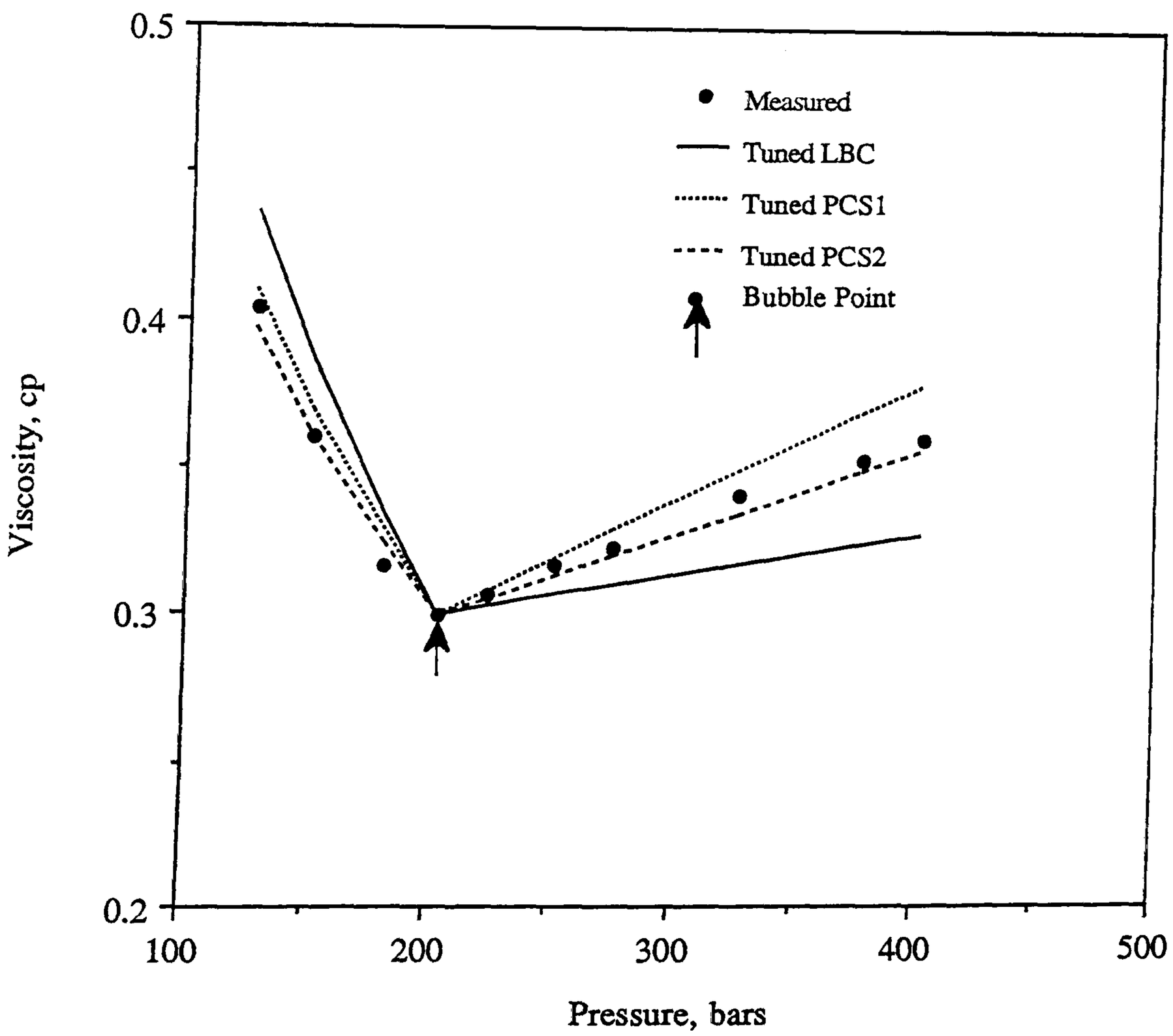

Figure 4.4.1b - Viscosity of North Sea Oil 1 at 97.8 deg C All Methods Individually Tuned at Bubble Point.

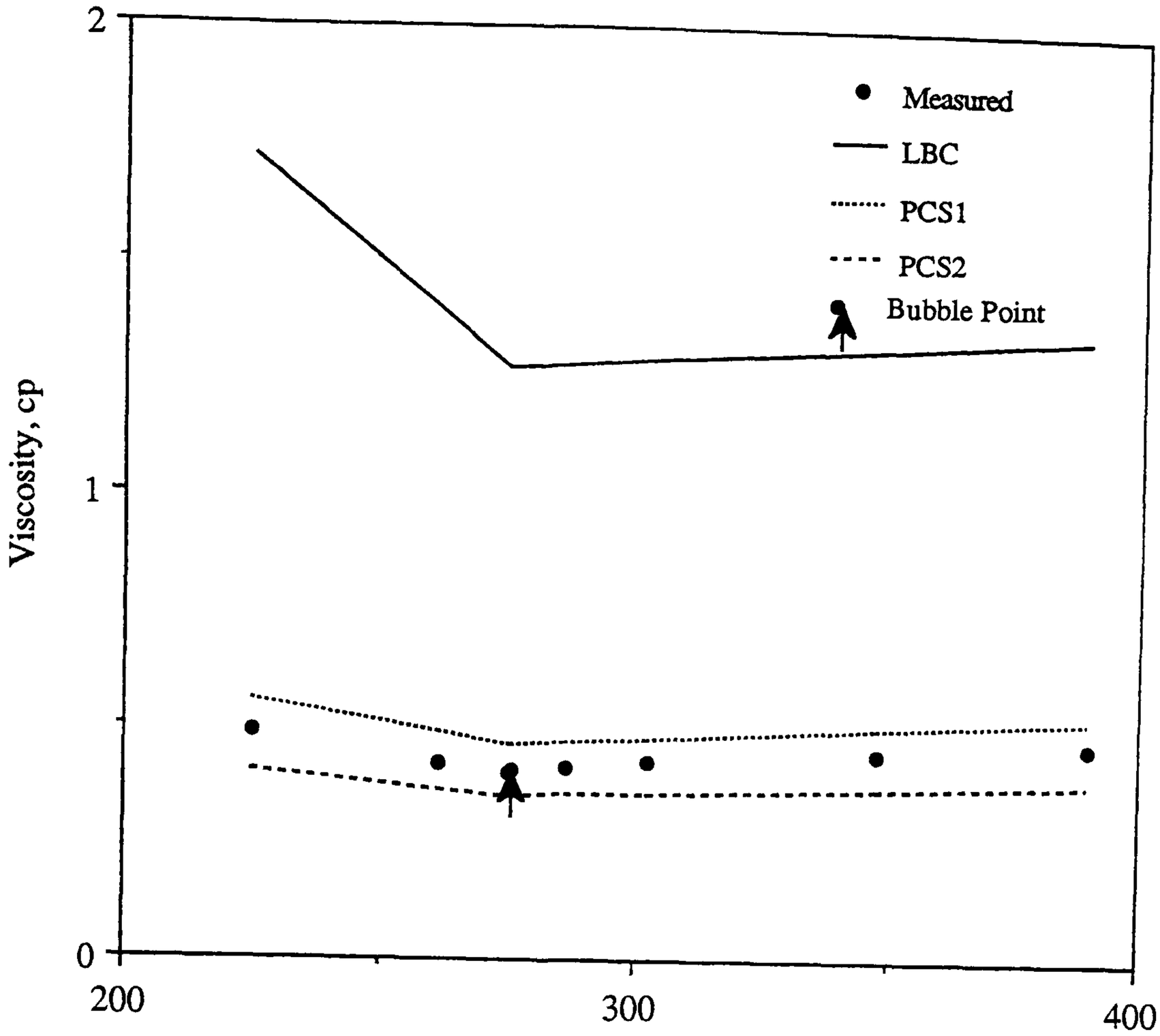

Figure 4.4.2a - Viscosity of North Sea Oil 2 at 93.3 deg C.

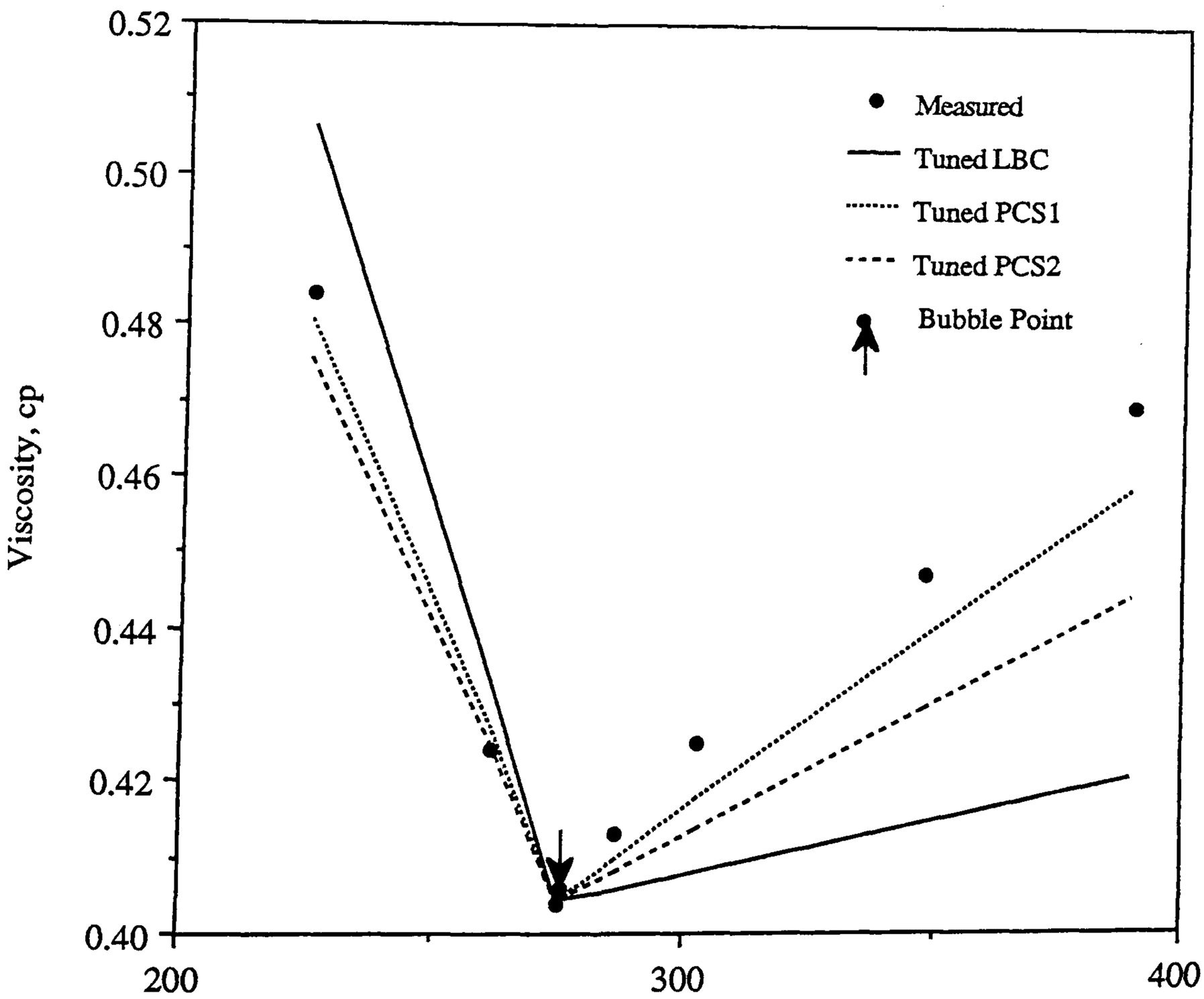

Figure 4.4.2b - Viscosity of North Sea Oil 2 at 93.3 deg C All Methods Individually Tuned at Bubble Point.

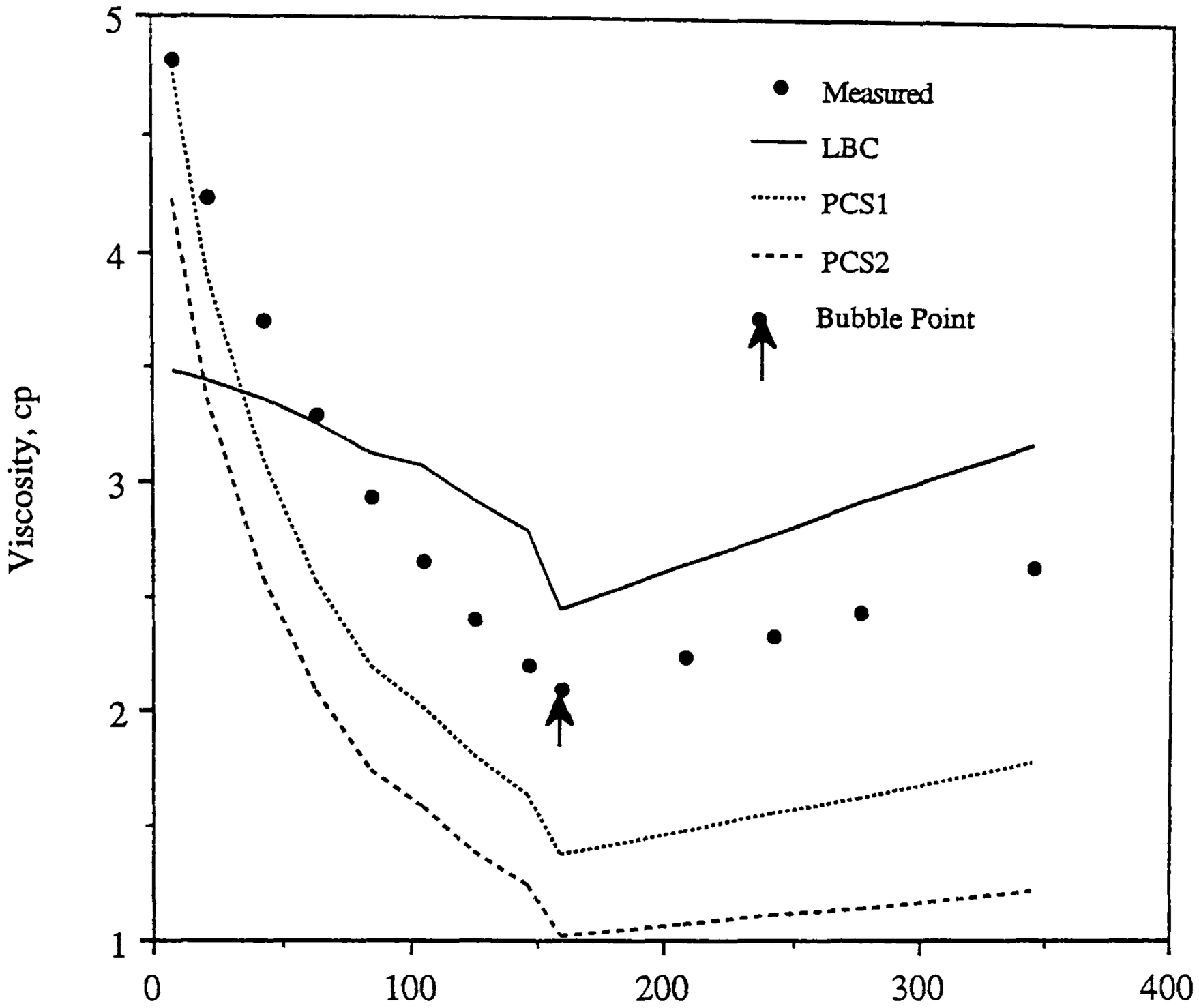

Figure 4.4.3a - Viscosity of North Sea Oil 3 at 71.1 deg C.

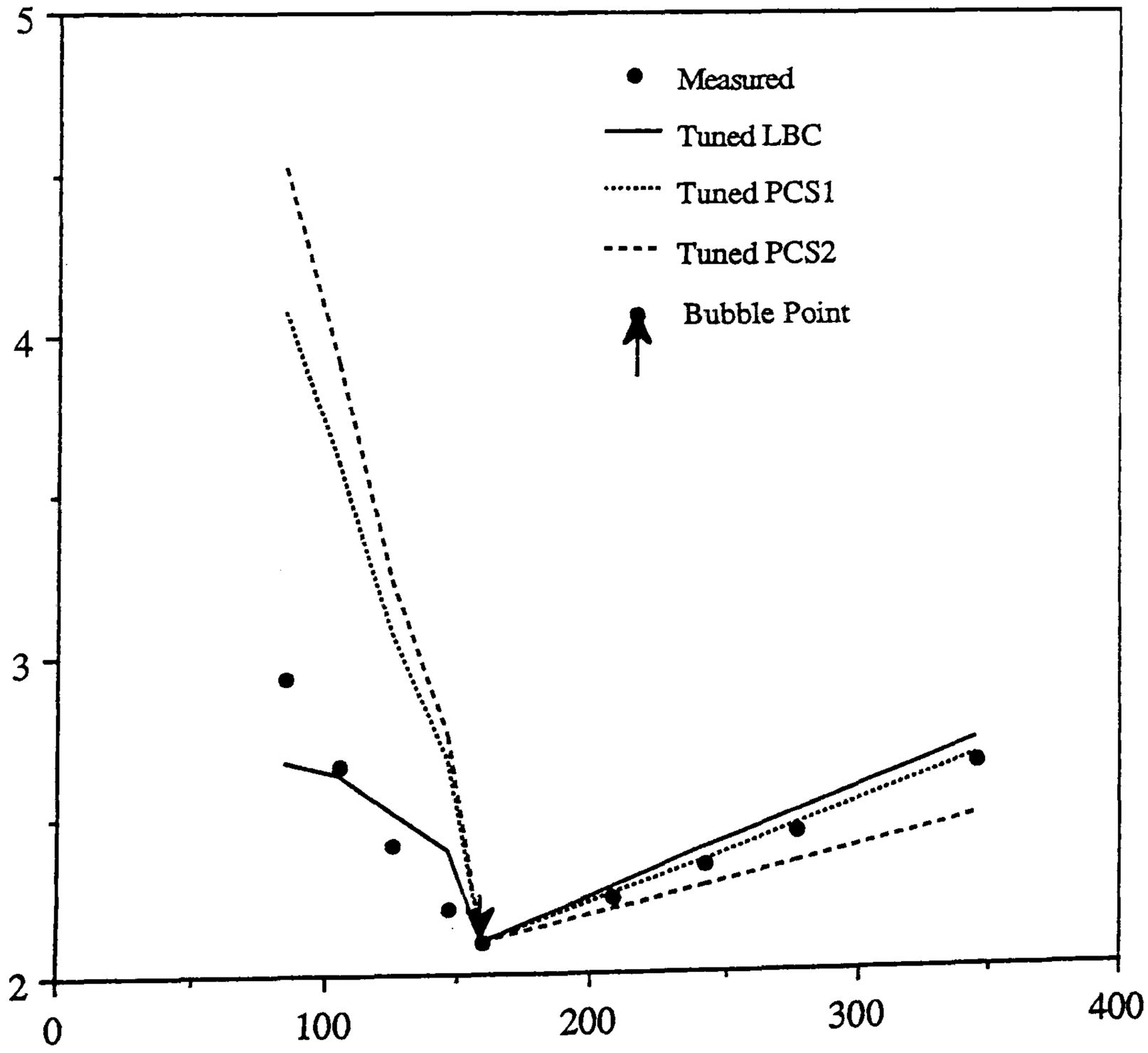

Figure 4.4.3b - Viscosity of North Sea Oil 3 at 71.1 deg C All Methods Individually Tuned at Bubble Point.

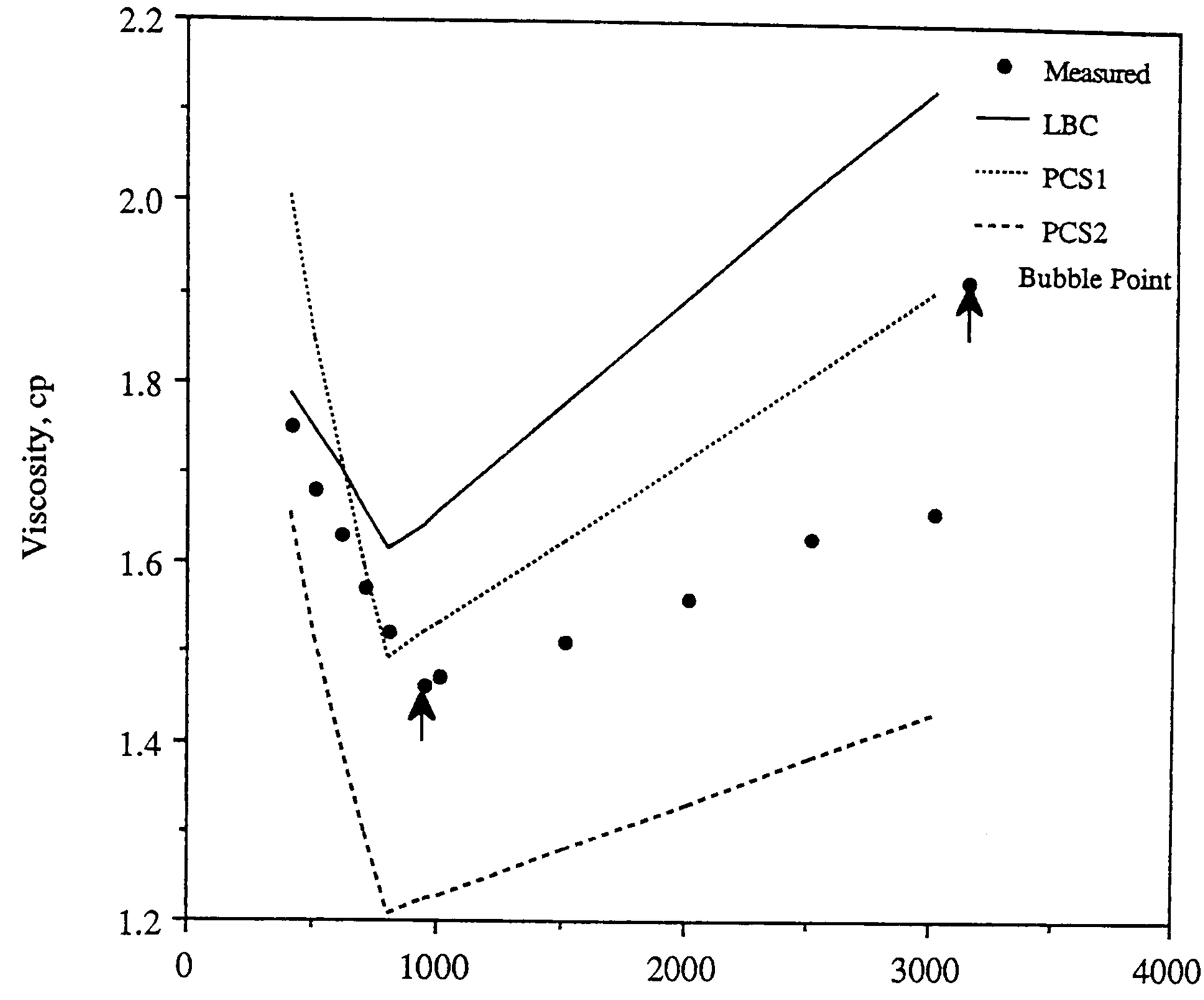

Figure 4.4.4a - Viscosity of Malaysian Oil Mixture 4 at 125 deg F.

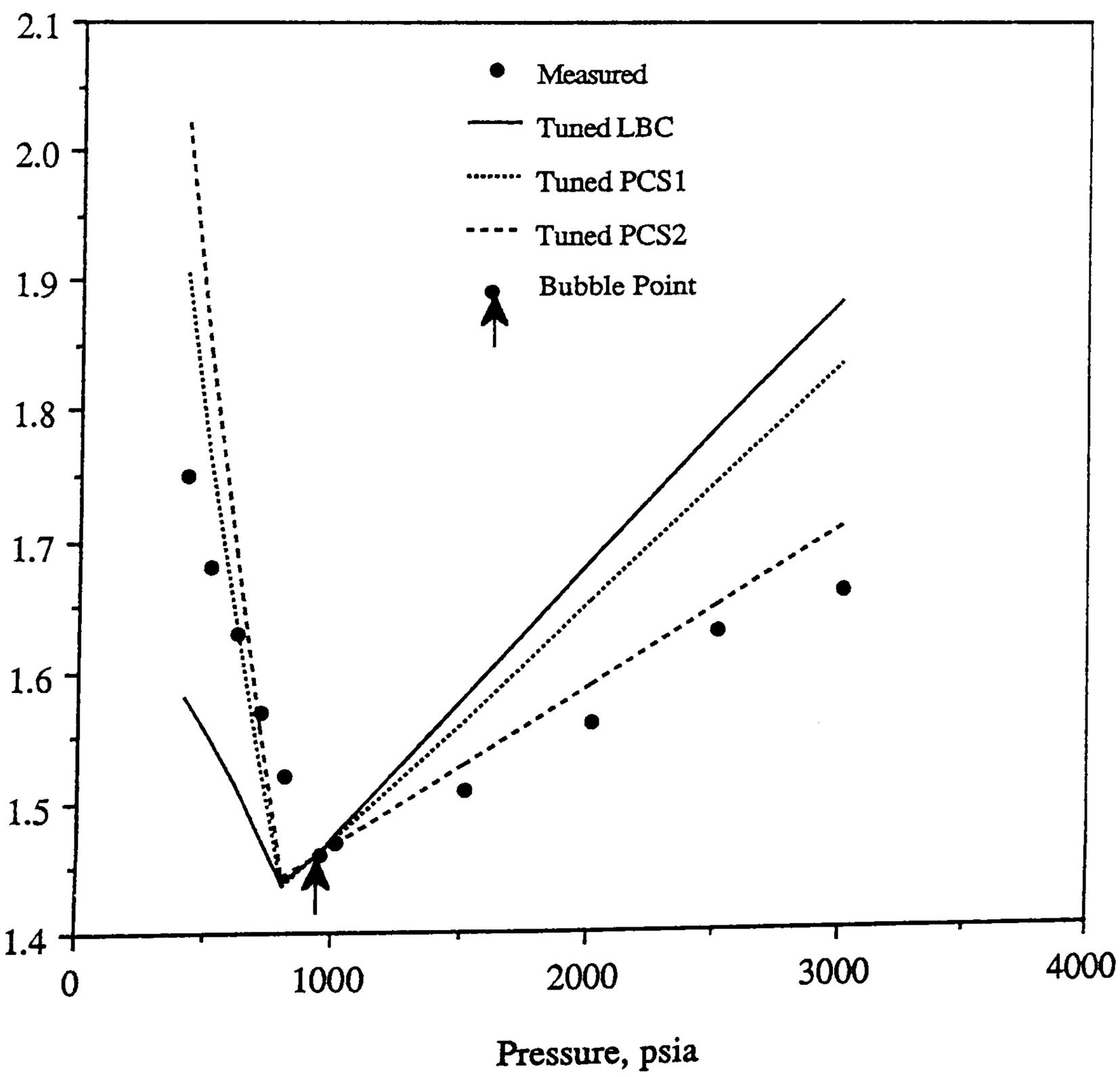

Figure 4.4.4b - Viscosity of Malaysian Oil 4 at 125 deg F All Methods Individually Tuned at Bubble Point.

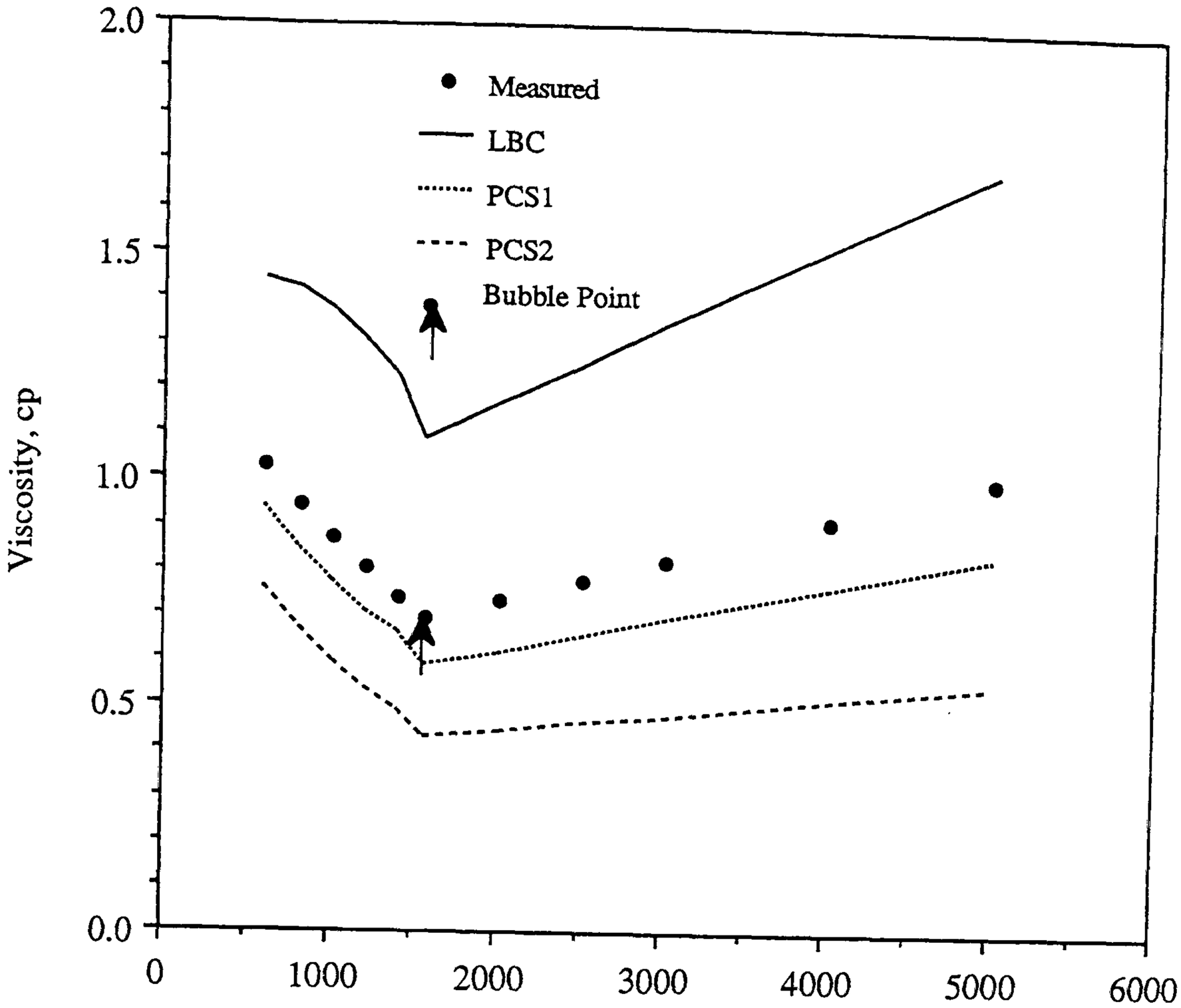

Figure 4.4.5a - Viscosity of Malaysian Oil 5 at 196 deg F.

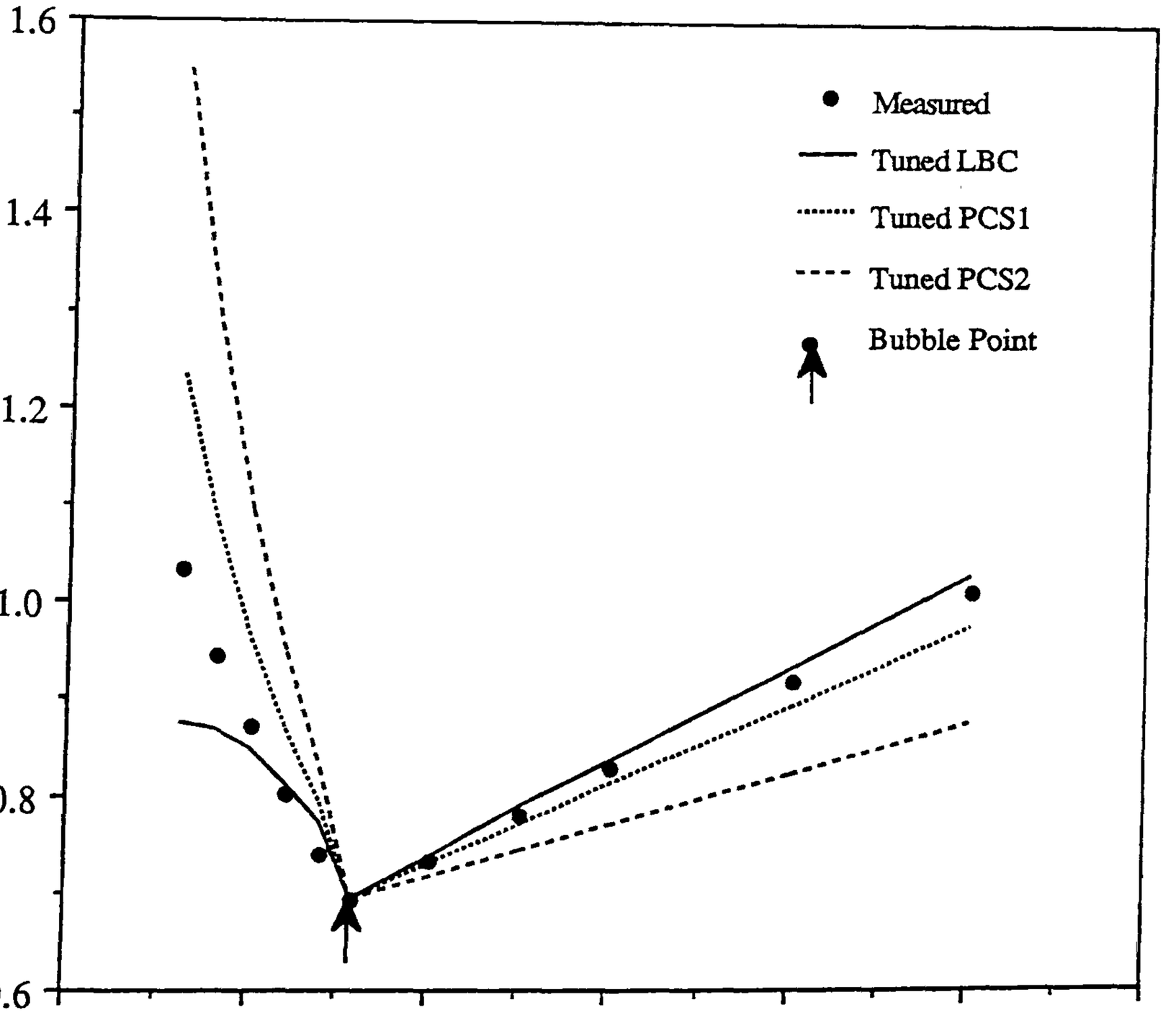

Figure 4.4.5b - Viscosity of Malaysian Oil 5 at 196 deg F All Methods Individually Tuned at Bubble Point.

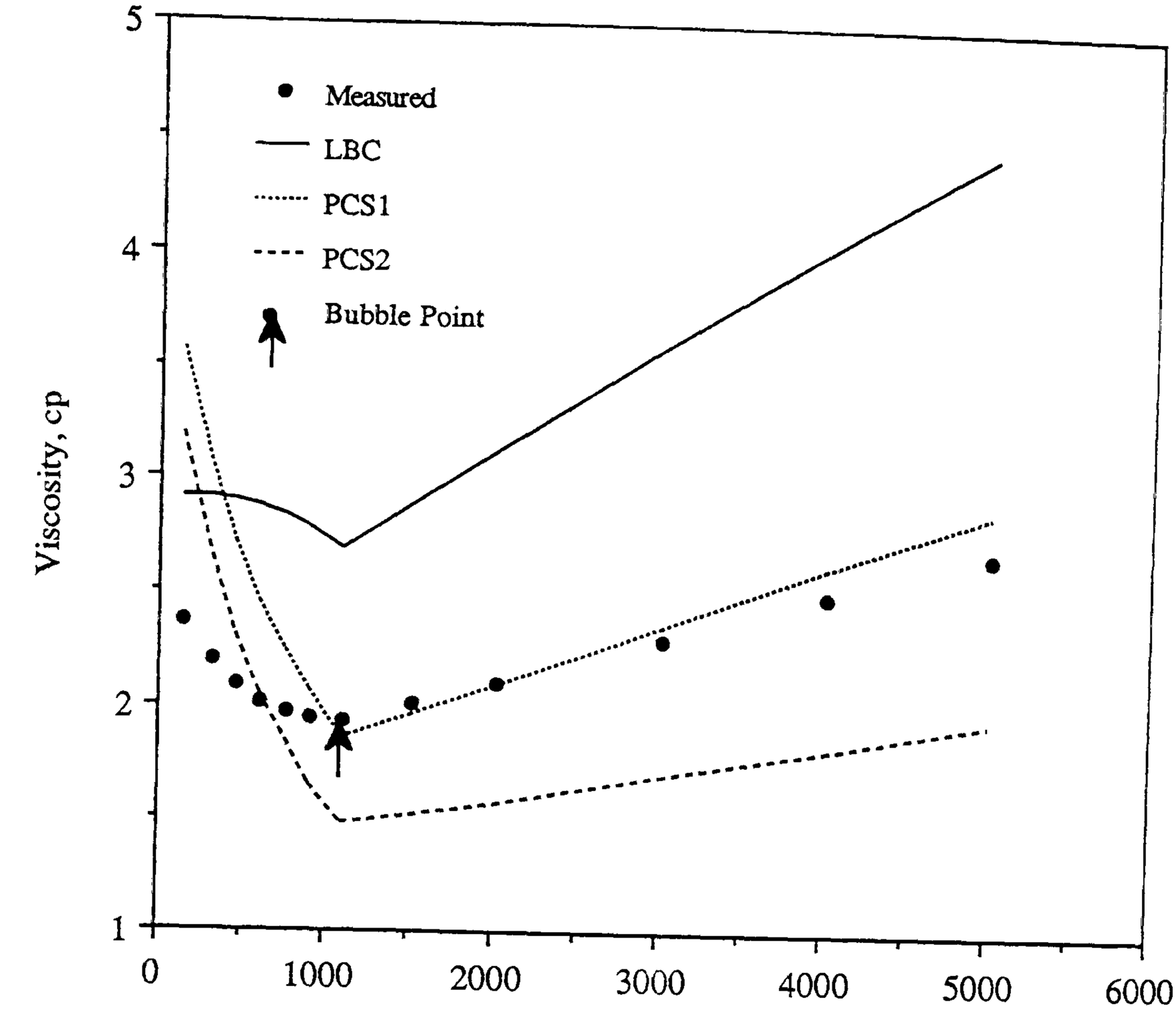

Figure 4.4.6a - Viscosity of Malaysian Oil 6 at 187 deg F.

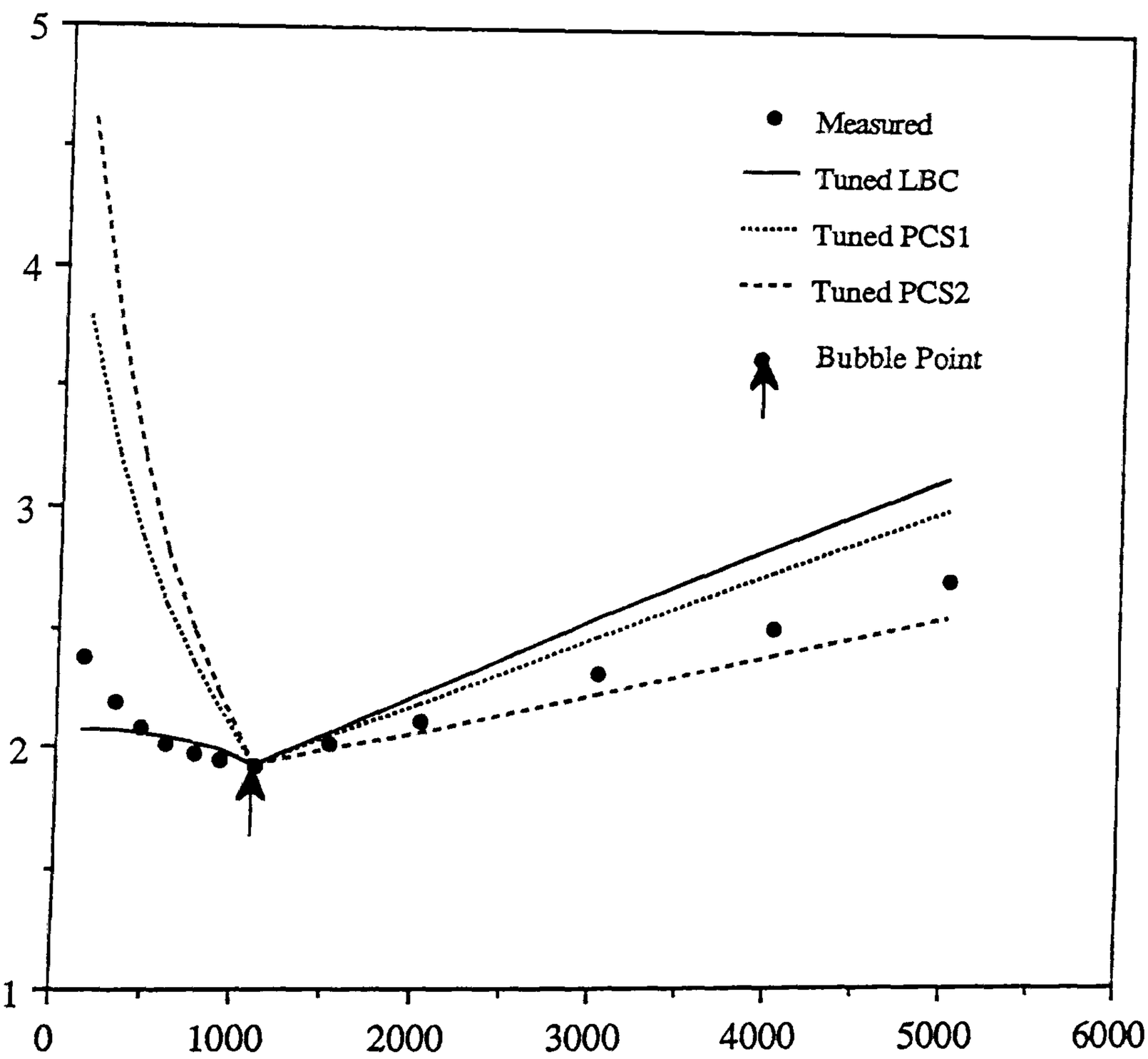

Figure 4.4.6b - Viscosity of Malaysian Oil 6 at 187 deg F All Methods Individually Tuned at Bubble Point.

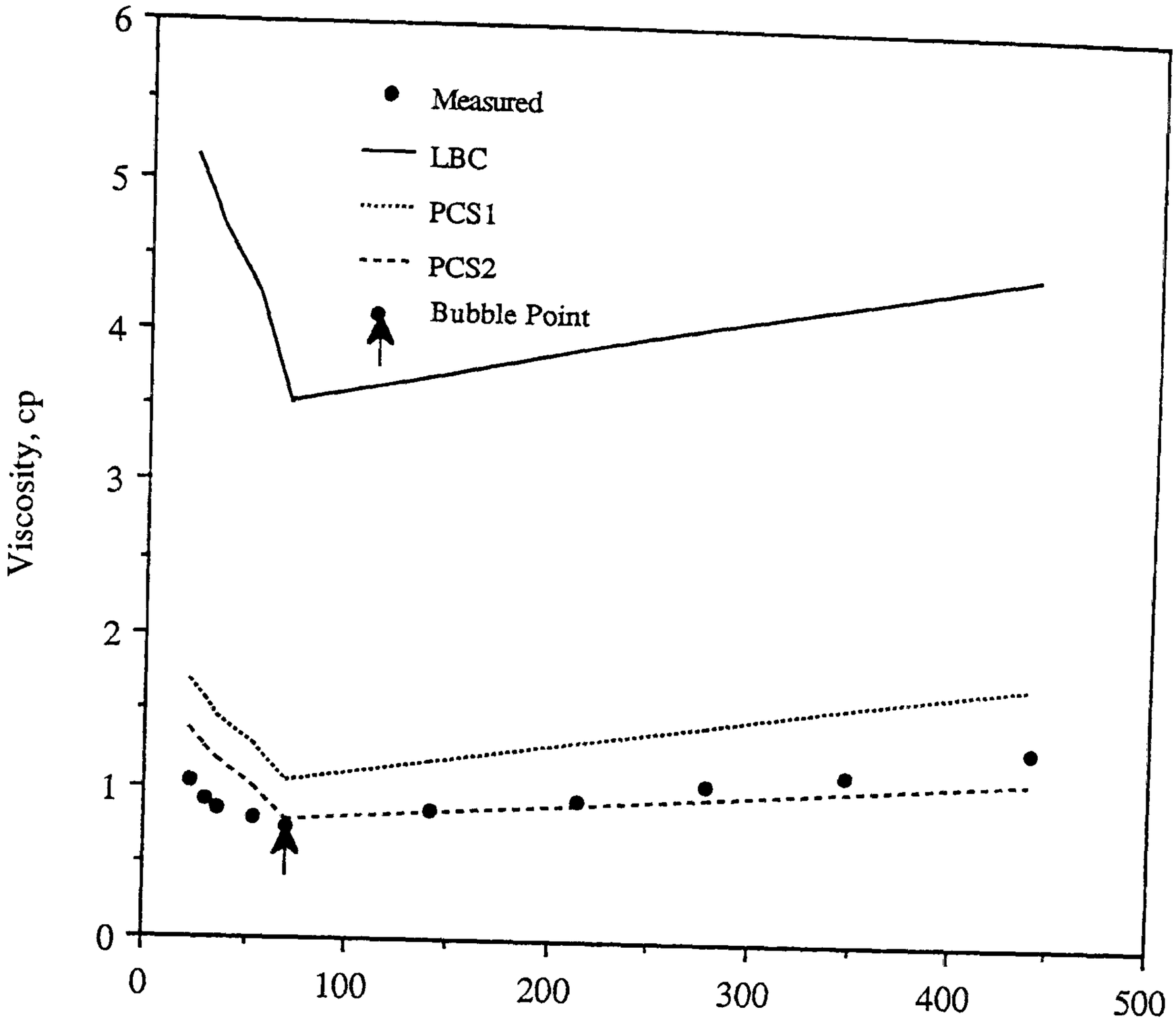

Figure 4.4.7a : Viscosity of North Sea Oil 7 at 353.2 K

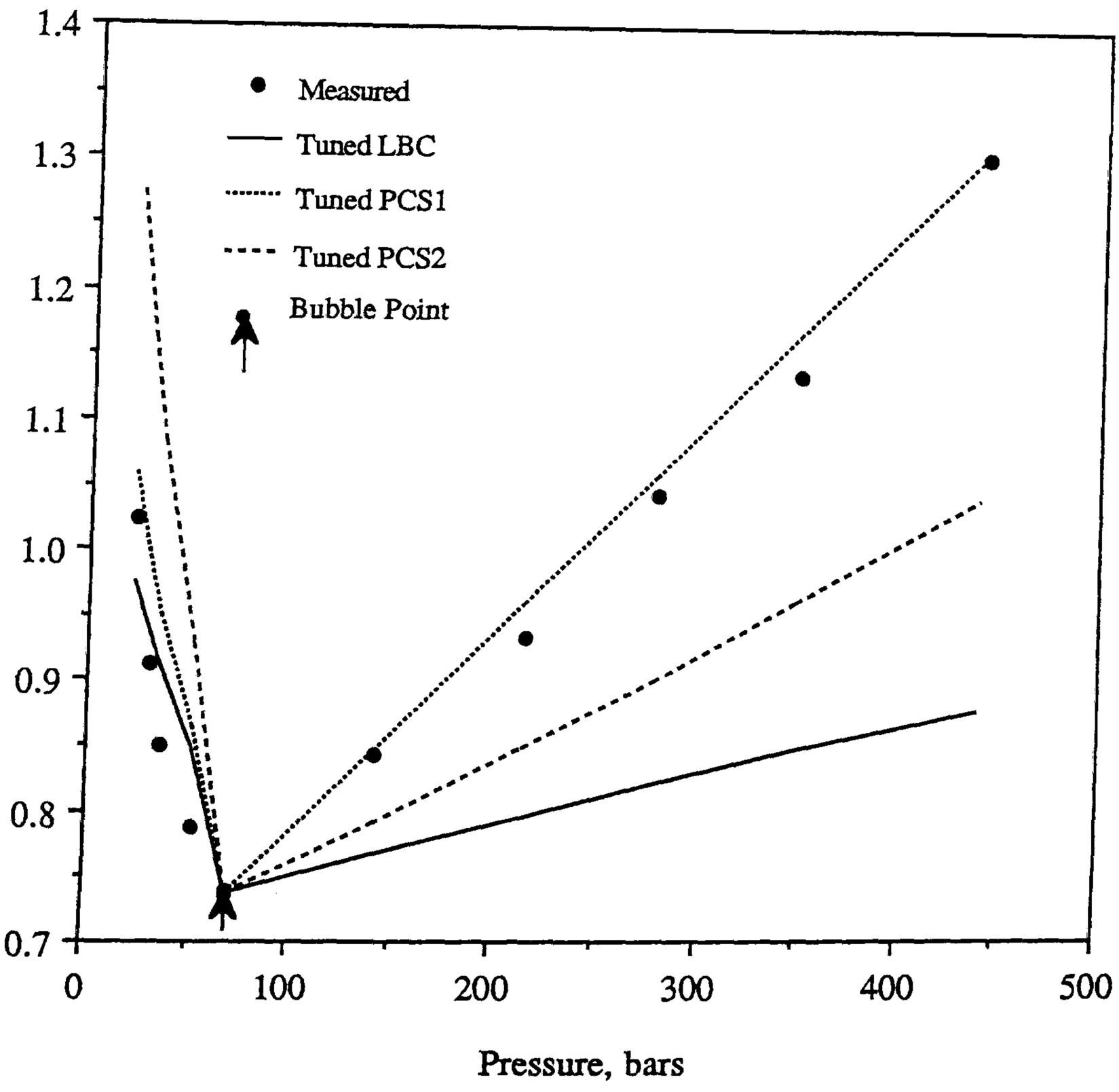

Figure 4.4.7b - Viscosity of North Sea Fluid 7 at 353.2 K All Methods Individually Tuned at Bubble Point.

References

1) Lohrenz, J., Bray, B.G. and Clark, C.R.: "Calculating Viscosities of Reservoir Fluids from their Compositions", *Journal of Petroleum Technology*, pp. 1171-1176, (Oct., 1964).

2) Pedersen, K.S. and Fredenslund, Aa.: "An Improved Corresponding States Model for Prediction of Oil and Gas Viscosities and Thermal Conductivities", *Chemical Engineering Science*, Vol. 42, pp. 182-186, (1987).

3) Ely, J.F. and Hanley, H.J.M: "Prediction of the Viscosity and Thermal Conductivity in Hydrocarbon Mixtures - Computer Program TRAPP", Proceedings of the Sixtieth Annual Convention of Gas Processors Association", pp. 20-29, (Mar., 1981).

4) Lee, A.L., Gonzalez, M.H. and Eakin, B.E.: "The Viscosity of Natural Gases", *Journal of Petroleum Technology*, pp. 997-1000, (Aug., 1966).

5) Stephan, K. and Lucas, K.: "Viscosity of Dense Fluids", Plenum Press, New York, (1979).

6) McCarty, R.D.: "A Modified Benedict - Webb - Rubin Equation of State for Methane using Recent Experimental Data", *Cryogenics*, (May, 1974).

7) Lee, A.L: "Viscosity of Light Hydrocarbons", Monograph on API Research Project 65, New York, (1965).

8) Lawal, A.S.L: "Improved Fluid Property Predictions for Reservoir Compositional Simulation", PhD Dissertation, The University of Texas at Austin, (1985).

9) Diller, D.E.: "Measurements of the Viscosity of Compressed Gaseous and Liquid Methane + Ethane Mixtures", *J. of Chem & Eng. Data*, Vol. 29, pp. 215-221, (1984).

10) Giddings, J.G., Kao, J.T.F. and Kobayashi, R.: "Development of a High Pressure Capillary - Tube Viscometer and its Application to Methane,

Propane, and their Mixtures in the Gaseous and Liquid Regions", *The Journal of Chemical Physics*, Vol. 45, No. 2, (Jul., 1966).

11) Diller, D.E.: "Measurements of the Viscosity of Compressed Gaseous and Liquid Nitrogen + Methane Mixtures", *International J. Thermophysics*, Vol. 3, No. 3, (1982).

12) Dewitt, K.J. and Thodos, G.: "Viscosities of Binary Mixtures in the Dense Gaseous State: the Methane and Carbon Dioxide System", In: SPE Reprint Ser. 13, Vol. 1, pp. 236-241, (1977).

13) Diller, D.E., Pollen, L.J.V. and Santos, F.V.D: "Measurements of the Viscosities of Compressed Fluid and Liquid Carbon Dioxide + Ethane Mixtures", *J. of Chem & Eng. Data*, Vol. 33, pp. 460-464, (1988).

14) Cullick, A.S. and Mathias, M.L.: "Densities and Viscosities of Carbon Dioxide and n - Decane from 310 to 403 K, and, 7 to 30 MPa", *J. of Chem & Eng. Data*, Vol. 29, pp. 393-396, (1984).

15) Kovarik, F.S. and Taylor, M.A.: "Viscosity Measurements of High - Pressure CO_2/Hydrocarbon Mixtures", AIChE, Annual General Meeting, New York, (1987).

16) Ali, J.K: "Evaluation of Correlations for Estimating the Viscosities of Hydrocarbon Fluids", *Journal of Petroleum Science and Engineering*, Vol. 5, pp. 351-369, (1991).

17) Jossi, J.A., Stiel, L.I. and Thodos, G.: "The Viscosity of Pure Substances in the Dense Gaseous and Liquid Phases", *AIChEJ*, Vol. 8, pp. 59 - 63, (1962).

18) Aasberg-Petersen, K., Knudsen, K. and Fredenslund, A.: "Prediction of Viscosities of Hydrocarbon Mixtures", *Fluid Phase Equilibria*, Vol. 70, pp. 293-308, (1991).

19) Pedersen, et. al : "Properties of Oils and Natural Gases", (Contrib. Petrol. Geol. & Eng., Vol. 5), Gulf Publishing Co., (1989).

20) Omar, M.I.: "Private Communication". (1991)

21) Twu, C.H: "An Internally Consistent Correlation for Predicting the Critical Properties and Molecular Weights of Petroleum and Coal-Tar Liquids", *Fluid Phase Equilibria*, Vol. 16, pp. 137-150, (1984).

22) Xu, D.: "FPE, Predictions of Fluid Phase Equilibria", Department of Petroleum Engineering, Heriot-Watt University, (1992).

23) Alani, G.H. and Kennedy, H.T.: "Volumes of Liquid Hydrocarbons at High Temperatures and Pressures", *Petroleum Transactions of AIME*, Vol. 219, pp. 288-292, (1960).

CHAPTER 5 : THE MODIFIED RESIDUAL VISCOSITY METHOD (THIS WORK)

5.1 : INTRODUCTION

This chapter presents a modification carried out to the residual viscosity correlation initially proposed by Jossi et. al.[1] for pure components and later extended by Lohrenz et. al.[2] to hydrocarbon mixtures. The residual viscosity approach utilises fluid density as a major parameter for predicting viscosity. Considering the fact that viscosity is a configurational property, the use of density to correlate seems to be logical. The residual viscosity method assumes that the change of viscosity from a condition dominated by the thermal energy (low pressure) to a condition dominated by the structure of molecules correlates with the density. This is a very severe assumption, but the fact that the method gives reliable results indicate that it is probably a valid assumption.

It has already been shown in the previous chapter, on comparative study of viscosity prediction methods, that the residual viscosity method proves to be a useful tool for reliable prediction of viscosity. This approach has been enjoying great acceptance and application in compositional reservoir simulators due to the fact that it is rather fast and more easily tuned to the experimental data (Section 4.4). Several authors have pointed out shortcomings associated with the residual method, such as strong dependence on the fluid density. Moreover, in this work another major drawback of this method has been indicated, which is its inability to accurately estimate the viscosity of fluids with reduced density higher than 2.5. In the next section a critical evaluation of the Jossi et.al. method and the Lohrenz et.al. method has been carried out which forms the basis of the proposed modifications.

5.2 : EVALUATION OF THE J-S-T[1] AND THE L-B-C[2] CORRELATIONS

In 1962 Jossi et.al.[1] proposed a correlation based on viscosity and PVT data on pure hydrocarbons up to n-pentane and some non-hydrocarbons. This method was later adopted

by Lohrenz-Bray-Clark[2] to develop their correlation for mixtures of hydrocarbon fluids. A large number of data on pure components and mixtures were employed to check the performance of these two correlations. Figure 5.2.1 shows the plot of percentage deviations of calculated viscosity for pure components vs. reduced density using the J-S-T correlation. This graph clearly shows that viscosities can be predicted with reasonable accuracy for reduced density up to about 2.5 and a general trend of large underpredictions (especially for heavier components) is evident for reduced density greater than 2.5. This also indicates that the method fails to recognise that the variation of residual viscosity with density is not uniform for all components. Jossi et.al. have assumed in their work that for reduced densities higher than 3.0 for components heavier than n-pentane the variation of residual viscosity with respect to reduced density would correspond to their constructed plot. The drawback of this assumption has been shown in the next section. A similar trend has been observed when the L-B-C method is applied to hydrocarbon mixtures, showing reasonably reliable predictions for reduced densities up to 2.5 and large underpredictions above 2.5. Figure 5.2.2 shows a plot of percentage deviations of calculated viscosity vs. reduced density for various binary mixtures.

However, it was also thought that these errors in predicted viscosity could be due to the use of simple molar mixing rules (especially for critical volume, since the method is highly sensitive to reduced density). Table 5.2.1 shows the results of viscosity prediction using two different types of mixing rules for critical volume namely; the simple molar mixing rule and the cubic mixing rule. However Table 5.2.1 proves the adequacy of the simple mixing rules for the purpose of viscosity calculations.

5.3 : DEVELOPMENT OF THE MODIFIED RESIDUAL VISCOSITY CORRELATION

The above evaluation of the J-S-T and the L-B-C correlation was conducive to propose a modification of the residual viscosity approach for the dense fluid phases. The modification has been carried out to the pure component correlation of J-S-T and subsequently applied to hydrocarbon mixtures.

Table 5.2.1 - Effect of Simple and Cubic Mixing Rules on Prediction of Viscosity Using the Lohrenz-Bray-Clark (L-B-C)[2] Correlation.

No	Mixture	Temp Kelvin	V_{cm}[simple] cc/gmmole	V_{cm}[cubic] cc/gmmole	Predicted [simple]	Predicted [cubic]	Exptl cp
1	.243C1+.757CO2	373	95.19	95.18	0.0462	0.0462	0.0445
2	.464C1+.536CO2	323	96.36	96.35	0.0230	0.0230	0.0227
3	.755C1+.245CO2	472	97.90	97.89	0.0379	0.0379	0.0367
4	.221C1+.779C3	311	180.09	177.98	0.0603	0.0586	0.0655
5	.388C1+.612C3	344	162.75	159.83	0.0234	0.0230	0.0241
6	.614C1+.386C3	411	139.28	136.37	0.0461	0.0446	0.0470
7	.455C1+.545C4	353	184.16	178.18	0.0412	0.0393	0.0457
8	.362C1+.638C4	353	198.58	193.01	0.0497	0.0473	0.0571
9	.146C1+.854C4	353	232.30	229.30	0.0696	0.0672	0.0846
10	.850C10+.150CO2	403	526.63	507.70	0.2460	0.1952	0.2695
11	.699C10+.301CO2	374	449.76	418.52	0.4074	0.2435	0.3905
12	.495C10+.505CO2	343	345.90	308.79	0.2793	0.1529	0.2893
13	.3C1+.7C10	411	451.86	421.81	0.1983	0.1355	0.2387
14	.5C1+.5C10	378	351.10	315.33	0.2221	0.1229	0.2743
15	.7C1+.3C10	344	250.34	220.30	0.1673	0.0927	0.2275
16	.094C6+.906C7	293	426.17	426.03	0.4188	0.4176	0.4007
17	.498C6+.502C7	293	401.11	400.70	0.3690	0.3659	0.3592
18	.906C6+.094C7	293	375.80	375.66	0.3207	0.3197	0.3193
19	.1C7+.9C10	293	585.85	584.99	0.6517	0.6420	0.8532
20	.5C7+.5C10	293	517.36	514.99	0.5650	0.5402	0.6332
21	.893C7+.107C10	293	450.25	449.34	0.4614	0.4529	0.4534
22	.101C8+.899C14	293	795.76	793.09	0.8343	0.8039	2.0497
23	.505C8+.495C14	293	659.24	651.91	0.7541	0.6705	1.2165
24	.903C8+.097C14	293	524.65	522.09	0.5922	0.5642	0.6482
25	.103C14+.897C16	293	937.60	937.35	1.0221	1.0189	3.3100
26	.496C14+.504C16	293	890.50	889.82	0.9410	0.9328	2.8361
27	.903C14+.097C16	293	841.60	841.36	0.8571	0.8544	2.4022

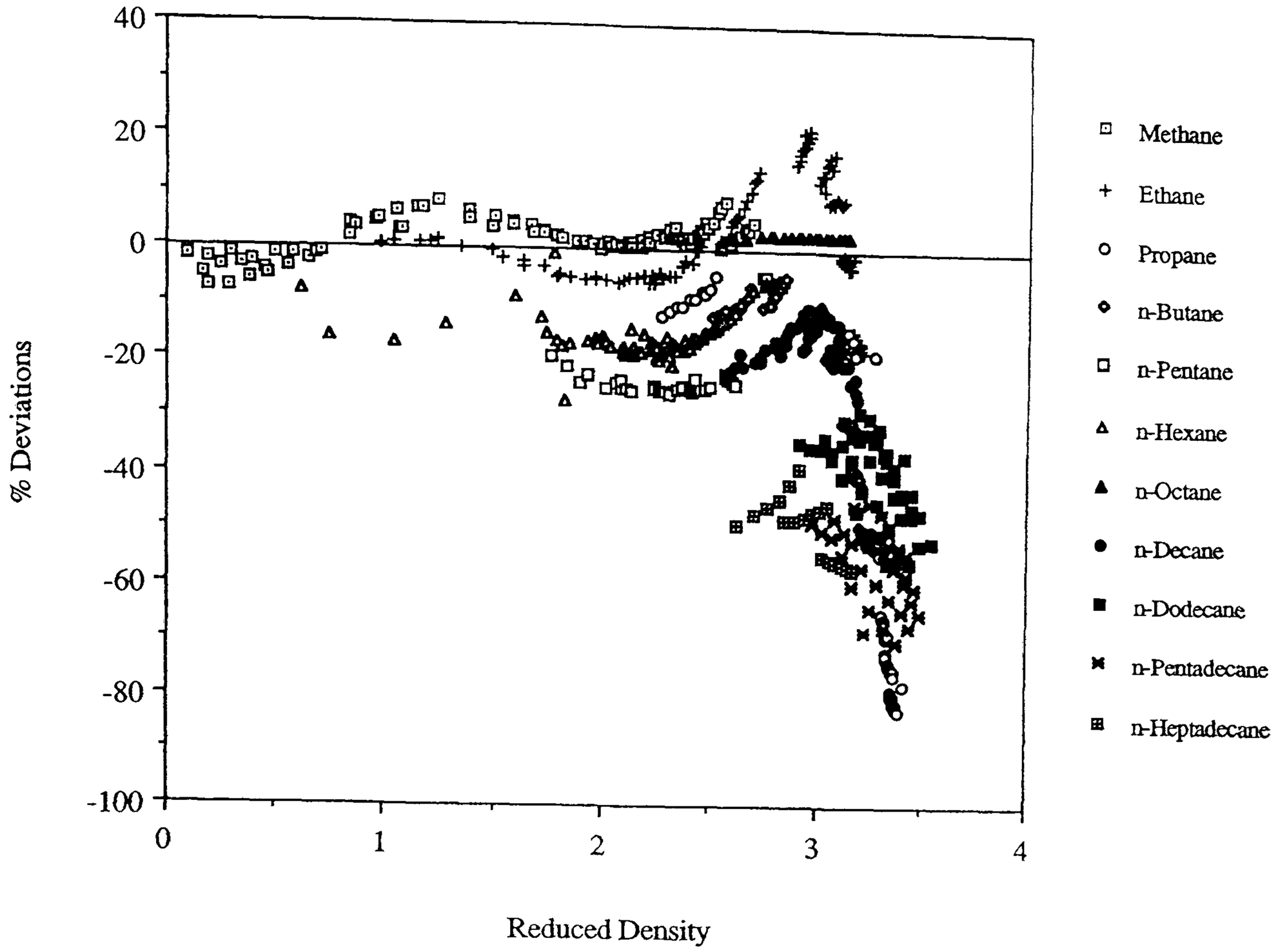

Figure 5.2.1 - Deviations of Calculated Viscosity from Experimental Value for the J-S-T Method for the Pure Components Investigated.

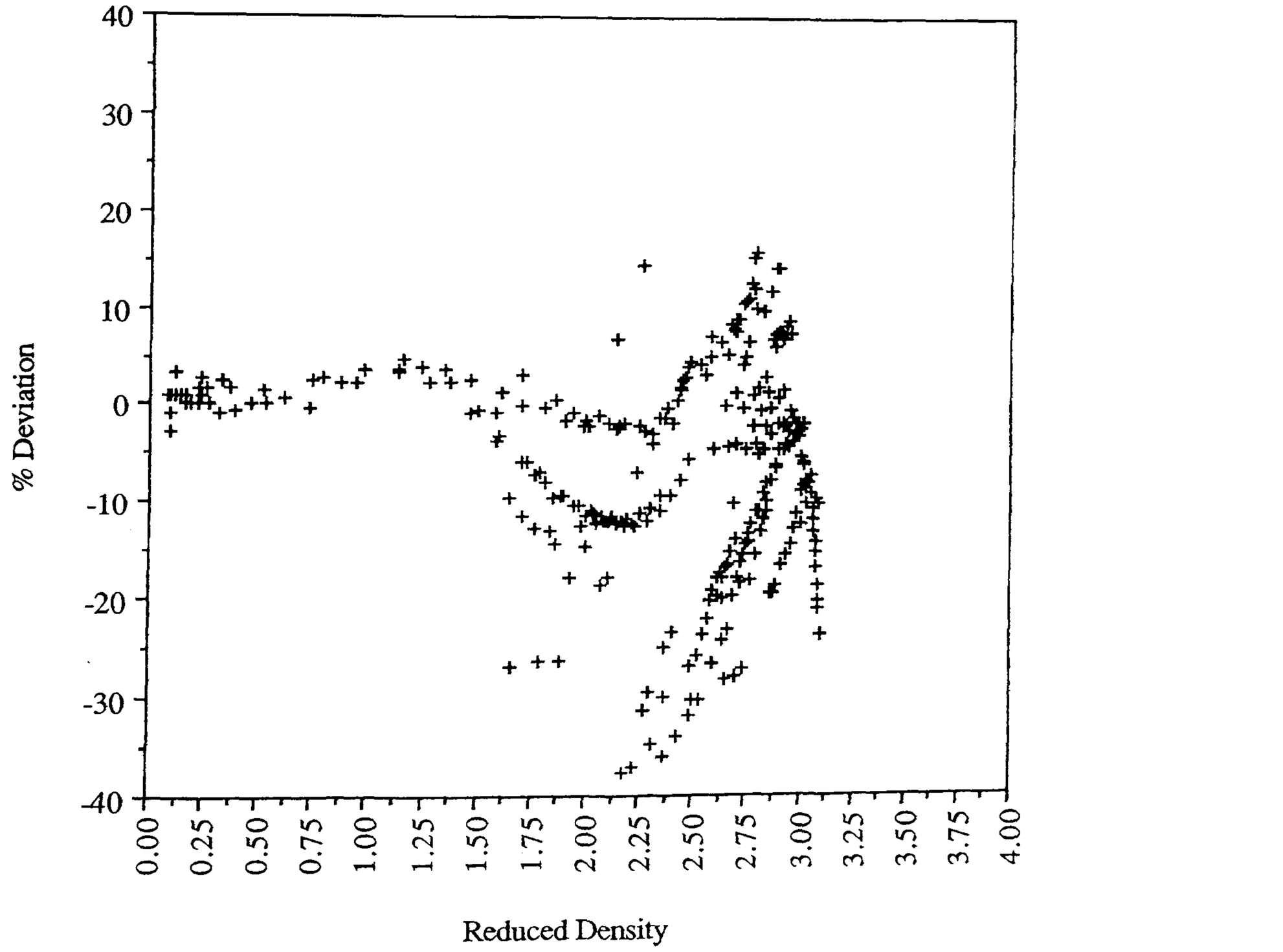

Figure 5.2.2 - Deviations of Calculated Viscosity from Experimental Value for the L-B-C Correlation for Binary Mixtures.

A large number of data on viscosity[3,4,5] and PVT[3,4,6] in dense fluid phase conditions for heavy n-alkanes was amassed for this purpose. All the data was quality checked before using them for modelling purposes. Figure 5.3.1 shows the plot of residual viscosity (RV), $(\eta-\eta^*)\lambda$ against reduced density for various compounds[3,4,5]. Where, η is the fluid viscosity, η^* is the low pressure gas phase viscosity and λ is the inverse of critical viscosity or viscosity reducing parameter defined by Eq. 2.2.2 a, Section 2.2. Along with all the points a curve for the J-S-T correlation has also been shown (Eq. 2.2.3, Section 2.2). It is evident from the graph that the points belonging to the group of (n-C_6, Toluene and n-C_8) follow the same trend as the J-S-T curve and exhibit that RV is also a function of a molecular property for heavier compounds. Note the gradual shifts in the RV curves as the alkane number increases. Another important feature of Figure 5.3.1 shows that all the curves converge at a reduced density of 2.5. This Figure is also indicative of the fact that the hypothesis put forward by Jossi et.al.[1] that the variation of residual viscosity with respect to the reduced density is uniform for all the substances is valid only for components up to normal octane. Hence it can be concluded that the J-S-T correlation is valid for any range of reduced density and components smaller with a molecular weight less than that of n-octane or for any compounds with reduced density less than 2.5.

The above exercise formed the basic groundwork for the modification, the solution was achieved in a very systematic way. In order to find out the dependence of RV on the component property, values for RV were computed from Figure 5.3.1 for isoreduced density values and were plotted against acentric factor. The formulation obtained by this method was presented at the 7th European Improved Oil Recovery (IOR) Symposium in Moscow, Russia[19]. However, later on the molecular weight was, chosen, instead of the acentric factor as the correlating parameter because the former is a more readily available parameter than acentric factor especially for the plus fractions of a real fluid. Figure 5.3.2 shows the plot of RV vs. molecular weight for various isoreduced densities. The graph demonstrates the dependency of RV on a component property. It is also interesting to note that the values of RV converge to zero as molecular weight decreases.

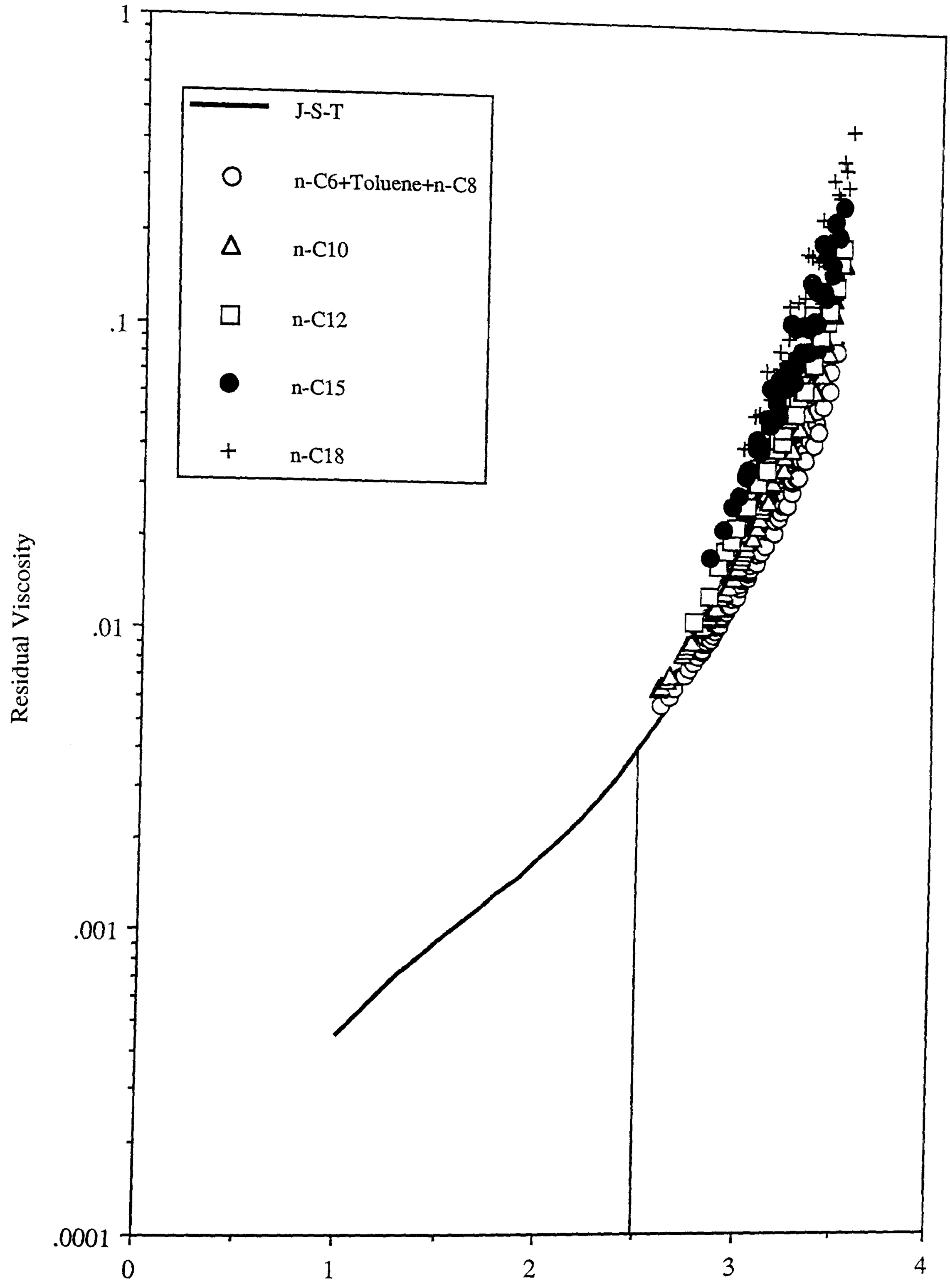

Figure 5.3.1 - Plot of Residual Viscosity vs Reduced Density

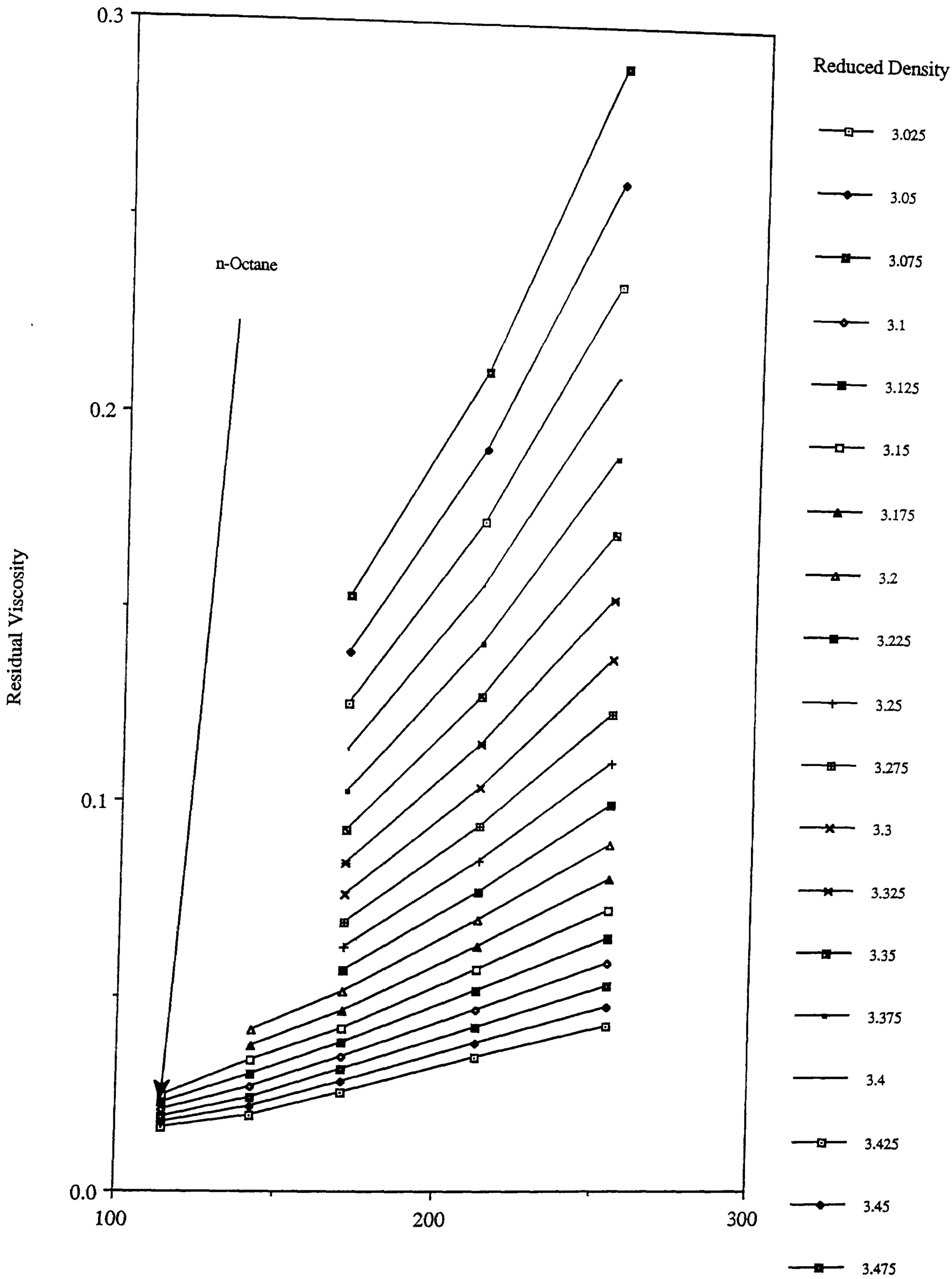

Figure 5.3.2 - Dependence of Residual Viscosity on Molecular Weight.

Considering Figure 5.3.1, also Figures 5.2.1 and 5.2.2 it was decided to maintain the original J-S-T correlation for reduced density up to 2.5. The modified correlation would therefore be valid for reduced density greater than 2.5. In order to maintain the continuity between the original and the modified correlation at a reduced density of 2.5, few values of RV calculated from the J-S-T correlation were considered in developing the set of correlations for all the pure components concerned. Figure 5.3.3 shows a plot of $\log_e(RV)$ vs. reduced density for the group of n-C_6, Toluene and n-C_8. Similar to Figure 5.3.3 plots for other components were also constructed and all the curves were fitted in terms of a second order polynomial, for the group of n-C_6, Toluene and n-C_8 for example:

$$\log_e(RV) = A + B\rho_r + C\rho_r^2 \qquad (5.3.1)$$

where, reduced density, ρ_r is given by:

$$\rho_r = \frac{\rho}{\rho_c}$$

and ρ_c is the critical density

where A, B and C from Figure 5.3.3 are :

$$A = -5.4054$$

$$B = -2.1979$$

$$C = 0.86652$$

Values of A, B and C for all the components were subsequently plotted vs. molecular weights as shown in Figure 5.3.4. A generalised correlation for A, B and C was thus formed as a function of molecular weight in terms of a second order polynomial. Hence, the modified correlation is:

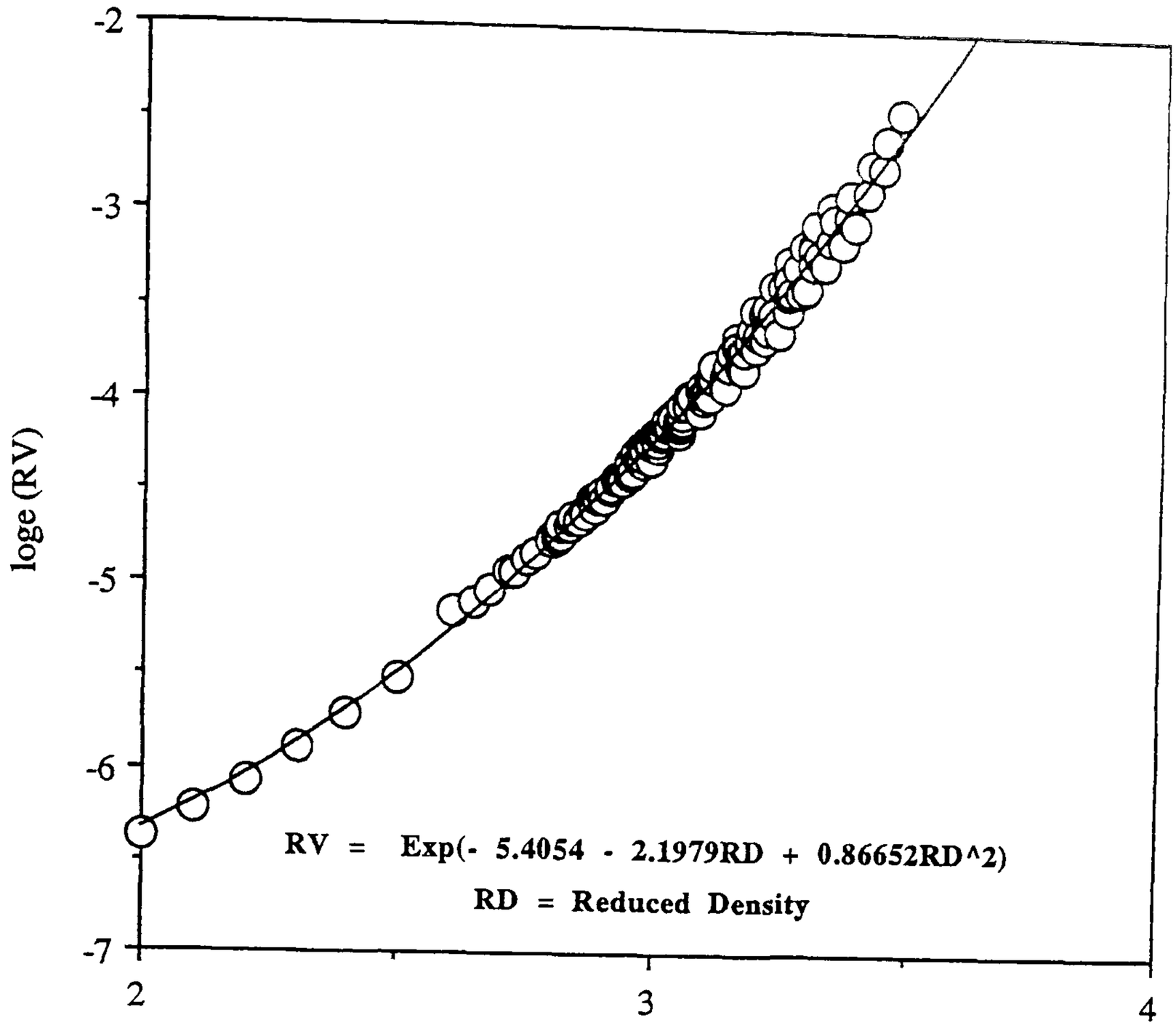

Figure 5.3.3 - Plot of loge(RV) vs Reduced Density for the Group, n-C6, Toluene and n-C8.

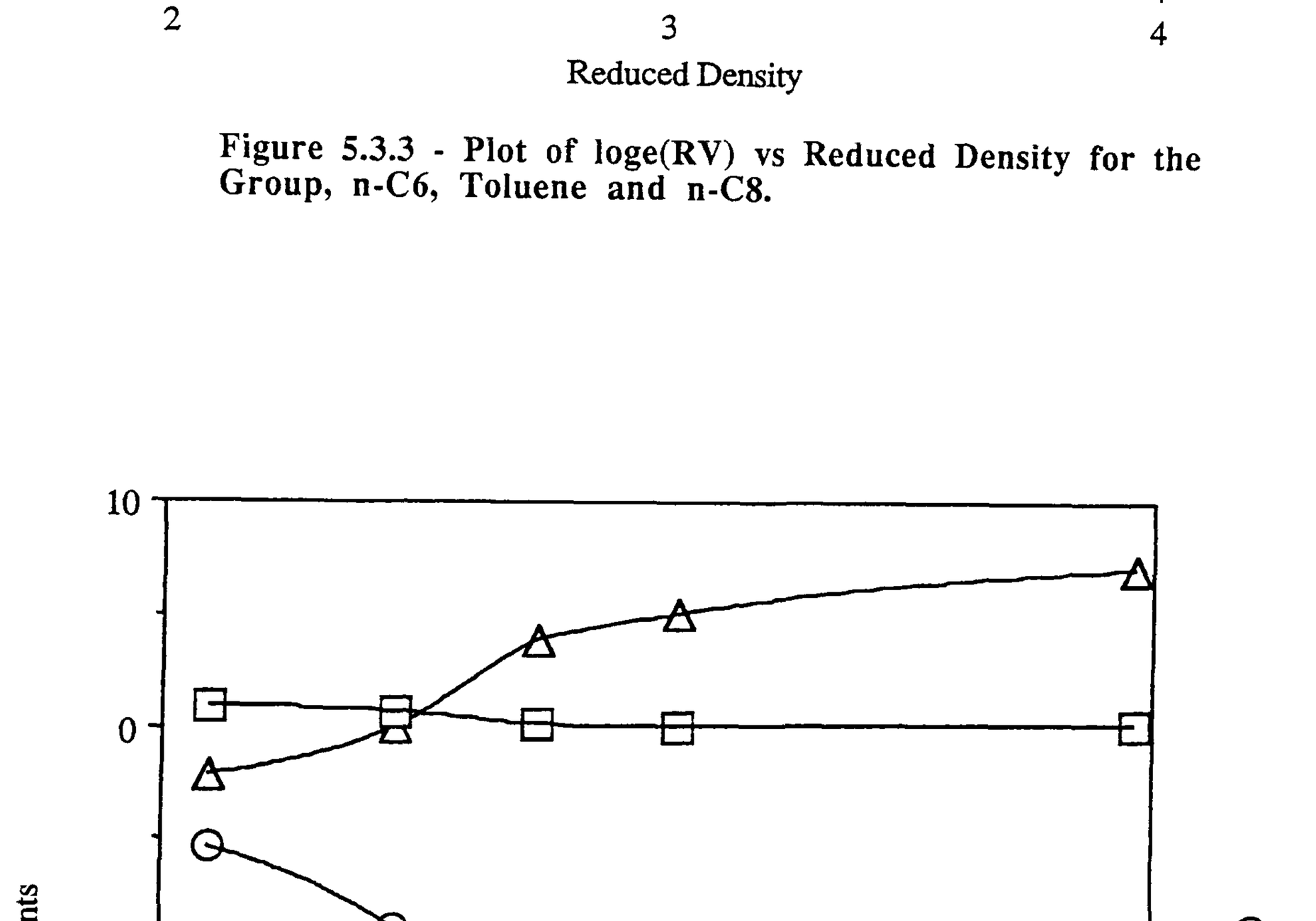

Figure 5.3.4 : Plot of Coefficients of Individual Compounds vs Molecular Weight.

for reduced density greater than 2.5

$$(\eta-\eta^*)\lambda = \text{Exp}\,[A + B\rho_r + C\rho_r^2] \tag{5.3.2}$$

where:

$$A = 9.8338 - 0.15568MW + 1.8935E^{-04}MW^2 \tag{5.3.3}$$

$$B = -12.150 + 0.10345MW - 1.3971E^{-04}MW^2 \tag{5.3.4}$$

$$C = 2.3990 - 1.6355MW + 2.5338E^{-05}MW^2 \tag{5.3.5}$$

and MW is the molecular weight.

The lowest value of molecular weight used in the above set of correlations is 114.232. The modified correlation was also compared with two methods from the group of corresponding states, namely; the extended corresponding states method (TRAPP) of Ely and Hanley[8] and the two reference component method of Petersen et.al.[7]. The statistical analysis of the developed modified correlation is provided in Table (5.3.1) and the percentage deviations are plotted against measured viscosity in Figure 5.3.5. The one reference method was not considered for comparison because it has already been shown that the two reference method is more reliable than the former one[7]. It was observed that in the TRAPP method the shape factor iteration loop did not converge at certain high pressure conditions. Similarly for the two reference method the deviations were found to be higher for components heavier than n-decane (the second reference component), refer to the average absolute deviation Table 1 of Reference[7].

5.3.1 : Continuity Between the Original and Modified Correlation

In order to check that the continuity is maintained when the correlations are changed as a result of varying reduced density, both correlations were applied to one pure component and one binary hydrocarbon mixture. Figure 5.3.1.1 shows the plot of residual viscosity vs. reduced density for n-decane. For reduced densities less than 2.5 the J-S-T correlation was

Table 5.3.1 - Statistical analysis for the modified residual viscosity correlation.

Pure Components

Data Points	Method	STDEV %	AAD %	BIAS %
278 excluding the very high pressure (> 20, 000 psi) points	**This work**	**8.4**	**6.6**	**-3.1**
	JST[1]	23.5	20.4	-14.0
	TRAPP[8]	13.7	10.7	-7.8
	2 reference[7]	14.1	9.2	5.3
356* all data points for developing the correlation	**This work**	**10.8**	**8.2**	**-3.2**
	JST	26.9	26.6	-21.5

* The TRAPP and 2-reference methods could not handle the data with P > 20, 000psi.

$$\text{AAD \%} = \frac{100}{N} \sum_{i=1}^{N} \text{ABS}\left(\frac{\eta_{pred} - \eta_{exp}}{\eta_{exp}}\right)$$

$$\text{BIAS \%} = \frac{100}{N} \sum_{i=1}^{N} \left(\frac{\eta_{pred} - \eta_{exp}}{\eta_{exp}}\right)$$

$$\text{STDEV \%} = \frac{100}{N} \text{SQRT}\left[\sum_{i=1}^{N}\left(\frac{\eta_{pred} - \eta_{exp}}{\eta_{exp}}\right)^2\right]$$

N : Number of data points

pred : predicted value

exp : experimental value

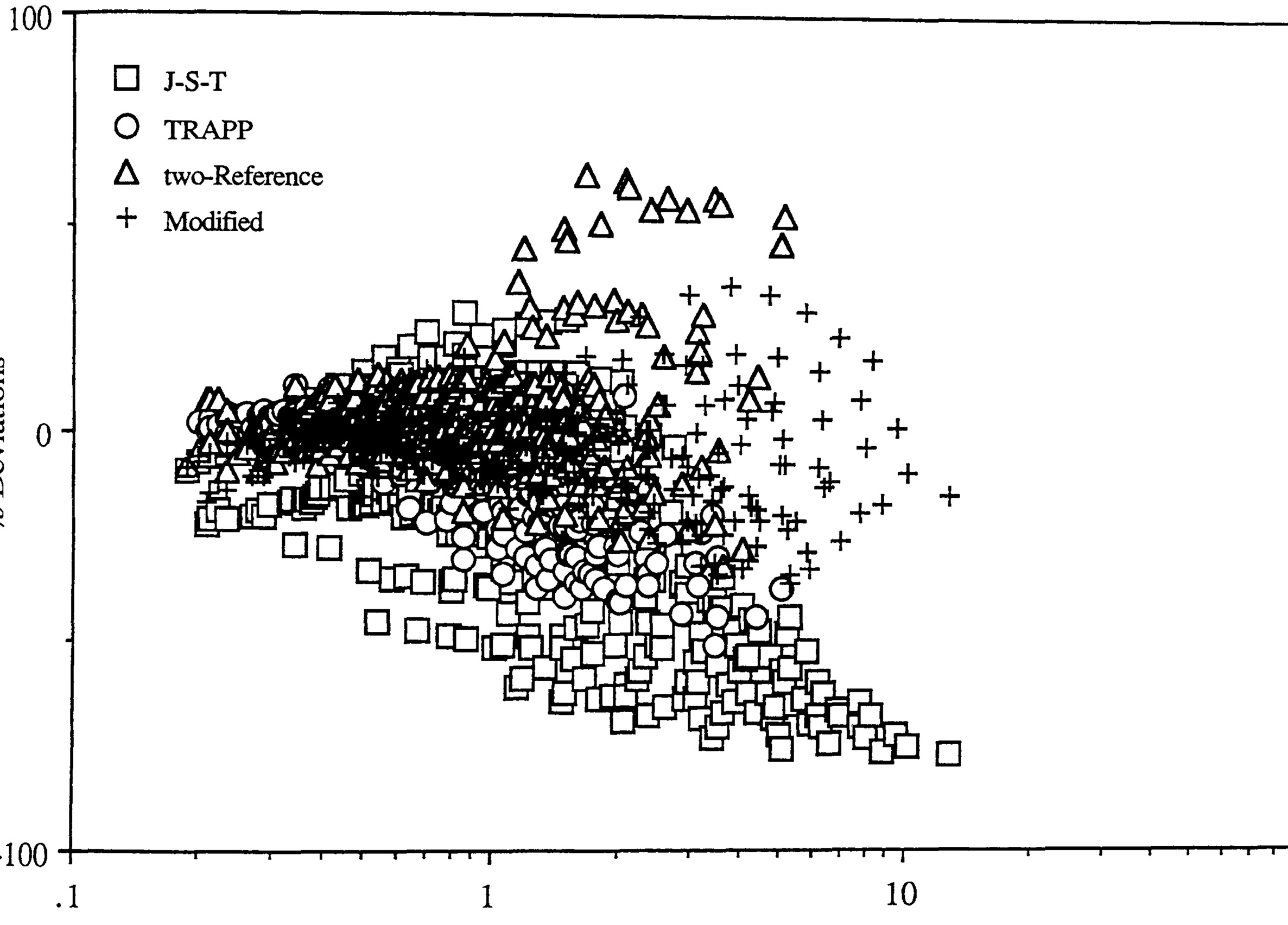

Figure 5.3.5 - Deviations of Calculated Viscosity from Experimental Values for Pure Components.

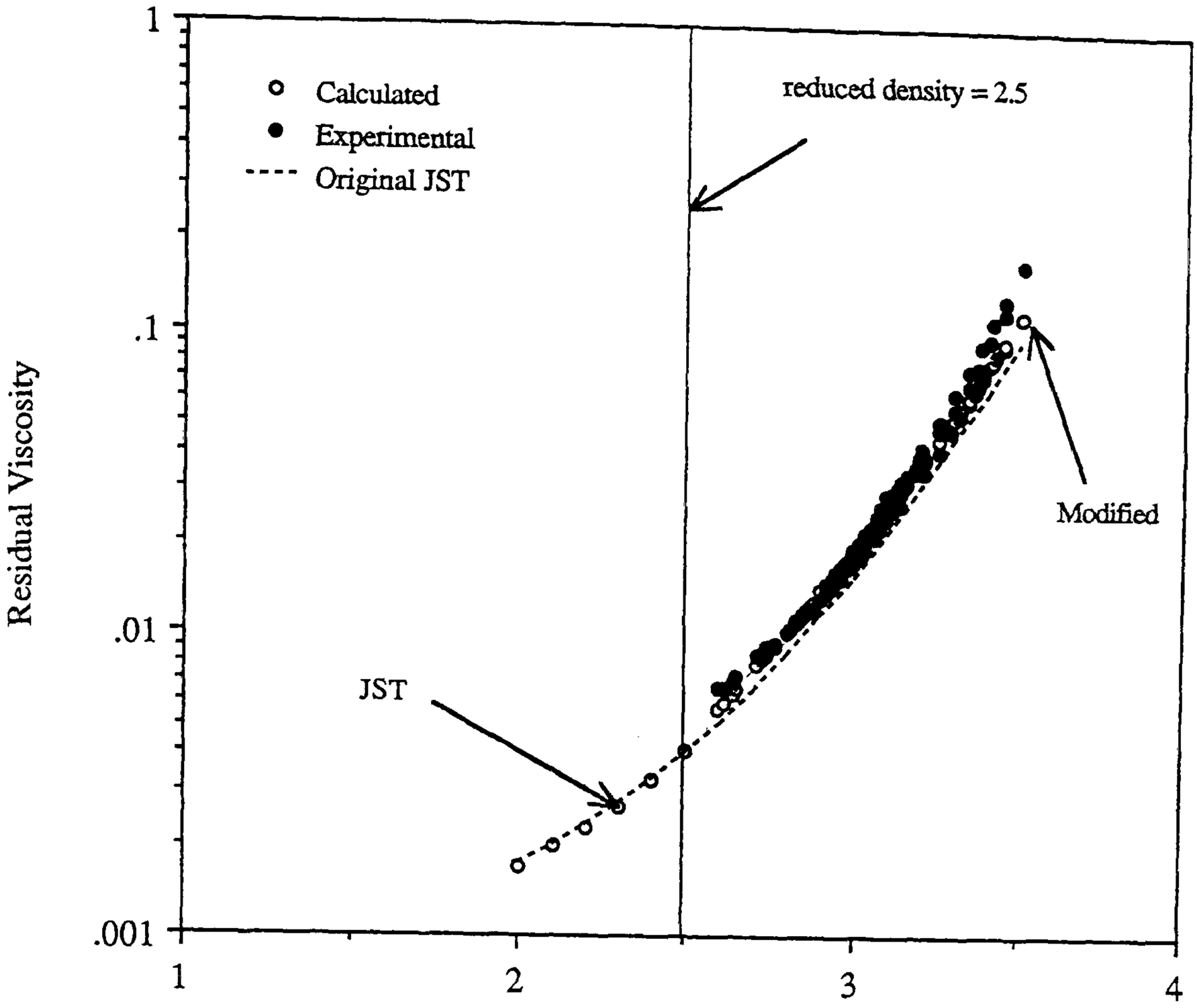

Figure 5.3.1.1 - Continuity between the Original and Modified Correlation for n-C10.

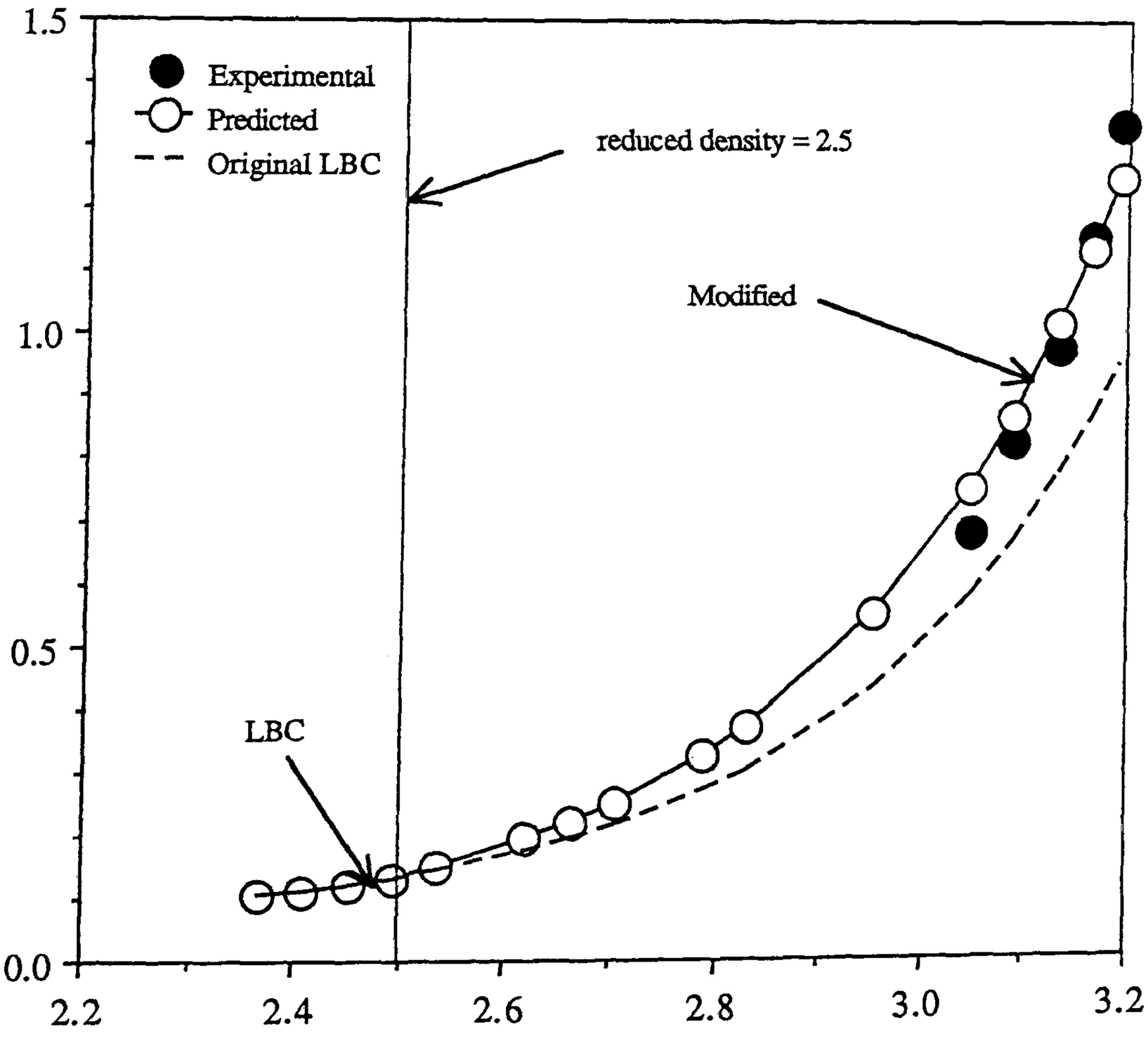

Figure 5.3.1.2 - Continuity Between the Original and Modified Correlation for a nC10+nC16 Binary Mixture.

applied and for reduced densities greater than 2.5 the modified correlation was used. The Figure clearly illustrates the continuity maintained between the two correlations as the value of reduced density changes, and a fairly smooth transition is achieved. Figure 5.3.1.2 shows graph of viscosity against reduced density for a n-decane and n-hexadecane binary mixture. The L-B-C correlation is applied to the reduced density data below 2.5 and the modified correlation is applied to the reduced density data above 2.5. This plot again indicates consistent predictions when the correlations are changed as a result of varying reduced density.

5.4 : APPLICATION OF THE MODIFIED RESIDUAL VISCOSITY METHOD TO SYNTHETIC HYDROCARBON MIXTURES

The modified residual viscosity correlation, Eq. 5.3.2-5.3.5, was applied to several synthetic hydrocarbon mixtures, ranging from simple binary mixtures to multicomponent mixtures[9,10,11,12,16] at a wide range of temperature and pressure conditions. All the data was quality checked prior to using it for comparison purposes. The experimental data used for comparison is measured by various techniques. The data from Reference 9 on various binary mixtures were measured by the Cannon-Ubeholde type viscometer which is generally employed in estimating viscosities of viscosity standards which are used for calibrating the rolling ball type viscometers. The viscosities of a binary mixture of carbon dioxide and n-decane[10] were obtained by the capillary tube viscometer. The viscosities of the binary mixture of toluene and n-hexane[11] were measured by the falling body viscometer. A conventional falling body viscometer similar to the rolling ball viscometer was used for measuring viscosity of higher alkanes and its mixtures at high pressures and temperatures[12]. The viscosities of the binary mixture of methane and n-decane[16] were measured by the oscillation cup viscometer.

The data on measured density was available in all the sources corresponding to the viscosity measurements except Reference 12 in which case the densities were calculated using the API method[13] for the binary mixture of n-decane-n-hexadecane and the quaternary mixture of n-

decane-n-dodecane-n-tetradecane-n-hexadecane respectively. The viscosity predictions were carried out using the original Lohrenz-Bray-Clark method[2], and the modified correlation. They were compared with two methods from the group of corresponding states namely; TRAPP[8] and the two-reference[7] method. The overall statistical analysis for all the methods is shown in Table (5.4.1). The percentage deviations vs. the measured viscosities are plotted in Figure 5.4.1. The modified correlation was found to have the lowest average absolute deviation and the standard deviation. This comparative study confirms that the modified correlation is significantly superior to the original L-B-C method and the deviations are less than those predicted by TRAPP and the two reference method.

5.5 : APPLICATION OF THE MODIFIED RESIDUAL VISCOSITY METHOD TO REAL RESERVOIR FLUIDS

The modified residual viscosity correlation was also applied to real reservoir fluids. A correlation for estimating the critical volume (V_c) of the plus fraction has also been developed. A total number of 39 data points were considered for developing the V_c correlation. The data presented in Reference 14 on experimental viscosity measurements on real reservoir fluids was employed to back calculate the values of V_c for the plus fractions by forcing the agreement between the experimental value and that predicted by the modified correlation. The developed correlation has been made a function of specific gravity and molecular weight of the plus fraction, similar to that proposed by Lohrenz et. al.[2] and has the following form:

$$V_c(C_{7+}) = -10.329 + 0.12570MW_{C7+} + 15.461SG_{C7+} - 0.08587MW_{C7+}SG_{C7+} \qquad (5.5.1)$$

The densities of all the 39 samples were predicted by the Alani and Kennedy equation of state[18] and the critical temperature and pressure of the plus fractions were estimated from the Twu[17] correlation. The range of specific gravity and molecular weight of the plus fraction for developing Eq. 5.5.1 was 0.6-0.9 (60/60) and 160-400 gm/gm-mole respectively. The volume calculated by Eq. 5.5.1 is in ft^3/lb-mole. The average absolute deviation of Eq. 5.5.1 is 1.5 % with a standard deviation of 1.9 %.

Table 5.4.1 - Statistical analysis for the modified residual viscosity correlation.

Synthetic Mixtures

Data Points	Method	STDEV %	AAD %	BIAS %
398	**This work**	**10.8**	**8.2**	**-3.1**
	LBC	22.4	16.0	-8.8
	TRAPP	24.5	17.3	-1.7
	2 reference	16.0	11.2	-4.0

Table 5.5.1 - Statistical analysis for the modified residual viscosity correlation.

Real Reservoir Fluids

Data Points	Method	STDEV %	AAD %	BIAS %
106	**This work**	**21.4**	**21.8**	**20.1**
	LBC	26.9	36.0	34.2

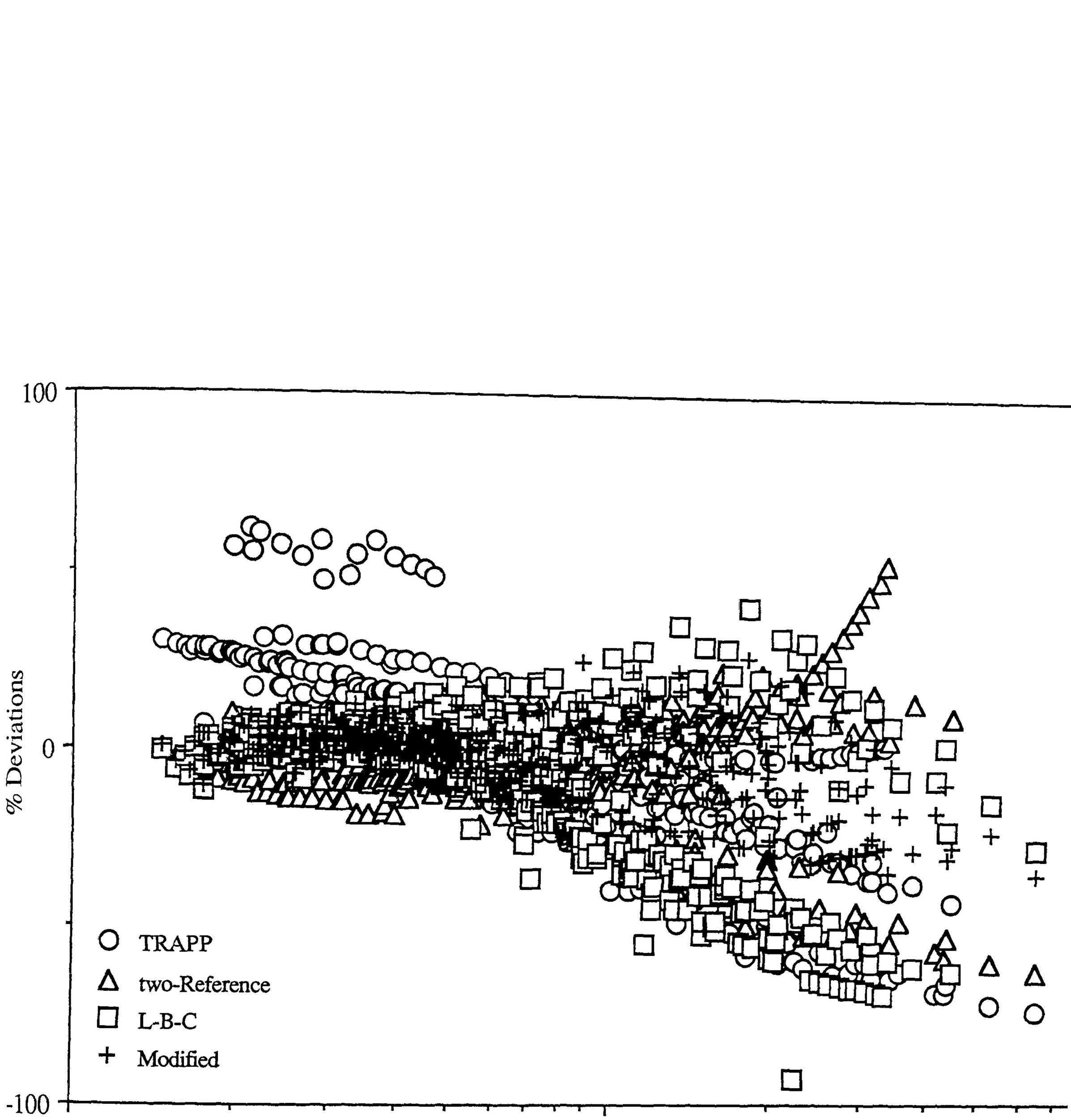

Figure 5.4.1 - Deviations of calculated viscosity from experimental value for synthetic mixtures.

The modified residual viscosity correlation and the Lohrenz et. al.[2] method were subsequently applied to a total number of 106 data points on real reservoir fluids[13,15]. The above developed correlation for the critical volume of the plus fraction was utilised for the modified correlation whereas the correlation developed by Lohrenz et. al.[2] was employed for the L-B-C method. The critical temperature and pressure were estimated from the Twu[17] correlation, and the fluid density at all conditions were estimated by the Alani and Kennedy equation of state[18]. The liquid phase compositions for all the samples were calculated by the in-house Vapour Liquid Equilibrium (VLE) model[20]. The statistical analysis for the tested fluids is provided in Table (5.5.1). The modified residual viscosity method again shows the lowest average absolute and standard deviation compared to the L-B-C method.

References

1) Jossi, J.A., Stiel, L.I. and Thodos, G.: "The Viscosity of Pure Substances in the Dense Gaseous and Liquid Phases", *AIChEJ*, Vol. 8, pp. 59 - 63, (1962).

2) Lohrenz, J., Bray, B.G. and Clark, C.R.: "Calculating Viscosities of Reservoir Fluids from their Compositions", *Journal of Petroleum Technology*, pp. 1171-1176, (Oct., 1964).

3) Oliveira, C.M.B.P. and Wakeham, W.A.: "The Viscosity of Five Liquid Hydrocarbons at Pressures Up to 250 MPa", *International J. of Thermophysics*, Vol. 13, No. 5, pp. 774-790, (1992).

4) Lee, A.L. and Ellington, R.T.: "Viscosity of n-Decane in the Liquid Phase", *Journal of Chem. Engg. Data*, Vol. 10, No. 4, pp. 346-348, (1965).

5) Hogenboom, D.L., Webb, W. and Dixon, J.A.: "Viscosity of Several Liquid Hydrocarbons as a Function of Temperature, Pressure an Free Volume", *J. Chem Phys.*, Vol. 46, No. 7, (April, 1967).

6) Cutler, W.G., McMickle, R.H., Webb, W. and Schiessler, R.W.: "Study of the Compression of Several High Molecular Weight Hydrocarbons", *J. Chem Phys.*, Vol. 29, No. 4, pp. 727-740, (October, 1958).

7) Aasberg-Petersen, K., Knudsen, K. and Fredenslund, A.: "Prediction of Viscosities of Hydrocarbon Mixtures", *Fluid Phase Equilibria*, Vol. 70, pp. 293-308, (1991).

8) Ely, J.F. and Hanley, H.J.M: "Prediction of the Viscosity and Thermal Conductivity in Hydrocarbon Mixtures - Computer Program TRAPP", Proceedings of the Sixtieth Annual Convention of Gas Processors Association, pp. 20-29, (Mar., 1981).

9) Cooper, E.F. and Asfour, A.A.: "Densities and Kinematic Viscosities of Some C_6-C_{16} n-Alkane Binary Liquid Systems at 293.15 K", *Journal of Chem. Engg. Data*, 36, pp. 285-288, (1991).

10) Cullick, A.S. and Mathis, M.L.: "Densities and Viscosities of Mixtures of Carbon Dioxide and n-Decane from 310 to 403 K and 7 to 30 MPa", *Journal of Chem. Engg. Data*, 29, pp. 393-396, (1984).

11) Dymond, J.H., Awan, M.A., Glen. and Isdale, J.D.: "Transport Properties of Nonelectrolyte Liquid Mixtures. VIII. Viscosity Coefficients for Toluene and for Three Mixtures of Toluene+Hexane from 25 to 100°C at Pressures up to 500 MPa", *International Journal of Thermophysics*, Vol. 12, No. 2, pp. 275-287, (1991).

12) Ducoulombier, D., Zhou, H., Boned, C., Peyrelasse, J., Saint-Guirons, H. and Xans,P.: "CONDENSED PHASES AND MACROMOLECULES, Pressure (1-1000 bars) and Temperature (20-100°C) Dependence of the Viscosity of Liquid Hydrocarbons", *Journal of Physical Chemistry*, 90, pp. 1692-1700, (1986).

13) Pedersen, et. al : "Properties of Oils and Natural Gases", (Contrib. Petrol. Geol. & Eng., Vol. 5), Gulf Publishing Co., (1989).

14) Lawal, A.S.L.: "Improved Fluid Property Predictions for Reservoir Compositional Simulation", PhD Dissertation, The University of Texas at Austin, (1985).

15) Omar, M.I.: "Private Communication" (1991).

16) Knapstad, B., Skjolsvik, P.A. and Oye, H.A.: "Viscosity of n-Decane-Methane System in the Liquid Phase", *Ber. Bunsenges. Phys. Chem.*, Vol. 94, pp. 1156-1165, (1990).

17) Twu, C.H: "An Internally Consistent Correlation for Predicting the Critical Properties and Molecular Weights of Petroleum and Coal-Tar Liquids", *Fluid Phase Equilibria*, Vol. 16, pp. 137-150, (1984).

18) Alani, G.H. and Kennedy, H.T.: "Volumes of Liquid Hydrocarbons at High Temperatures and Pressures", *Petroleum Transactions of AIME*, Vol. 219, pp. 288-292, (1960).

19) Dandekar, A., Danesh, A., Tehrani, D.H. and Todd, A.C.: "A Modified Residual Viscosity Method for Improved Prediction of Dense Phase Viscosities", Presented at the 7th European Improved Oil Recovery (IOR) Symposium in Moscow, Russia, October 27-29, (1993).

20) Xu, D.: "FPE, Predictions of Fluid Phase Equilibria", Department of Petroleum Engineering, Heriot-Watt University, (1992).

CHAPTER 6 : CONCLUSIONS AND RECOMMENDATIONS

6.1 : CONCLUSIONS

The following conclusions can be drawn from the study presented in this work:

1. The concept of relating residual viscosity to reduced density is confirmed as a simple and useful approach for estimating fluid viscosities.
2. The tuning study performed on the L-B-C method and three other methods from the principle of corresponding states, on real reservoir fluids, revealed that the L-B-C method is computationally fast and easily tuned to the experimental data compared to the other methods. The method also had lowest average absolute deviation among the group of tuned models.
3. The residual viscosity methods of J-S-T (pure components) and L-B-C (mixtures) have been critically evaluated and it has been demonstrated that the variation of residual viscosity with respect to reduced density is not uniform for all the substances. These methods predict the fluid viscosities within a reasonable range of accuracy for reduced densities less than 2.5. Whereas both methods largely underpredict the viscosities for fluids having reduced density greater than 2.5.
4. A modification of the J-S-T method has been proposed, based on experimental viscosity data from literature on pure heavy hydrocarbons. The residual viscosity has been made a function of molecular weight and reduced density. The modified method has been applied to a large number of data on pure hydrocarbons and its synthetic mixtures at a wide range of temperatures and pressures. The modified method is shown to have the lowest average absolute and standard deviation compared to the original methods and two other methods from the group of corresponding states.

5. A correlation for estimating the critical volume of the plus fraction of a real reservoir fluid for the modified correlation has been developed. The modified residual viscosity correlation is also shown to be superior to the L-B-C method for real reservoir fluids.

6. All methods from the group of principle of corresponding states, (one reference or two reference) methods and the TRAPP (Ely and Hanley) were found to be highly inaccurate for dense fluid phase conditions. The methods were also found to be unreliable at high pressures, the conditions at which the variation of fluid viscosity is not uniform with respect to the reference component.

6.2 : RECOMMENDATIONS

Following are the recommendations which could be made from the study:

1. If reliable and accurate density data is available, the residual viscosity method is highly recommended for estimation of gas phase viscosities. However, in the absence of density data, the principle of corresponding states (one reference) method is best recommended.

2. The modified residual viscosity method is recommended when viscosity predictions are required for dense phase fluid mixtures ($\rho_r > 2.5$) provided the density data supplied is of reasonable accuracy.

3. The extended principle of corresponding states (TRAPP) or the principle of corresponding states method with two reference components is recommended for hydrocarbon mixtures where the density data are scarce.

4. There exists a room for modification of the principle of corresponding states method with two reference components. The method has been found to be unreliable for fluids having molecular weights more than n-decane (the second reference component). The prediction capability of the method can be significantly improved by introduction of a third reference component heavier than n-decane.

5. The principle of corresponding states method with one reference component and the residual viscosity method are best recommended for the purposes of tuning in a compositional reservoir simulator.

6. A more accurate and reliable correlation for the critical volume (V_c) of the plus fraction of a real reservoir fluid could further improve the accuracy of the modified residual viscosity correlation for real reservoir fluids.